



Institut für Anorganische und Analytische Chemie

Determination of non-thiophenic sulfur  
compounds in vacuum gas oils -  
Ligand Exchange Chromatography and Ultra High  
Resolution Mass Spectrometry as tools to gain deeper  
insight into higher boiling petroleum cuts

**Inaugural-Dissertation**

zur Erlangung des Doktorgrades der Naturwissenschaften im  
Fachbereich Chemie und Pharmazie der  
Mathematisch-Naturwissenschaftlichen Fakultät der Westfälischen  
Wilhelms-Universität Münster

vorgelegt von  
**Isabelle Möller**  
aus Lünen  
– 2014 –

---

Dekan:	Prof. Dr. Bart J. Ravoo
Erster Gutachter:	Prof. Dr. Jan T. Andersson
Zweiter Gutachter:	Prof. Dr. Uwe Karst
Tag der mündlichen Prüfung:	<b>20.10.2014</b> .....
Tag der Promotion	<b>20.10.2014</b> .....

*Je mehr man schon weiß, je mehr hat man noch zu lernen. Mit dem Wissen nimmt das Nichtwissen in gleichem Grade zu oder vielmehr das Wissen des Nichtwissens.*

Friedrich von Schlegel



## Contents

<b>Nomenclature</b>	<b>V</b>
<b>1 Introduction</b>	<b>1</b>
<b>2 Crude oil: composition, origin and processing</b>	<b>4</b>
2.1 Petroleum: The supercomplex mixture . . . . .	4
2.2 Sulfur in fossil material . . . . .	6
<b>3 Scope of work</b>	<b>11</b>
<b>4 High resolution mass spectrometry</b>	<b>12</b>
4.1 Orbitrap mass spectrometry . . . . .	16
4.2 Fourier transform ion cyclotron resonance mass spectrometry . . . . .	17
4.3 Graphical methods for data interpretation . . . . .	19
4.3.1 Kendrick plots . . . . .	20
4.3.2 Pseudograms . . . . .	21
4.3.3 Box plot modification . . . . .	21
<b>5 LEC on metal ion treated stationary phases</b>	<b>24</b>
5.1 State-of-the-art: LEC for the analysis of sulfur containing compounds . . .	24
<b>6 LEC phases for the separation of sulfur compounds</b>	<b>31</b>
6.1 Separation on zinc chloride silica gel . . . . .	33
6.2 Separation on chromium sulfate silica gel . . . . .	34
6.3 Separation on cadmium acetate silica gel . . . . .	36
6.4 Separation on cobalt nitrate silica gel . . . . .	38
6.5 Separation on <i>h</i> Ag-MPSG and silver cartridges . . . . .	39
6.6 Conclusions . . . . .	43
<b>7 Chromatographic separation &amp; further analysis of VGOs</b>	<b>44</b>
7.1 State-of the art . . . . .	44
7.1.1 Chromatographic separation of petroleum . . . . .	44
7.1.2 Methylation reaction of sulfur containing compounds . . . . .	45
7.1.3 FT-ICR MS for the analysis of petroleum . . . . .	46
7.1.4 FT-ICR MS for the analysis of sulfur compounds . . . . .	48

---

7.2	Preseparation of vacuum gas oils . . . . .	50
7.3	Methylation of non-thiophenic sulfur compounds . . . . .	54
7.4	Separation of vacuum gas oils . . . . .	57
7.4.1	Separations of VGOs on PdSO <sub>4</sub> -Alox . . . . .	58
7.4.2	Separations of VGOs on <i>h</i> Ag-MPSG . . . . .	70
7.4.3	Separations of VGOs on Ag <sup>+</sup> -cartridges . . . . .	76
7.4.4	Online HPLC-MS separations on PdSO <sub>4</sub> -Alox . . . . .	82
7.4.5	Comparison between the different phases for the separation of VGOs	92
7.4.6	Effects of the ionization technique on the resulting mass spectra .	94
7.5	Sulfur content, sulfur balance and mass balance of the separated fractions	101
7.5.1	Determination of the total sulfur content via TXRF . . . . .	101
7.5.2	Repeatability, mass and sulfur balance . . . . .	103
7.6	Conclusions . . . . .	111
<b>8</b>	<b>Alternative approaches towards the disulfide analysis</b>	<b>115</b>
8.1	State of the art: Analysis of disulfides . . . . .	115
8.2	Reduction of disulfides with tris(2-carboxyethyl)phosphine . . . . .	116
8.3	Reduction of disulfides and derivatization with ethyl iodoacetate . . . . .	118
8.4	Reduction and derivatization with iodoacetic acid . . . . .	120
8.5	Reduction and direct determination via ESI-MS as thiolates . . . . .	122
8.6	Reduction and derivatization with maleic anhydride . . . . .	124
8.7	Iodine-catalyzed addition of disulfides to alkenes . . . . .	125
8.8	Reduction and detection via photometry . . . . .	128
8.8.1	Derivatization with monobromobimane . . . . .	128
8.8.2	Derivatization with benzofurazan sulfides . . . . .	129
8.9	Isolation of sulfides by oxidation with tetrabutylammonium periodate . .	131
8.10	Conclusions . . . . .	136
<b>9</b>	<b>Summary</b>	<b>138</b>
<b>10</b>	<b>Appendix</b>	<b>141</b>
10.1	Experimental . . . . .	141
10.1.1	General preparation of metal coated silica gel . . . . .	141
10.1.2	General preparation of metal coated alumina . . . . .	141
10.1.3	Preparation of silver nitrate titania . . . . .	141
10.1.4	Preparation of silver nitrate alumina . . . . .	141

---

10.1.5	Preparation of heat-treated Ag-MPSG . . . . .	142
10.1.6	Preparation of Ag <sup>0</sup> silica gel . . . . .	142
10.1.7	Preparation of silver nanoparticle silica gel . . . . .	142
10.1.8	Preparation of phenyl silica gel . . . . .	143
10.1.9	Preparation of silver coated cationic ion exchanger . . . . .	143
10.1.10	Preparation of copper silica gel . . . . .	143
10.1.11	Preparation of palladium 8-hydroxyquinoline silica gel . . . . .	143
10.1.12	Preparation of PdSO <sub>4</sub> -Alox . . . . .	144
10.1.13	Vacuum gas oils . . . . .	144
10.1.14	Separation of standards on stationary phases . . . . .	144
10.1.15	SARA fractionation of VGOs . . . . .	145
10.1.16	Preseparation on alumina . . . . .	145
10.1.17	Separation of VGOs on stationary phases . . . . .	145
10.1.18	Separation of VGOs on Ag <sup>+</sup> -cartridges . . . . .	146
10.1.19	Derivatization by methylation with methyl iodide . . . . .	146
10.1.20	Derivatization by methylation with oxonium salts . . . . .	147
10.1.21	Reaction monitoring by NMR . . . . .	147
10.1.22	Reduction of disulfides with TCEP . . . . .	147
10.1.23	Reduction of disulfides and derivatization with ethyl iodoacetate . . . . .	148
10.1.24	Reduction of disulfides and derivatization with iodoacetic acid . . . . .	148
10.1.25	Reaction of disulfides and thiols with maleic anhydride . . . . .	148
10.1.26	Isolation of sulfides by oxidation with TBAPI . . . . .	149
10.1.27	Derivatization of standards with mBBr . . . . .	149
10.1.28	Iodine-catalyzed addition of disulfides to 4-fluorostyrene . . . . .	150
10.1.29	Synthesis of benzofurazan sulfides . . . . .	150
10.1.30	Derivatization of standards with nitrobenzofurazan sulfides . . . . .	150
10.2	Instrumental . . . . .	152
10.2.1	GC-FID parameters . . . . .	152
10.2.2	GC-AED analysis . . . . .	152
10.2.3	GC-MS parameters . . . . .	153
10.2.4	RP-HPLC parameters . . . . .	153
10.2.5	ESI-Orbitrap MS . . . . .	154
10.2.6	APCI- and APPI Orbitrap MS . . . . .	154
10.2.7	APCI-FT-ICR MS . . . . .	155
10.2.8	APLI-Orbitrap MS . . . . .	155

---

10.2.9 NMR . . . . .	156
10.2.10 TXRF . . . . .	156
10.3 Additional figures . . . . .	157
<b>11 References</b>	<b>180</b>



## Nomenclature

ACDA	2-amino-1-cyclopentene-1-dithiocarboxylate
APCI	atmospheric pressure chemical ionization
APLI	atmospheric pressure laser ionization
APPI	atmospheric pressure photoionization
DBE	double bond equivalent
DTT	dithiothreitol
EC	electrochemical cell
EI	electron impact ionization
ESI	electrospray ionization
FT-ICR	Fourier-transform ion cyclotron resonance
FT-ICR MS	Fourier-transform ion cyclotron resonance mass spectrometry
FWHM	full width at half maximum
GC x GC SCD	comprehensive two-dimensional gas chromatography with sulfur chemi-luminescence detector
GC-FID	gas chromatography with flame ionization detector
GC-MS	gas chromatography with mass spectrometric detector
HPLC	high performance liquid chromatography
HSAB	hard and soft acids and bases
KMD	Kendrick mass defect
LEC	ligand exchange chromatography
m/z	mass-to-charge ratio
mBBr	monobromobimane
MOF	metal-organic framework
MPSG	mercaptopropyl silica gel
MS	mass spectrometry
NCAC	nitrogen containing aromatic compounds
NMR	Nuclear Magnetic Resonance
PAH	polycyclic aromatic hydrocarbon
PANH	Polyaromatic nitrogen heterocycles
PASH	polyaromatic sulfur heterocycles
RP	reversed phase
SARA	saturates, aromatics, resins, asphaltenes
SG	silica gel
TBAPI	tetrabutylammonium periodate

TCEP	tris(2-carboxyethyl)phosphine
TIC	total ion current
VGO	vacuum gas oil

## 1 Introduction

Since industrialization, our modern world has a continuously increasing need for energy. Until today the greatest share of the produced energy is generated from fossil materials, like petroleum, natural gas and coal. [1] After the incident in Fukushima in March 2011, the German government decided on a nuclear power phase out until 2022. [2] As the energy transition towards renewable energies is related to high costs and the installation of the needed infrastructure in Germany is not yet completed, fossil materials are still of high importance as primary energy sources.

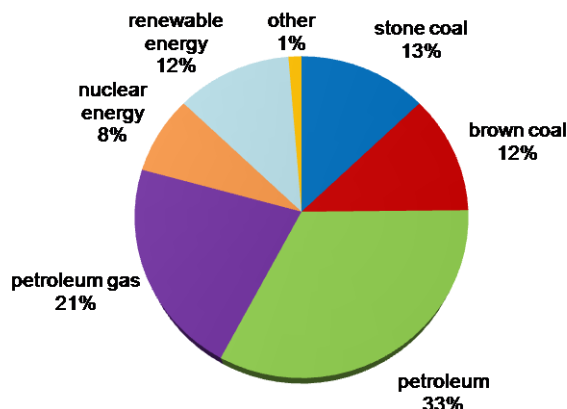


**Figure 1:** Primary energy sources in Germany in 2012. [1]

Whereas in western countries like Germany or the United States, fossil materials hold a stagnating or rather decreasing stake of the total energy consumptions, industrially emerging countries like China and India still have an ever growing demand for energy and the share of fossil fuels of the total energy consumption is still rising (see figure 2). Furthermore, fossil material is becoming an important factor in world politics. Ongoing conflicts in the Middle East, e.g. the Iraq wars, also resulted in an increase of the price for petroleum. The political power of fossil fuels recently became obvious in the conflict in the Ukraine, where Russia repeatedly threatened to turn off the gas tap not only cutting off the supply for the Ukraine itself, but parts of the European Union as well. The increasing demand in connection with the unstable political situation in some oil producing countries has led to a drastic price increase. The price for the OPEC reference basket, a weighted average price for petroleum blends and an important benchmark for the crude oil price development, has tripled in the last ten years (see figure 3). The

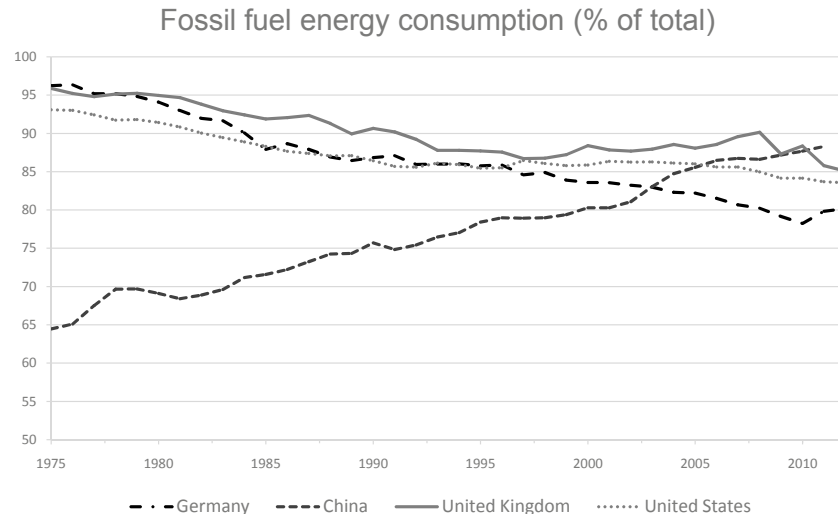


**Figure 2:** Share of fossil fuels to total energy consumption in selected countries from 1975 till today. [3]

world finance crisis in 2008 lead to a short time reduction of the price and since 2011 the prize has stabilized at around 105\$ per barrel, but the finite deposits will surely lead to another price increase in the future.

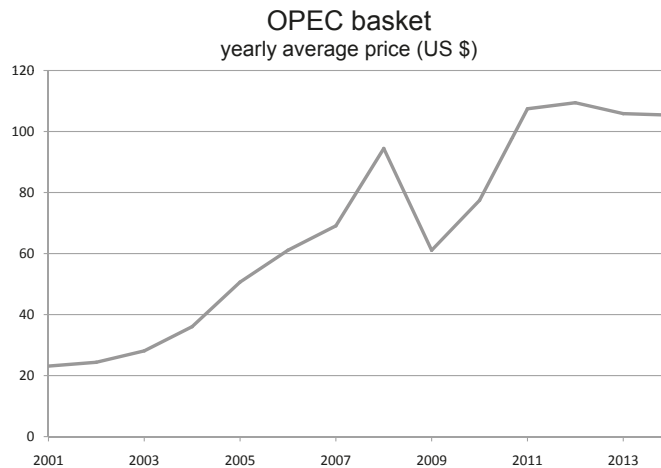


**Figure 3:** Development of the price in US Dollar for 1 barrel of the OPEC reference basket from 2001 until today. [4]

Due to this limitation of the deposits of fossil material, more efficient methods of processing crude oils are of huge economical interest. As the high consumption and growing demand will continue, the amount of easily processable crude oils decreases unceasingly,

so that even the heavier crudes as well as crude oils with higher content of heteroaromatic compounds become of increasing interest for the petroleum industry. [5] Due to legal requirements, the amount of heteroatomic compounds like sulfur and oxygen containing compounds in petroleum products has to be drastically reduced to be used as automotive fuel. In the EU directive 2003/17/EC, which took effect in January 2009, all diesel and gasoline used in the European Union is limited to a maximum sulfur content of 10 ppm. The reduction of the sulfur in automotive fuels has led to drastic reduction of emissions from motor vehicles and allowed the development of more efficient engines and exhaust gas treatment. A study presented by the German Federal Environmental Agency in 2014 predicts a reduction of the SO<sub>2</sub> emissions by about 50%, the NO<sub>2</sub> emissions by about 70% and the particulate emission from exhaust by about 80% between 2010 and 2030. [6]

Whereas in road transport strict sulfur limits have been legally enforced for several years, the limits in shipping traffic are still relatively lax. The International Maritime Organization (IMO) decided in October 2008 that the sulfur content of marine fuels should be reduced. From January 2012, the amount of sulfur in ship diesel should be reduced from 4.5% to 3.5% and progressively to 0.5% in 2025 at the latest. [7] In their directive 2005/33/EG the European Union already limited the sulfur content of marine fuels to 1.5% in all marine shipping traffic and 0.1% in inland shipping and while anchoring in European harbors. Hence, marine traffic still plays a larger part in the emissions caused by sulfur rich fuels than road traffic.

To reduce the sulfur content to comply with legal limitations, costly processes like desulfurization are needed. The different kinds of sulfur compounds present in the crude oils are susceptible to this process to a diverse degree. Whereas sulfides and thiols are readily desulfurized under relatively mild conditions, substituted aromatic sulfur compounds are recalcitrant to the known desulfurization methods. Therefore, detailed insight into the composition of a crude oil is extremely important for the oil processing industry. An easy distinction between sulfur classes in the crude oil is highly desirable and of huge economical interest.

## 2 Crude oil: composition, origin and processing

### 2.1 Petroleum: The supercomplex mixture

As petroleum, also known as crude oil, has been formed from marine sediments buried and kept under heat and pressure, its composition depends on the nature of the sediments, the underground environment, i.e. temperature, pressure and the possible presence of inorganic catalysts and the migration of liquids and gases underground to places where reservoirs are built. [8] The formation of petroleum is illustrated in figure 4: Biological material such as zooplankton and algae settles to the bottom of the sea and is mixed with sediments under anaerobic conditions. [9] The more layers are settled on top, the more heat and pressure are elevated in lower layers and during *diagenesis* the organic matter is converted into kerogenes, a waxy material. When the material is exposed to more heat, liquid and gaseous hydrocarbons are formed in a cracking process called *catagenesis*. Depending on the conditions present either natural gases, crude oils or carbon residue is formed.

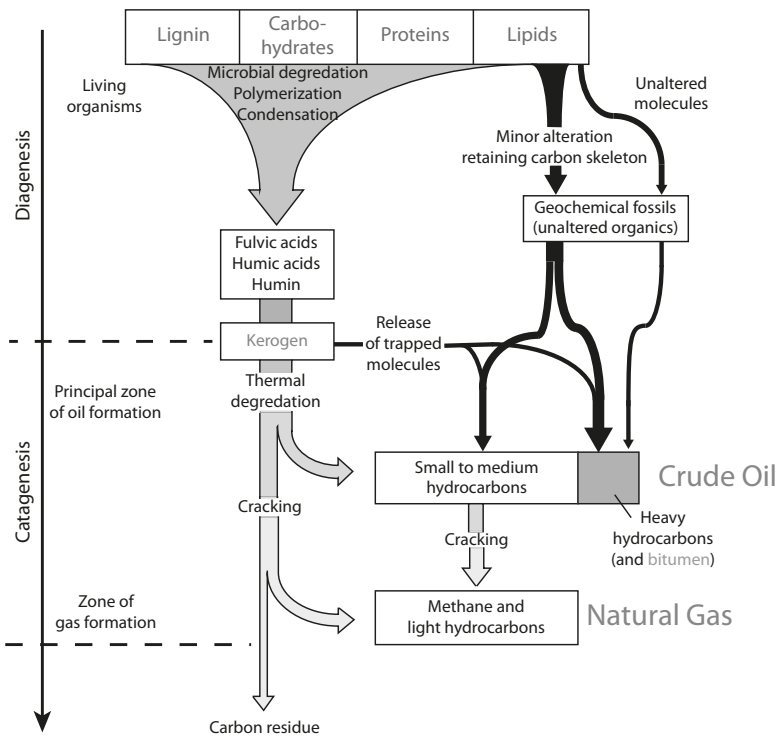
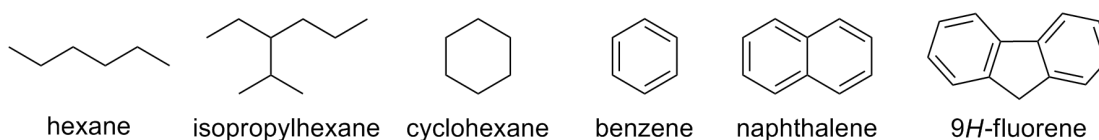


Figure 4: Scheme of the formation of petroleum. [9]

As various factors influence the formation, the physico-chemical properties like color, density or viscosity of crude oils can vary strongly. For example, the color ranges from light yellow to black, viscosity from free flowing to nearly solid. Petroleum is the most complex mixture known to mankind, whereby hydrocarbons are the most prevalent species at about 75% of most crude and refined oils and less than 50% in heavy oils. [10] Hydrocarbons can be divided into straight-chain alkanes, branched alkanes, cycloalkanes and aromatics (see figure 5). The aromatic hydrocarbons can be further classified in mono- and polycyclic aromatic hydrocarbons (PAHs). Alkenes also can occur in petroleum, but only in rare cases. [10] In addition to hydrocarbons, also compounds



**Figure 5:** Exemplary structures of different types of hydrocarbons.

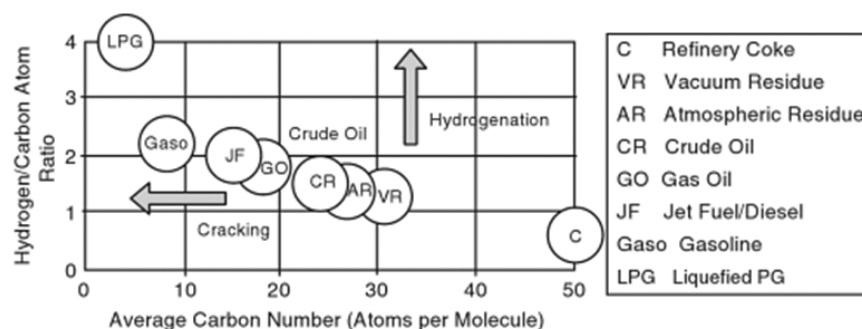
containing heteroatoms like oxygen, nitrogen or sulfur can be found. These elements can also be incorporated in aromatic systems, creating polycyclic aromatic oxygen compounds (PAOHs), polycyclic aromatic nitrogen heterocycles (PANHs) and polycyclic aromatic sulfur heterocycles (PASHs).

The classification of crude oils is done according to chemical composition or physical properties. For instance, specific gravity is used to classify a crude oil into light, medium or heavy. In the refinery classification is also done according to the boiling point of the fractions during the distillation process. Typical fractions and their yield during distillation are listed in table 1.

The table illustrates nicely that only small amounts of the distillation products are the highly desirable low boiling fractions, whereas the biggest shares are build by high boiling fractions and residue. Therefore in addition to distillation, each crude oil undergoes a multi-step process called *refining*. Solid components, metals and insoluble fractions are removed, distillation according to boiling point is performed, heteroatom compounds are removed by catalysts, and chemical conversions like *cracking* processes are done to increase the amount of aliphatic hydrocarbons in the processed oil. The effects of the cracking are also illustrated in figure 6.

**Table 1:** Crude distillation products[11]

	Yield (wt%)	True boiling temperature (°C)
<b>Atmospheric distillation</b>		
Refinery gases (C1-C2)	0.10	-
Liquid petroleum gases (LPG)	0.69	-
Light straight run (LSR)	3.47	32-82
Heavy straight run (HSR)	10.17	82-193
Kerosene (Kero)	15.32	193-271
Light gas oil (LGO)	12.21	271-321
Heavy gas oil (HGO)	21.10	321-427
<b>Vacuum distillation</b>		
Vacuum gas oil (VGO)	16.80	427-566
Vacuum residue (VR)	20.30	>566

**Figure 6:** Distribution of carbon number in petroleum products. [12]

During the refining process the average carbon number of the molecules present in the oil are reduced and the hydrogen/carbon atom ratio is increased. The hydrocarbons are cleaved to shorter chains and unsaturated bonds are saturated with hydrogen.

## 2.2 Sulfur in fossil material

Depending on the age of deposits, depth of occurrence and geological origin, the sulfur content in petroleum and its products varies strongly. [13] In crude oils and natural bitumen sulfur contents between 0.05% and 14% have been reported. [14] In a study of 9,000 crude oil samples an average sulfur content of 0.65% could be found, whereas the distribution is bimodal with a minimum at 1% sulfur content. [9] This minimum



can be used to classify crude oils into low-sulfur or sweet (sulfur content below 1%) and high-sulfur or sour material (sulfur content higher than 1%).

As elemental sulfur and dissolved hydrogen sulfide are only a minor class of the total sulfur, most of the sulfur is found in organic sulfur compounds. Those compounds range from low to high molecular weight. [14] In general, organic sulfur compounds can be classified in aromatic and aliphatic sulfur compounds and typical compound classes of both are displayed in figures 7 and 8.

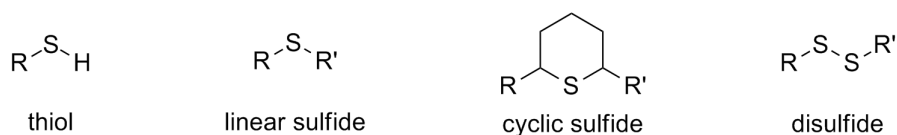


**Figure 7:** Typical non-thiophenic sulfur compounds.

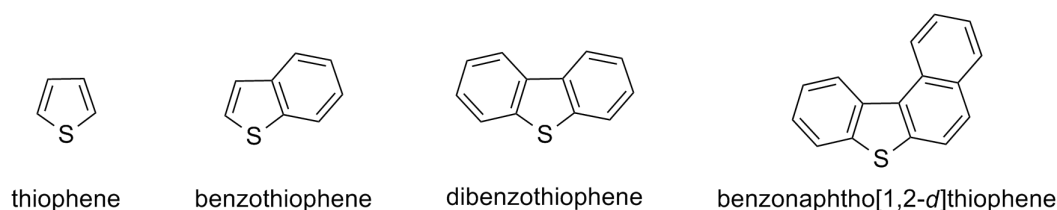


**Figure 8:** Typical thiophenic sulfur compounds (PASHs).

In addition to those compound classes, endless variations can be found. [13, 15] For some selected examples see figure 9: Different stages of hydrogenated PASHs (**1**, **2**), bridged or caged structures like thioadamantanes (**3**), cyclic sulfides with adjacent aromatic ring structures or aromatic S<sub>2</sub> compounds like thienothiophene derivatives (**9**) have already been described in the literature. During the aging of petroleum the distribution of the sulfur compound classes is shifted towards more highly aromatized structures. Immature oils still hold large amounts of non-thiophenic sulfur, whereas in mature oils mainly the more thermally stable condensed aromatic sulfur is present. [16] As chromatographic and physico-chemical properties can vary significantly between the classes of sulfur compounds, they can be separated by means of chromatography.

For the formation of organic sulfur compounds three major theories were proposed:

- **Biosynthesis:** The sulfur is incorporated into the hydrocarbon framework by a biosynthetic pathway. [17] This assumption is based on a common structural

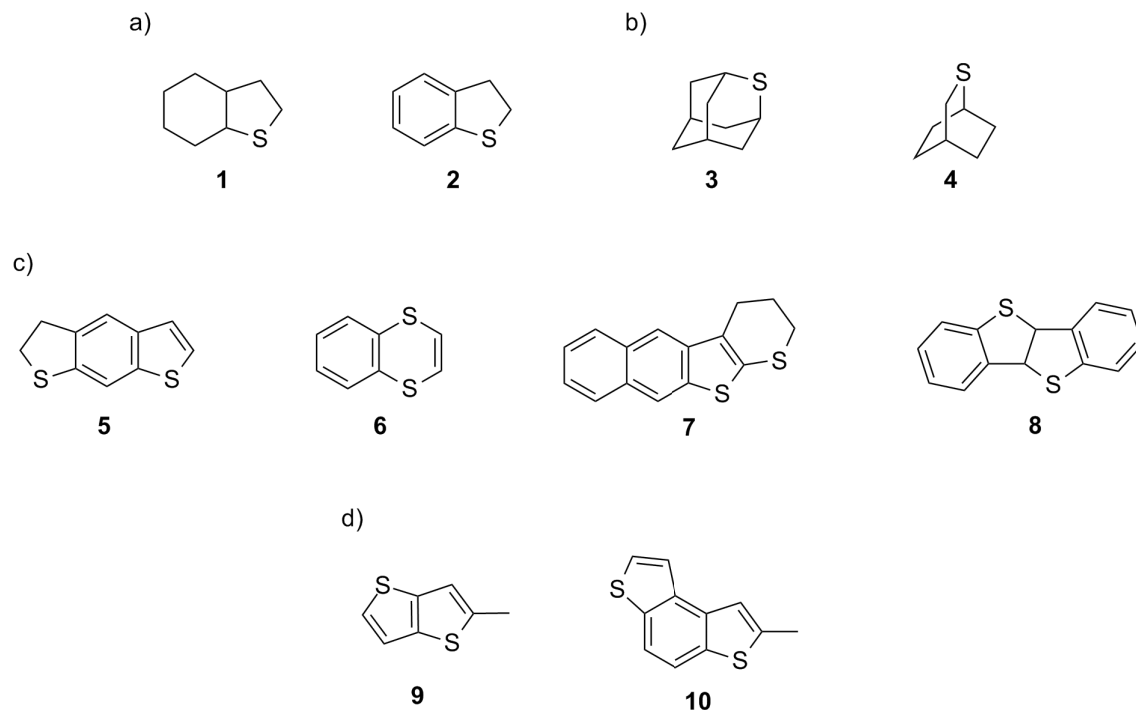


**Figure 9:** Other sulfur containing compounds in fossil fuels. [15]

a) (partially) hydrogenated PASHs, b) bridged sulfidic structures, c) aromatic-sulfidic sulfur hybrids, b) aromatic S<sub>2</sub> compounds.

feature of several bicyclic, tetracyclic and hopane sulfides, the position of the sulfur atom in the organic framework.

- **Formation during early diagenesis:** Inorganic sulfur species, like H<sub>2</sub>S<sub>2</sub>, HS<sup>-</sup> or HS<sub>x</sub><sup>-</sup> are incorporated into organic material. [18, 19]. The inorganic sulfur is provided through bacterial sulfate reduction. [20, 21]
- **Reaction of elemental sulfur with hydrocarbons:** Organic sulfur compounds originate during early maturation from the reaction of *n*-alkanes in the oil with elemental sulfur. [22] This assumption was supported by simulation experiments. [19]

DAMSTE et al showed that the reaction of hydrocarbons with elemental sulfur is not the major origin of sulfur containing compounds in sediments and immature crude oils by comparing distribution patterns of desulfurized organic sulfur compounds to the corresponding hydrocarbons. [19] It was found that the formation during early diagenesis is the most probable major origin of sulfur incorporation, as the intramolecular sulfur incor-

poration reactions can take place with suitable precursors at this time of the petroleum formation. [16, 19, 23] The proposed mechanism for the incorporation of sulfur is displayed in figure 10 and examples of sulfur compounds and their presumed precursors are given in figure 11. These intermolecular reactions also lead to the formation of higher molecular weight compounds and therefore might be a reason for the relatively high amount of sulfur containing compounds in high boiling fractions like asphaltenes.

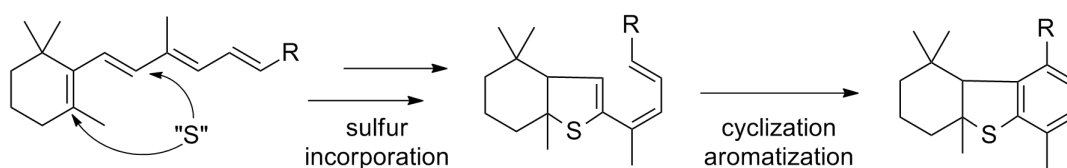


**Figure 10:** Proposed mechanism for the formation of sulfur containing compounds from terpenoids. [23]

When taking a look at the manifold compound classes displayed in figures 7 to 9, it is obvious that a distinction between thiophenic and non-thiophenic sulfur is not trivial and even identification of compound classes like sulfides and disulfides is difficult. Using mass spectrometry, only elemental formulas can be generated. For further distinction of the constitution of the molecule, chromatography is essential. Via group type separations the sulfur classes can be pre-separated and combined with the information gathered by MS-analysis possible structures can be proposed.

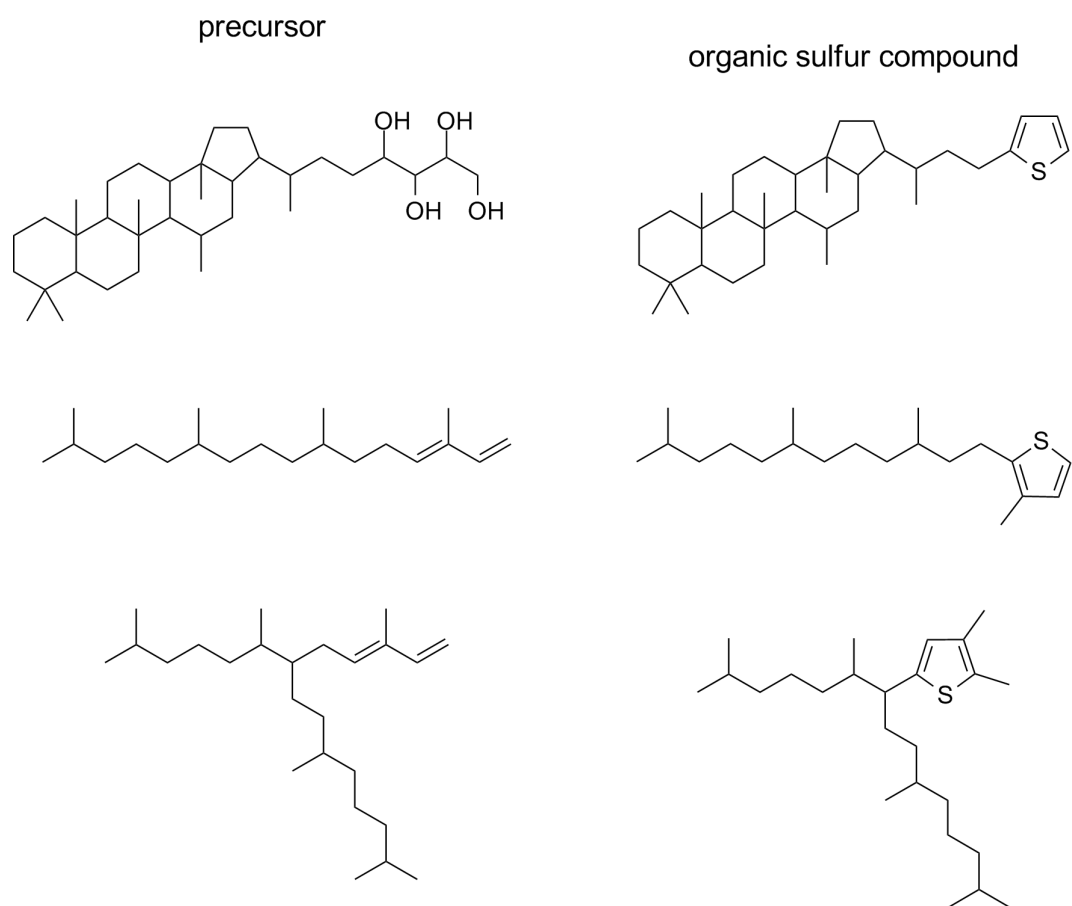


**Figure 11:** Examples of sulfur compounds and their presumed precursors. Top: bacteriohopanetetrol, middle: phyta-1,3-diene, bottom: a highly branched isoprenoidalkadiene. [16]

### 3 Scope of work

Until today no easy and robust determination of non-thiophenic and thiophenic sulfur in vacuum gas oils suitable for routine analysis is known.

The goal of this work is to develop a chromatographic separation for the determination of sulfides and disulfides in petroleum cuts, which is intended to be transferable to routine analysis in industry. Therefore, the method developed has to be robust, simple and easy to used without prior knowledge of the used techniques.

Within the means of metal treated ligand exchange chromatography stationary phases the separation of different sulfur species will be developed using standard substances and verified using several vacuum gas oils of different sulfur content and composition. The tested stationary phases vary in supporting material, the metal ion used to impregnate, the counter ion or the ligand binding the metal ion to the stationary phase.

Ultra high resolution mass spectrometry will be used to gain further insight into the composition of the samples. Therefore, various ionization techniques, as ESI, APCI, APPI and APLI will be applied to the separated fractions and the resulting mass spectra are compared after processing. Also, for the first time the newly developed palladium based ligand exchange chromatography phase is coupled to a ultra high resolution mass spectrometer. The differences between the phases used for open column chromatography and high performance liquid chromatography phases are also discussed. As a complementary technique GC x GC with sulfur chemiluminescence is also applied to the fractions separated in open column chromatography to further validate the results gained by mass spectrometry.

As the established methods are intended to be suitable for routine analysis in industry, the quality of the separations is also confirmed by establishing the recovery as well as mass and sulfur balance.

For disulfidic and sulfidic sulfur alternative routes for the determination of these compound classes are also tested, several originating from biochemical standard procedures. For disulfides often the reduction to thiols is needed for the subsequent derivatization, whereas sulfides are oxidized to sulfoxides to be isolated.

## 4 High resolution mass spectrometry (high res MS)

In mass spectrometry stable ions are separated and identified according to their mass-to-charge ratio ( $m/z$ ). Depending on the analytical problem the instrumental setup (see figure 12) may vary as there are many variations of ionization source, mass analyzer and detector. As these components are independent from each other, the three building

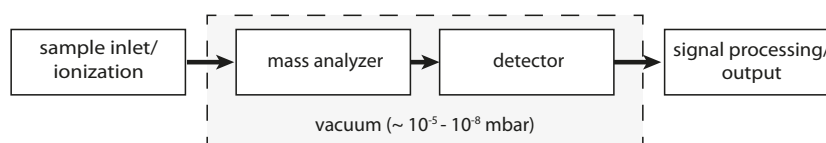


**Figure 12:** Schematic construction of a mass spectrometer. (based on [24])

blocks can be combined at will. For this work four different ionization sources, i.e. electrospray ionization (ESI), atmospheric pressure chemical ionization (APCI), atmospheric pressure photoionization (APPI) and atmospheric pressure laser ionization (APLI) were used:

**ESI:** In ESI the solution containing the analytes is passed through a charged capillary and dispersed by electrospray. While the solvent is evaporated, Coulomb fissions occur in highly charged droplets as repulsion increases. The size of droplets is reduced until free ions are present in the gas phase (see figure 13).

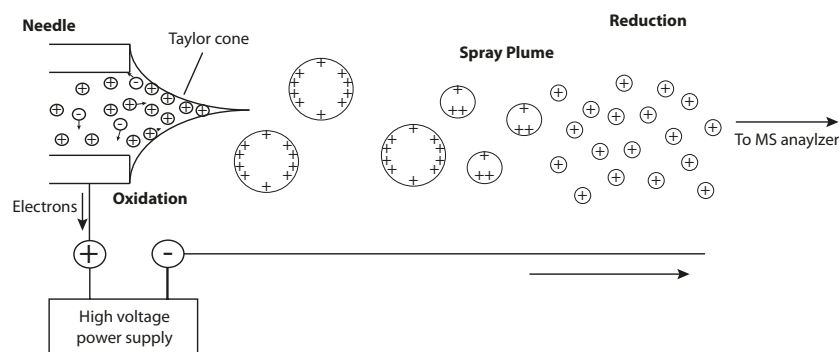


**Figure 13:** Schematic diagram of an ESI-source. (based on [25])

ESI is a very soft ionization technique. Molecules detected will usually be  $[M+H]^+$  or alkali metal adducts such as  $[M+Na]^+$  in positive mode and  $[M-H]^-$  in negative mode, respectively. Also multiply charged ions are possible. [26]

**APCI:** The main difference between APCI and ESI is that in APCI the solvent is evaporated before ionization. The solution of the analytes is introduced through a capillary and nebulized in a nitrogen stream. The sample is evaporated in a heating unit (300-400 °C). At a corona discharge needle ionization takes place (see figure 14). Solvent or nebulizer gas molecules are ionized first and are able to secondarily ionize the analytes by collision as displayed in figure 15.

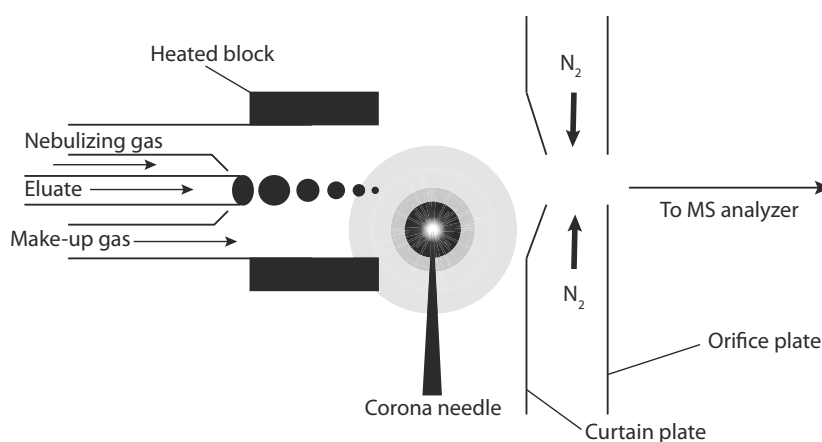


**Figure 14:** Schematic diagram of an APCI-source. (based on [27])

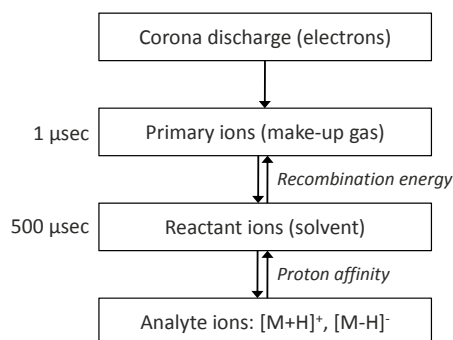


**Figure 15:** Diagram of the ionization mechanism in APCI. (based on [27])

APCI is a harsher ionization technique than ESI.  $[M+H]^+$  in positive and  $[M-H]^-$  in negative mode, respectively, are still the main occurring ions, but also fragmentation is possible. In contrast to ESI, APCI also allows higher flow rates up to  $600 \mu\text{L}/\text{min}$ [26].

**APPI:** Analogous to APCI, in APPI the solution of the analytes is nebulized and heated to high temperatures (300-400 °C). Instead of a corona needle, the ionization occurs by photons created by a UV source (see figure 16). [28, 29]

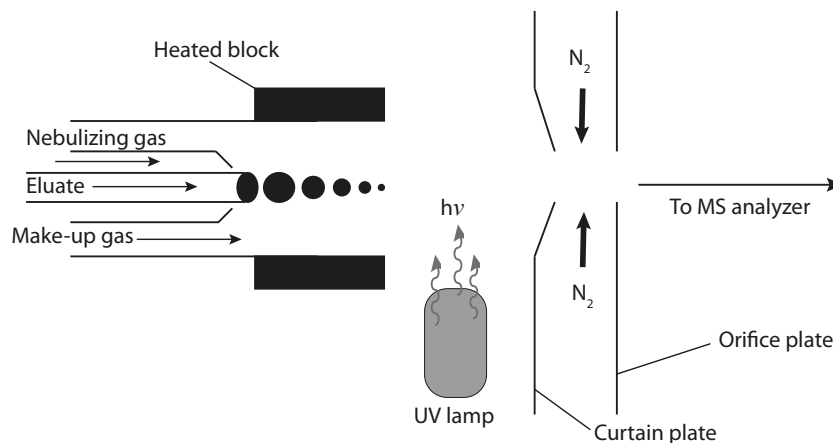
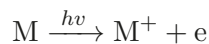
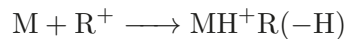


**Figure 16:** Schematic diagram of an APPI-source. (modified from [27])

The basic mechanism of ionization in APPI is therefore:



For molecules with low proton affinity the molecular ion  $M^+$  is actually observable, but the ion most frequently observable in APCI is typically  $MH^+$ . Therefore, chemical reactions have to occur after photoionization. The two general mechanisms proposed for the generation of  $MH^+$  from  $M$  are displayed in the following equations. [30]



Protonation by charge carrier  $R^+$



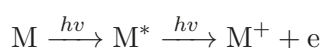
Hydrogen atom abstraction from a protic molecule  $P$

To increase the ionization efficiency of the analyte, often easily photoionizable compounds are used as dopants, e.g. toluene or acetone. [29] Concerning "softness", APPI is similar to APCI, as the conditions are very similar. In contrast to ESI some thermal degradation may occur. APPI is able to ionize less polar or even nonpolar compounds, but the analyte must be photoionizable. [31]



**APLI:** Mechanism and experimental setup for APLI are very closely related to APPI.

The ionization source setup is similar to the one displayed in figure 16, but instead of a UV lamp a laser is installed. Typically KrF\* or frequency quadrupled Nd:YAG lasers are used. In contrast to APPI, APLI is a multi photon ionization:[32–34]



In a first step the molecule is excited and when the excited molecule absorbs a second photon within its short lifetime of excitation, ionization occurs. Therefore, a high photon flux density of about 100 W/cm<sup>2</sup> is needed. Due to this two step excitation and ionization progress, APLI is a rather selective ionization technique and can only be applied to nonpolar and aromatic compound classes. Hence, it is ideal for the ionization of PAHs. If the analyte itself is not ionizable via APLI, a label molecule can be introduced via derivatization. This chromophore itself is then APLI susceptible and like in fluorescence labeling, the analyte is detected after derivatization.

With the ionization techniques available a wide field of analytes can be ionized. A scheme for the typical ranges of application for each technique is displayed in figure 17. In general the sulfur containing compounds present in petroleum are rather nonpolar compounds, with a wide range of molecular mass, also strongly depending on the boiling point of the respective VGO fraction.

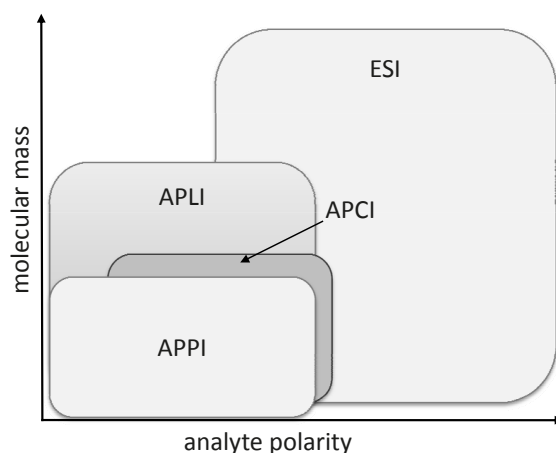


**Figure 17:** Polarity range of suitable analytes for the ionization with different mass spectrometric ionization techniques. (based on [31])

Therefore, techniques like APPI or APCI will be the ionization techniques of choice without further treatment, as ESI will be suitable only after the generation of thiophenium ions after methylation. For APLI aromatic ring systems are needed, therefore it may not be suitable for non-thiophenic sulfur compounds, but only for PASHs. But a comparison between the mass spectra recorded using APLI and other techniques like APCI might give detailed information about the aromatic character of the compounds present in the samples. Compounds ionizable with both APLI and APCI are more likely to be aromatic, whereas compounds with the same amount of double bond equivalents (DBE) only ionizable with APCI are most likely saturated and build up by naphthene rings. The intelligent and pointed combination of different ionization techniques therefore can be used to create a deeper insight into the sample composition.

#### 4.1 Orbitrap mass spectrometry

The Orbitrap mass spectrometer is the latest modification of an ion trap. In contrast to conventional ion traps like PAUL and PENNING traps, only electrostatic fields are used to confine the ions in the Orbitrap. The electrostatic attraction between the ions and the walls of the inner electrode is balanced by centrifugal forces, so that the ions circulate around the inner electrode in elliptical orbits (see figure 18).

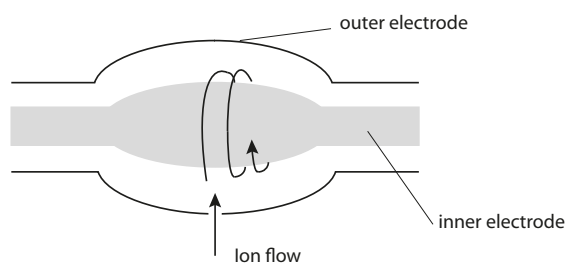


**Figure 18:** Scheme of an Orbitrap mass analyzer cell. (based on [35])

Commercially introduced in 2005, the Orbitrap analyzer consists of cup shaped outer electrodes facing each other and a spindle like electrode in the center. When a voltage is applied between these electrodes, a linear electric field is generated along the axis. Therefore, oscillations along the direction will be harmonic, whereas ions are attracted towards the central electrode by radial field components. [36] The injection takes place tangentially through a slot with a deflector electrode. When the field strength is chosen accordingly, the ions are kept on a nearly circular spiral inside the trap while, caused by the axial electric field, being pushed towards the widest part of the trap. These

axial oscillations are then detected by induction of an image current on the outer electrodes. The current is Fourier-transformed into the frequency domain and subsequently converted into mass spectra. [37]

With an optimized geometric design, the Orbitrap is reported to possess a maximum full width at half maximum (FWHM) resolving power of 350,000 at  $m/z$  524 and even 600,000 at  $m/z$  194 as well as a single-shot dynamic range of 25,000. [38] Also all Orbitrap instruments have a high mass accuracy of  $<2$ -3 ppm when used with an external and  $<1$ -2 ppm with an internal calibrant. [39]

## 4.2 Fourier transform ion cyclotron resonance mass spectrometry (FT-ICR MS)

In FT-ICR the  $m/z$  of an ion is measured by monitoring the cyclotron frequency of the ion in a static high magnetic field. To keep the ions in a defined space for the measurement, i.e. the measuring cell, a second electric field is applied axially.

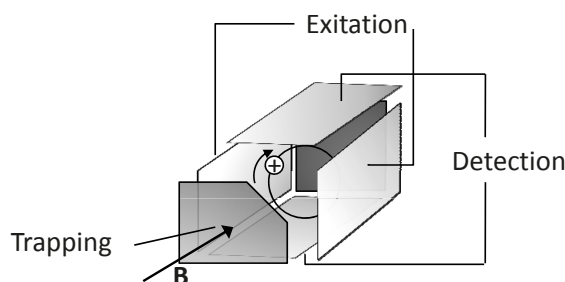


**Figure 19:** Scheme of a cubic FT-ICR mass analyzer cell. (based on [40])

As the FT-ICR was introduced in the 1970ies by COMISAROW and MARSHALL, [41] the instrumental setup has evolved since then. In addition to the cubic analyzer cell, displayed in figure 19, also cylindrical, end-caps segmented, open-ended and matrix-shimmed configurations of the ion trap are known in ICR. [40] In general, three kinds of electrodes are needed: excitation, detection and end capping, i.e. trapping of the ions. The high magnetic field and the trapping electrodes are used to confine the ions in the analyzer cell. As a result, the trapped ions rotate arbitrarily in the plane perpendicular to the magnetic field and are trapped in the center of the cell by the electric field of the trapping electrodes. To be able to detect the ions, the previously statistically distributed ions have to be synchronized in ion packages. This is done by exciting the synchronous cyclotron motion of the ions by applying RF voltage to the exciting electrodes of the

cell. [42] The now synchronized circulating ions induce image currents on the detection electrodes and the changes in the potential of the detection electrodes are recorded and again processed after Fourier-transformation, analogous to the Orbitrap.

The magnetic field strength  $B$  also influences several ICR performance parameters. As the ICR frequency is directly proportional to  $B$ , an increase of  $B$  also increases the resolution for example. The angular cyclotron frequency  $\omega$  of an ion of the mass  $m$  and charge  $q$  in a magnetic field  $B$  is expressed by:

$$\omega = \frac{q}{m} B$$

Mathematical relations of the first derivative with respect to  $m$  directly lead to the mass resolving power  $m/\Delta m$ :

$$\frac{m}{\Delta m} = \frac{qB}{m\Delta\omega}$$

Several other parameters like upper mass limit, maximum number of trapped ions, signal-to-noise ratio, dynamic range, mass accuracy, and more are also depended on the magnetic field strength, therefore magnets with increasingly higher field strength are developed. In June 2014 the first 21 T magnet was installed in a FT-ICR system. [43]

For FT-ICR instruments the dynamic range for a single-shot analysis is significantly higher than for the Orbitrap, but limited to 50,000. [44] Broadband measurements of ions of  $200 < m/z < 1000$  detected simultaneously showed a FWHM resolving power of 300,000 at 9.4 T, [40] but also resolving powers of 1,200,000 at  $m/z$  400 and 12 T have been reported. [45] The mass accuracy of FT-ICR instruments is very high, reportedly less than 0.5 ppm even for highly complex samples. [46].

Comparing FT-ICR with Orbitrap it is clear that FT-ICR is able to achieve higher resolving powers due to the development of magnets with higher field strength. But depending on the analytical problem Orbitrap MS might be sufficient for the detection of compounds of interest, especially in combination with chromatographic pre-separations. A comparison of physical and analytical features of the two techniques as well as a diagram showing the resolving power of the instrument as a function of  $m/z$  are displayed in figures 20 and 21, respectively.

Especially when taking a look at the resolving powers of the different instruments, it is obvious that for some ranges of  $m/z$  a conventional FT-ICR mass spectrometer has no great advantage over an Orbitrap mass spectrometer, whose measurements are considerably cheaper due to the lack of the magnet and which is more widespread in institutions.

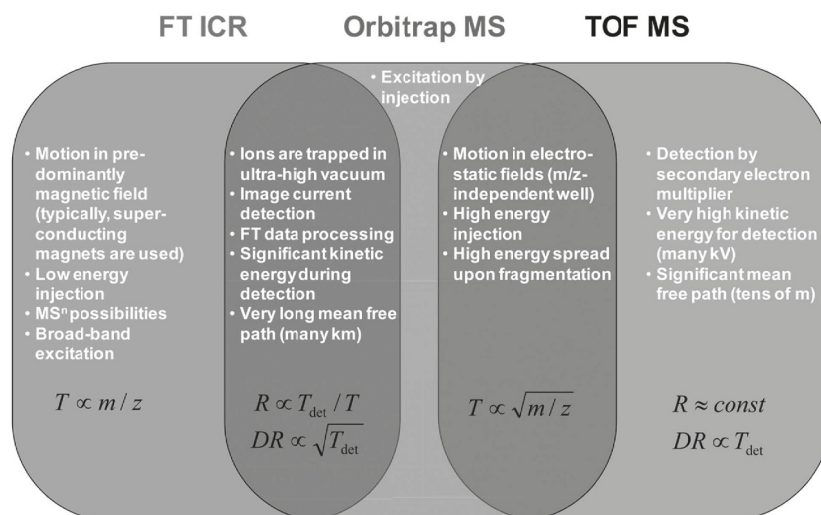


**Figure 20:** Comparison of physical and analytical features of different high resolution mass spectrometers. [37]

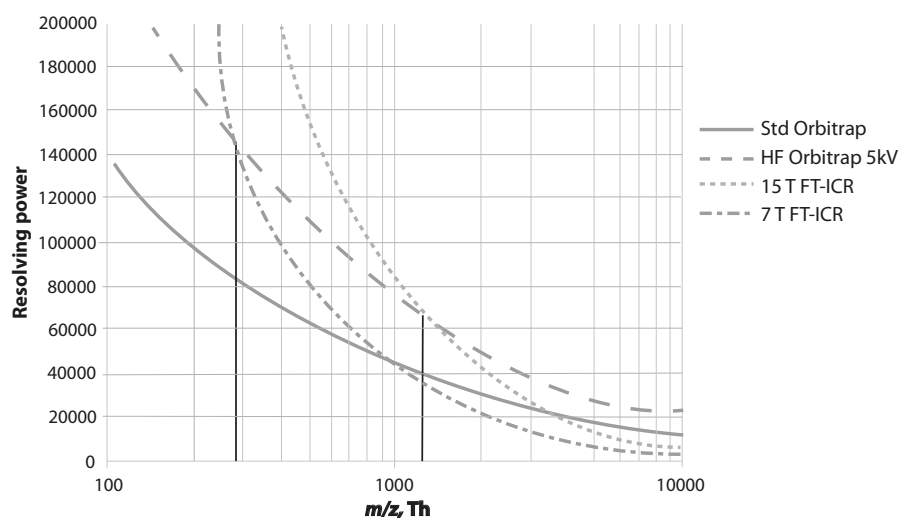


**Figure 21:** Resolving power as a function of  $m/z$  for different high resolution mass spectrometers. (based on [38])

### 4.3 Graphical methods for data interpretation

As a high resolution mass spectrum of crude oils contains several 10,000 peaks, it is often hard to interpret. [47] In addition to the actual compound peaks, various ionization techniques also generate multiple ions of one analyte, e.g. radicals or adducts. Therefore data interpretation is indispensable. The advancing development of computational data analysis has made statistical and graphical interpretations possible.

### 4.3.1 Kendrick plots

Developed by Edward KENDRICK[48], the Kendrick mass is often used to identify homologous series of compounds. To calculate the Kendrick mass of a given molecule, its exact IUPAC mass is divided by a constant. When dealing with hydrocarbon structures, often the CH<sub>2</sub> fragment is used. Therefore, the nominal mass of CH<sub>2</sub> is divided by its exact mass:

$$\text{Kendrick mass} = \text{IUPAC mass} \cdot \frac{14.00000}{14.01565}$$

Alternatively, the Kendrick mass can be normalized for other functional groups or building blocks like O, N, H<sub>2</sub>O or COO<sup>-</sup>. The huge advantage of using Kendrick masses is that molecules of similar structure, e.g. homologous series, can be easily identified, as their peaks always differ by an integer multiple of 14 Da. The Kendrick mass defect (KMD) can easily be calculated from the Kendrick mass:

$$\text{Kendrick mass defect} = \text{nominal mass} - \text{exact Kendrick mass}$$

For the Kendrick mass analysis, the Kendrick mass defect is plotted against the nominal Kendrick mass (see figure 22). The so generated plots easily give an overview over

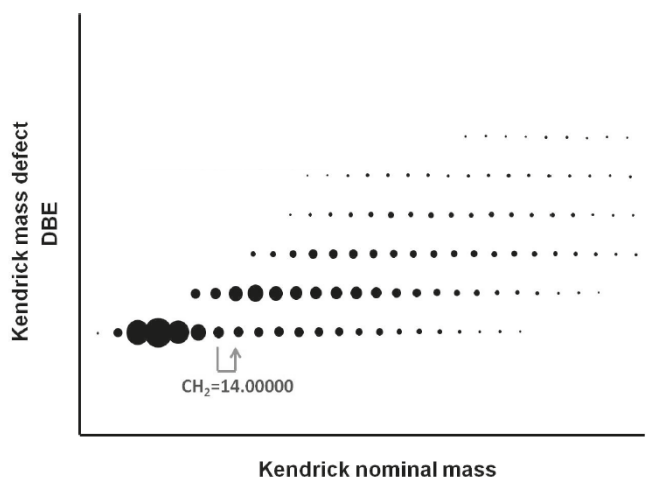


**Figure 22:** Showcase example of a Kendrick plot. [49]

complex spectra: along one horizontal line in the plot, ions with the same Kendrick mass defect, but different Kendrick masses are lined up, e.g. an homologous series of alkyl substituted compounds. When moving to higher Kendrick mass defects, the

degree of saturation decreases, e.g. ring closure occurs or double bonds are added. By reflecting the abundance of the peaks in the mass spectra by the size of the dots used in the Kendrick plot, another dimension can be added to the display.

Nowadays often a modification of Kendrick plots is used to visualize mass spectra. Instead of the Kendrick mass defect and Kendrick nominal mass, often double bond equivalents (DBE) and exact mass are used. As the Kendrick mass defect is proportional to the degree of saturation, i.e. the double bond equivalent, this change can easily be made. One advantage of using the DBE instead of the KMD is that the aromaticity of the analytes becomes directly visible in the plot.

### 4.3.2 Pseudograms

For some analytical questions even Kendrick plots might have a high complexity. To further simplify the data, PANDA developed the so called pseudograms. [50] In these diagrams the intensities of one horizontal line of the Kendrick plot is plotted against the Kendrick or exact mass. The resulting visualization resembles a gas chromatogram and is used to compare mass distributions of single double bond equivalents or to visualize dominance within different double bond equivalent ranges.

To get an overview of the different visualization techniques, figure 23 shows the correlation between mass spectrum, Kendrick plot and pseudogram.

### 4.3.3 Box plot modification

Due to the large amount of data acquired, even Kendrick plots can get very complicated, especially when comparing different fractions of one separation or several single separation with each other. Therefore, box plots were modified to summarize the information in a Kendrick plot.

Traditionally, box plots are used in statistics to illustrate large data sets by depicting groups of data through quartiles, i.e. 25% of the data points. The upper and lower quartiles are not included in the box, but displayed as whiskers. Box plots are a useful tool to visualize variability and distribution, as the spacing of the different parts of the diagram is directly connected to the degree of dispersion of the data points.

To use box plots for the visualization of Kendrick plots, instead of the second and third quartile for the extension of the box, the DBE ranges of the main intensities were chosen. The DBE with signals with relative intensities of 50% were picked as a threshold value. The whiskers now indicate the maximum range of the DBE distribution. An example

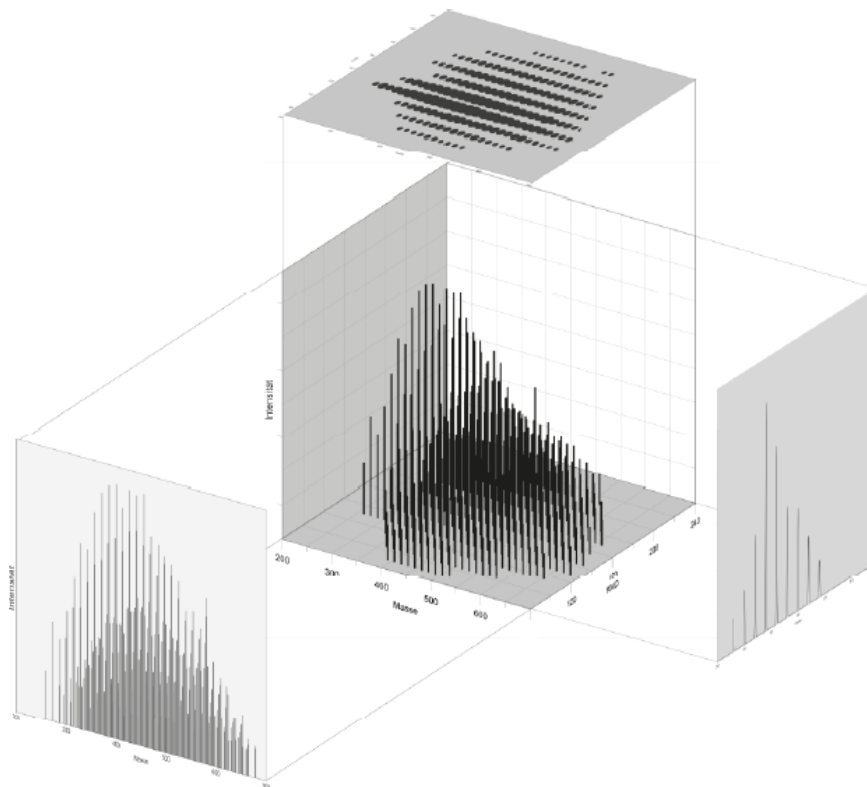


**Figure 23:** Relation between different kinds of visualization. Middle: 3-dimensional data set, bottom-left: mass spectra, top: Kendrick plot, right: pseudogram[51]

for the conversion of a Kendrick plot to the corresponding box plot is displayed in figure 24.

Apparently, the main information of the DBE distribution from the Kendrick plot is indicated in the box plot. Information about the C-atom number distribution will get lost during conversion, but in this work for the distinction between thiophenic sulfur compounds, being mainly of highly aromatic character, and non-thiophenic sulfur compounds, being mainly of low or no aromatic character, the DBE distribution is the main tool to analyze the sulfur class at hand.



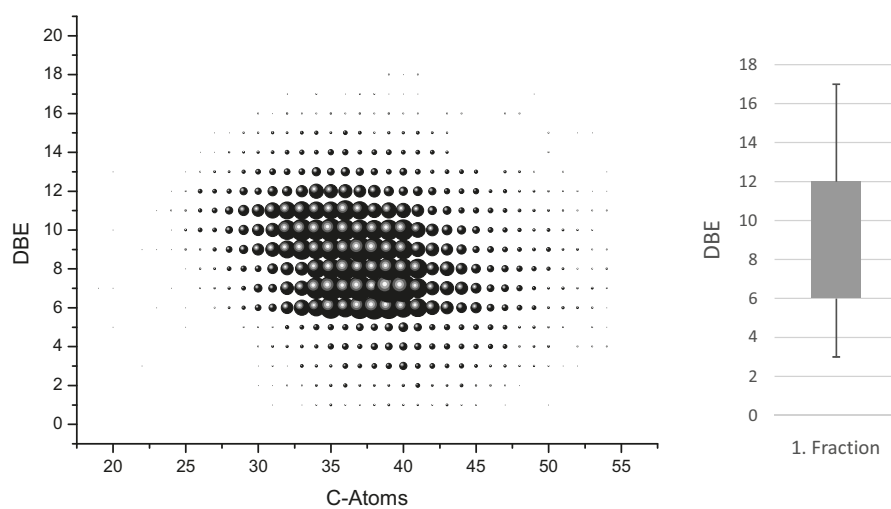


**Figure 24:** Comparison between Kendrick plot and box plot.

Displayed are the S1 compounds of the 1. fraction of the separation of Albacora Leste 369-509 °C on PdSO<sub>4</sub>-Alox. Left: Kendrick plot, right: box plot.

## 5 Ligand exchange chromatography on metal ion treated stationary phases

The term ligand exchange chromatography (LEC) was first introduced by HELFFERICH in 1961. [52] The main difference to conventional adsorption or ion exchange chromatography is the interaction of the analyte and the coordination sphere of the complexed metal ion instead of an interaction of the analyte and the surface of the stationary phase, as found in conventional normal phase chromatography. [53] For a starting point to choose possible metal ions for LEC, PEARSON's HSAB concept can be considered (HSAB: Hard and soft acids and bases [54]). But to ensure the ligand exchange is still possible, the resulting complexes of analyte and metal ion must not be kinetically inert. Too strong interactions would lead to irreversible binding of the analyte to the stationary phase, therefore the metal ion and the analyte should have similar 'softness' or 'hardness', but not be too similar.

As the separation abilities of the phase strongly depend on the metal ion used, LEC is easily modifiable and tunable to the specific need of the chromatographic problem.

As analytes a wide range of anions or neutral molecules are suitable for LEC. Free electron pairs and electron donor properties are the main requirements for those ligands, therefore a wide field of organic molecules, i.e. amines, alcohols, acids or sulfides, can be analyzed by LEC and even compounds that do not form complexes on their own, like ketones, ethers or esters are separable, as they can undergo  $\pi$ -interactions with the electron gap of the metal ion. Thus, LEC is a useful tool for many analytical problems in organic chemistry and biochemistry.

### 5.1 State-of-the-art: LEC for the analysis of sulfur containing compounds

In the literature various approaches for the usage of LEC for the separation of sulfur containing compounds can be found.

#### Copper containing phases

Aryl and alkyl sulfides could be separated from aromatic hydrocarbons on a copper ion loaded cation exchange resin. [55] After a pre-separation on an alumina and silica gel column, the aromatic fraction was loaded on the copper ion loaded cation exchange resin. The phase strongly adsorbed sulfides from a pentane solution, while hydrocarbons were eluted in the order of the increasing number of aromatic rings. Subsequently, the sulfides were recovered by backwashing the column with a mixture of pentane and ethyl

ether. All sulfides could be recovered without loss and the method was applicable to a wide range of molecular weight, making it suitable for high boiling samples as well.

Copper(II) 2-amino-1-cyclopentene-1-dithiocarboxylate (ACDA) bound to silica gel has also been used for the separation of dialkyl sulfides. [56] The retention of the sulfides was affected by the length of the alkyl chain and the degree of branching. The more branched sulfides could be eluted earlier than the linear sulfides. When treating the ACDA silica gel with silver ions instead of copper, the separation of the sulfides was still efficient, but the elution order of the di-*n*-alkyl sulfides was reversed compared to the copper treated phase.

For the isolation of aliphatic sulfur compounds from crude oils, also copper chloride treated silica gel was applied. [57] Due to their higher nucleophilicity, aliphatic sulfur compounds were bound more strongly to the phase and could be recovered by elution with a mixture of chloroform and ethyl ether. The interaction of alkyl disulfides with the stationary phase was found to be weaker than the interaction of the corresponding sulfides. Thus, significant amounts of the disulfides were already eluted in early fractions of the separation.

Also copper based metal-organic frameworks (MOFs) have been reported for the adsorption of sulfur containing compounds in liquid fuels. [58] The commercially available MOF Basolite C300, based on copper(II) benzene-1,3,5-tricarboxylate, was used to adsorb dibenzothiophene. It was found that the interactions between the sulfur atom and the surface of the framework were stronger for copper based MOFs than for iron and aluminum based MOFs due to bonding of the sulfur to the metal and  $\pi$ -complexation of the analyte. For a set of PASHs, a selectivity ranking was determined as: 4,6-dimethyl dibenzothiophene > 4-methyl dibenzothiophene > dibenzothiophene > benzothiophene. As the MOFs in this study were only used for the adsorption, no data about the possible release of the sulfur containing compounds was presented. In a different study concerning the adsorption of sulfur containing compounds on MOFs, it could be shown that these materials are regenerable at 373 K by using small volumes of *n*-octane or toluene. [59]

### Silver containing phases

For the analysis of crude oils, also silver nitrate coated silica gel was used to separate sulfides after several pretreatment steps. [60] After deasphalting, a crude oil sample was separated on silica gel and the "apolar" fraction, eluted with ethyl acetate in hexane, was further separated on the silver coated silica gel. This phase was prepared by suspending silica gel in a water/ethanol solution of silver nitrate and subsequent activation at 140 °C.

The apolar fraction was separated into a hydrocarbon and a sulfidic fraction on the silver phase and the obtained fractions further analyzed using GC-MS.

Also silver nitrate coated silica gel was applied to the separation of thiaadamantanes from Chinese oil samples. [61] For the preparation, silver nitrate was dissolved in water and silica gel was added. After drying at 120 °C, the phase was used to collect two fractions. The thiaadamantanes were eluted with a mixture of dichloromethane and methanol and subsequently characterized using GC-MS and GC-MS/MS.

An alternative preparation of a silver coated silica gel was described by VIVILECCHIA et al. [62] Silica gel was first deprotonated by washing the column with sodium hydroxide and then coated with silver ion by passing a solution of silver nitrate in methanol through the column. After further washing and drying steps, a golden-yellow to golden-brown material could be gained. The material was successfully applied for the separation of PANCs in crude oil samples.

Instead of silica gel, also titania has been applied for the preparation of stationary phases for the adsorption of sulfur containing compounds. [63] Titania was treated with an aqueous solution of silver nitrate and calcinated at 450 °C to generate this stationary phase. The phase was treated with dibenzothiophene in octane and the PASH was adsorbed efficiently. Regeneration took only place at 525 °C, making this phase more suitable for deep desulfurization than for chromatographic purposes.

### **Palladium containing phases**

Also palladium chloride LEC has been used to separate sulfur containing compounds. NISHIOKA used palladium chloride coated silica gel to separate a crude oil sample into PAHs, PASHs and other types of aromatic sulfur compounds, e.g. aromatic sulfides. [64] This early palladium phase separation did not properly distinguish between PAHs and PASHs, so that both fractions were eluted with the same solvents, a mixture of chloroform and hexane. The remaining aromatic sulfur compounds were eluted using a mixture of chloroform and ethyl ether as an eluting solvent. Besides aromatic sulfides, also aromatic disulfides, dithianes and thianthrenes could be shown to be recoverable on this LEC phase, but only partially as some portion of these analytes remained on the column.

Bigger ligands to bind the palladium, like ACDA have also been successfully used to separate PASHs and sulfides in fossil material. [65] The chelating ACDA ligand was introduced to reduce column bleeding by binding the metal ion to the stationary phase more strongly. PAHs were eluted using hexane as a mobile phase, whereas the PASHs

could be released from this phase either by addition of isopropanol or by back flushing the column with hexane. However, for more complex samples like vacuum residue, sulfur compounds were found to elute too early in previous fractions. [66] Furthermore, sulfides were partially retained on the phase as well.

Mercaptopropyl silica gel (MPSG) is another modification of the palladium coated silica gel used for the analysis of sulfur containing compounds in crude oils. [67] In contrast to the previously described ACDA phase, the synthesis is much simpler and MPSG is even commercially available as a scavenger for various metals. This phase was reported to separate a crude oil into a PAH, a PASH and a sulfidic fraction, whereas the PASHs can be released by the addition of isopropanol as a competitive ligand. For the elution of the sulfides, the addition of isopropanol saturated with ammonia is necessary. The strong interaction of the sulfides makes them only partially recoverable and the addition of the strong competitive ligand ammonia drastically reduces the reusability of the phase, as conditioning is difficult.

Furthermore, 8-hydroxyquinoline silica gel impregnated with palladium chloride has also been used for the isolation and determination of PASHs from crude oils. [68] After a pre-separation on silica gel into an aliphatic and aromatic fraction, the aromatic fraction was further separated into PAHs and PASHs by an 8-hydroxyquinoline silica gel, coated with palladium chloride. The PAH fraction was eluted with a mixture of cyclohexane and dichloromethane, while addition of isopropanol as competitive ligand yielded the PASHs in a separate fraction.

### **Other metal containing phases**

Silica gel coated with nickel chloride has been applied to isolate sulfur containing compounds from deasphalted crude oil samples. [69] PASHs and sulfides could be concentrated and were eluted using benzene. Disulfides were not found in any of the low-, medium- and high-sulfur samples used in this study.

LEC can also be used as stationary phase in gas chromatography. Nickel and zinc treated liquid crystals based on 4-decanoyldithiobenzoic acid as stationary phase in GC were used to separate PASHs and dialkyl sulfides. [70] The nickel mesophase was more stable over a wider temperature range (140-230 °C, compared to 137-173 °C for the zinc phase). In addition to vapor pressure and polarity of the compounds, molecular geometry of the analytes was found to strongly affect the retention on the phases. Using standard substances, it could be shown that the nickel phase is able to separate PAHs, whereas the zinc based phase is able to separate dialkyl sulfides.

For the enrichment of sulfides and thiols in water samples, also metal-loaded cation exchange materials have been used. [71] Tin, lead, copper and silver salts were tested for the loading of the cation exchange resins. For that purpose, commercially available cation exchange cartridges were loaded with the respective metal ions by passing an aqueous solution of the corresponding salts through the cartridge. After washing, standard compounds in a methanolic solution were applied. To elute the analytes, several solvents were tested, including toluene, acetonitrile, chloroform and dichloromethane. Cartridges loaded with tin ions were found to form the weakest bonds, whereas strong interactions were observable for lead, silver and copper treated cartridges. In fact, the bonds formed between silver and copper ions and the analytes were that strong that not all analytes could be recovered. Therefore, the best results could be obtained using lead ion treated cation exchangers.

### **Studies about various metal containing phases**

Various metal salts, i.e. mercury acetate, silver nitrate, zinc chloride, cadmium acetate and copper acetate, were applied to TLC plates and used for the separation of sulfur containing compounds in high boiling petroleum cuts. [72] The supporting material of the TLC phases was either silica gel or alumina. *N*-hexane was used as a developing solvent. Mercury and silver salts were found to be efficient for the sulfur class separation, thus a mercury loaded silica gel was applied to the separation of a Kuwaiti crude oil. Thiols, sulfides and disulfides could be separated from PAHs on TLC plates and the sulfides were subsequently identified using mass spectrometry.

Alkyl phenyl sulfides with varying length of the alkyl chain and degree of branching were separated on TLC plates treated with mercury, silver, cadmium and lead salts. [73] The best separations could be achieved with mercury and silver salts in solvents of a moderate polarity. The solvents used to develop the plates were chloroform or ethyl acetate. Silver, mercury and lead were found to increase the retention of the sulfides compared to untreated TLC plates, whereas no change in retention was observable for the tested cadmium coated phases. Silver and mercury were especially well suited for the separation of the individual alkyl phenyl sulfides, as retention factors differed most, when separating the analytes on this phases.

Thiols, which are easily retained on most stationary phases, were separated on LEC phases based on  $\beta$ -hydroxydithiocinnamic acid and its ethyl ester, that were treated with copper, cadmium and mercury ions. [74] The synthesized chelating resins were suspended in a solution of the metal salt in water and an acetic acid-sodium acetate buffer. After

drying, the material was packed into HPLC columns. Standard compounds were used for breakthrough studies and chromatographic separations. For the separations, buffered solutions and acetonitrile were used as mobile phases. The best results were achieved on the  $\beta$ -hydroxydithiocinnamic acid ethyl ester stationary phase treated with copper, as it was the most hydrophobic phase tested.

The separation of sulfur compounds in vacuum gas oils was also tested on LEC phases using copper, silver, mercury and palladium ions by GHALOUM et al. [75] Silica gel was treated with aqueous solutions or solutions of the particular metal salts in dichloromethane and activated at 200 °C after drying. VGO samples were pre-separated using activated alumina and the aromatic fraction subsequently further separated on the LEC phases. Repeatability, mass and sulfur balance and further characterization of the sulfur compounds by elemental analysis was performed. The order of efficiency of the LEC phases in separating sulfur containing compounds was described as: palladium chloride (in water) > silver nitrate > mercury chloride > copper sulfate > palladium chloride (in dichloromethane).

Palladium chloride, iron chloride, copper sulfate, silver nitrate and tin chloride were used in LEC for the separation of sulfur compounds in a Kuwaiti diesel.[76] To compare the effectiveness, three different supporting materials were tested, two silica gels with different particle sizes and alumina. Three fractions were collected. Whereas for tin, silver and palladium phases two fractions containing sulfur compounds were observable, as some sulfur species could be retained more strongly, on iron and copper coated phases all sulfur containing compounds were eluted in one fraction without further distinction.

The studies vary in the results for the quality of the separation on LEC phases based on some metal ions, like zinc, which is in some studies reported as being efficient for the separation of sulfur compounds and in some as not. But palladium and silver based stationary phases were reported to be efficient for the separation of sulfur containing compounds in all studies.

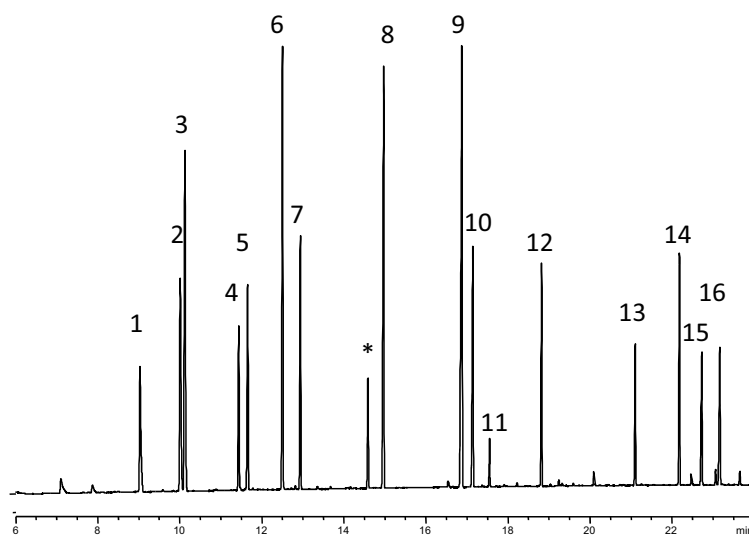
When analyzing disulfides, which were not further considered in many of the studies, the reducing ability of transition metal should be considered. Platinum, copper, mercury, cobalt as well as their salts and complexes, for example, are reported to be able to cleave the disulfide bond. [77–80] Therefore, many LEC phases, suitable for the separation of sulfides and PASHs, might not be applicable to the separation of disulfides, but result in a cleavage of the disulfide bond. The resulting thiolate or thiol species interact very

strongly with nearly all stationary phases and are therefore retained irreversibly. This could be one of the reasons why no phase for the separation of disulfides and sulfides in fossil material has been described yet.



## 6 Metal based LEC phases for the separation of sulfur containing compounds

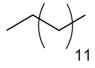
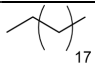
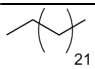
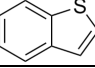
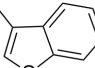
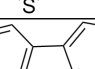
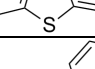
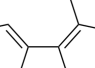
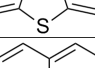
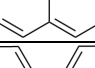
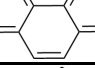
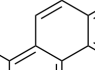
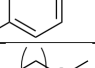
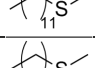
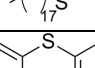
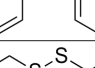
In this work, several metal salts were used to create LEC stationary phases based on silica gel, alumina and titania. The synthesis of the phases can be found in section 10.1. The metal salts were chosen according to known thiometalates in the literature. [81–84] As crude oil is a supercomplex mixture, the separation was first tested with standard substances for all tested metal phases. Therefore, typical candidates of the different group types were chosen and standard solutions of 1 mg/mL were prepared. The group types include alkane, PAHs, PASHs, sulfides and disulfides. For sulfides and disulfides both aromatic and aliphatic standards were chosen, as the aromatic ring system can strongly influence the interaction of an analyte with the stationary phase as many LEC phases are able to interact with  $\pi$ -electrons. Also the variation in the electron density at the sulfur atom between aromatic and non-aromatic sulfur compounds can effect the chromatographic behavior. The standards used are displayed in table 2 and the GC-FID chromatogram of a standard mixture is shown in figure 25.



**Figure 25:** GC-chromatogram of the standards used for the evaluation of LEC phases:  
1: *t*-butyl disulfide 2: naphthalene, 3: benzothiophene, 4: *n*-butyl disulfide, 5: 3-methyl-benzothiophene, 6: tetradecane, 7: dodecyl methyl sulfide, 8: phenyl sulfide, 9: dibenzothiophene, 10: phenanthrene, 11: phenyl disulfide, 12: eicosane, 13: octadecyl methyl sulfide, 14: tetracosane, 15: benzonaphtho[1,2-*d*]thiophene, 16: chrysene, \*: contamination.

**Table 2:** Used standard substances.

Number was chosen according to the elution order of the compounds in GC-FID.

Group type	Substance	Structure	N°
alkanes	tetradecane		6
	eicosane		12
	tetracosane		14
PASH	benzothiophene		3
	3-methylbenzothiophene		5
	dibenzothiophene		9
	benzonaphtho[1,2-d]thiophene		15
PAH	naphthalene		2
	phenanthrene		10
	chrysene		16
sulfides	dodecyl methyl sulfide		7
	octadecyl methyl sulfide		13
	phenyl sulfide		8
disulfides	<i>n</i> -butyl disulfide		4
	<i>t</i> -butyl disulfide		1
	phenyl disulfide		11

To obtain comparable results, the separations were performed using the same eluting solvents for each LEC phase. The choice of solvents was based on separations of sulfur

containing compounds in literature [67] and previous experiments. [85] The used method is described in section 10.1.14.

As more than thirty different stationary phases were tested, the results of the separations are summarized in the appendix (see tables 14-17). Ten of the tested phases, including cadmium chloride, lead nitrate, manganese chloride and copper nitrate silica gel as well as cadmium acetate and vanadium chloride alumina, showed no separating abilities for the given analytes at all. No retention of any of the standards could be noted. On the other hand, several phases interacted too strongly with some of the analytes, generally the disulfidic standards. On thirteen of the tested stationary phases at least some disulfides were retained irreversibly, whereas aromatic disulfides could be recovered more often than aliphatic disulfides. For sulfides this problem was less immanent. Only on five of the phases some sulfides could not be recovered, of which two retained only aromatic sulfides (silver nitrate titania and copper acetate silica gel) and three only aliphatic sulfides (copper(I) chloride silica gel, vanadium chloride alumina and commercial available  $\text{Ag}^+$  cartridges).

The results for the phases with the best performance will be discussed in detail in the following sections.

### 6.1 Separation on zinc chloride silica gel

The first phase to be discussed is zinc chloride silica gel. As during the separation of the standard solution all analytes can be recovered in the first two fractions, the third fraction is left out for clarity, when displaying the results in figure 26.

The zinc chloride silica gel phase is able to isolate aromatic non-thiophenic compounds from the standard mixture. Alkanes, PASHs, PAHs and aliphatic sulfides and disulfides are not retained and elute in the first fraction. However, in the second fraction phenyl sulfide (**8**) and octadecyl methyl sulfide (**13**) can be eluted. The selectivity of this phase is remarkable, as thiophenic and sulfur-free aromatics and also aliphatic non-thiophenic sulfur are not retained. Selectivity for sulfur or interactions with  $\pi$ -electrons do not seem to be the separation mechanisms for this phase.

Also the elution of the standard compounds seems to be at least partially incomplete, as the ratio of the peak heights of the individual peaks is changed. In the second fraction the intensity of the phenyl sulfide (**8**) is weaker than the one of the octadecyl methyl sulfide (**13**), whereas the aliphatic sulfide was the more dominant one in the standard solution. Therefore the aromatic sulfide must be partially retained on the stationary phase.

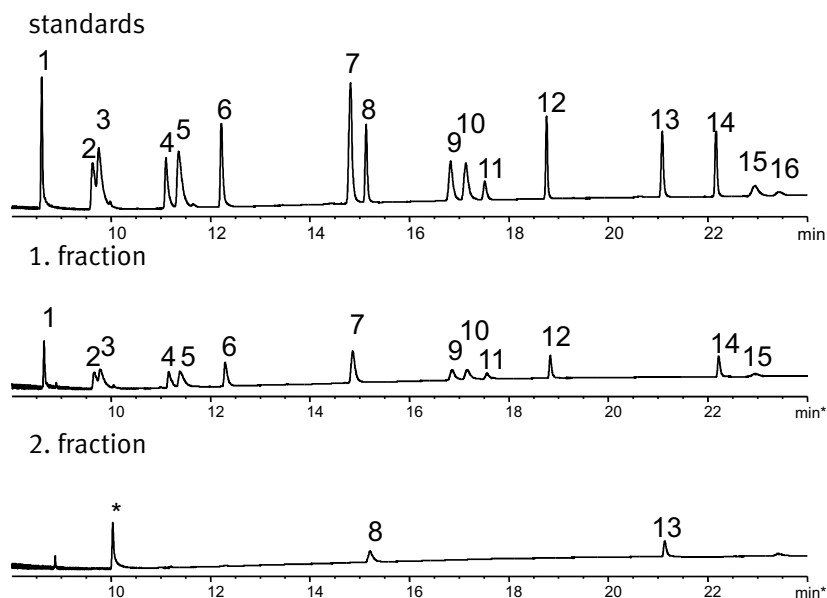


**Figure 26:** GC-FID chromatogram of the standard separation on zinc chloride silica gel.

Elution: 1. fraction: cyclohexane, 2. fraction: cyclohexane:dichloromethane 2:1.

1: *t*-butyl disulfide 2: naphthalene, 3: benzothiophene, 4: *n*-butyl disulfide, 5: 3-methylbenzothiophene, 6: tetradecane, 7: dodecyl methyl sulfide, 8: phenyl sulfide, 9: dibenzothiophene, 10: phenanthrene, 11: phenyl disulfide, 12: eicosane, 13: octadecyl methyl sulfide, 14: tetracosane, 15: benzonaphtho[1,2-*d*]thiophene, 16: chrysene, \*: contamination.

Zinc chloride silica gel could therefore only be used to isolate aromatic non-thiophenic sulfur to a limited extent, but as the double bond equivalents of the non-thiophenic fractions of real world samples show, many non-aromatic non-thiophenic sulfur compounds are present in crude oils (see sections 7.1.4 and 7.4). Hence, the zinc chloride silica gel is not suitable for the analysis of the total non-thiophenic sulfur, as aliphatic compounds cannot be separated from other compound classes, because they are not retained on the phase strongly enough.

## 6.2 Separation on chromium sulfate silica gel

When the standard solution is separated on chromium sulfate silica gel, all analytes can be recovered in the first two fractions. For clarity, the third fraction is therefore left out when displaying the results in figure 27.

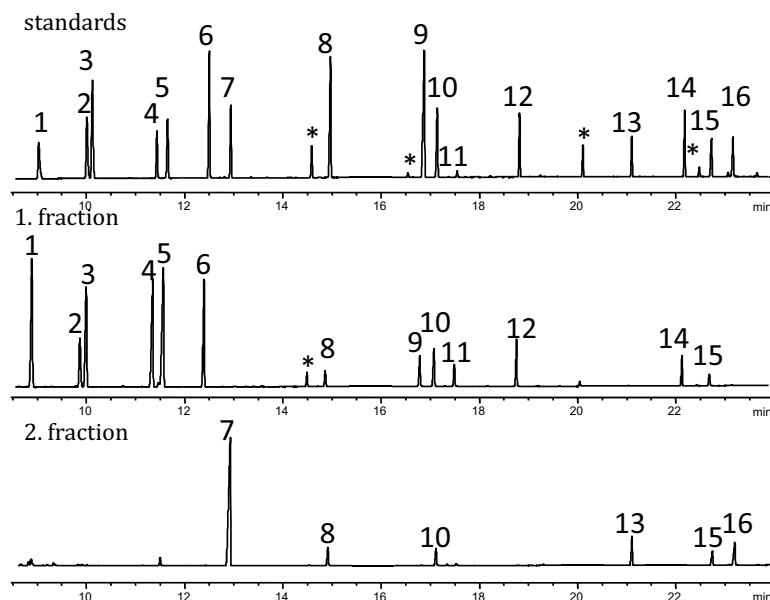


**Figure 27:** GC-FID chromatogram of the standard separation on chromium sulfate silica gel.

Elution: 1. fraction: cyclohexane, 2. fraction: cyclohexane:dichloromethane 2:1

1: *t*-butyl disulfide 2: naphthalene, 3: benzothiophene, 4: *n*-butyl disulfide, 5: 3-methylbenzothiophene, 6: tetradecane, 7: dodecyl methyl sulfide, 8: phenyl sulfide, 9: dibenzothiophene, 10: phenanthrene, 11: phenyl disulfide, 12: eicosane, 13: octadecyl methyl sulfide, 14: tetracosane, 15: benzonaphtho[1,2-*d*]thiophene, 16: chrysene, \*: contamination.

Chromium sulfate silica gel is able to separate sulfides from other substance classes. Whereas alkanes, PASHs, disulfides and most PAHs are not retained on the phase and can be eluted in the first fraction, the sulfides can interact more strongly with the chromium ions and are therefore only eluted in the second fraction. In addition, the phase seems to be able to interact with  $\pi$ -electron systems, as some of the larger aromatic compounds, especially the four-ring-aromatics, are also eluted in the second fraction. Even an increase in the amounts of solvents or activation of the stationary phase at higher temperatures could not reduce the retention of these compounds.

As already seen for the zinc chloride stationary phase, some analytes are partially retained on the chromium sulfate silica gel. In the first fraction the higher boiling compounds have reduced intensities compared to the standard mixture, whereas only reduced intensities for the lower boiling substances is to be expected. Due to the high volatility of the smaller compounds, they might easily be lost during evaporation of the solvents. But as in this case the signals for the higher boiling compounds are decreased, partial

retention of these compounds on the phase occur. Especially noticeable is the change in peak ratios for the compounds **9-11**. the intensity of dibenzothiophene (**9**) is drastically reduced, especially compared to phenyl disulfide (**11**). In the untreated standard mixture their ratio is about 15:1, whereas in the first fraction of the separation a ratio of 4:3 can be found. Significant amounts of dibenzothiophene therefore must be retained on the phase and are not eluted at all. A similar effect is observable in the chromatogram of the second fraction. Dodecyl methyl sulfide (**7**) is overly dominant in this fraction, implying a partial retention of the remaining compounds eluting in the fraction.

The carry-over observable for the separation on chromium sulfate silica gel is even enhanced when substituting the silica support for alumina. On chromium sulfate alumina also three-ring-aromatics, like phenanthrene and dibenzothiophene are eluted in the second fraction (see table 16 in the appendix). Furthermore, the retention of the sulfides is reduced, so that all sulfides can be found in the first fractions. Traces of the aromatic sulfides and disulfides are also present in the second fraction, which also implies  $\pi$ -interactions of the stationary phase with aromatic analytes. Hence, for the desired separation chromium sulfate silica is more suitable than alumina.

In conclusion, this phase is able to preconcentrate sulfidic compounds, but not to isolate them from larger aromatic ring systems, as large  $\pi$ -systems of the analytes interact with the stationary phase and yield in increased retention. Disulfides do not interact strongly, so they are directly eluted without any retention. Partial retention of the standards was observable for both fractions, so that the phase would not be suitable for mass and sulfur balances.

### 6.3 Separation on cadmium acetate silica gel

When the standard solution is separated on cadmium acetate silica gel, all analytes can be recovered in the first two fractions. For clarity, the third fraction is therefore left out when displaying the results in figure 28.

The results for the separation of standards on cadmium acetate silica gel are similar to the previous separation on chromium sulfate silica gel. Alkanes, disulfides, most PAHs and PASHs are not retained on the phase, but directly eluted in the first fraction. Sulfides can be found in the second fraction, as they seem to interact more strongly. The aromatic phenyl sulfide (**8**) already starts to eluate in the first fraction, but even in both fractions combined, the total amount of recovered phenyl sulfide is very low. Hence, the phenyl sulfide seems to be partially retained on the stationary phase. In the

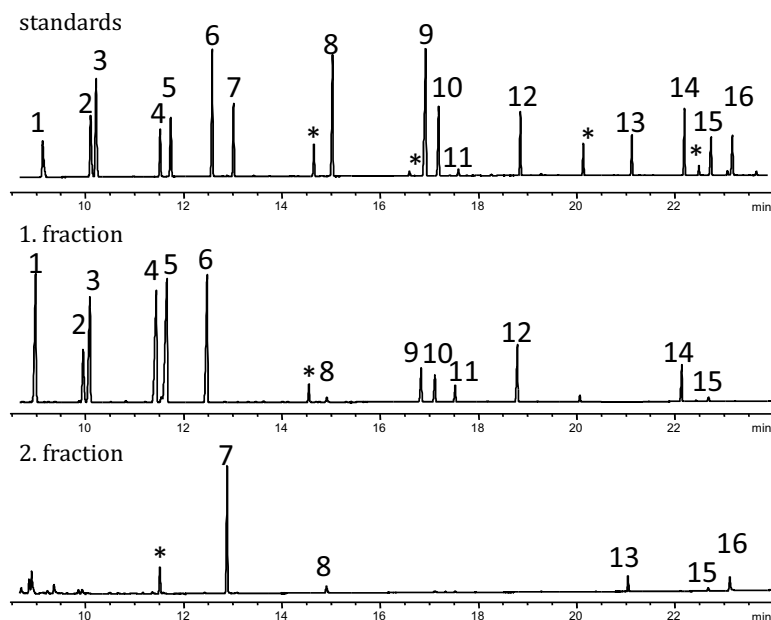


**Figure 28:** GC-FID chromatogram of the standard separation on cadmium acetate silica gel.

Elution: 1. fraction: cyclohexane, 2. fraction: cyclohexane:dichloromethane 2:1

1: *t*-butyl disulfide 2: naphthalene, 3: benzothiophene, 4: *n*-butyl disulfide, 5: 3-methylbenzothiophene, 6: tetradecane, 7: dodecyl methyl sulfide, 8: phenyl sulfide, 9: dibenzothiophene, 10: phenanthrene, 11: phenyl disulfide, 12: eicosane, 13: octadecyl methyl sulfide, 14: tetracosane, 15: benzonaphtho[1,2-*d*]thiophene, 16: chrysene, \*: contamination.

second fraction again also the four-ring-aromatic compounds can be found, whereas in this case the PASHs already start to elute in the first fraction and the PAHs are found in the second fraction only. The  $\pi$ -interactions of the cadmium acetate silica gel and the analytes seem to be weaker than seen on the chromium phase.

Partial retention of the analytes is observable for this stationary phase as well. As already seen for the separation on chromium sulfate silica gel, the intensities of the high boiling compounds in the first fractions are decreased compared to the more volatile compounds. Again, the intensity of the dibenzothiophene peak (9) is drastically reduced. Compared to phenyl disulfide (11), the ratio of the peak heights changes from 15:1 in the standard mixture to 5:2 in the first eluted fraction. In the second fraction again dodecyl methyl sulfide (7) is overly dominant. The peak heights for phenyl sulfide (8) and the remaining larger aromatic compounds eluted in this fraction are even lower than seen for the separation on chromium sulfate silica gel. Again, an increase of eluting solvent

volume or activation of the stationary phase did not improve the separation.

When substituting the silica support for alumina, no retention at all is observable. All analytes are eluted in the first fraction (see table 17 in the appendix). This also proves that the kind of supporting material has a huge effect on the separating abilities of the stationary phase. Even if metal salt, preparation and separation remain similar, a change in the supporting material can drastically change the chromatographic properties of the stationary phase.

#### 6.4 Separation on cobalt nitrate silica gel

Again, as all analytes can be recovered in the first two fractions, the third fraction of the separation on cobalt nitrate silica gel is left out for clarity when displayed in figure 29.

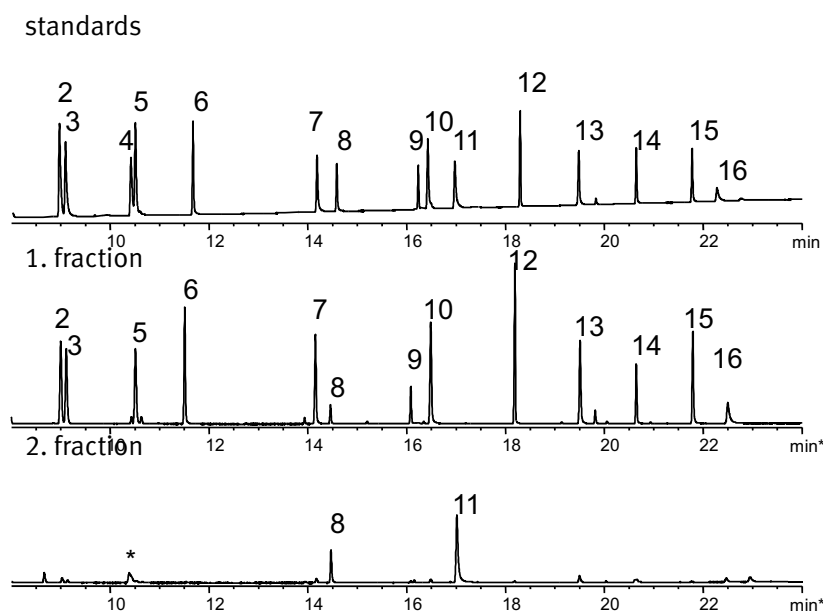


**Figure 29:** GC-FID chromatogram of the standard separation on cobalt nitrate silica gel.

Elution: 1. fraction: cyclohexane, 2. fraction: cyclohexane:dichloromethane 2:1.

1: *t*-butyl disulfide 2: naphthalene, 3: benzothiophene, 4: *n*-butyl disulfide, 5: 3-methylbenzothiophene, 6: tetradecane, 7: dodecyl methyl sulfide, 8: phenyl sulfide, 9: dibenzothiophene, 10: phenanthrene, 11: phenyl disulfide, 12: eicosane, 13: octadecyl methyl sulfide, 14: tetracosane, 15: benzonaphtho[1,2-*d*]thiophene, 16: chrysene, \*: contamination.



The separation on cobalt nitrate silica gel is similar to the one on zinc nitrate silica gel. Alkanes, PAHs, PASHs and aliphatic sulfides are not retained on the phase and readily elute in the first fraction, whereas the aromatic non-thiophenic compounds, i.e. phenyl sulfide and phenyl disulfide, are isolated in the second fraction. In contrast to the zinc phase, the aliphatic disulfides cannot be recovered on the cobalt nitrate silica gel column. It is interesting to see that the interactions between aromatic and aliphatic disulfides vary that much, that the aromatic disulfide is easily recovered with moderately polar solvents as cyclohexane-dichloromethane, whereas the aliphatic disulfides cannot be eluted, even with the addition of ammonia as competitive ligand and an increased polarity due to the addition of isopropanol.

Compared to the previously described phases, the peak intensities for the separation on cobalt nitrate silica gel are not altered as drastically. Only small alteration between the ratios of the peak heights are observable, when comparing the untreated standard solution to the separated fractions. The peak height of dibenzothiophene (**9**) is slightly reduced. The ratio between the peak heights of dibenzothiophene (**9**) and phenanthrene (**10**) change from 6:10 in the standard mixture to 5:13 in the first fraction of the separation. Apart from that no major retention of the elutable compounds is observable.

The cobalt nitrate silica gel phase is only suitable for isolation of aromatic non-thiophenic sulfur. Considering the peak heights of the two compounds in fraction 2, the recovery of the sulfide seems to be incomplete, as the ratio of peak heights is shifted towards the disulfide. This indicates that the phenyl sulfides could probably not be eluted quantitatively. Aliphatic disulfides are also irreversibly retained on the phase, making the cobalt nitrate silica gel not suitable for the desired determination of non-thiophenic sulfur.

## **6.5 Separation on heat-treated silver mercaptopropano-silica gel (*h*Ag-MPSG) and silver cartridges**

As silver based stationary phases have been successfully used for the separation of fossil material both in the literature [65, 76, 86–89] and our working group [85, 90, 91], several variations of silver ion coated stationary phases were tested. As a showcase, the separations on heat-treated silver mercaptopropano-silica gel (*h*Ag-MPSG) and silver cartridges ( $\text{Ag}^+$ -cartridges) will be discussed.

When separating the standard mixture on *h*Ag-MPSG (see figure 30), three fractions were collected. The first fraction contains alkanes, smaller PAHs and PASHs. However, the second fraction contains larger aromatic compounds, the smaller aliphatic sulfide, i.e.

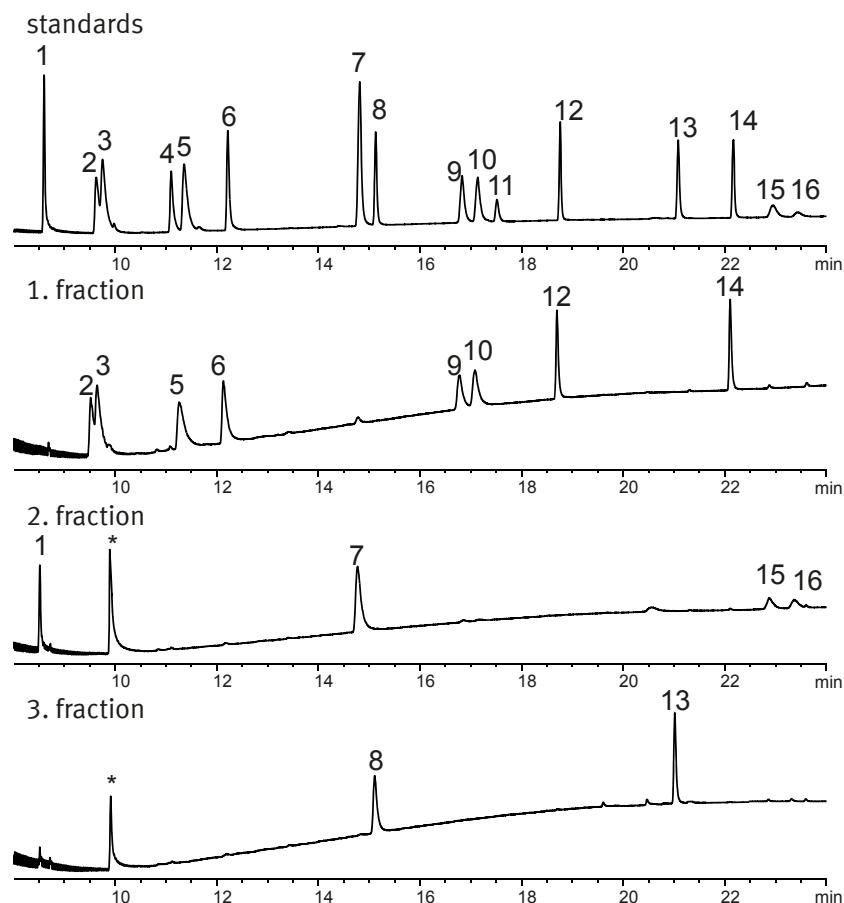


**Figure 30:** GC-FID chromatogram of the standard separation on heat-treated silver mercaptopropano-silica gel (*h*Ag-MPSG).

Elution: 1. fraction: cyclohexane, 2. fraction: cyclohexane:dichloromethane 2:1, 3. fraction: cyclohexane:dichloromethane 2:1 + 5% ammonia saturated isopropanol.

1: *t*-butyl disulfide 2: naphthalene, 3: benzothiophene, 4: *n*-butyl disulfide, 5: 3-methylbenzothiophene, 6: tetradecane, 7: dodecyl methyl sulfide, 8: phenyl sulfide, 9: dibenzothiophene, 10: phenanthrene, 11: phenyl disulfide, 12: eicosane, 13: octadecyl methyl sulfide, 14: tetracosane, 15: benzonaphtho[1,2-*d*]thiophene, 16: chrysene, \*: contamination.

dodecyl methyl sulfide and tertiary-butyl disulfide as the only recoverable disulfide. The bulky tertiary butyl group might therefore slightly inhibit the interactions of the disulfide with the stationary phase, so that it can be released more easily than the other disulfides used. The phenyl disulfide might undergo additional  $\pi - \pi$ -interactions, which would lead to an even higher retention of this analyte. The fact that the four-ring-aromatics, i.e. benzonaphthothiophene and chrysene are also eluted in this fraction, supports this

claim. Silver phases are known to be able to separate aromatics according to the size of their aromatic ring system [91] and therefore larger aromatics experience stronger interactions with the phase and are retained more strongly. The third fraction isolates the remaining sulfides, i.e. phenyl sulfide and octadecyl methyl sulfide. Here again, the aromatic character of the phenyl sulfide leads to higher retention and the difference in the eluting fractions of the two aliphatic sulfides is caused by the variation of the electron density at the sulfur atom caused by the longer alkyl chain. As no  $\pi$ -electrons to interact with the stationary phase are present in either substance the difference in electron density of the sulfur atoms must be great enough to allow early elution for the short chained sulfide and stronger retention for the longer alkyl chained sulfide.

Concerning the ratio of the peak heights, no remarkable changes are noticeable when separating the standard mixture on *h*Ag-MPSG. The peak for dodecyl methyl sulfide (**7**) appears to be slightly reduced compared to the peak of the other substances eluting in this fraction, but due to the slightly increased peak width, the peak area is comparable. Lastly, the separation on  $\text{Ag}^+$ -cartridges will be discussed. These silica gel based cartridges are commercially available and were purchased from *Supelco*. Due to the small amount of stationary phase in the columns and as the packing material is not sold unpacked, this phase strongly limits the application due to possible overloading and the lack of applicability for HPLC. All other synthesized stationary phases could just be generated from material with a smaller particle size and packed into an HPLC column. But as the exact preparation of the silver cartridges is unknown and only one particle size (60  $\mu\text{m}$ ) is available, the transition to HPLC is not possible for this phase.

Figure 31 shows the separation of the standard mixture on  $\text{Ag}^+$ -cartridges. The first fraction contains alkanes, as well as the two-ring-aromatics. Often in group type separations these small aromatic compounds elute in earlier fractions, as the aromatic system is still very small and  $\pi - \pi$ -interactions between the analytes and the stationary phases cannot be strong enough to successfully retain the small aromatics. What is remarkable here, is that the signals for the alkanes seem to be reduced, compared to the standard mixture. The small aromatics (**2 + 3**) are a lot more abundant than the alkanes (**6, 12 + 14**). As the alkanes are not expected to interact with the stationary phase and have a higher volatility than the aromatics, the separation on  $\text{Ag}^+$ -cartridges must be treated with caution. A rerun of the separation yielded similar results. The second fraction nicely separates the larger aromatics, including PASHs and PAHs, as well as the phenyl disulfide. Here again, the ability of silver ions to separate according to the size of the aromatic ring system is applied. The third and final fraction contains the aliphatic disul-

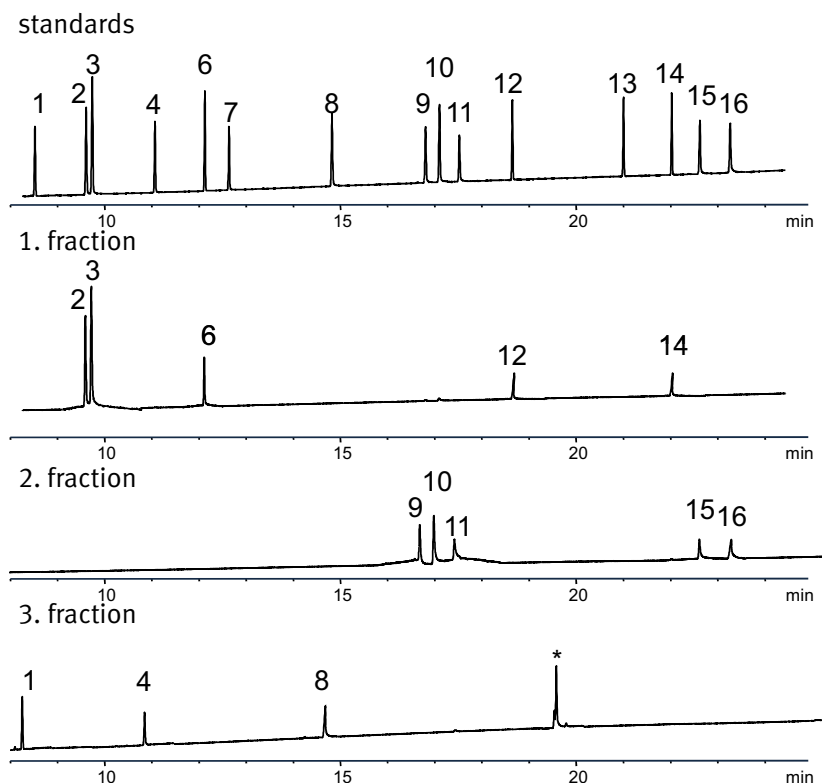


**Figure 31:** GC-FID chromatogram of the standard separation on commercially available  $\text{Ag}^+$ -cartridges.

Elution: 1. fraction: cyclohexane, 2. fraction: cyclohexane:dichloromethane 2:1, 3. fraction: cyclohexane:dichloromethane 2:1 + 5% ammonia saturated isopropanol.

1: *t*-butyl disulfide 2: naphthalene, 3: benzothiophene, 4: *n*-butyl disulfide, 5: 3-methylbenzothiophene, 6: tetradecane, 7: decylmethyl sulfide, 8: phenyl sulfide, 9: dibenzothiophene, 10: phenanthrene, 11: phenyl disulfide, 12: eicosane, 13: octadecyl methyl sulfide, 14: tetracosane, 15: benzonaphtho[1,2-*d*]thiophene, 16: chrysene, \*: contamination.

fides, as well as the aromatic sulfide. The aliphatic sulfides cannot be recovered from the stationary phase. As it is observable that the aromatic disulfide elutes earlier than the aliphatic disulfides, it is probable that the aliphatic sulfides as well undergo stronger interactions with the silver ions than the aromatic sulfides. Even stronger competitive ligands than ammonia might be able to release the aliphatic sulfides. But as the silver cartridges are not very stable towards amines, or other complexing agents, the choices of suitable ligands are limited. Reusability would also be effected, as strong binding ligands make regeneration and equilibration of the phase impossible. As the cartridges are meant to be disposable, this would be of minor concern.

The Ag<sup>+</sup>-cartridges therefore can be used to separate aromatic sulfides and aliphatic disulfides from the standard mixture. Aromatic disulfides coelute with larger aromatics and aliphatic sulfides could not be recovered. As only SPE-cartridges are available, no transition to HPLC can be done and compared to the other tested phases, the cartridges are rather pricy.

## 6.6 Conclusions

Ligand exchange chromatography is a flexible and versatile technique. Through endless combinatory possibilities of metal ion, counter ion, supporting material and surface modification, the chromatographic properties can be easily adjusted. Even if the HSAB concept and complex stability constants can be taken as a general guideline for the binding between stationary phase and analyte, it is impossible to predict the exact separation on a given phase. Among all tested stationary phases none could completely perform the desired separation. It was possible to isolate sulfides from the standard mixture, to collect fractions containing aromatic sulfides and aliphatic disulfides, but never to isolate the total non-thiophenic sulfur selectively. Often  $\pi - \pi$ -interactions of the larger aromatic ring systems occurred, causing a carry-over of four-ring-aromatics into the non-thiophenic fraction. Also many phases were not able to release disulfides at all, as the interaction of this sulfur class with the metal ions was too strong.

The best results could be achieved using silver based stationary phases. Especially the Ag<sup>+</sup>-cartridges were able to release all types of disulfides and aromatic sulfides. As the aliphatic sulfides cannot be recovered from this phase, for the total analysis of non-thiophenic sulfur the combination of two different columns, e.g. the already established Pd-MPSG column[67] or the PdSO<sub>4</sub>-Alox column[85] combined with the cartridges could be used. The palladium phases are able to separate sulfides from PASHs, but disulfides are irreversibly retained.

A simultaneous separation of a sample on both phases could possibly result in a sulfidic and a disulfidic fraction. For that purpose further experiments need to be conducted, as due to the lack of time and laboratory space the experiments could not be concluded in the scope of this work.

## 7 Chromatographic separation and further analysis of vacuum gas oils

### 7.1 State-of the art

#### 7.1.1 Chromatographic separation of petroleum

As simplification of the matrix is essential when dealing with supercomplex mixtures, traditional chromatographic techniques like the SARA fractionation (SARA: saturates, aromatics, resins, asphaltenes) have been extensively used for the separation of fossil material. A typical separation scheme is displayed in figure 32.

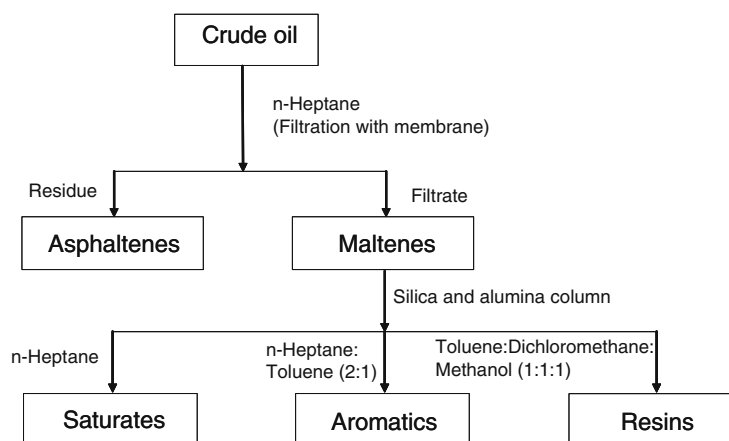


**Figure 32:** One of the commonly used fractionation schemes of crude oil (SARA). [92]

This technique has been widely used for the fractionation of crude oils based on the chemical composition of the fractions [47] and numerous modifications of this separation are known. For example when using a combination of polarity chromatography by combining different kinds of silica gel, e.g. basic and acidic, crude oils can be separated according to pH in addition to the conventional SARA fractionation. [93] In addition to the traditional silica gel stationary phases also other chromatographic separations were performed on crude oils. PAHs and asphaltenes in crude oils can also be separated on a caffeine based HPLC phase[94] or using nematic liquid crystals as phases for the separation of PAHs in gas-liquid chromatography. [95] Also amino-functionalized stationary phases have been applied for the group type separation in saturates, aromatics, and polars or according to ring size. [96] Using a combination of anion- and cation-exchange chromatography, coordination chromatography, and adsorption chromatography heavy-

end distillates from crude oils have been separated into acids, bases, neutral-nitrogen compounds, saturates and aromatics. [97] Furthermore, comprehensive two-dimensional gas chromatography (GCxGC) is a widely used technique to analyze pre-separated crude oils. GCxGC has been applied to separate and identify biomarker molecules isolated from crude oils, including alkylated aromatics, PASHs, steranes, triterpanes, and triaromatic steranes. [98] Also it can be used to identify homologous series of alkyl substituted compounds and to classify a specific group of compounds, e.g. C4-substituted benzenes. [99] In addition to chromatographic techniques, also NMR spectroscopy was applied for the analysis and characterization of crude oils. [100]

For different compound classes in petroleum also selective techniques have been developed. For phenols, for example, a TLC separation with subsequent spectrophotometric determination after derivatization using the Folin-Ciocalteu reagent [101] or a gas chromatographic separation with atomic emission detection after derivatization with ferrocenecarboxylic acids. [102] Acids in petroleum samples were isolated using gel permeation chromatography on a cross-linked polystyrene gel. [103] For the separation of nitrogen containing compounds LEC phases based on zirconium and hafnium as well as metal organic frameworks (MOFs) were applied. [104]

For PASHs the classical technique for determination is GC due to the availability of several sulfur selective detectors. [105] GCxGC with sulfur chemiluminescence detector has been used to group separate, identify and quantify sulfur containing compounds in crude oils. [106, 107] In liquid chromatography palladium based stationary phases have been widely used to separate PASHs from PAHs, e.g. Pd-MPSG and Pd-ACDA. [67, 92] Besides the chromatographic methods the sulfur compounds in crude oil were also analyzed using XANES spectroscopy. [108]

### 7.1.2 Methylation reaction of sulfur containing compounds

When trying to analyze sulfur containing compounds like PASHs and sulfides with weak ionization techniques, e.g. ESI-MS, derivatization is inevitable. As PASHs, in contrast to some nitrogen aromatics, cannot be deprotonated or protonated in ESI, a methyl group is introduced at the sulfur atom. The sulfur is indeed incorporated into the aromatic system, but not completely nonreactive. Strong electrophilic attacks, e.g. of carbenium ions, are therefore possible and can be used to generate thiophenium ions. [109] These ions are now already charged, making the compound classes of PASHs and sulfides accessible for ESI-MS and other else wise weak ionization techniques. [110] In the literature the reaction is also described for sulfides and disulfides. [111–113] In case

of disulfides often trimethyl- or triethyloxonium tetrafluoroborate are used as alkylation agents (figure 33), whereas for PASHs and sulfides a combination of methyl iodide and silver tetrafluoroborate is more often used. In both cases the stabilizing counterion is

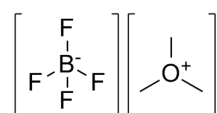


**Figure 33:** The alkylation agent trimethyloxonium tetrafluoroborate.

tetrafluoroborate, but methyl iodide has the advantage that the formation of the stable tertiary carbenium ion is favored by the precipitation of weakly soluble silver iodide when adding silver tetrafluoroborate. The formation of a silver iodide precipitate is instantly observable when combining the methyl iodide with silver tetrafluoroborate implying an  $S_N1$  reaction as displayed in figure 34.

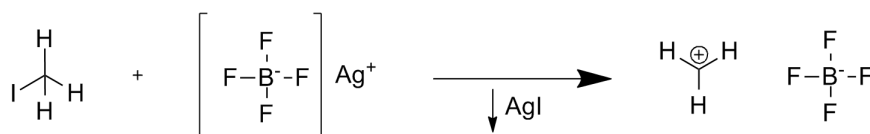


**Figure 34:** Activation of methyl iodide.

As this reaction only takes place when the silver salt is added, methyl iodide is easier to store. Methyl iodide can be completely evaporated due to its low boiling point of 42 °C, so that excess of methylation agent can be removed by evaporation. Trimethyloxonium tetrafluoroborate already is a cation. In contrast to methyl iodide to start the alkylation only the addition of one substance is needed, therefore the reaction time is easier to control. Trimethyloxonium tetrafluoroborate cannot be evaporated as it is a solid, but it can easily be quenched by addition of water.

### 7.1.3 Fourier-transform ion cyclotron resonance mass spectrometry for the analysis of petroleum

As petroleum is the most complex mixture known, high resolution mass spectrometry was always an interesting tool for the analysis of this material, so that the earliest commercial high resolution mass spectrometers were even developed for the analysis of petroleum distillates. [44]



Introduced in 1974[41], Fourier-transform ion cyclotron resonance mass spectrometry (FT-ICR MS) has nowadays improved to one of the most often used techniques for the mass spectrometric analysis of petroleum and its products due to its ultrahigh resolving power (resolving power of about 1,200,000 at  $m/z$  400 and 12 T has been reported [45]). For supercomplex mixtures like petroleum even these high resolutions will not be sufficient to resolve single  $m/z$ , but be a helpful tool for the analysis of functional groups or other group types previously separated by chromatography. As various ion sources can be coupled to FT-ICR, a huge variety of compound classes can be detected. For example, via coupling of electrospray ionization (ESI) to FT-ICR several thousands of individual  $m/z$  could be identified in a crude oil. [44]

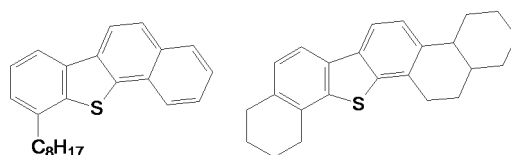


**Figure 35:** An example for isomers present in crude oils. Both compounds have the chemical formula  $C_{24}H_{26}S$  and can therefore not be distinguished in mass spectrometry.

However, one should always keep in mind that mass spectrometry can only provide us with elemental composition. Especially in super complex mixtures isomers are widely present in the sample (see figure 35) and cannot be resolved by mass spectrometry.

Also the ionization technique strongly affects the resulting chromatograms. Depending on the type of ionization source, different compound classes or  $m/z$  ranges are over-proportionally favored and therefore overrepresented in the mass spectra (see also figure 36). [114] The most commonly used technique ESI favors compounds with a higher molecular mass than the atmospheric pressure ionization techniques. Again it could be shown that

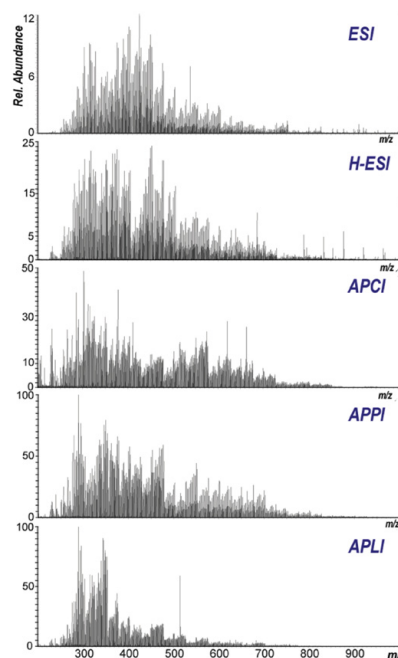


**Figure 36:** FT-ICR mass spectra of asphaltenes in positive ionization mode for the mass range 200-1000 Da[114]

APLI is only able to ionize a fraction of the the compounds compared to the other techniques.

GASPAR et al [115] also show that especially when analyzing crude oils, ion suppression occurs and hugely affects the number of detectable compounds. In their study they separated a crude oil into different fractions and performed FT-ICR measurements with atmospheric pressure chemical ionization (APCI) of the bulk crude oil and each of the fractions (see figure 37). After each separation step even more compounds could be assigned by the software than were assignable in the previous separation step.

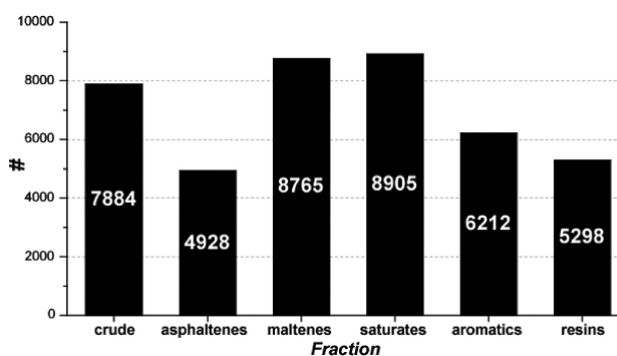


**Figure 37:** Number of assigned formulas found in a bulk crude oil and its corresponding separated fractions. [115]

The same phenomena was observed by CHO et al in APPI FT-ICR MS. [116] Therefore, chromatography is essential for the correct characterization of fossil material, as without prior separation many analytes get suppressed in mass spectrometry and even with its ultrahigh resolution FT-ICR is not able to completely resolve a mass spectra of petroleum.

#### 7.1.4 Fourier-transform ion cyclotron resonance mass spectrometry for the analysis of sulfur compounds

For the analysis of sulfur containing compounds in petroleum samples via high resolution mass spectrometry mainly two different techniques have been applied: ESI-ionization after methylation or photoionization at atmospheric pressure, using APPI or more recently APLI.

For the speciation of sulfur containing compounds in crude oil fractions APPI has been applied, but the simultaneous generation of protonated molecules and parent ions as well as ion radicals in the source generate additional signals to the already complex

sample and make compositional assignment even harder. [117] In addition, APPI also generates signals for other photoionizable compounds and hence the spectra are further unnecessarily complicated. With ultrahigh mass resolving power and the extraordinary mass accuracy of FT-ICR MS, sulfur speciation of petroleum might be achieved by APPI. [118] APLI has been applied similarly to APPI. However, its ionization mechanism is more selective than that of APPI. In petroleum samples mainly aromatic compounds like PASHs and PAHs are ionized, but PAHs present in the sample can act as dopants for other compounds and increase ionizability. [34] In APLI-MS of an unseparated crude oil, as well as APPI and APCI, the amount of S species is smaller than to be expected from values received from elemental analysis, but APLI is able to ionize a wider range of compounds than APPI, especially low boiling nonpolar analytes. [114]

As nonpolar compounds like PASHs cannot be ionized directly by soft ionization techniques like ESI, they have to be converted to the corresponding thiophenium ions first. [92] This approach has the advantage that non-sulfur containing compounds like PAHs remain neutral and therefore do not produce signals in the mass spectrum. Especially as aromatic hydrocarbons often dominate in petroleum cuts, this is an extremely useful simplification and also a concentration of PASHs, which are usually only present in small amounts. As in contrast to gas chromatography no volatility of the compounds is needed this technique can also be applied to high boiling fractions and even vacuum residues. [119] But ESI after methylation also has its limits. For higher aromatic ring systems as present in compounds with a DBE >20 the spectra are not representative. [120]

Most recently silver cationization has been presented as a new technique for the ionization of sulfur containing compounds in crude oils. Instead of a methylation reaction the sample is treated with a solution of silver triflate in methanol/toluene. Silver triflate is chosen, so that  $\text{Ag}^+$  adducts are more easily formed when adding the analytes. [121] Subsequently the formed  $\text{Ag}^+$  adducts are analyzed using ESI FT-ICR MS. In the resulting mass spectra the sulfur containing compound classes S1 and S2 are the most abundant in the mass spectra, whereas these classes cannot be ionized at all in ESI without the addition of silver ions. In contrast to the ESI MS after methylation here again also hydrocarbons like PAHs can react and are detected. [122, 123] Thus, even hydrocarbons with a DBE <4 could be identified. [121] In addition to silver ions also palladium(II) ions have been used to promote ionization of sulfur containing compounds in ESI-MS. [124] Here again, the signal intensity for S1 compounds was largely enhanced by the addition of the metal ion, but also PAHs can interfere with the signals. One great downside of using metal ions for the ionization is the isotopy of the metals.

Due to the different isotopes of the metals each signal is split up into multiple signals of weaker intensity, therefore adding additional complexity to the spectra. Compounds of low abundance in the sample are even further reduced in intensity and might be not detectable anymore. Also for sensitive mass spectrometric instrument the introduction of large amounts of metal salts into the instrument might be problematic.

## 7.2 Preseparation of vacuum gas oils

Fractionation of the samples according to SARA would drastically reduce the complexity of the sample and enrich the analytes of interest as a large percentage of the given sample consists of aliphatic saturated hydrocarbons. Also other compounds, like nitrogen containing aromatic compounds (NCAC), sulfoxides or other polar compounds, should be removed if possible, as they might also interact with the stationary LEC phases and occupy interaction positions, so that the capacity for sulfur retention is reduced. Furthermore, compounds like sulfoxides or thiols might complicate the detection of non-thiophenic sulfur due to their own sulfur content. Therefore, a separation according to the scheme displayed in figure 38 was planned.

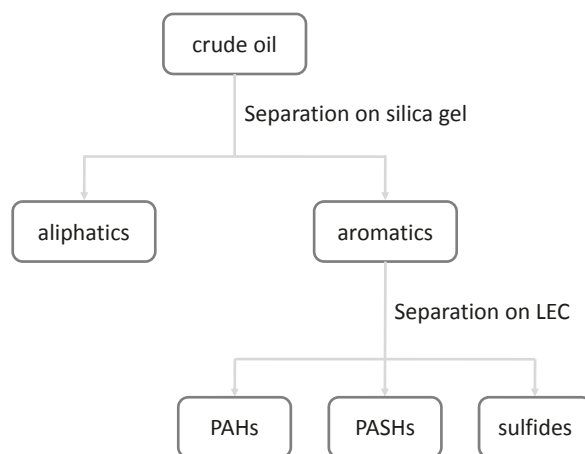


**Figure 38:** Ideal separation of a crude oil according to SARA with subsequent separation on a LEC phase.

As a showcase example, the separation of Karachaganak will be discussed. The fractions of Karachaganak 369-509 °C, separated according to the procedure described in section 10.1.15, were methylated with iodomethane and analyzed via ESI-Orbitrap. The cor-

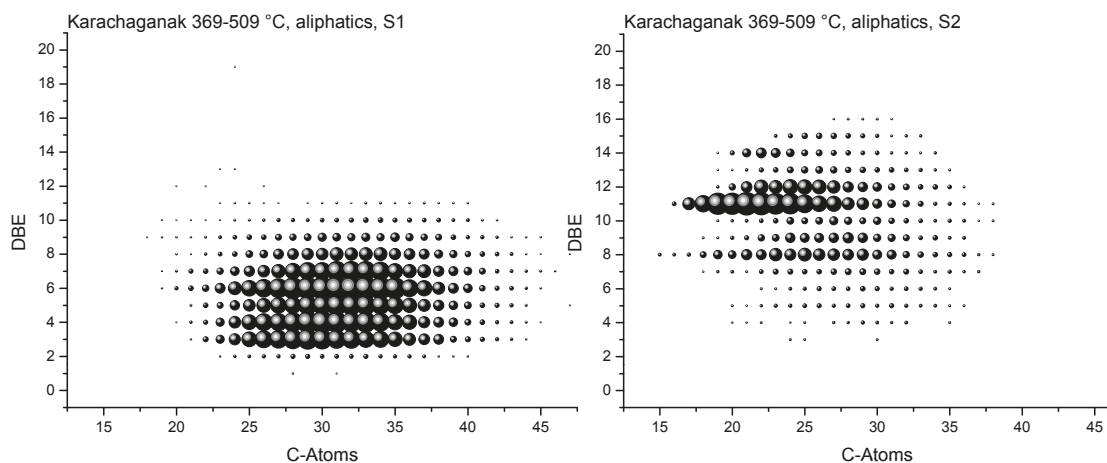


**Figure 39:** Kendrick plots of the S1 and S2 compounds in the aliphatic fraction of the SARA fractionation of Karachaganak 369-509 °C according to the scheme in figure 38.

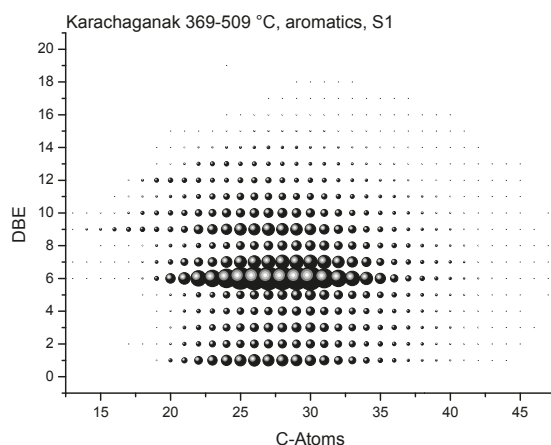


**Figure 40:** Kendrick plot of the S1 compounds in the aromatic fraction of the SARA fractionation of Karachaganak 369-509 °C according to the scheme in figure 38.

responding Kendrick plots for the S1 and S2 compounds of the aliphatic and aromatic fraction are displayed in figures 39 and 40.

The aliphatic fraction contains of S1 compounds with a lower DBE as to be expected. Compounds with  $3 < \text{DBE} < 7$  are the most abundant ones, the total range of DBE spreading from 2 to 11. The dominant lines present at DBE 3 and 6 indicate the presence of thiophenes and benzothiophenes in this fraction. The S2 compounds in this fraction are surprisingly of a higher DBE with dominant lines at DBE 8 and 11, corresponding to the S2 equivalents of dibenzothiophenes and benzonaphthothiophenes. The range of DBE is 4 to 15 and therefore slightly higher than seen for the S1 compounds. Also the degree of alkylation differs. Whereas the S1 compounds have a higher degree of alkylation

(20-45 carbon atoms), slightly shorter alkyl chains can be found for the S2 compounds (15-40 carbon atoms). For the aromatic fraction only S1 compounds are displayed, as only single statistically distributed S2 compounds could be assigned, when analyzing this fraction. Compared to the aliphatic fraction, now even more saturated compounds like cyclic sulfides (DBE 1) can be found. The most prominent line can be found at DBE 6, corresponding again to benzothiophenes, but also dibenzothiophenes (DBE 9-11) and benzonaphthothiophenes (DBE 12-15) are present in this fraction. For  $6 < \text{DBE} < 10$ , also smaller compounds with only 12-20 carbon atoms can be found. Apart from that, the alkylation patterns is nearly identical to the one found for the S1 compounds in the aliphatic fraction. To gain more insight on the behavior of disulfides during this separation, disulfide standards were spiked to Karachaganak 96-369 °C and the SARA separation was performed. As displayed in the corresponding GC-FID chromatograms in figure 41, both standard substances could be recovered in the aromatic fraction.

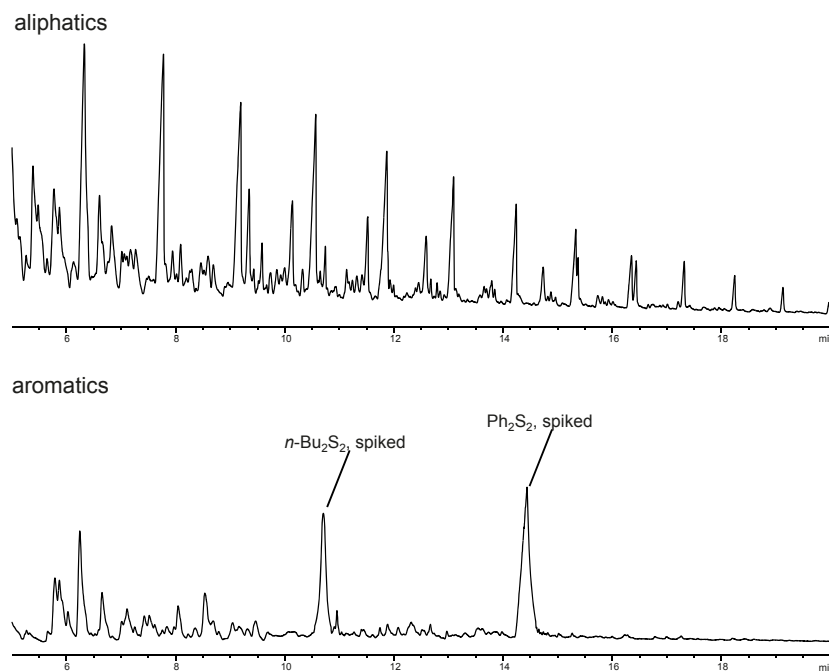


**Figure 41:** GC-FID chromatograms of the aliphatic and aromatic fraction of the SARA fractionation of Karachaganak 96-369 °C spiked with disulfide standards. Separation according to the scheme in figure 38.

It is obvious that a preseparation according to the SARA scheme is not suitable for the analysis of non-thiophenic sulfur compounds, as in both the aromatic and the aliphatic

fraction there are sulfur containing compounds with low double bond equivalents. Interestingly the S1 compounds with a DBE of 1 are only found in the aromatic fraction, whereas the aliphatic fraction contains sulfur compounds with a DBE up to 10. Also the GC-chromatograms show that disulfides, even when bearing aliphatic substituents, are more strongly retained on stationary phases, also on as silica gel. Both of the disulfide standards, n-butyl disulfide and phenyl disulfide, are eluted in the aromatic fraction. The SARA method is mainly established to analyze polyaromatic compounds, non-thiophenic sulfur is often not of major interest and therefore not extensively studied. These results now show that the SARA fractionation cannot be used as a tool to remove only saturated hydrocarbons as sulfur containing compounds also elute in the aliphatic fraction. Using the aliphatic fraction alone would also result in false results as especially S1 compounds of low DBE and aromatic and aliphatic disulfides can only be found in the aromatic fraction.

As the classical SARA fractionation could not be applied successfully to the analytical problem, but pre-separation was desired to reduce the amount of unwanted compound classes, a modified pre-separation according to the scheme displayed in figure 42 was performed.

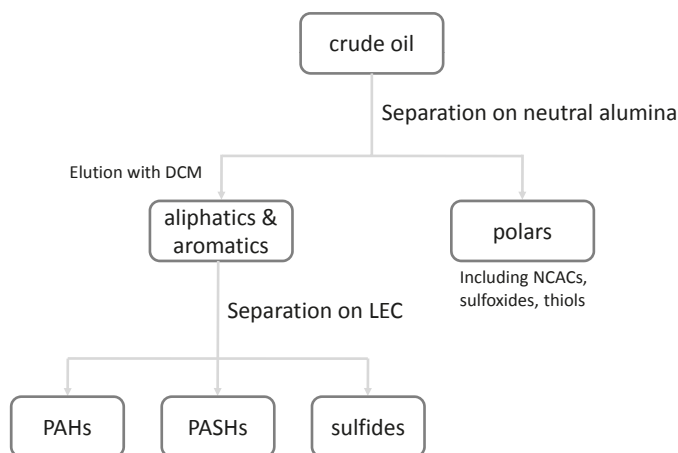


**Figure 42:** Separation scheme including pre-separation on alumina to remove polar compounds.

Instead of collecting isolated aliphatic and aromatic fractions, a combined fraction was directly eluted using dichloromethane. Other polar compounds, like NCACs, sulfoxides, thiols or asphaltenic compounds remained on the alumina column. Saturated hydrocarbons were of course still present in the collected fraction, but as they are not ionizable in

the used mass spectrometric techniques and are not retained on the stationary phases, but directly eluted, their influence on the separation and detection is minor.

### 7.3 Methylation of non-thiophenic sulfur compounds

The methylation of sulfur heterocycles with iodomethane and silver tetrafluoroborate has been performed in our working group for routine analysis of crude oils. Nevertheless, the methylation of disulfides has not been studied here yet. For later mass spectrometric investigations it is important that the compounds of interest are present as ions. Therefore, the methylation of sulfides and disulfides was tested to determine if already established methods for producing ions is also applicable to sulfides and disulfides. The reaction scheme of both methylating reactions is displayed in figures 43 and 44. As

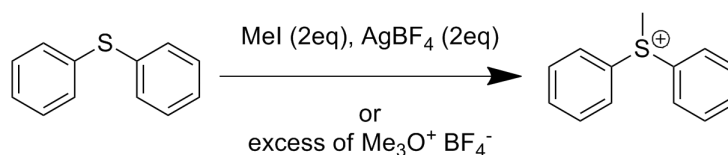


**Figure 43:** Reaction scheme of methylation of phenyl sulfide.

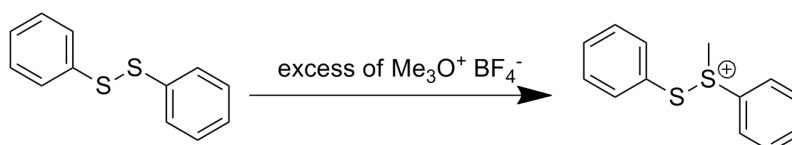


**Figure 44:** Reaction scheme of methylation of phenyl disulfide.

already mentioned, the methylation of sulfides and disulfides is a very important aspect. If it is possible to methylate sulfides and disulfides in different ways, the ionization and therefore the MS signal would also differ. Selective methylation of single compound classes would facilitate the identification of substances, especially when the general presence of disulfides is concerned, as a methylation method selective for disulfides would greatly simplify the matrix. And even in later states of work, mass spectrometry would be an important issue for validation and for identification. Therefore, the methylation reaction was monitored via NMR.

NMR data show that when methylating phenyl sulfide with iodomethane an immediate conversion to the sulfonium ion takes place (see figure 45). Even in the sample taken



instantly after adding the methylation agent, no signals of the starting material are visible in the NMR and the integral of the signal from the introduced methyl group equals three protons, confirming that the conversion is complete at this time.

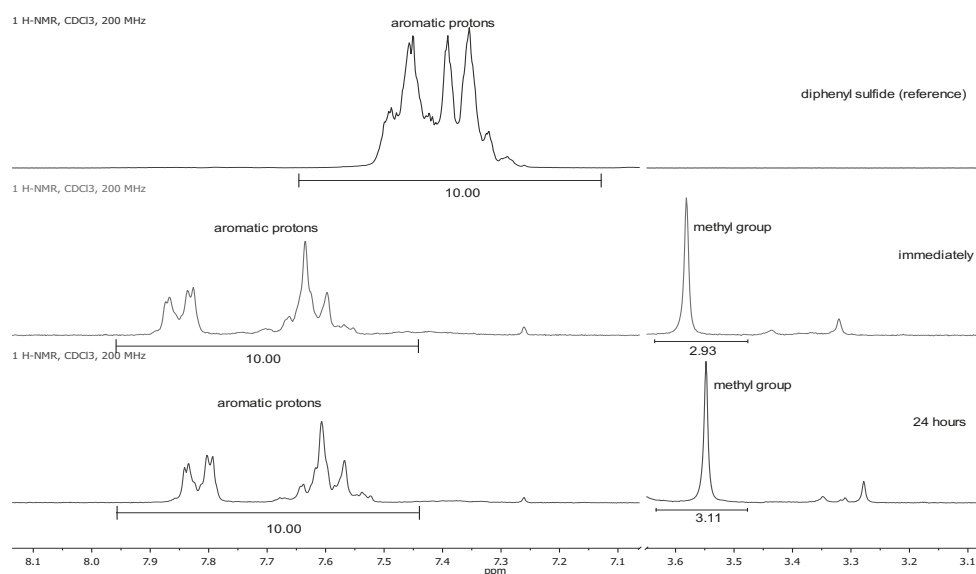


**Figure 45:** NMR spectra of the methylation of phenyl sulfide with iodomethane.

- 1: sample before reaction, reference
- 2: sample immediately after addition of methylating agent
- 3: sample after 24 h reaction time.

The conversion with trimethyloxonium tetrafluoroborate (see figure 46) is much slower than with iodomethane. After 30 min only small amounts of methyl sulfonium are present, the conversion seems to be nearly complete after 24 hours.

Trimethyloxonium tetrafluoroborate therefore proved to be a milder methylating agent than iodomethane. Additional studies showed that polyaromatic sulfur heterocycles are methylated by trimethyloxonium tetrafluoroborate only to a small extent, so that for the mass spectrometric determination of sulfides trimethyloxonium tetrafluoroborate can be very useful as it is more selective towards sulfides and more gentle than iodomethane, a reagent that is able to methylate even polyaromatic hydrocarbons in the ring after longer reaction times.

Because of the good results for phenyl sulfide, the methylation with trimethyloxonium tetrafluoroborate was also tested with the corresponding disulfide, phenyl disulfide. The

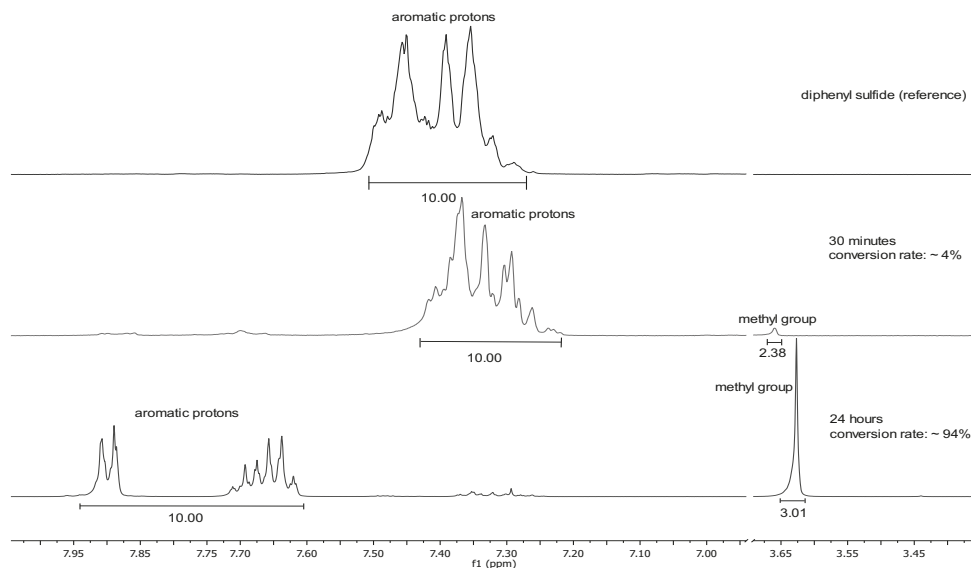


**Figure 46:** NMR spectra of the methylation of phenyl sulfide with trimethyloxonium tetrafluoroborate.

- 1: sample before reaction, reference
- 2: sample after 30 min reaction time
- 3: sample after 24 h reaction time.

disulfide reacts more slowly than the sulfide and even after 24 hours a complete conversion to the methylated product had not taken place (see figure 47). Trimethyloxonium tetrafluoroborate is not the methylation agent of choice for disulfides, because conversion is very slow and incomplete. In addition to the methyl group also two additional signals appear in the higher field range at 3.22 ppm and 3.17 ppm. The signal at 3.22 ppm could correspond to another methyl group, possibly originating from a disulfide that was methylated twice. But as no comparable literature values were available this assumption can not be confirmed. As the signals of the products and the starting material overlap multiply, no quantification of the amount of disulfide converted can be made. Considering the still remarkably high signals for the aromatic protons of the starting material, only a small fraction of it was converted during the reaction.

The methylation experiments showed that both sulfides and disulfides can be methylated but to different extents. Whereas sulfides readily react, disulfides barely react after 24 h of methylation time at all. As the reaction with the oxonium salts is significantly slower for sulfides as well, for the further experiments iodomethane will be used, as it readily

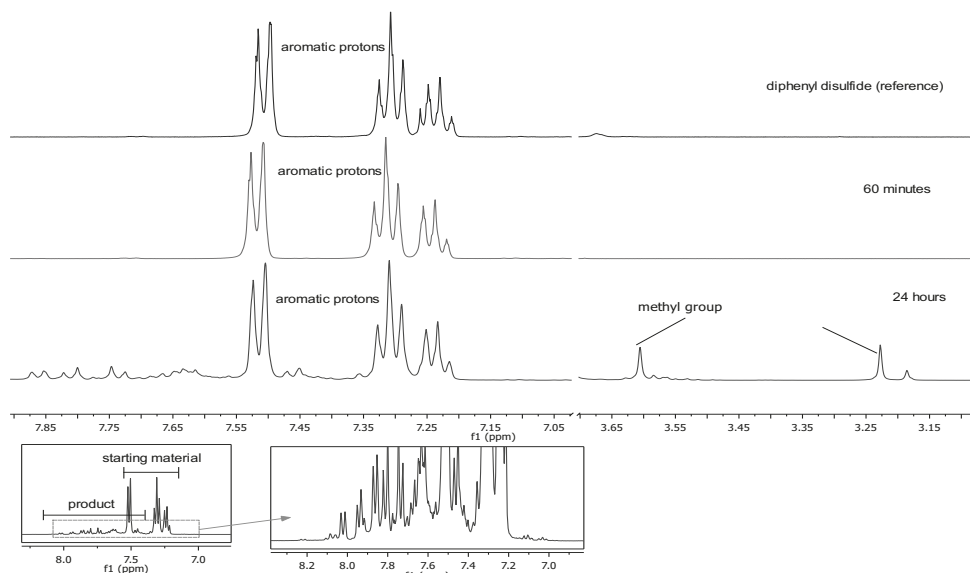


**Figure 47:** NMR spectra of the methylation of phenyl disulfide with trimethyloxonium tetrafluoroborate.

- 1: sample before reaction, reference
- 2: sample after 60 min reaction time
- 3: sample after 24 h reaction time.
- 4: magnification of spectra after 24 h reaction time.

reacts with sulfides within seconds, drastically reducing expenditure of total analysis time.

#### 7.4 Separation of vacuum gas oils

In the previous chapter several different stationary phases have been evaluated using standard compound mixtures. To verify the results for real world samples, the three phases with the best performance were used to separate vacuum gas oils (compare section 6). For this purpose, mainly the samples supplied by BP with boiling points of 369-509 °C and 509-550 °C are used.

The stationary phases used to separate these crudes are:

**PdSO<sub>4</sub>-Alox:** It is able to separate aliphatics, polyaromatic hydrocarbons (PAHs), PASHs and sulfides. Disulfides are irreversibly retained on this phase.

**hAg-MPSG:** This stationary phase is able to separate a standard mixture into aliphatics, aromatics including PASHs and non-thiophenic sulfur, but some non-thiophenic sulfur cannot be released from the column.

**Ag-Cartridges:** With standard substances these cartridges were able to separate a crude oil into aliphatics, aromatics including PASHs and non-thiophenic sulfur. Even disulfides can be released from this material, but only partially.

To analyze the separated fractions different mass spectrometric techniques were applied, including APCI-FT-ICR and ESI-, APCI-, APPI- and APLI-Orbitrap. Furthermore, for a selected set of samples GC x GC SCD analysis was performed by BP. In addition to the open column chromatographic separations, also HPLC separations on the PdSO<sub>4</sub>-Alox phase were performed and via coupling of the HPLC to APCI-Orbitrap online-mass spectra could be recorded.

#### 7.4.1 Separations of VGOs on PdSO<sub>4</sub>-Alox

The separation of the samples on PdSO<sub>4</sub>-Alox in open column chromatography was first checked with GC-FID and GC-AED (see exemplarily for Albacora Leste figures 48 and 49, for the remaining samples see section 10.3).

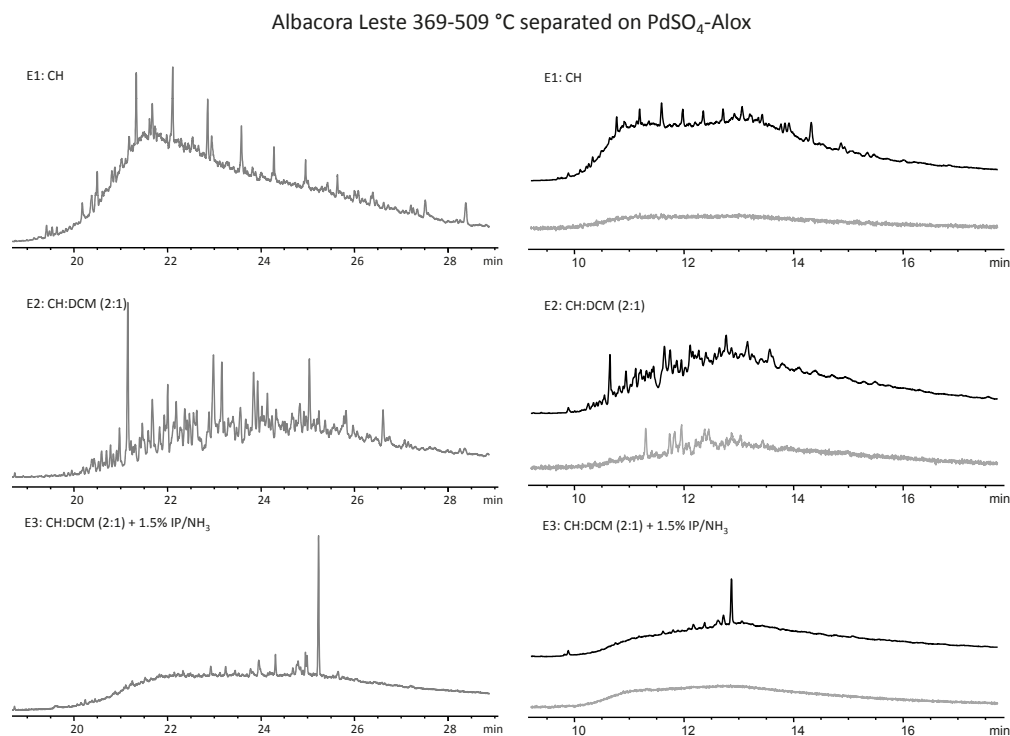


**Figure 48:** GC chromatograms of the separation of Albacora Leste 369-509 °C on PdSO<sub>4</sub>-Alox. Left: GC-FID, right: GC-AED with carbon (upper) and sulfur trace (lower).

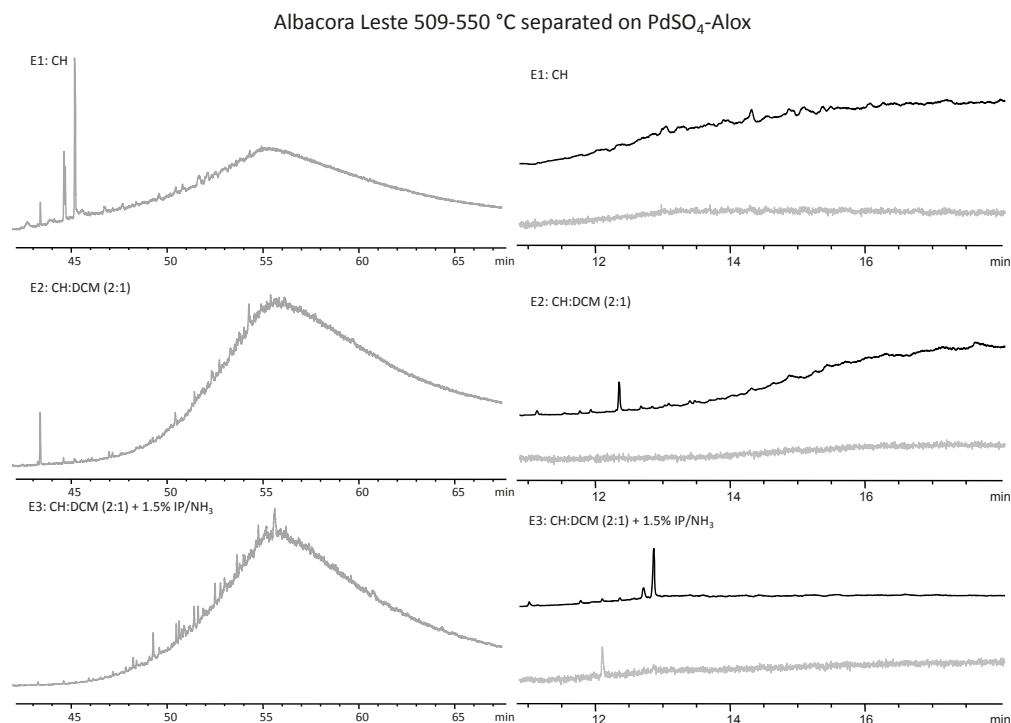


**Figure 49:** GC chromatograms of the separation of Albacora Leste 509-550 °C on PdSO<sub>4</sub>-Alox. Left: GC-FID, right: GC-AED with carbon (upper) and sulfur trace (lower).

Due to the high complexity of the sample, even the GC chromatograms are very complex and only occasionally isolated peaks are detected. For the first fraction, the characteristic regular pattern of homologous series of alkanes can be found for the lower boiling fraction Albacora Leste 369-509 °C. For lower boiling petroleum cuts, gas chromatography is the standard technique for analysis. But when taking a closer look at the results for the high boiling fraction with a boiling point of 509-550 °C (see figure 49), it becomes obvious that GC analysis is limited. Due to the size of the compounds, even for simple alkanes numberless constitutional isomers are possible. The supercomplex mixture petroleum therefore is just too complex to be resolved, even with huge theoretical plate numbers (GC: about 50,000, HPLC: about 5,000[26]). The higher boiling the petroleum cuts, the more the gas chromatogram cannot be resolved into individual peaks and only humps appear through the entire chromatogram. In GC-AED the concentrations of the individual sulfur compounds in the samples are too low after separation, so that the detection of those compounds via AED is not possible as the limit of detection is not reached. The one exception is the second fraction of Albacora Leste 369-509 °C, where individual signals for the aromatic sulfur compounds present in the fraction can be found

in the AED chromatogram. For a successful sulfur detection with AED, therefore the fractions of several separations need to be combined, while losing the information about the quality of each individual separation. Hence, sulfur determinations were hereinafter performed using either GCxGC SCD or external determination of the total sulfur in a fraction according to DIN EN ISO 20884.

After the separation on the palladium sulfate phase, mass spectrometry is applied to obtain more information, especially from the high boiling fractions either using ESI-MS after methylation or APCI-MS without pretreatment. To illustrate the efficiency of the separation of vacuum gas oils on PdSO<sub>4</sub>-Alox, the Kendrick plot of the S1 compounds of the separation of Albacora Leste 369-509 °C are displayed in figures 50 to 52 as an example and summarized in a box plot displayed in figure 53. For clarity the box plots for the other samples can be found in section 10.3 in the appendix.

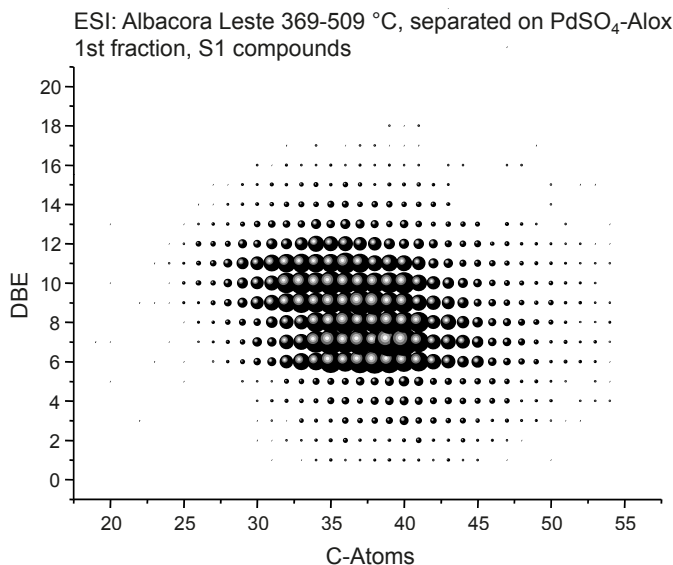


**Figure 50:** Kendrick plot of the S1 compounds in the first fraction of the separation of Albacora Leste 369-509 °C on PdSO<sub>4</sub>-Alox.

By taking a look at the Kendrick plots presented, it becomes obvious that PdSO<sub>4</sub>-Alox is not able to elute PASHs in one fraction. Already in the first fraction numerous sulfur containing compounds with DBE ranging mainly between six and twelve, corresponding to benzothiophenes and dibenzothiophenes, can be found. A breakthrough of smaller PASHs like thiophenes and benzothiophenes is not surprising, as this is also the case

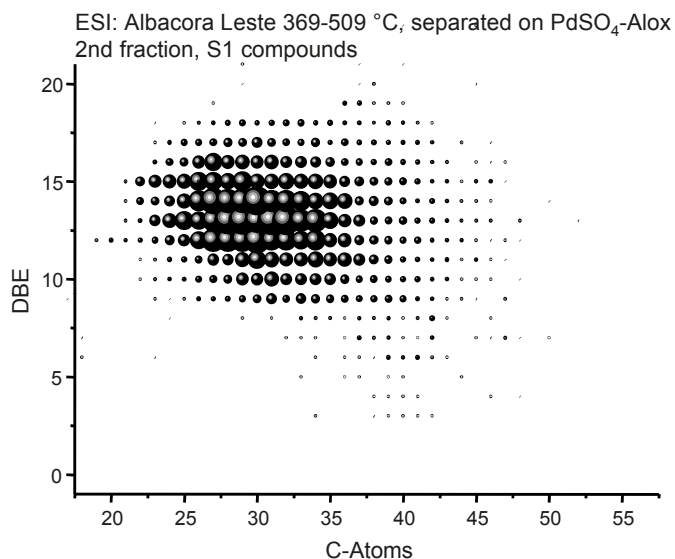


**Figure 51:** Kendrick plot of the S1 compounds in the second fraction of the separation of Albacora Leste 369-509 °C on PdSO<sub>4</sub>-Alox.

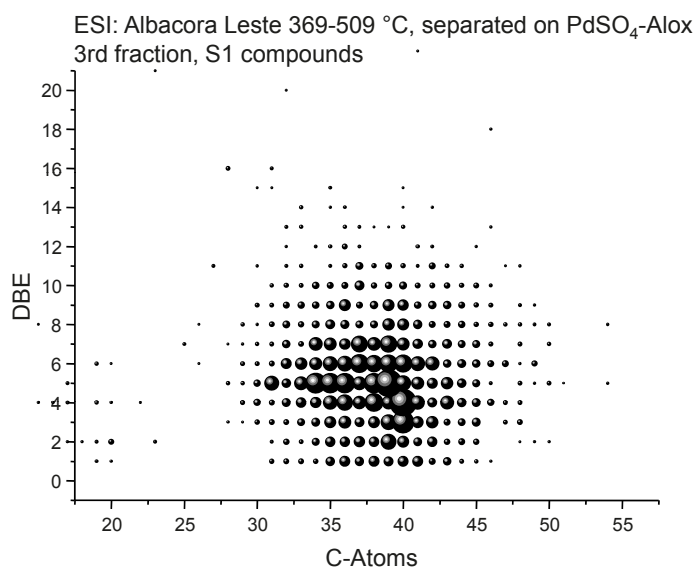


**Figure 52:** Kendrick plot of the S1 compounds in the third fraction of the separation of Albacora Leste 369-509 °C on PdSO<sub>4</sub>-Alox.

when separating a crude oil on well established LEC phases like Pd-MPSG. But the early elution of larger PASHs like dibenzothiophenes shows that the interaction of the palladium ion with the sulfur containing analytes, being bound on the PdSO<sub>4</sub>-Alox, is different from the interactions on the Pd-MPSG. Instead of by a ligand, the palladium

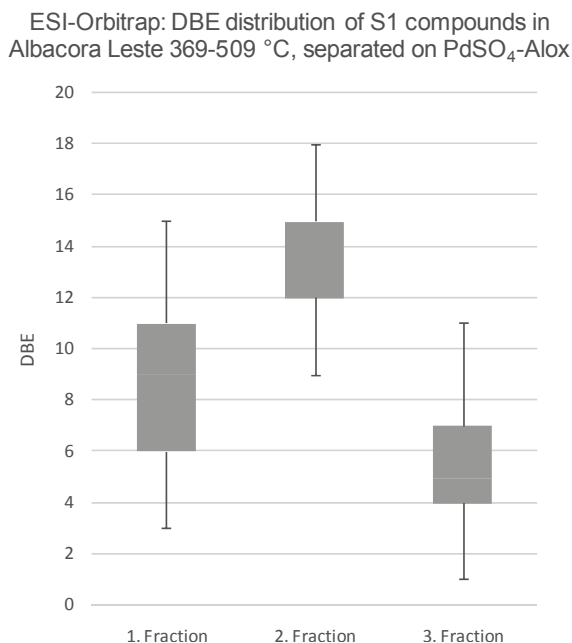


**Figure 53:** Box plot of the S1 compounds of the separation of Albacora Leste 369-509 °C on PdSO<sub>4</sub>-Alox.

is directly deposited onto the supporting material. Also the change in color during preparation from brownish-reddish via metallic deposition towards dark gray (see figure 54) is an indication that the oxidation state of the palladium ion is at least partially changed during this process.



**Figure 54:** Preparation of PdSO<sub>4</sub>-Alox. Left: directly after addition, middle: after 2 h, right: after 5 h.

The second fraction contains the larger PASHs as expected. Some dibenzothiophenes (DBE 9-11), but mainly benzonaphthothiophenes (DBE 12-14) and even larger PASHs with DBE 15-17 like benzophenanthrothiophenes can be found in this fraction. This highly aromatic content of the second fraction contrasts with the low DBE compounds



found in the third fraction. Starting at DBE 1, corresponding to cyclic sulfides, various degrees of unsaturated sulfides are present in this fraction. The higher DBE compounds with a DBE up to 10 found in this fraction might be aromatic sulfides or naphthenic ring structures.

To further characterize the sulfur containing compounds in the fractions, GCxGC SCD measurements were performed. The resulting chromatograms are displayed in figure 55.

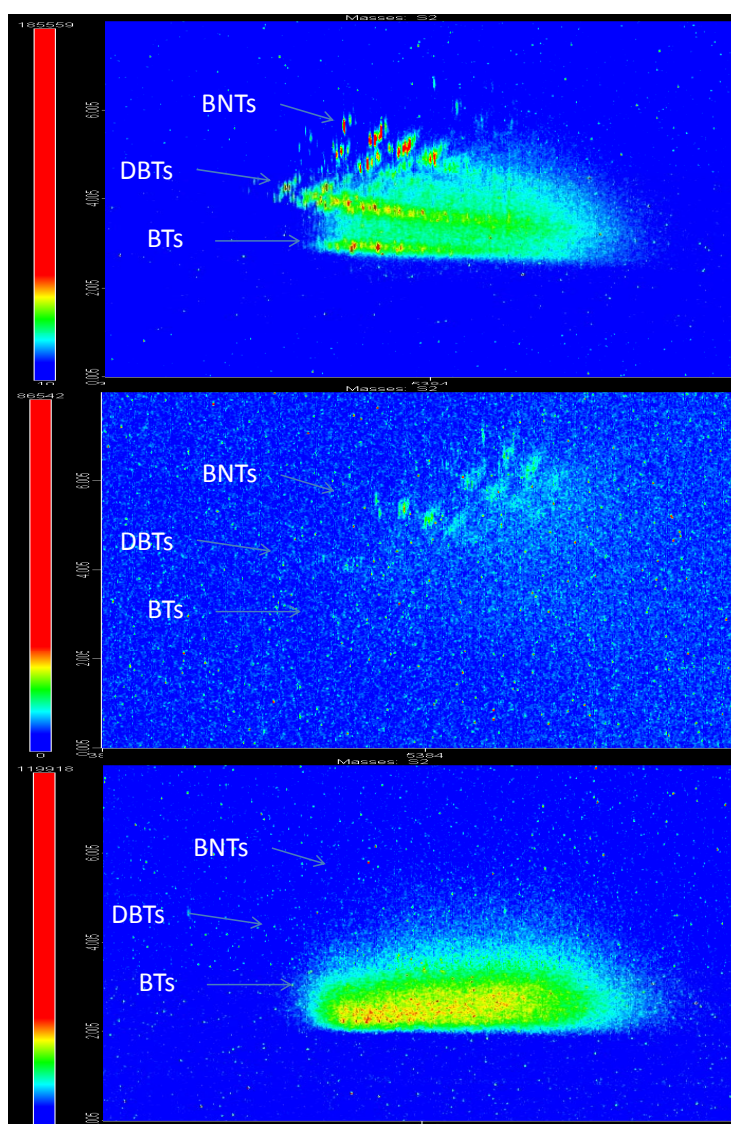


**Figure 55:** GCxGC SCD chromatograms of the separation of Albacora Leste 369-509 °C on PdSO<sub>4</sub>-Alox. Top: first fraction, middle: second fraction, bottom: third fraction.

GCxGC nicely confirms the results already seen in the Kendrick plots. In the first fraction PASHs have been found, including benzothiophenes, dibenzothiophenes and some benzonaphthothiophenes. The chromatogram of the second fraction shows the presence of larger PASHs, including the remaining benzonaphthothiophenes which were not eluted with the first fraction and benzophenanthrothiophenes or similar. In the third fraction no PASHs are present in the GCxGC SCD chromatogram, supporting the assumption that all sulfur in the third fraction is non-thiophenic. Hence, GCxGC measurements are in excellent agreement with the data collected by ESI-MS after methylation. The sulfur containing compounds eluted in the third fraction of the separation on PdSO<sub>4</sub>-Alox are most probably sulfides with multiple naphthenic ring units or aromatic side chains, but no PASHs that were eluted belatedly.

As a further proof of the presence of non-thiophenic sulfur in the third fraction UV/Vis spectra were recorded. Figure 56 shows the resulting spectra.

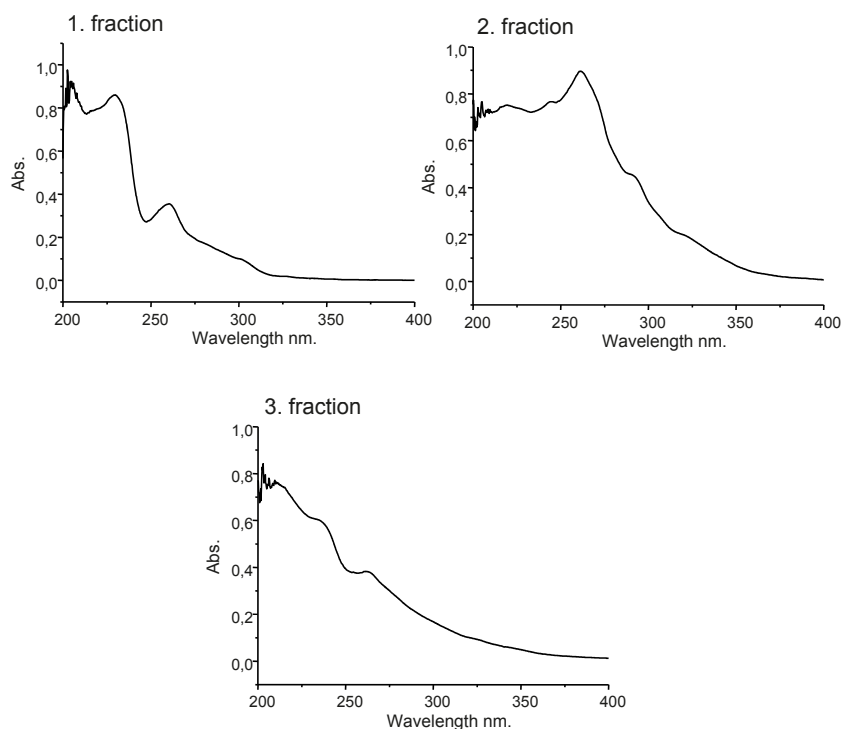


**Figure 56:** UV/Vis spectra of the separated fractions of Albacora Leste 369-509 °C separated on PdSO<sub>4</sub>-Alox. Upper left: first fraction, upper right: second fraction, bottom: third fraction.

The different composition of absorbing molecules in each fraction becomes immediately evident. Absorption in the aromatic range ( $\lambda = 200\text{-}300\text{ nm}$ ) is noticeable in all three fractions, but the proportion of the aromatic region is visibly reduced in the third fraction and declines quickly, whereas the spectra of the second fraction is at its maximum at about 260 nm. UV/Vis spectra suggest that aromatic structures are still present in the third fraction, but in combination with GCxGC data, excluding the possibility of the presence of remaining PASHs, it is probable and plausible that sulfidic compounds with aromatic sidechains make up a proportion of this fraction's sulfur containing compounds. The separations of Albacora Leste 509-550 °C and the three Karachaganak samples (96-369 °C, 369-509 °C and 509-550 °C) gave analogous results. The box plots for these separations can be found in section 10.3. For the high boiling fractions, however GCxGC reaches its limits in terms of thermal stability of the column and resolution. As already seen for the GC-FID and GC-AED chromatograms (compare figure 49), no individual signals can be detected when analyzing these high boiling samples. Figure 57 displays the GCxGC chromatograms of the separated fractions of Albacora Leste 509-550 °C separated on PdSO<sub>4</sub>-Alox.

The nice resolution of individual compound classes, e.g. different kinds of PASHs, that could be seen for the lower boiling fraction Albacora Leste 369-509 °C in figure 55 is now replaced by an undifferentiated spot for the first and second fraction. In the second fraction, still traces of benzophenanthrothiophenes and higher PASHs can be found and resolved, but the first and the third fraction can only be distinguished by the shape of the spots and the position. The compounds present in the third fraction elute a little bit earlier from the second dimension column, whereas the compounds in the first fraction are slightly more strongly retained on the GC column. Again, compared to the lower boiling fraction Albacora Leste 369-509 °C, this could be an indication for the presence of non-thiophenic sulfur in the third fraction, as for the lower boiling fraction it could be shown that PASHs have a stronger retention in the second dimension than non-thiophenic sulfur. But as the resolution of the GCxGC chromatograms is not sufficient for definite conclusions, these chromatograms were neglected in further discussions.

For the Karachaganak sample a third fraction with a boiling point of 96-369 °C was provided. Here, GCxGC is an ideal technique for the characterization of the sample as the compounds in this low boiling fraction have not as complex alkylation patterns due to their lower molecular weight. Therefore, the resolution is better, so that nearly individual compounds can be detected (see figure 58).

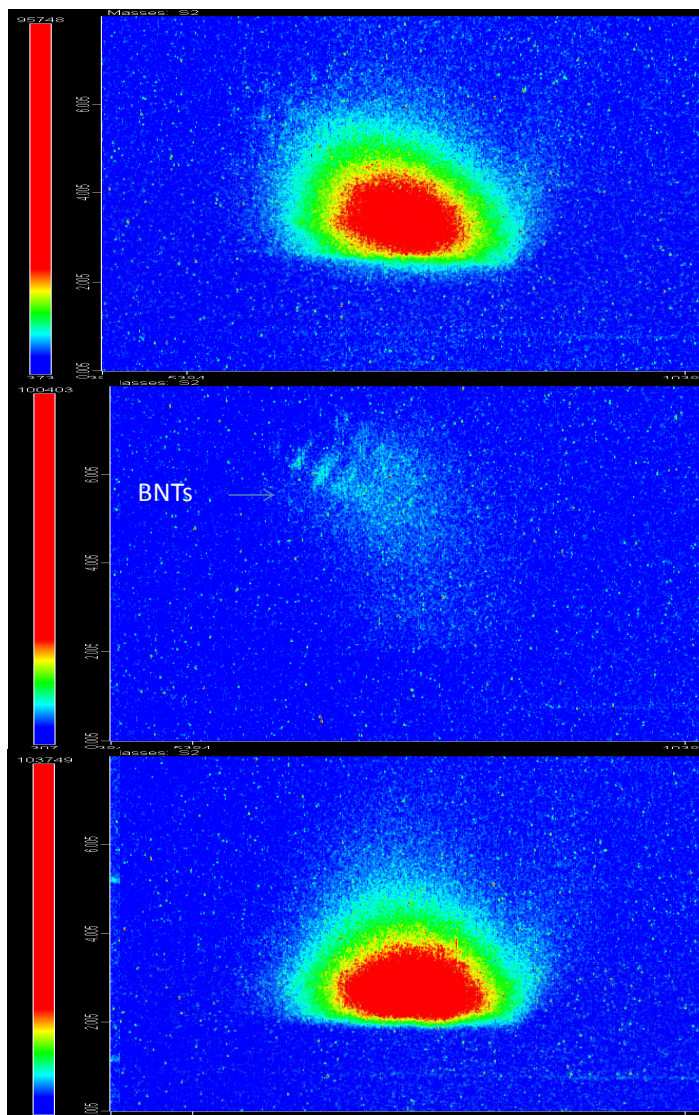


**Figure 57:** GCxGC SCD chromatograms of the separation of Albacora Leste 509-550 °C on PdSO<sub>4</sub>-Alox. Top: first fraction, middle: second fraction, bottom: third fraction.

The separation of the Karachaganak sample seems to be successful when considering only the GCxGC data, but when taking a closer look at the corresponding Kendrick plots of the S1 compounds of an identical separation (displayed in figure 59), the two data sets do not fit. In GCxGC clearly the most dominant sulfur containing compounds in the second fraction are dibenzothiophenes (DBE 9-11), but these compound class is scarcely present in the corresponding Kendrick plot. Also in the Kendrick plot of the second fraction an early elution of compounds with low DBE is observable, that does

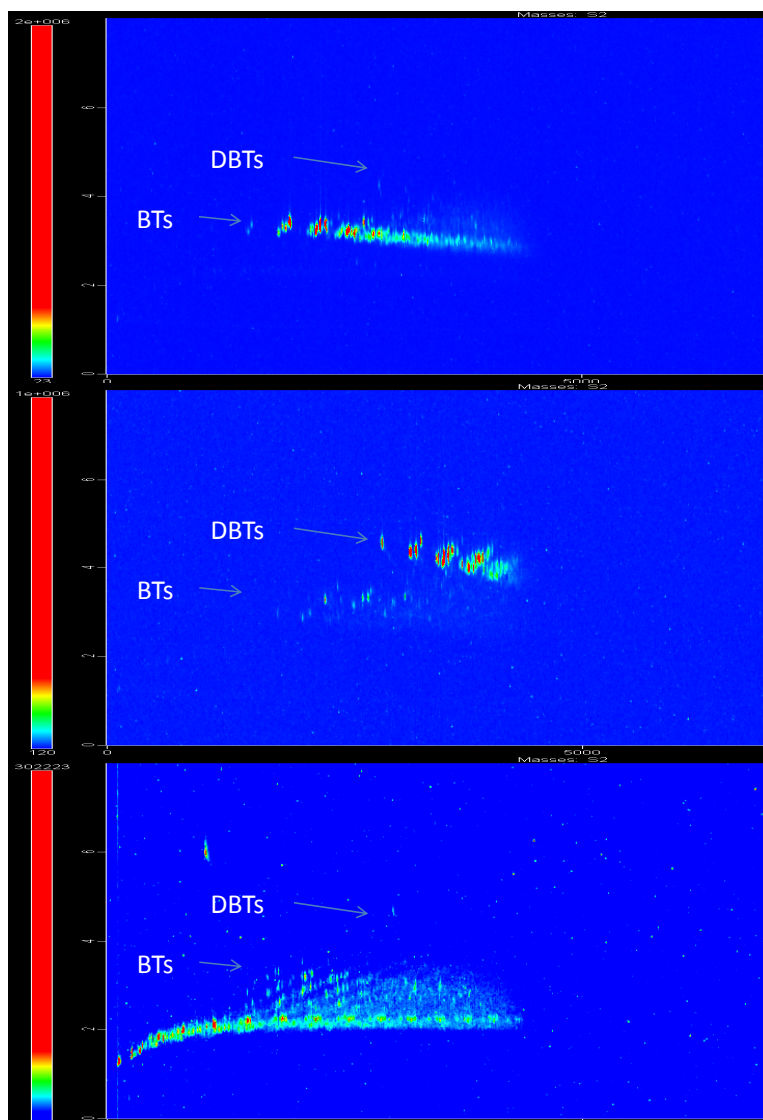


**Figure 58:** GCxGC SCD chromatograms of the separation of Karachaganak 96-369 °C on PdSO<sub>4</sub>-Alox. Top: first fraction, middle: second fraction, bottom: third fraction.

not appear in the GCxGC chromatogram. Either intensities of the signals of the sulfur containing compounds vary strongly between GCxGC SCD and ESI-Orbitrap or the repeatability of the separation is insufficient for this particularly low boiling sample.

As the molecular weight and the boiling point are lower for the compounds in this fraction, also the degree of aromatization and the size of the aromatic ring systems are expected to be smaller than in the higher boiling fractions. As to be expected,

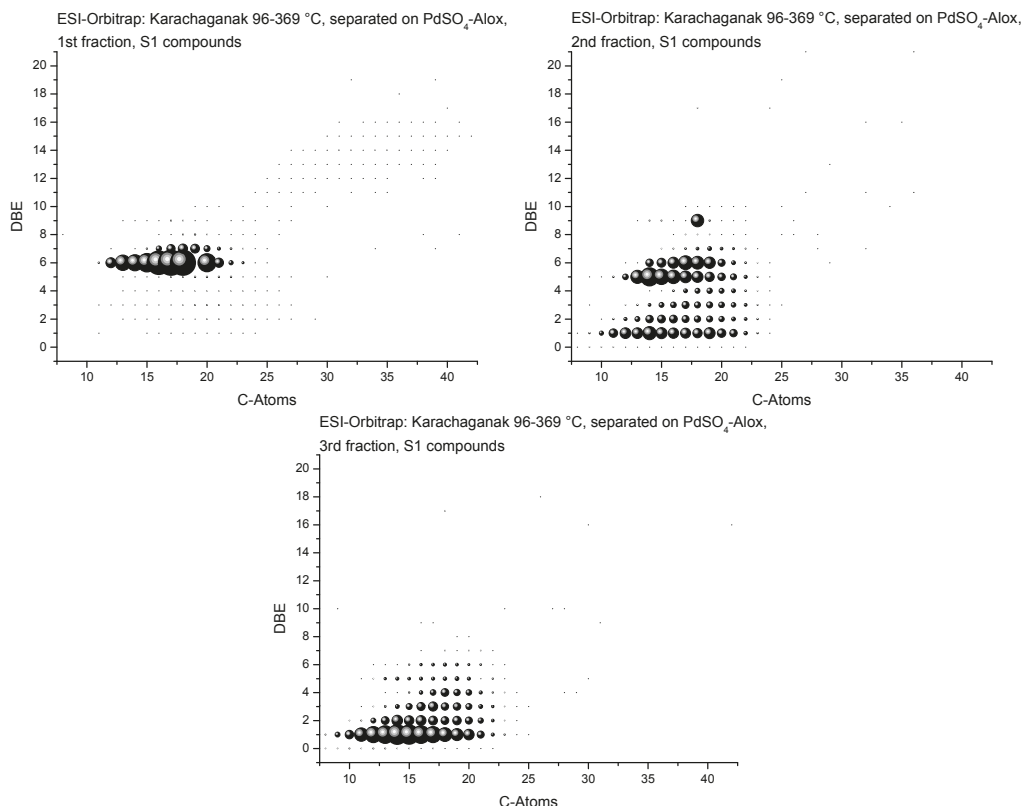


**Figure 59:** Kendrick plots of the S1 compounds of the separation of Karachaganak 96-369 °C on PdSO<sub>4</sub>-Alox, analyzed with ESI-Orbitrap after methylation. Upper left: first fraction, upper right: second fraction, bottom: third fraction.

dibenzothiophenes are the largest sulfur aromatics detectable in the sample. The first fraction mainly consist of benzothiophenes, whereas dibenzothiophenes and remaining benzothiophenes make up the compounds in the second fraction. Again, a successful separation into thiophenic and non-thiophenic sulfur is observable for this sample, as neither benzothiophenes nor dibenzothiophenes are eluted in the third fraction, but only non-thiophenic sulfur compounds. The sulfidic sulfur in this fraction is most likely of a rather aliphatic character, as the retention on the second dimension is even lower than for the the small PASHs. Furthermore, the molecular weight distribution seems to be widely spread, as the compounds are eluted in the first dimension over a wide time range. A significant amount of compounds is eluted very early indicating a high vapor pressure and therefore a low molecular weight. The MS analysis of this fraction is tricky, as during evaporation steps in the pretreatment especially compounds with high vapor pressure are most likely to get lost. On the contrary, in APCI and related techniques

the background noise for  $m/z < 200$  is so high that a distinction between signals from the analyte and background signals is not possible. As this is exactly the main  $m/z$  range for the Karachaganak 96-369 °C sample, mass spectra and the resulting plots generated from this sample should be treated with caution.

The separation on PdSO<sub>4</sub>-Alox has been successfully applied to the other VGO samples as well. Only when separating Winter ANS 509-550 °C, a deterioration of the quality of the separation was observable in early experiments. Sulfides were already partially eluted in the second fraction when using the previously used amount of 8 g stationary phase to separate 200 μL sample. An increase of stationary phase to 32 g proved that the early elution was caused by overloading of the stationary phase. The Kendrick plots of the second and third fraction of both separations with 8 and 32 g stationary phase, respectively, are shown in figure 60.

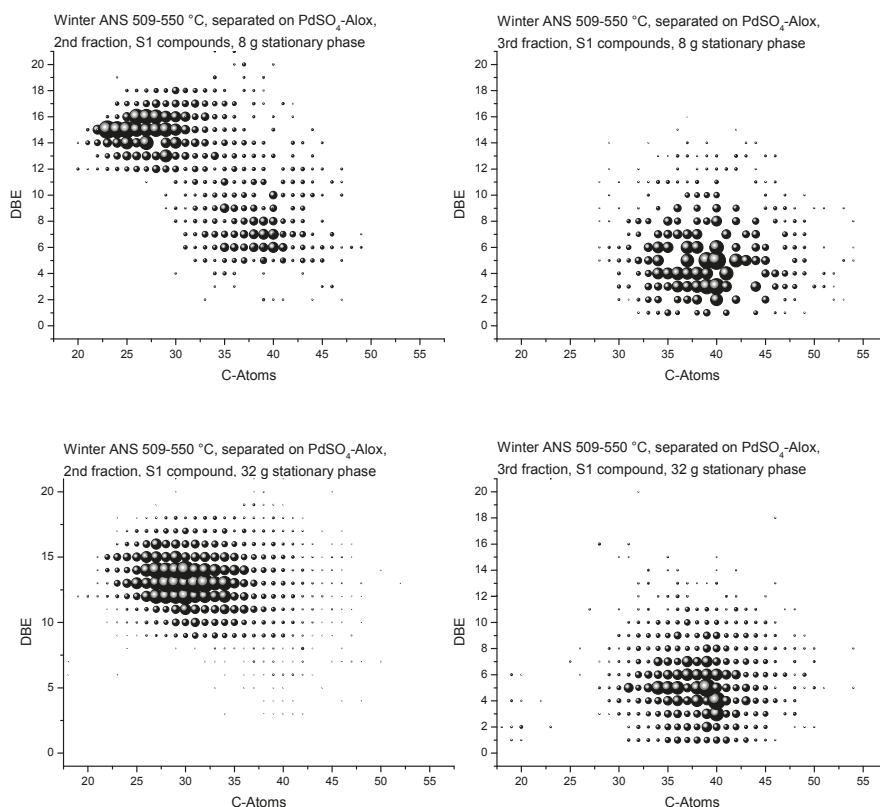


**Figure 60:** Kendrick plots of the second and third fraction of the separation of Winter ANS 509-550 °C on PdSO<sub>4</sub>-Alox with different amounts of stationary phase. Top: 2nd and 3rd fraction, 8 g stationary phase; bottom: 2nd and 3rd fraction, 32 g stationary phase.

In the case of Winter ANS thiophenic and non-thiophenic sulfur is even more easily distinguishable as the high aromatic PASHs are shifted towards lower carbon atom numbers compared to the sulfidic sulfur containing compounds. In both separations the second fractions consist of an aromatic PASHs pattern of benzophenanthrothiophenes and larger PASHs, when increasing the amount of stationary phase also dibenzothiophenes are retained more strongly and eluted in the PASH fraction. For the low amount of stationary phase in addition the sulfidic sulfur compounds with a larger number of carbon atoms are eluted in the second fraction. The compounds with  $5 < \text{DBE} < 10$  and between 30 and 50 carbon atoms are congruent with the ones found in the sulfidic fraction. In addition, when increasing the amount of stationary phase these compounds are not longer found in the second fraction, but in the third fraction only. This supports the assumption that overloading of the phase occurred and is responsible for the lower separation ability. Hence, for all further experiments the increased amount of 32 g stationary phase was used for the separation to ensure sufficient separation capacities and minimize overloading.

#### 7.4.2 Separations of VGOs on *h*Ag-MPSG

As already seen for the separation of the samples on PdSO<sub>4</sub>-Alox, the fractions were first checked with GC-FID and GC-AED. As an example again to allow a better comparison, the chromatograms for Albacora Leste 369-509 °C are displayed in figure 61. The corresponding chromatograms for the remaining samples can be found in the appendix in section 10.3. The GC chromatograms for the separation on *h*Ag-MPSG are comparable to the ones obtained from PdSO<sub>4</sub>-Alox (see figure 48). Again, the regular pattern of a homologous series of alkanes is visible in the GC-FID chromatogram of the first fraction and individual signals for sulfur containing compounds are only detectable in the second fraction of the GC-AED chromatograms.

APCI- and ESI-MS measurements were performed on the samples to gain deeper insight about the composition of the fractions. To visualize the separation of vacuum gas oils on *h*Ag-MPSG, as an example, the Kendrick plots of the S1 compounds of the separation of Albacora Leste 369-509 °C are displayed in figures 62 to 64 and further summarized in a box plot displayed in figure 65. For clarity, the box plots of the separations of the other samples can be found in section 10.3 in the appendix.



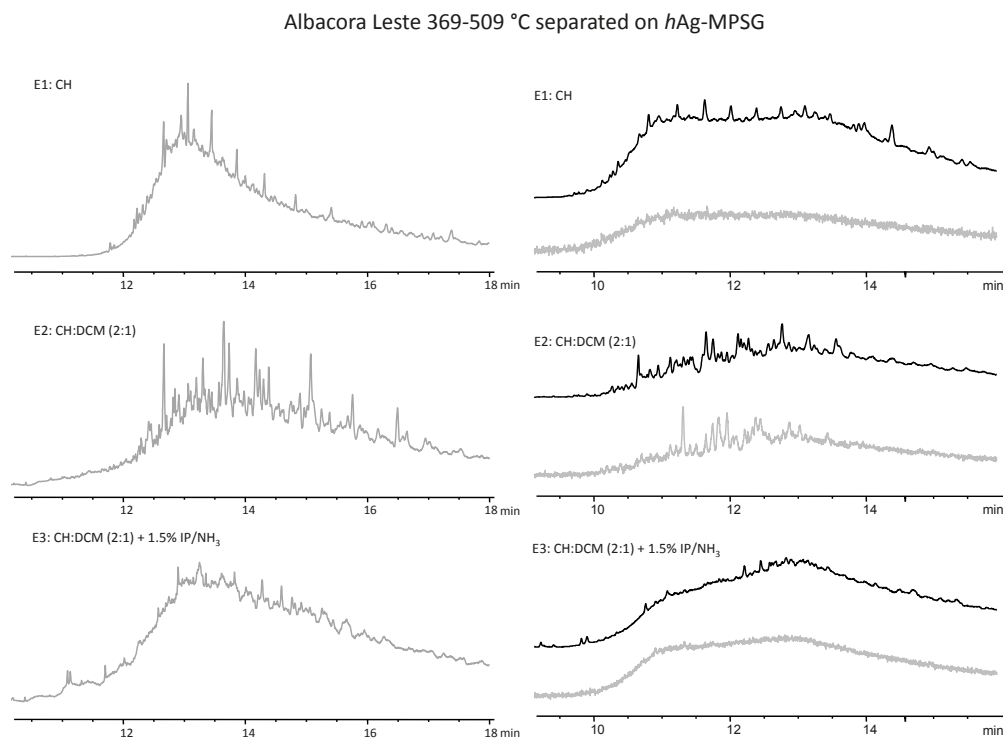


**Figure 61:** GC chromatograms of the separation of Albacora Leste 369-509 °C. Left: GC-FID, right: GC-AED with carbon (upper) and sulfur trace (lower).

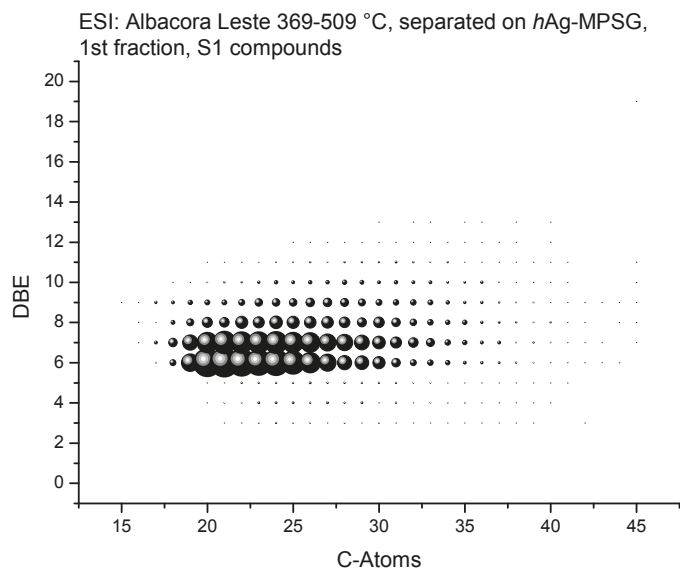


**Figure 62:** Kendrick plot of the S1 compounds in the first fraction of the separation of Albacora Leste 369-509 °C on *h*Ag-MPSG.

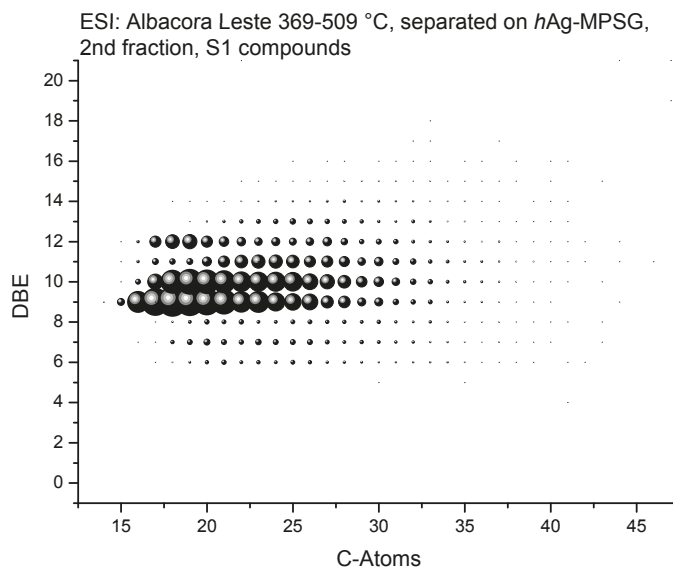


**Figure 63:** Kendrick plot of the S1 compounds in the second fraction of the separation of Albacora Leste 369-509 °C on *h*Ag-MPSG.

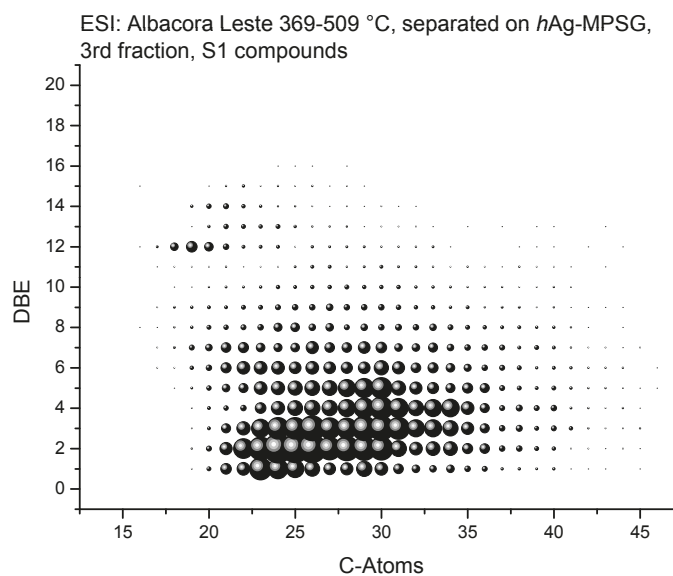


**Figure 64:** Kendrick plot of the S1 compounds in the third fraction of the separation of Albacora Leste 369-509 °C on *h*Ag-MPSG.

The first thing that comes to mind when looking at the Kendrick plots of this separation is the drastically lower maximum DBE of the compounds compared to the separation on PdSO<sub>4</sub>-Alox. Whereas compounds with a DBE up to 20 could be detected when analyzing the sample using the palladium based phase (compare figure 51), now the maximum

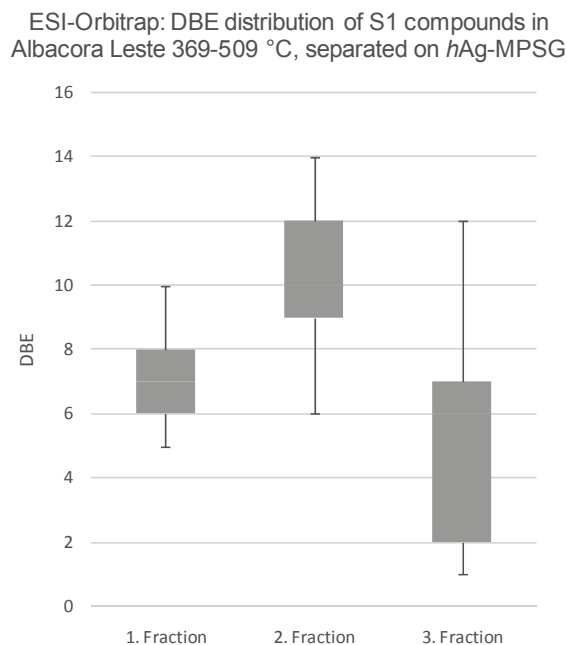


**Figure 65:** Box plot of the S1 compounds of the separation of Albacora Leste 369-509 °C on *h*Ag-MPSG.

DBE is 14. As the fractions from both separations were treated in the same manner, it is possible that the silver phase has a stronger interaction with larger aromatic ring systems, which are therefore retained more strongly on the phase. All in all, the Kendrick plots for the separation on the silver phase are less complex and rather simple. In the first fraction only benzothiophenes and traces of dibenzothiophenes are found, the second fraction consists of the remaining dibenzothiophenes and benzonaphthothiophenes. In the third fraction lower DBE sulfur containing compounds can be found, starting at a DBE of 1, representing cyclic sulfides. Also the main intensities of the compounds range around the non-aromatic DBE range of 1-3. Interestingly, some remaining benzonaphthothiophenes (DBE 12-14) are also eluted in this fraction. This is exactly the opposite situation from the one seen for the high boiling fractions on PdSO<sub>4</sub>-Alox. Instead of an overloading effect, now the higher PASHs are retained more strongly on the stationary phase and therefore carried over into later fraction. This also supports the assumption that the *h*Ag-MPSG phase interacts more strongly with larger aromatic compounds.

Further evidence for this assumption can be found in the literature. NOCUN and ANDERSSON describe the use of a silver based LEC stationary phase for the separation of PASHs according to the size of the aromatic ring system. [91] Using the  $\pi$ - $\pi^*$ -interactions of the silver ions with the condensed aromatic ring systems, it is possible to separate ben-

zothiophenes, dibenzothiophenes and benzonaphthothiophenes into different fractions. The same basic interactions are now observable for the *h*Ag-MPSG separations. Larger aromatic ring systems, e.g. benzonaphthothiophenes are more strongly retained and can only be eluted in later fractions than the smaller PASHs.

For further information and clarification GCxGC SCD measurements were obtained. The resulting chromatograms are displayed in figure 66.

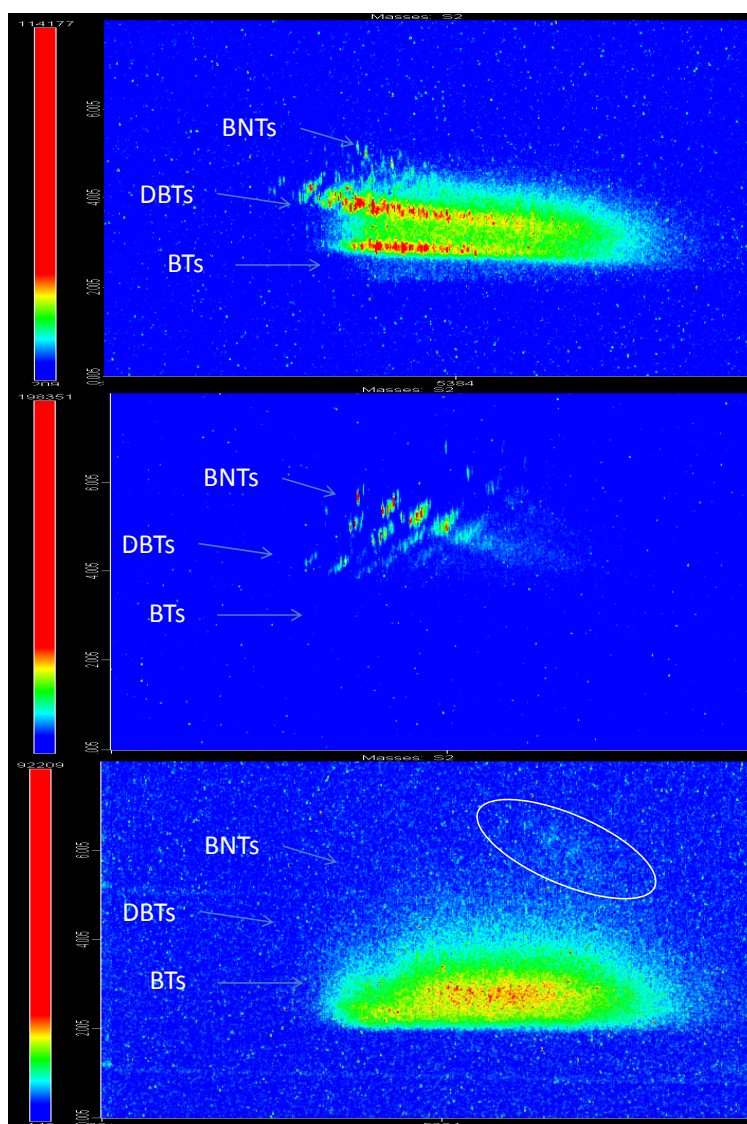


**Figure 66:** GCxGC SCD chromatograms of the separation of Albacora Leste 369-509 °C on *h*Ag-MPSG. Top: first fraction, middle: second fraction, bottom: third fraction.

Compared to the Kendrick plots, in the GCxGC chromatograms more PASHs can already be found in the first fraction. Besides benzothiophenes, also large amounts of dibenzothiophenes and even traces of benzonaphthothiophenes are observable in the GCxGC chromatogram of the first fraction. In the second fraction the remaining higher PASHs, including dibenzothiophenes, benzonaphthothiophenes and larger PASHs, are found. The pattern of the larger PASHs rises steeper than for the smaller sulfur aromatics and only low intensities can be found in the plot of the second fraction. Again this observation is in contrast to the data gained from ESI-MS experiments, where only compounds with a maximum DBE of 14, corresponding to benzonaphthothiophenes, could be assigned. The chromatogram of the third fraction shows mainly sulfidic sulfur as expected, but also traces of large PASHs can be found. GCxGC hence supports the observation made in ESI-MS that higher aromatized PASHs are more strongly retained on the silver phase and are therefore carried over into later fractions. This could be problematic especially for higher boiling samples, as the degree of aromaticity and molecular weight of the sample increase with increasing boiling point of the fraction. The carry over of larger aromatics will therefore be even more relevant for high boiling vacuum cuts.

Interestingly, when taking a look at higher boiling samples like Winter ANS 509-550 °C no enhanced retention effects of higher PASHs are observable (see figure 67).

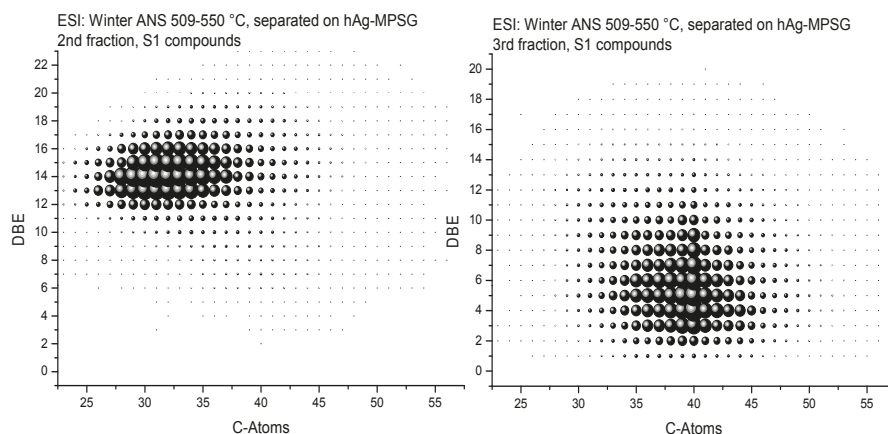


**Figure 67:** Kendrick plot of the S1 compounds in the second and third fraction of the separation of Winter ANS 509-550 °C on *hAg*-MPSG.

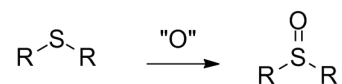
Here a nice separation between PASHs and non-thiophenic sulfur can be found and also higher DBE compounds are again detectable. The DBE range reaches up to about 20, which is even slightly higher than for the corresponding separation on PdSO<sub>4</sub>-Alox (see

fig. 60). At first sight, the chromatographic behavior and separation abilities of the *h*Ag-MPSG seem to be contradictory, but can be well explained by the preparation of the phase. To obtain the desired properties the synthesized Ag-MPSG is heat treated. This process was first reported by PENASSA. [90] What is tricky about this process is that the material is not very stable at elevated temperatures and easily burned when exposed to high temperatures or left at elevated temperatures for an extended period of time. During the heating the color of the material changes from pale yellow over dark yellow and orange towards brown and even black when it is exposed to too high temperatures. The best chromatographic results could be obtained from dark gamboge material, therefore the aim of every synthesis was to achieve similarly colored material. But between individual batches variations are unavoidable. This variation in the preparation might result in the slightly different chromatographic properties observed between the separations of different crude oils. The silver phase is therefore hard to handle and not suitable for routine analysis.

#### 7.4.3 Separations of VGOs on Ag<sup>+</sup>-cartridges

As the GC-FID and GC-AED chromatograms of the separations on *h*Ag-MPSG and PdSO<sub>4</sub>-Alox only gave little information and already met their limits in terms of limit of detection, the even less concentrated fraction from the separation on the silver ion cartridges were directly analyzed using mass spectrometry. Again, to allow a better comparison the separation of Albacora Leste 369-509 °C is chosen as an example.

In contrast to the previously shown mass spectrometric data, now for the first time APCI spectra will be discussed. Compared to ESI, there is one particular aspect to keep in mind when analyzing sulfur containing compounds in APCI. The conditions in the source are harsher than in ESI, so that the oxygen from the air present in the source is able to at least partially oxidize sulfides present in the ion source (see figure 68).



**Figure 68:** Oxidation of sulfides within the APCI source

Therefore, not only S1 compounds, but also S1O compounds need to be taken into consideration, when discussing the elution of the sulfides from the stationary phases. Furthermore, as sulfoxides can be present in the untreated sample, a pre-separation on alumina is absolutely necessary to remove the S1O compounds originating from the

sample to make sure all detected S1O species in the mass spectra were indeed generated in the source, especially as sulfoxides would also be eluted in the non-thiophenic fractions together with the corresponding sulfides, as could be shown in standard separations (see figure 69).

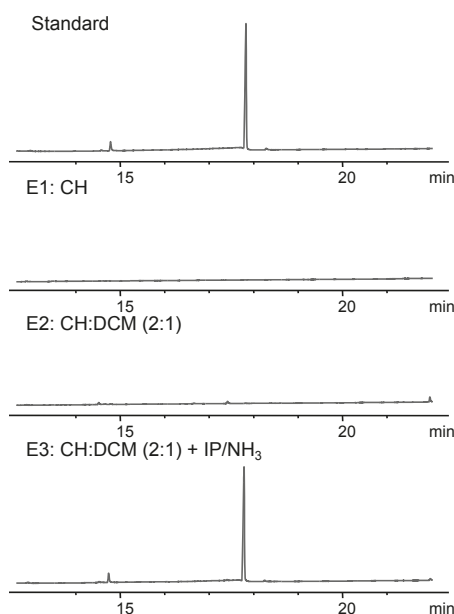


**Figure 69:** GC-FID chromatograms of the separation of phenyl sulfoxide on  $\text{Ag}^+$ -cartridges. Standard solution (top), 1st fraction, 2nd fraction, 3rd fraction (bottom), \*= contamination.

But as the capacity of the  $\text{Ag}^+$ -cartridges is anyway reduced compared to the self-prepared stationary phases as they are prepacked and only below 1 g of stationary phase is in one cartridge, a preseparation is almost indispensable to reduce other components of the crude oil like PANHs or other polars, which could occupy interaction sites on the stationary phase and further reduce the capacity of the cartridge. And the preseparation can also be used as a dilution step of the crude oil. As the pre-separated crude is redissolved in cyclohexane, the dosage of the small volume loaded on the cartridges is easier to measure due to the dilution by the solvent.

The Kendrick plots of the APCI-MS results for the individual fractions are now displayed in figures 70 to 72. As S1O compounds could be assigned in the third fraction, they will also be displayed. In the remaining fractions no S1O compounds were found. The distribution of S1 and S2 compounds in the fraction is also illustrated in the box plots

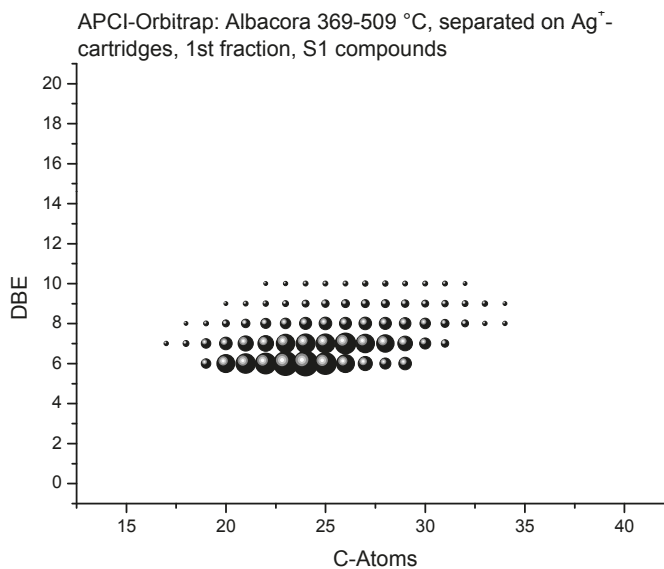


**Figure 70:** Kendrick plot of the S1 compounds in the first fraction of the separation of Albacora Leste 369-509 °C on Ag<sup>+</sup>-cartridges.

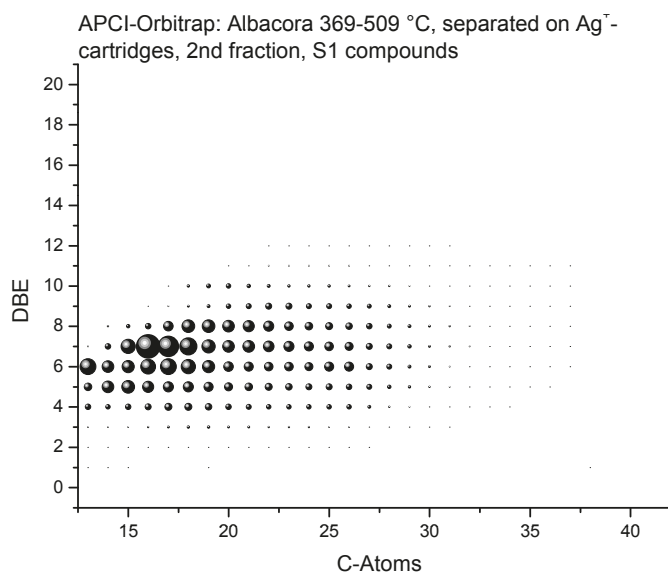


**Figure 71:** Kendrick plot of the S1 compounds in the second fraction of the separation of Albacora Leste 369-509 °C on Ag<sup>+</sup>-cartridges.

in figure 73. The corresponding box plots for the remaining samples can be found in the appendix in section 10.3.

On a first glance, the results are similar to the ones obtained on the *h*Ag-MPSG. The first fraction contains mainly benzothiophenes with additional naphthenic rings (see figure



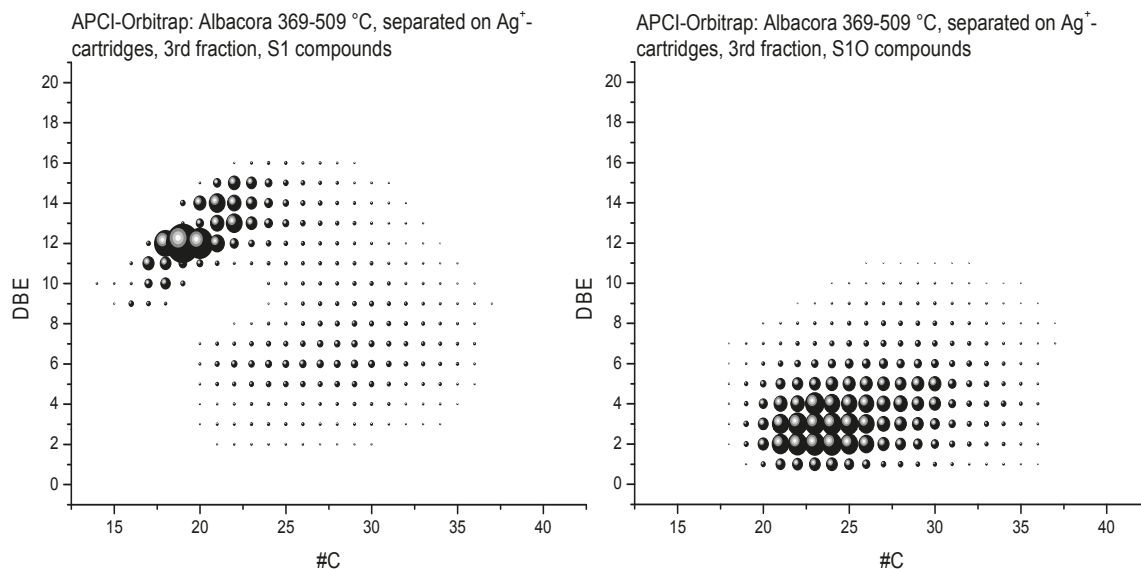


**Figure 72:** Kendrick plot of the S1 and S10 compounds in the third fraction of the separation of Albacora Leste 369-509 °C on Ag<sup>+</sup>-cartridges.

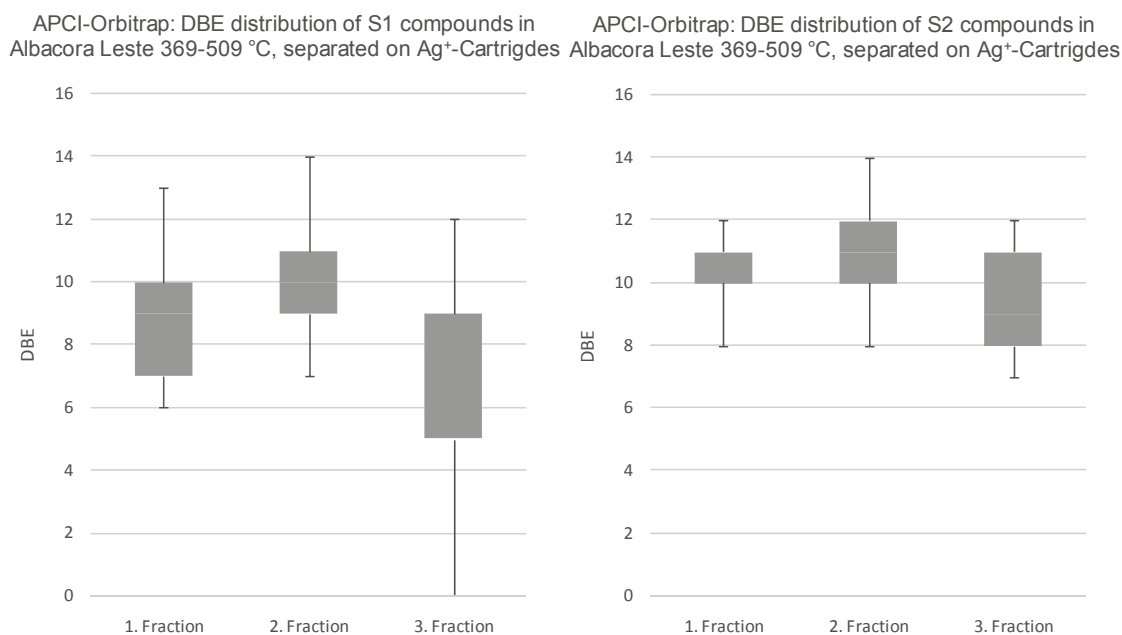


**Figure 73:** Box plot of the S1 and S2 compounds of the separation of Albacora Leste 369-509 °C on Ag<sup>+</sup>-cartridges.

70), in the second fraction also benzothiophenes as well as dibenzothiophenes can be found (see figure 71). Only in the third fraction the higher aromatic sulfur containing compounds like benzonaphthothiophenes and benzophenanthrothiophenes can be eluted.

Again, the interactions of the silver ions with the large aromatic ring systems seem to delay the elution of 4- and 5-ring PASHs so that the larger PASHs are carried over in the third fraction instead of eluting in the second fraction. In the Kendrick plots for the third fraction also nicely the effect of the oxidation of sulfides in the APCI source is shown. Whereas the PASHs with their high DBE range are only found in the Kendrick plot of the S1 compounds, the sulfidic sulfur compounds with  $1 < \text{DBE} < 10$  and 20 to 30 carbon atoms are present in both the plot for the S1 and the S1O compounds. The distribution patterns of both plots in this area are almost identical.

Using APCI also some S2 compounds could be assigned in the mass spectra. Their distribution is illustrated on the right side of figure 73. All S2 compounds found are rather aromatic and can be found in all three fraction. This indicates that the two sulfur atoms in the S2 compounds are probably integrated in aromatic structures, e.g. as thienothiophenes. The presence of S2 compounds in the third fraction might be either caused by a carry-over of PASHs with two sulfur atoms due to stronger interactions with the silver ions or the presence of mixed species of PASHs with a sulfidic sidestructure, e.g. partially hydrated thienothiophenes. But these are only speculations, as simple MS experiments alone are not sufficient for structural clarification. Fragmentation or NMR experiments can be further approaches in this matter.

Albacora Leste 369-509 °C, in fact, showed one of the worst separations on the silver ion cartridges. Karachaganak 369-509 °C and 509-550 °C, as well as Winter ANS 509-550 °C, could be separated more efficiently with less effects of the carry-over of larger PASHs. Therefore, in addition the Kendrick plots of the separated fractions of Winter ANS 509-550 °C on the  $\text{Ag}^+$ -cartridges are compiled in figure 74.

As the analyzed fraction is higher boiling than the Albacore Leste sample discussed previously, the compounds present in the Winter ANS sample have a higher degree of unsaturation and alkylation due to their higher boiling point. Also compared to Albacora Leste, Winter ANS also has a higher degree of aromatization (see table 13. Here, dibenzothiophenes and benzonaphthothiophenes are eluted in the first fractions, whereas the 5- and even 6-ring sulfur aromatics are found in the second fraction together with remaining 3- and 4-ring PASHs. The scattered pattern of the distribution of compounds in the first and second fraction do not originate in the sample, but are caused by instrumental errors during the measurement. As the processing of the data is extensive, those errors are not self-evident when recording the mass spectra and only obvious after post-processing. As the access to the instrument was limited, no additional measurement could be performed. In contrast to the separation of Albacora Leste 369-509 °C on

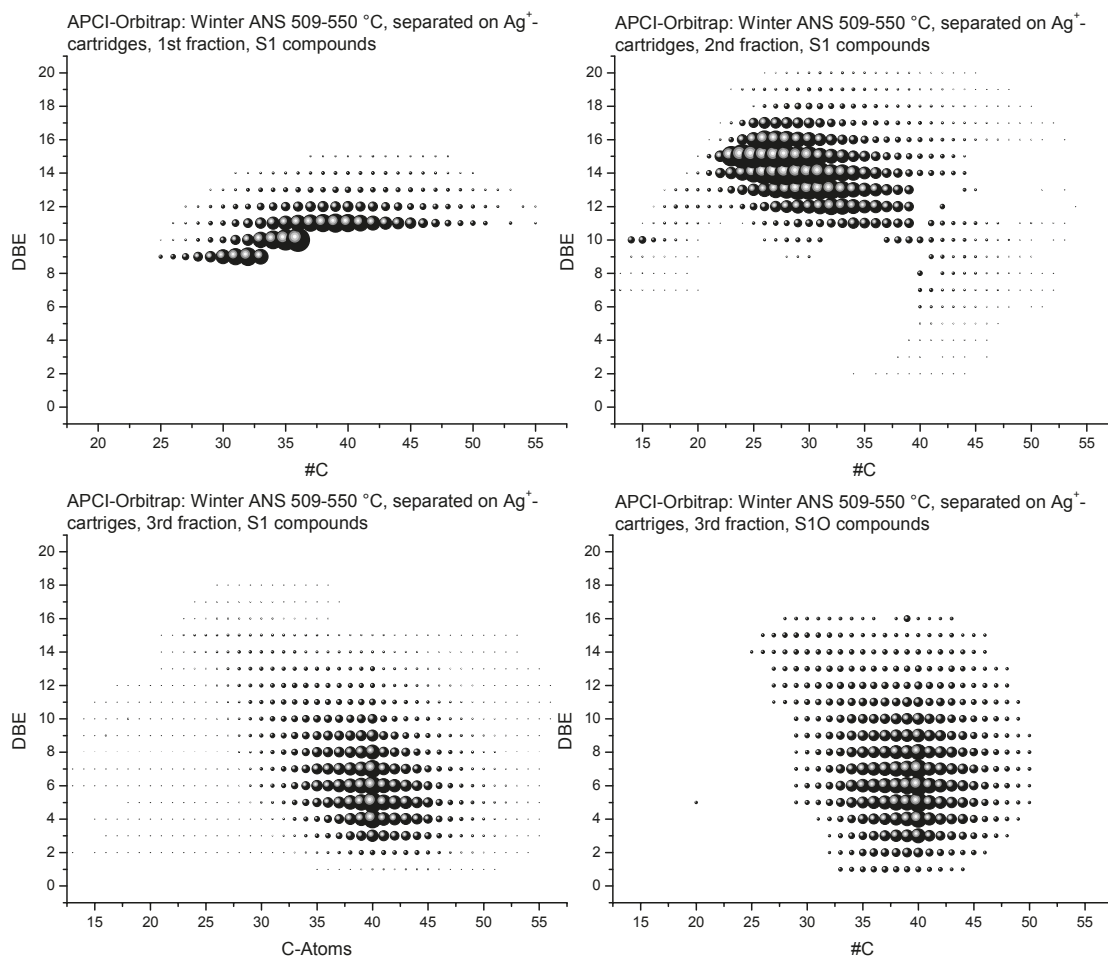


**Figure 74:** Kendrick plot of the S1 and S1O compounds in the fractions of the separation of Winter ANS 509-550 °C on Ag<sup>+</sup>-cartridges.

the very same material, there is nearly no carry-over of PASHs in the third fraction, as can be seen by comparing the plots for the S1 and S1O compounds of the third fraction. The regularly distributed sulfidic sulfur compounds can be detected as S1 and are also partially oxidized to S1O compounds in the sample. Again, of course S1 compounds already present in the sample have been removed prior to the separation on the silver ion cartridges by a pre-separation on alumina.

As the separations on Ag<sup>+</sup>-cartridges were performed at a later stage of this work, no GCxGC measurements are available for the fractions as the access to the GCxGC instrument was limited. But as APCI proved to be suitable as a tool for the discrimination of PASHs and sulfidic sulfur in separated fractions, the quality of the separation could be verified by mass spectrometry. The silver ion cartridges showed for some samples an

increased interaction of large PASHs and therefore a carry-over of these aromatic sulfur compounds into the non-thiophenic fraction. Due to its limitations concerning size of the column and amount of stationary phase used for a separation, the number of interactions sites on the phase and therefore the capacity of the column is also very limited. Supercomplex mixtures like crude oils or VGO easily overload the column and pre-separations are indispensable. Due to SPE automation units, the separation might be well suitable for routine analysis. Compared to the other prepared stationary phases, the amounts of solvents needed for the separation are significantly reduced and the quality of the material is consistent as the cartridges are commercially available.

#### 7.4.4 Online HPLC-MS separations on PdSO<sub>4</sub>-Alox

In addition to the separations of VGOs in open column chromatography on the tested LEC phases, the developed separations were transferred to HPLC. For this purpose 10  $\mu\text{m}$  material was used for the preparation of the phases and the resulting material was packed into stainless steel HPLC columns at 400 bar. For both PdSO<sub>4</sub> and *h*Ag-MPSG the HPLC separations were first tested using UV-detection. Fractions of several runs were collected and subsequently analyzed via ESI-MS after methylation. Even this early experiments could show that the separation on *h*Ag-MPSG is not easily transferable to HPLC. The HPLC-UV chromatogram of the separation of standard substances on *h*Ag-MPSG is displayed in figure 75. In addition the box plot of the S1 compounds of the separation of Albacora Leste 369-509 °C is displayed in figure 76 and confirms that no efficient separation between thiophenic and non-thiophenic sulfur could be achieved using *h*Ag-MPSG in HPLC.

The third fraction contains a very wide DBE range of compounds from 1 to 13. In addition, an overlapping with the range of compounds previously eluted in the second fraction occurs. As carry-over of higher aromatic PASHs was already observable in the open column separations on this phase, it is very probable that the very same effects also hinder a good separation in HPLC. Hence, the *h*Ag-MPSG phase was not further used in HPLC due to weak performance.

For PdSO<sub>4</sub>-Alox also first fractions were collected and subsequently analyzed via ESI-MS after methylation. As better separations could be achieved than using the silver base phase, in the next step the HPLC phase was directly coupled to APCI-Orbitrap MS. Again when using APCI, sulfides are partially oxidized in the ionizing cells, so that they are detectable as S1O compounds as well as S1 compounds. To ensure the detected S1O

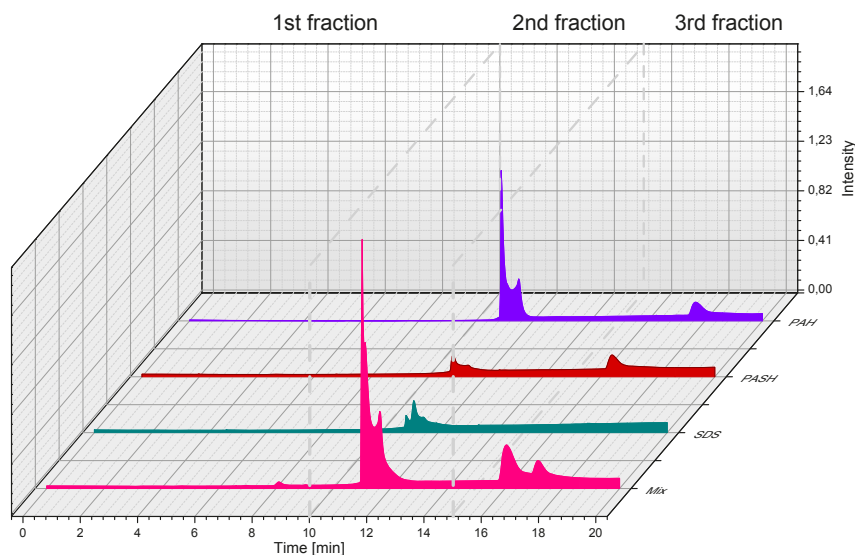


**Figure 75:** HPLC-UV chromatogram of the separation of several standard mixtures on *hAg-MPSG*.

PAHs (top): naphthalene, phenanthrene, chrysene; PASHs: benzothiophene, 3-methylbenzothiophene, dibenzothiophene, benzonaphtho[1,2-*d*]thiophene; sulfides & disulfides: phenyl sulfide, dodecyl methyl sulfide, octadecyl methyl sulfide, *n*-butyl disulfide, *t*-butyl disulfide, phenyl disulfide; combined mixture (bottom).

1st fraction: cyclohexane, 10 min,

2nd fraction: cyclohexane:dichloromethane 2:1, 5 min,

3rd fraction: cyclohexane:dichloromethane 2:1 + 15% isopropanol,

flow rate: 3 mL/min, detection at 254 nm.

species are generated in the source and do not originate in the sample prepreparations on alumina are absolutely necessary to remove sulfoxides originating from the sample. Also the prepreparations remove other polars like PANHs that might occupy the already limited interactions sites on the HPLC column. The removal of these compounds, which interact with the phase very strongly, prior to the separation also enhances the reusability of the HPLC phase. Polar compounds like PANHs would bind to the phase nearly irreversibly therefore each separation including this compound classes would further deactivate the interaction sites on the column as they are permanently blocked by the polars. This problem is less significant in open column chromatography as the column material can be replaced easily, whereas the process of column packing in HPLC is more time consuming and complicated.

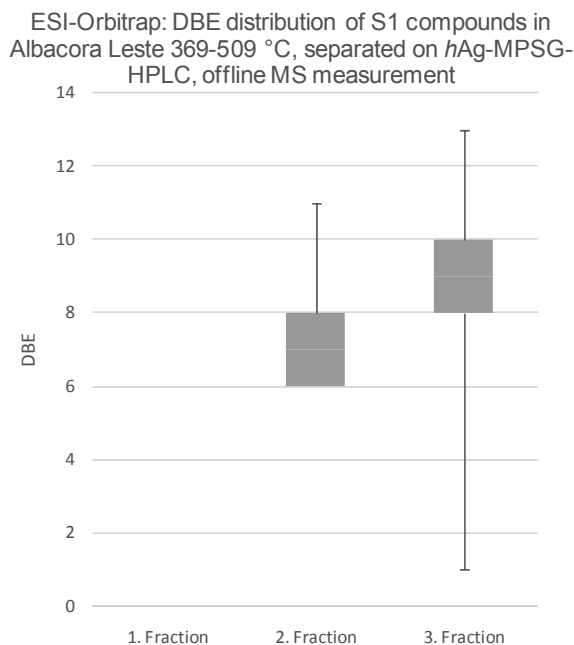


**Figure 76:** Box plot of the S1 compounds of the HPLC-separation of Albacora Leste 369-509 °C on *h*Ag-MPSG.

To optimize the HPLC separation, first standards were separated. A previous optimization in HPLC-UV was difficult, as not all desired analytes had sufficient or distinguishable UV absorption, so optimization was done using the HPLC-MS system. The optimized HPLC gradient for the separation of standards and later VGO samples is displayed in table 3.

**Table 3:** Optimized HPLC gradient for the separation of the samples.

Time min	% A [cyclohexane]	% B [dichloromethane]	% C [isopropanol]
0	100	0	0
4	67	33	0
8	52	33	15

For the standard separation the following standard substances were used:

- Polyaromatic hydrocarbons (PAHs):  
naphthalene, phenanthrene, chrysene

- Polyaromatic sulfur heterocycles (PASHs):  
benzothiophene, 3-methylbenzothiophene, dibenzothiophene, benzonaphtho[1,2-*d*]thiophene
- sulfides:  
dodecyl methyl sulfide, octadecyl methyl sulfide, phenyl sulfide
- disulfides:  
*n*-butyl disulfide, *t*-butyl disulfide, phenyl disulfide

Aliphatic compounds were not included in the standard mixture, as APCI is not able to ionize this compound class, due to the lack of electrons susceptible to chemical ionization in alkanes.

The total ion current (TIC) of the separation of a standard mixture is displayed in figure 77.

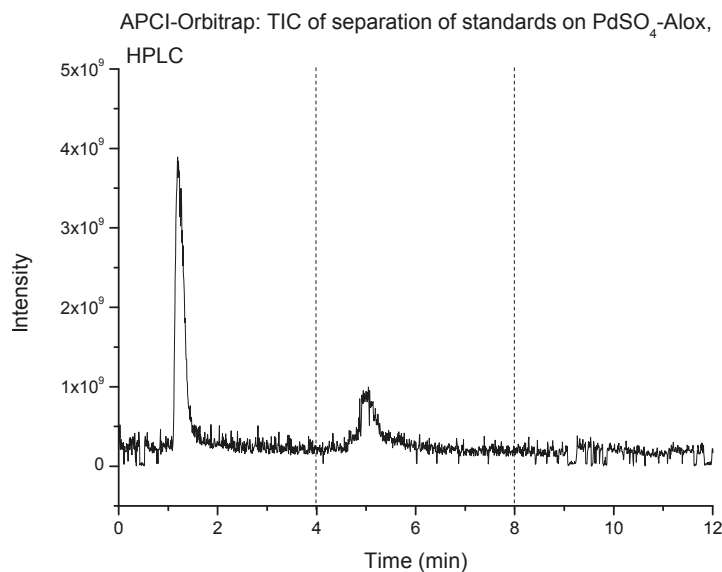


**Figure 77:** TIC of the HPLC-separation of a standard mixture on PdSO<sub>4</sub>-Alox.

Compared to the offline open column separation, the separation on HPLC is of a completely different quality, yielding fractions with a composition that differs significantly from the ones obtained in open column chromatography. PAH and PASH standards could be found eluting in the first fraction, whereas the sulfidic standard compounds were detected as S1O species in the second fraction. Even for standards the ionization efficiency of the disulfides was too small, so that the disulfides could not be detected in

the mixture, even in direct injection without prior HPLC separation. This also means that when analyzing the VGO samples, the S2 compounds assignable in the mass spectra are most likely no disulfides, but other S2 compounds, e.g. thienothiophenes or sulfide-PASH-hybrids.

For reason of comparability, again the results for the HPLC separation of Albacora Leste 369-509 °C will be discussed. The corresponding diagrams for the remaining samples can be found in section 10.3 in the appendix. The TIC of this separation is displayed in figure 78.

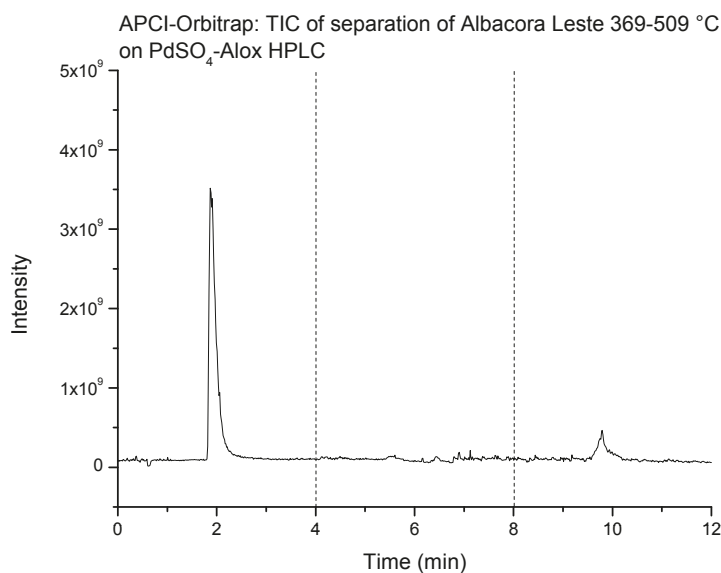


**Figure 78:** TIC of the HPLC-separation of Albacora Leste 369-509 °C on PdSO<sub>4</sub>-Alox.

In contrast to the standard separation a significant peak is visible in the third fraction when separating the VGO sample. In return the peak of the second fraction, where the sulfidic compounds were found in the standard separations, is now drastically reduced and for Albacora Leste 369-509 °C hardly visible. For the further evaluation of the quality of the separation, Kendrick plots were created of the compounds assignable by the MS software (see figures 79 to 81).

In the first fraction S1 is the only assignable sulfur containing compound class besides large amounts of aromatic hydrocarbons. The character of the S1 compounds in this fraction is rather aromatic with the highest abundance for compounds with  $9 > \text{DBE} > 16$ , corresponding to dibenzothiophenes and benzonaphthothiophenes. Due to possible



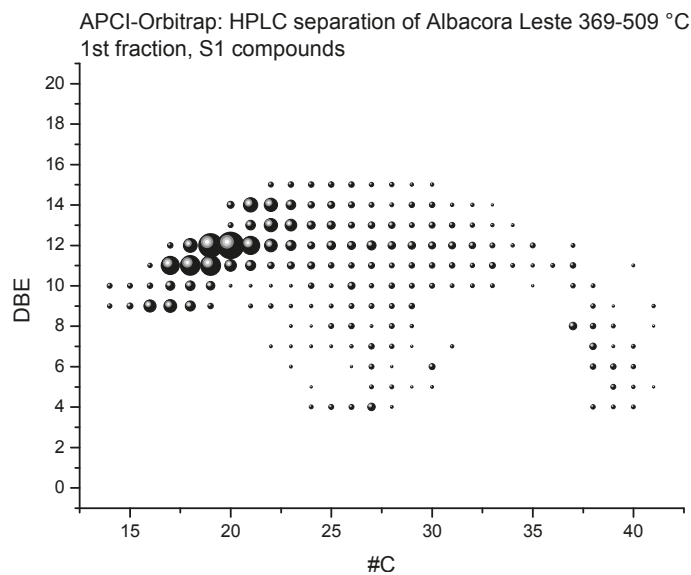


**Figure 79:** Kendrick plot of the S1 compounds in the first fraction of the HPLC-separation of Albacora Leste 369-509 °C on PdSO<sub>4</sub>-Alox.

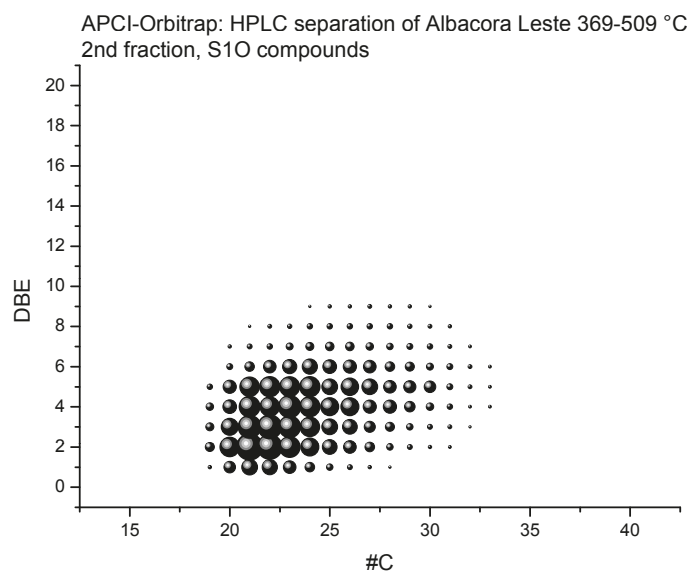


**Figure 80:** Kendrick plot of the S1O compounds in the second fraction of the HPLC-separation of Albacora Leste 369-509 °C on PdSO<sub>4</sub>-Alox.

overloading effects, some sulfur containing compounds with a DBE between 4 and 8 can be also found.

The biggest difference to the separation in open column chromatography is the content of the second fraction. Whereas in open column chromatography the main share of PASHs

was eluted in the slightly more polar second fraction, in HPLC only non-thiophenic sulfur compounds can be detected as S1O species. In fact, S1O is the only assignable compound class in this fraction. From standard experiment sulfidic sulfur would indeed be expected to elute in this fraction and the oxidation of the sulfides was also observable for the standard solution.

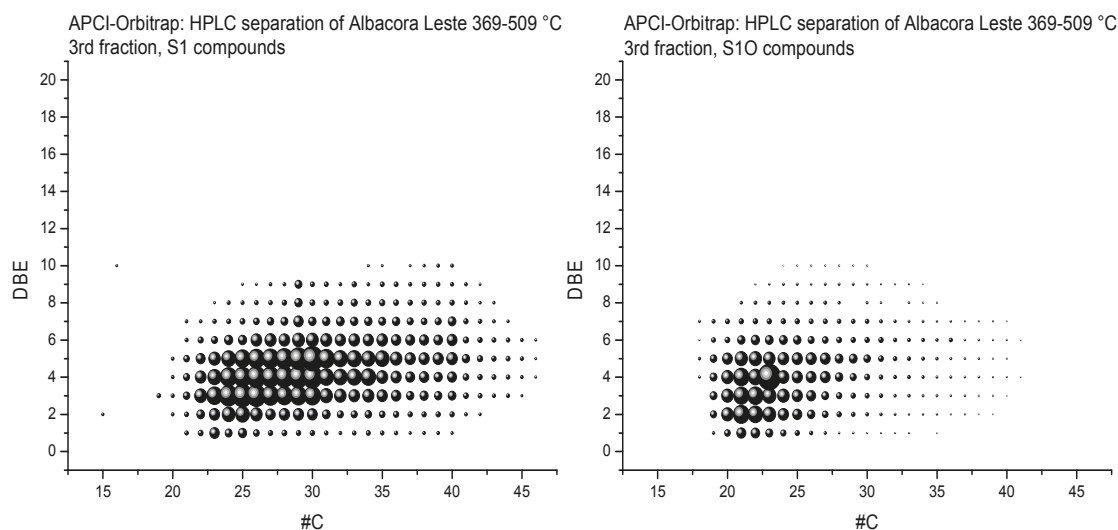


**Figure 81:** Kendrick plot of the S1 and S1O compounds in the third fraction of the HPLC-separation of Albacora Leste 369-509 °C on PdSO<sub>4</sub>-Alox.

Even more interestingly, further non-thiophenic sulfur is eluted in the third fraction. As is clearly visible in the TIC, this is not a carry-over or slow bleeding of the peak of the second fraction, but a clearly separated individual peak. As the polarity of the solvents needs to be strongly enhanced to be able to elute these compounds, their polarity and binding strength must be different from that of the sulfidic sulfur eluted in the second fraction. The assignable compound classes in the third fraction were S1 as well as S1O, again in contrast to the second fraction where only S1O compounds could be found. The DBE range is similar to the one found in the second fraction, but a much larger variation in alkylation, apparent in the wide range of carbon atoms. In the second fraction the maximum number of carbon atoms in the sulfides is 33, whereas in the third fraction compounds with up to 46 carbon atoms are present.

In figure 82 an overlay of the S1 and S1O compounds, found in the third fraction, is shown to further illustrate the similarity of the two Kendrick plots.

Except for some compounds with less than 20 carbon atoms and more than 40 carbon

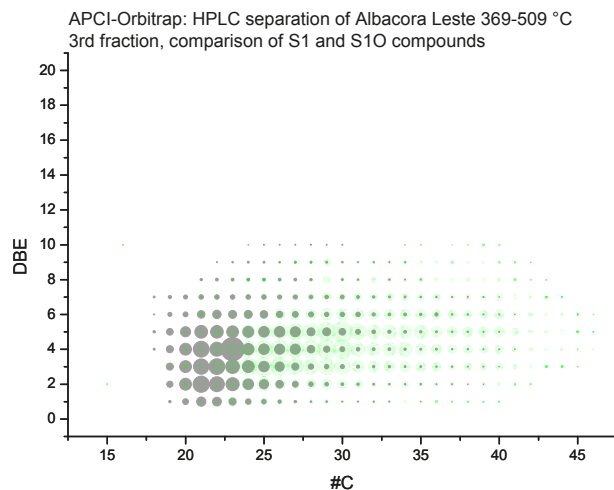


**Figure 82:** Overlay of the Kendrick plot of the S1 and S1O compounds in the third fraction of the HPLC-separation of Albacora Leste 369-509 °C on PdSO<sub>4</sub>-Alox.  
Gray: S1O compounds, green: S1 compounds.

atoms the plots are rather similar, even if intensities do vary. This also supports the assumption that sulfidic sulfur containing compounds are at least partially oxidized within the ionization source. The fact that sulfidic sulfur can be found in two separate fraction eluted with solvents of different polarity implies the presence of two independent classes of sulfidic sulfur within the sample. As these results were reproducible for the other VGO samples and boiling point ranges as well, this is not just a structural unique characteristic of the Albacora sample.

To further illustrate that the separation including the presence of two individual sulfidic sulfur classes is also applicable to higher boiling fractions and different samples, the results for Winter ANS 509-550 °C are discussed. The TIC for the HPLC separation of Winter ANS 509-550 °C on PdSO<sub>4</sub> is displayed in figure 83, the corresponding Kendrick plots in figures 84 to 86.

For the separation of Winter ANS 509-550 °C the peak in the TIC for the second fraction is more defined than seen for Albacora Leste 369-509 °C. In the first fraction, in addition to aromatic hydrocarbons and S1 compounds, also S2 compounds were assignable. Both S1 and S2 compounds are highly aromatic with DBEs between 12 and 19, corresponding to benzonaphthothiophenes (DBE 12-14), benzophenanthrothiophenes (15-17) and even 6-ringed PASHs for the S1 compounds. Due to this high aromaticity the S2 compounds are very likely to be polyaromatic thienothiophene derivatives.

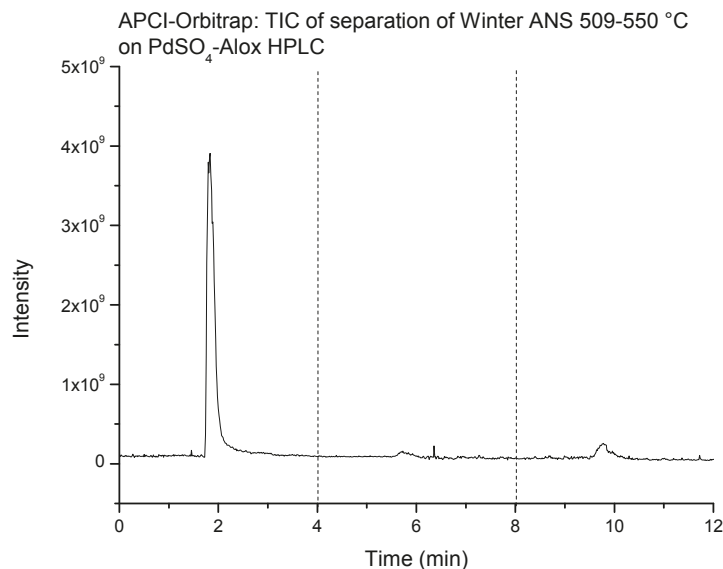


**Figure 83:** TIC of the HPLC-separation of Winter ANS 509-550 °C on PdSO<sub>4</sub>-Alox.

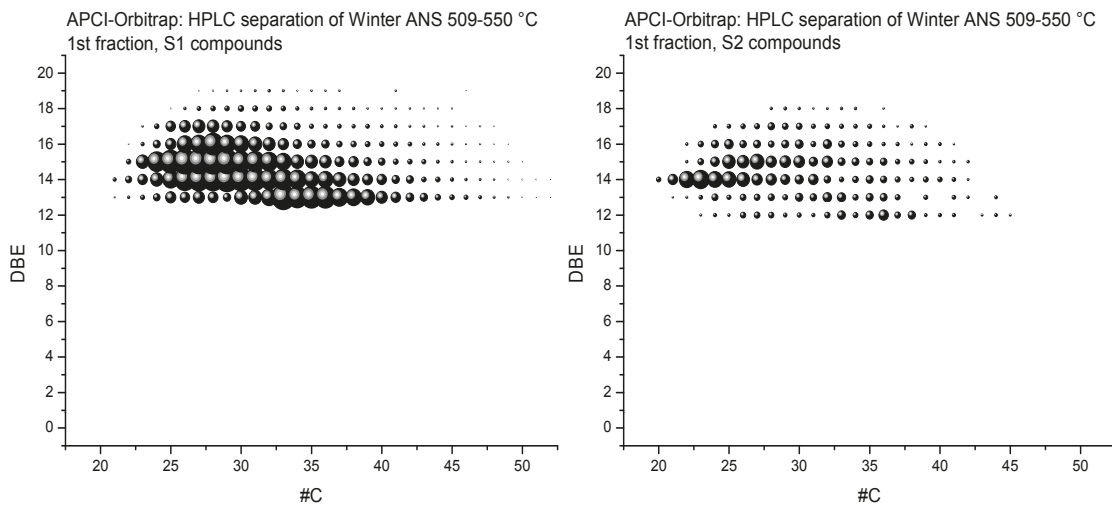


**Figure 84:** Kendrick plot of the S1 and S2 compounds in the first fraction of the HPLC-separation of Winter ANS 509-550 °C on PdSO<sub>4</sub>-Alox.

The second and third fraction consist of non-thiophenic sulfur compounds, as for both fractions S1O species are detectable. For the second fraction again S1O is the only assignable compound class, whereas S1 and S1O species can be found in the third fraction. Cyclic sulfides corresponding to DBE 1 can only be found in the second fraction. Also the DBE range in this fraction is slightly wider than in the third, ranging from DBE 1 to 14. In the third fraction only compounds with DBEs between 1 and 12 are

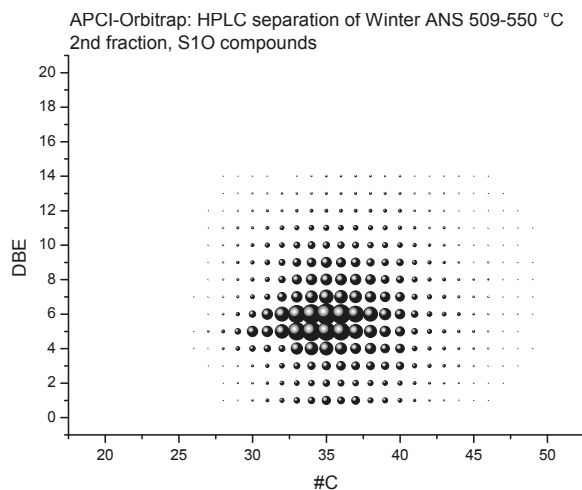


**Figure 85:** Kendrick plot of the S1O compounds in the second fraction of the HPLC-separation of Winter ANS 509-550 °C on PdSO<sub>4</sub>-Alox.

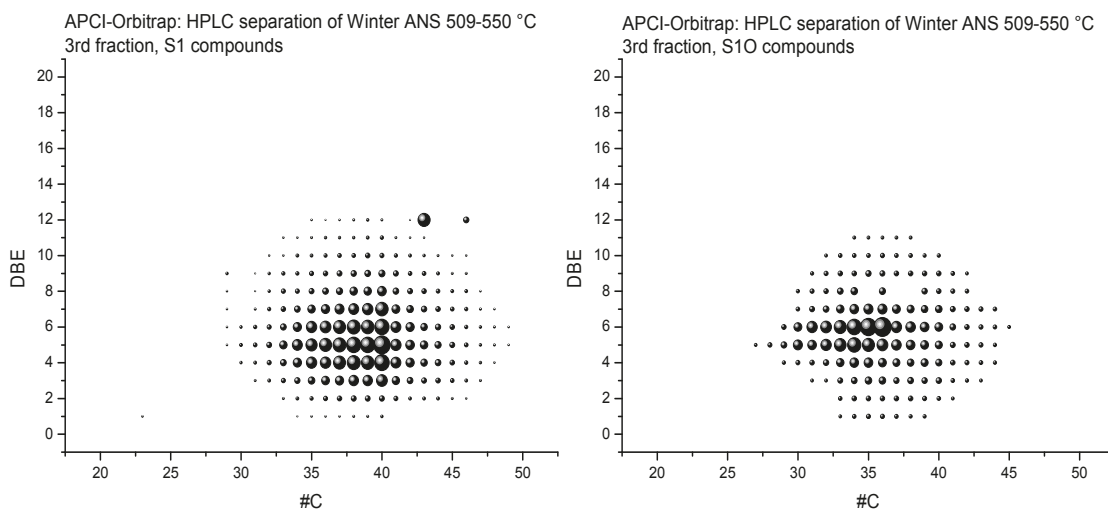


**Figure 86:** Kendrick plot of the S1 and S1O compounds in the third fraction of the HPLC-separation of Winter ANS 509-550 °C on PdSO<sub>4</sub>-Alox.

present. In contrast to the separation of the Albacora Leste sample, here the extent of the alkylation pattern of both fractions is similar, whereas the second fraction is still shifted towards slightly lower carbon atom numbers.

When PdSO<sub>4</sub>-Alox is used in HPLC, VGO samples can be successfully separated into thiophenic and non-thiophenic sulfur. The DBE range of the detected PASHs is slightly lower than in mass spectrometric analysis after open column chromatography. Also all PASHs do not interact as strongly with the stationary phase as seen in open column

chromatography and therefore already eluted in the first fraction together with PAHs and aliphatic hydrocarbons, which cannot be detected using APCI. Sulfidic sulfur compounds can be separated into two different chromatographic fractions using solvents of different polarity. The second fraction of the separation contains non-thiophenic sulfur compounds with a lower amount of carbon atoms and a wider range of unsaturation and includes cyclic sulfides. All of the sulfides present in this fraction are oxidized in the ion source analogously to the aliphatic and aromatic sulfides used in standard separations. The third fraction also includes non-thiophenic sulfur compounds, which could only be eluted with the addition of a significant amount of isopropanol to increase the polarity and to serve as a competitive ligand. These sulfidic compounds are only partially oxidized in the ion source, so that S1 compounds can still be detected in the fraction, but the distribution patterns of S1 and S1O compounds in the Kendrick plots are nearly congruent. Compared to the sulfides found in the second fraction, the non-thiophenic sulfur compounds in the third fraction have a higher degree of alkylation and a more narrow range of unsaturation, starting at a DBE of 2. As both DBE range and number of carbon atoms are similar for the sulfides found in the two fractions, only constitution might differ between the fractions. Due to steric effects or changes in the electron density at the sulfur atom, the interaction of the sulfur atom and the stationary phase can be altered in more branched sulfides compared to linear sulfides, so that elution of the compounds is affected. This effect was also described by ORR. [125, 126] Branching and the position of the branching could be shown to have an effect on the elution of sulfides in liquid-liquid chromatography. As further experiments for structure elucidation, like NMR or IR, of further isolated and concentrated compounds would be needed to receive clear proof, of course only assumptions can be made to explain the differences between the two individual classes of sulfidic sulfur compounds.

#### 7.4.5 Comparison between the different phases for the separation of VGOs

Three stationary phases, PdSO<sub>4</sub>-Alox, hAg-MPSG and Ag<sup>+</sup>-cartridges, were extensively tested for the separation of several VGO samples with different boiling points. For both of the silver ion based phases stronger interactions of sulfur containing compounds with large condensed aromatic ring systems could be observed, that resulted in a carry-over of larger PASHs into the non-thiophenic sulfur fraction. The PdSO<sub>4</sub> could be applied to open column chromatography and HPLC, whereas the separation in HPLC differs strongly from the ones obtained by open column chromatography, as the retention of PASHs is reduced and sulfidic sulfur can be separated into two individual fractions. A

comparison between the tested phases and the well established Pd-MPSG as a reference is presented in table 4.

**Table 4:** Properties of the different stationary phases

PdSO <sub>4</sub> -Alox	PdSO <sub>4</sub> -Alox HPLC	<i>h</i> Ag-MPSG	Ag <sup>+</sup> -cartridges	Pd-MPSG
easy to prepare, 1-pot synthesis,	easy to prepare, 1-pot synthesis, has to be packed	2-step synthesis, tricky heating process, low consistency in quality of material	no preparation necessary as prepacked cartridges are commercially available	2-step synthesis, eventually packing of HPLC columns
PASHs up to DBTs coelute with PAH in 1st fraction, clean separation between PASHs and sulfidic sulfur, disulfides are retained	PASHs elute in 1st fraction, two different kinds of sulfides found, disulfides are retained	PASHs up to DBTs coelute with PAH in 1 <sup>st</sup> fraction, clean separation between PASHs and sulfidic sulfur, disulfides are retained	PASHs up to DBTs coelute with PAH in 1 <sup>st</sup> fraction, aromatic sulfides and disulfide are eluted in third fraction	well established for the separation of PAHs and PASHs, sulfides are only partially recovered, disulfides are retained irreversibly
time consuming open column separation, offline MS detection possible with various techniques	quick separation (12 min) and online MS detection via APCI possible	time consuming open column separation, offline MS detection possible with various techniques	time consuming SPE separation, no upscaling possible as only fixed volume cartridges available, offline MS detection possible with various techniques	use in open column and HPLC separations, HPLC has even better performance, therefore offline and online MS detection possible
Use of costly palladium, but reduced amounts compared to Pd-MPSG	Use of costly palladium, but reduced amounts compared to Pd-MPSG, quick separation needs less solvents	Use of cheaper silver,	Price of ca 7€ per cartridge	Large amounts of palladium needed

In conclusion, the chromatographic phase should be chosen according to the analytical problem and the nature of the sample. For an excellent separation of PAHs and PASHs the well established separation on Pd-MPSG is the method of choice as here the smaller

PASHs are retained best. Early elution is only observable for thiophenes and benzenes. For a routine analysis of non-thiophenic sulfur, which should be easily feasible and simple to handle also for users without previous knowledge of the technique, the separation on  $\text{Ag}^+$ -cartridges should be used as the stationary phase is prepacked and commercially available. Due to the limited amount of stationary phase a preseparation on alumina is necessary and the silver ion phase is still easily overloaded. Furthermore, disulfide standards could be recovered from this phase. That makes the separation on  $\text{Ag}^+$ -cartridges the only tested separation, where disulfides could be eluted at all. For a more detailed characterization of the non-thiophenic S1 compounds in a sample,  $\text{PdSO}_4$ -Alox as a HPLC phase can be used. Here, no separation into PAHs and PASHs is observable, so only few information can be gained about the thiophenic sulfur using this phase. Also as seen for the silver ion cartridges, preseparations on alumina are necessary, as the interaction sites are limited and the reusability of the phase would be drastically reduced when injecting non-recoverable substances.

#### 7.4.6 Effects of the ionization technique on the resulting mass spectra

To compare the effects of the ionization technique on the resulting mass spectra, again Albacora Leste 369-509 °C will be discussed as an example. As the mass spectra themselves are supercomplex and a comparison between them can only be superficial, the Kendrick plots for the S1 compounds are compared in figures 87 and 88.

The four Kendrick plot series differ strongly. Whereas for ESI and APCI the sulfur containing compounds are regularly and evenly distributed, in the Kendrick plots for the mass spectra ionized using APPI and APLI more irregularities occur. APCI seems to favor smaller molecular weight compounds, as molecules with lower carbon atom number can be detected using this technique. In ESI the main intensities of the compounds are shifted to slightly higher DBE, giving more emphasis on compounds with a lower degree of saturation. This becomes especially apparent when comparing the Kendrick plots for the third fraction, which include the non-thiophenic sulfur. In ESI main intensities can be found at 4 to 6, in APCI only at DBE 2 to 5. The intensities of the sulfidic compounds without any possible aromatic structure ( $\text{DBE} < 3$ ) are enhanced in APCI compared to ESI.

The Kendrick plots for the fractions ionized with APLI and APPI are surprising. According to the underlying ionization mechanism of these two techniques the more aromatic a compound is, the better it should be ionizable due to the increased number of  $\pi$ -electrons in the condensed aromatic ring system. Especially APLI should be selective



for condensed aromatic systems, as the secondary excitation necessary for ionization is adapted to fit the energy levels of condensed aromatics. Nevertheless, APLI only yields an irregular rather statistical distribution of signals especially for the two aromatic fractions. Only in the third fraction broken lines of homologous series can be observed. Also total intensities are very low and close to the limit of detection. In APPI the intensities are also distributed irregularly, but the lines of homologous series are less broken. The assigned compounds in APPI have even lower carbon atom numbers than seen in APCI, starting at compounds with only 10 carbon atoms, compared to 15 in APCI and about 20 in ESI. Also the distribution of the sulfur containing compounds especially in the third fraction is extremely widely scattered, including compounds with DBEs up to 20 and carbon atom numbers between 10 and 40. The range of the compounds with the highest intensities is similar to the APCI data. For APLI no conclusions about the maximum intensities can be made due to the irregular distribution.

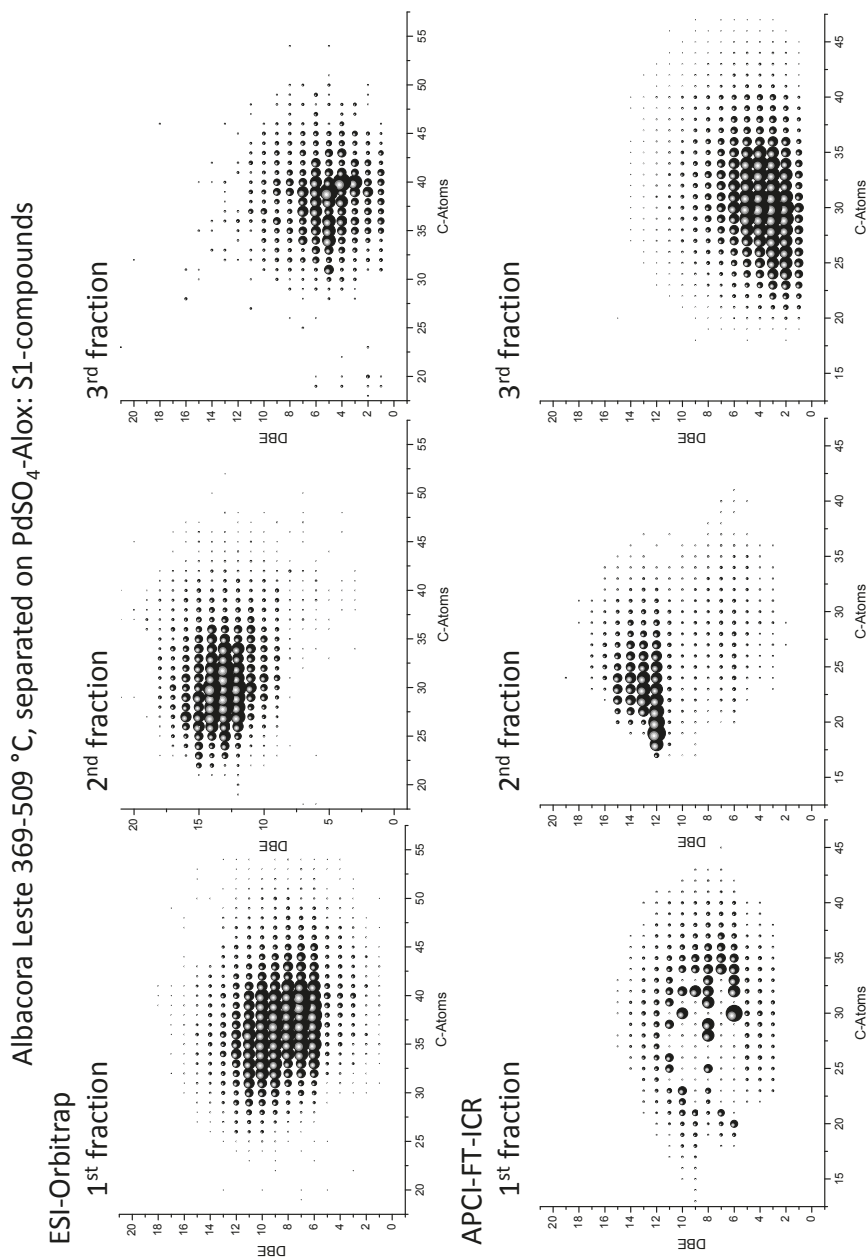


**Figure 87:** Comparison of different ionization techniques for Albacora Leste 369-509 °C. Displayed are the Kendrick plots of the S1 compounds in the three eluted fractions on PdSO<sub>4</sub>-Alox. Upper row: ESI-Orbitrap MS after methylation, bottom row: APCI-FT-ICR MS.

Albacora Leste 369-509 °C, separated on PdSO<sub>4</sub>-Alox: S1-compounds

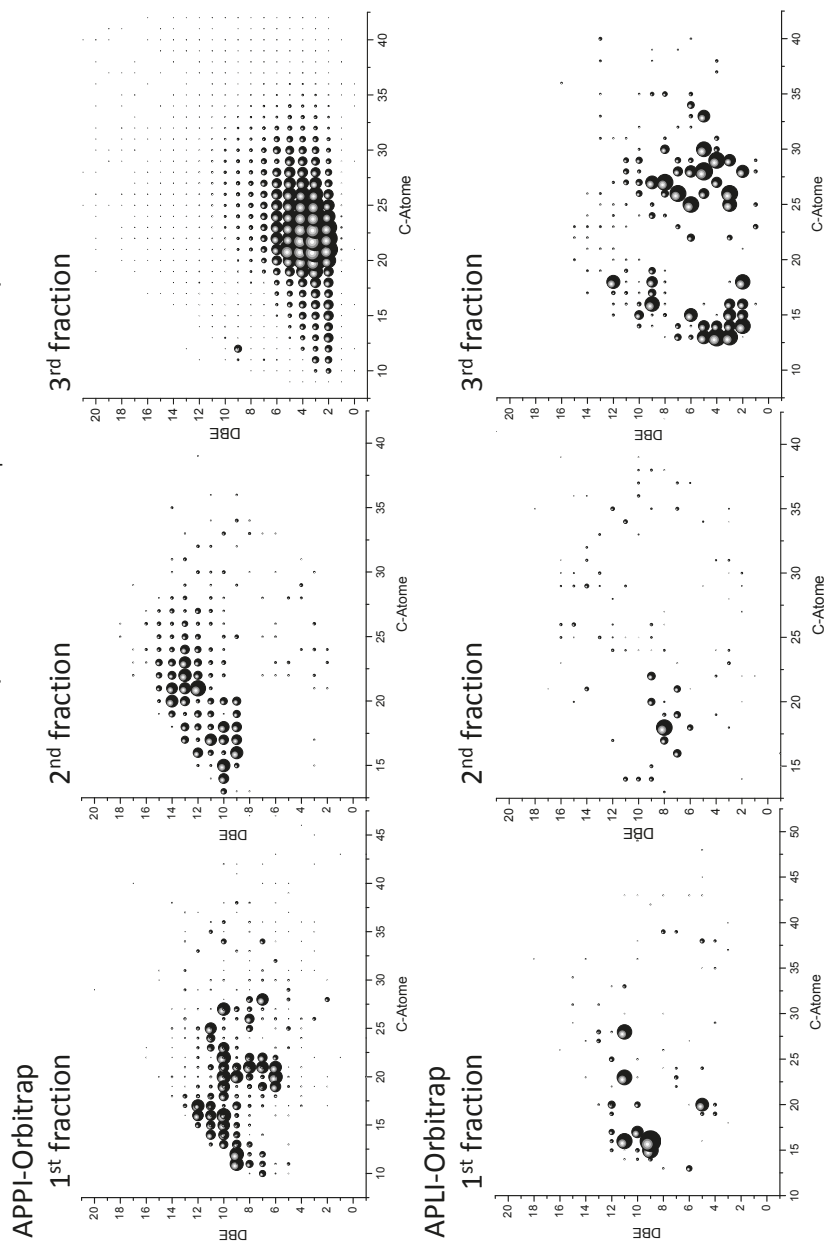


**Figure 88:** Comparison of different ionization techniques for Albacora Leste 369-509 °C. Displayed are the Kendrick plots of the S1 compounds in the three eluted fractions on PdSO<sub>4</sub>-Alox. Upper row: APPI-Orbitrap MS, bottom row: APPI-Orbitrap MS.

APPI and APLI does only seem to be applicable to the analysis of the fractions obtained from the separations without further optimization of the instrumental parameters, as both APPI and APLI have been successfully applied to the analysis of various crude oil samples and their sulfur containing compounds. [34, 45, 115, 116, 118, 127, 128]. ESI after methylation and APCI are of a similar quality and both suited for the analysis and generation of Kendrick plots. Of course, intensities of the peaks should always be treated with caution as different techniques favor different analytes during ionization. [114, 129] These results were similar for the remaining separated VGO samples. The corresponding box plots for differently ionized samples can also be found in the appendix in section 10.3.

In the analysis of the higher boiling fractions with a boiling point of 509-550 °C, a structural distinctive factor in form of a dominant line of compounds with 40 carbon atoms could be found in non-thiophenic fraction of the separated VGOs. To further illustrate that C40 compounds in the sample fall out of the series and that this behavior is not caused by a discrimination by the stationary phase or the ionization technique, pseudograms of the homologous series of S1 compounds with a DBE of 6 in the third fraction of the separation of Albacora Leste 509-550 °C on the tested stationary phases are displayed in figure 89.

Even though the relative intensities for the different compounds vary between the separations and between ESI after methylation and APCI, the C40 compounds are the most abundant species in all homologous series. This further implies that the dominance of these compounds is not caused by the separation or overrepresentation during the mass spectrometric detection, but that the class of C40 S1 compounds is more abundant in the sample itself.

To check if this is a special feature of the Albacora Leste sample, also pseudograms of the analogous compounds found in the third fractions of the separations of other high boiling samples like Winter ANS 509-550 °C and Azeri 509-550 °C were generated and are displayed in figure 90

For Winter ANS 509-550 °C, C40 still are the most dominant of the S1 compounds with 6 DBE in the third fractions, but the effect is less drastic than seen for Albacora Leste 509-550 °C. The intensities for the C40 compounds protrude just slightly from the nearly Gaussian distribution of the remaining peaks. For Azeri 509-550 °C the effect is again more drastic. The intensity of the C40 compounds here is considerably increased for both separations on PdSO<sub>4</sub>-Alox and *h*Ag-MPSG. The results reflect the ones obtained

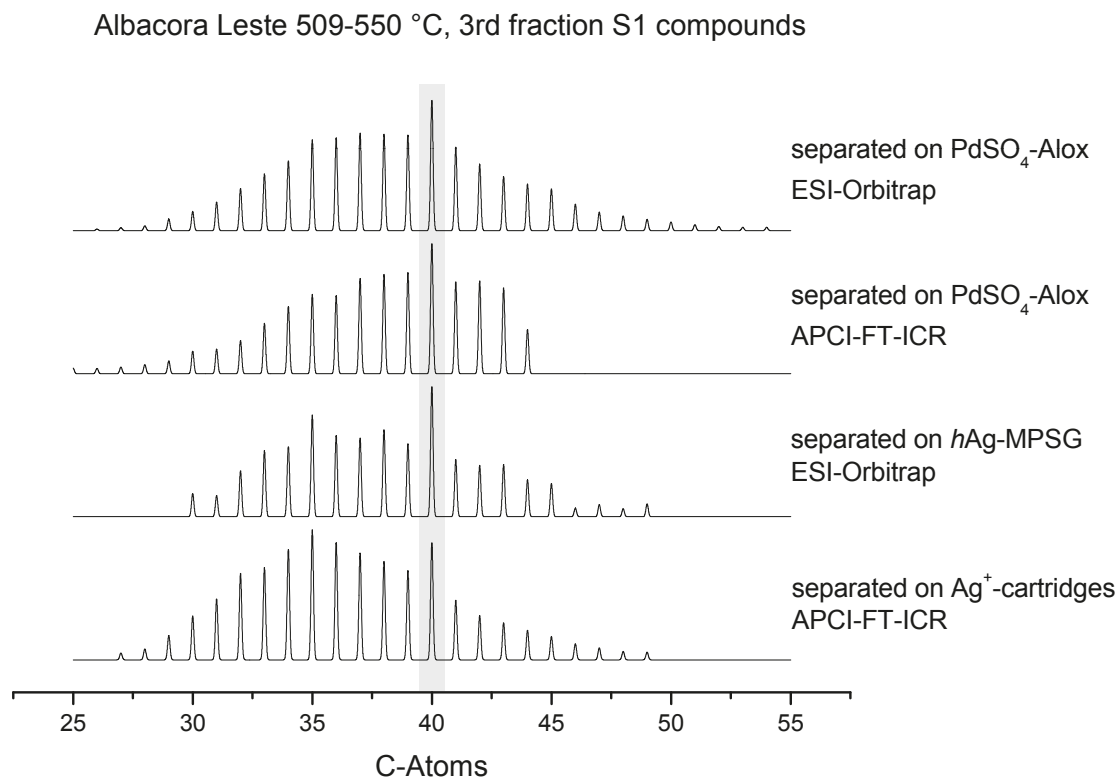


**Figure 89:** Pseudograms of the homologous series of S1 compounds with DBE=6 found in the third fractions of Albacora Leste 509-550 °C on different stationary phases and with different MS ionization.

from the Albacora Leste sample. The increased intensities for C40 compounds can be found for different VGO samples of different geographic origin and the results can be reproduced using different stationary phases and MS techniques.

A possible explanation for this dominant line of C40 compounds can be found in the origin of crude oils. One origin of sulfur containing compounds in petroleum is the addition of sulfur to isoprenoid structures. The class of carotenoids, organic pigments found in plants and other photosynthetic organism, is based on a C40 backbone, which can be varied at defined positions (see figure 91).

Carotenoids play an important role during photosynthesis. For example, an important enzymatic cycle in phytoplankton is the xanthophyll cycle, where epoxy groups are removed from xanthophylls to quench light energy to prevent damage from excessive stimulation of the photosynthesis apparatus. In algae therefore diadinoxanthin is enzymatically converted to diatoxanthin as illustrated in figure 92. [130]

VGO fractions 509-550 °C, 3rd fractions, S1 compounds, DBE=6

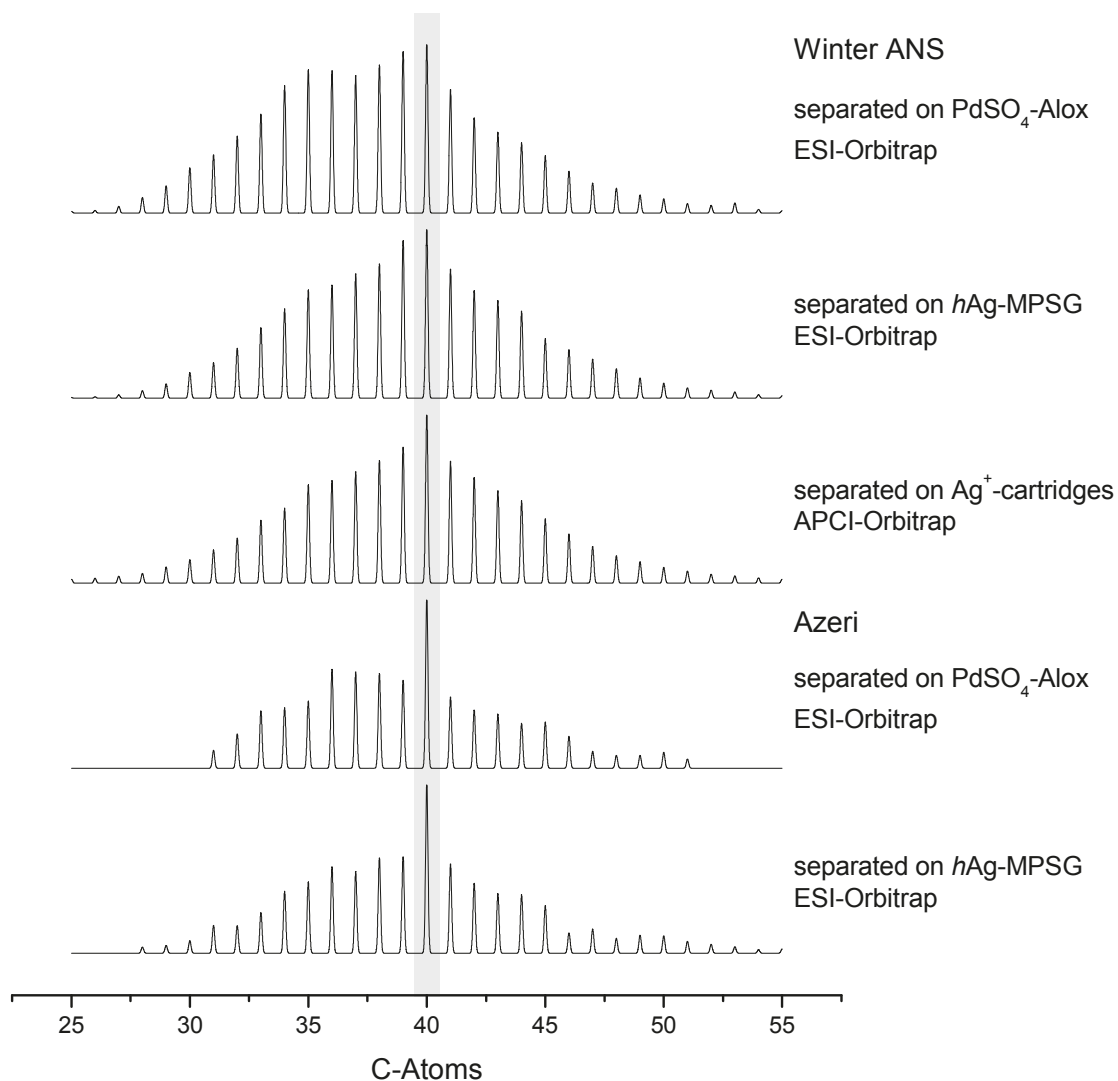


**Figure 90:** Pseudograms of the homologous series of S1 compounds with DBE=6 found in the third fractions of Winter ANS 509-550 °C and Azeri 509-550 °C on different stationary phases and with different MS ionization.

The presence of carotenoid based structures in sediments has been described in the literature [131, 132], and carotenoid based sulfides were described to be present in petroleum and its products. [19, 23, 131, 133, 134] Thus, the overdominant C40 compounds in the high boiling fractions are very probably originating from carotenoid based structures in the sediments during formation of the crude oils.

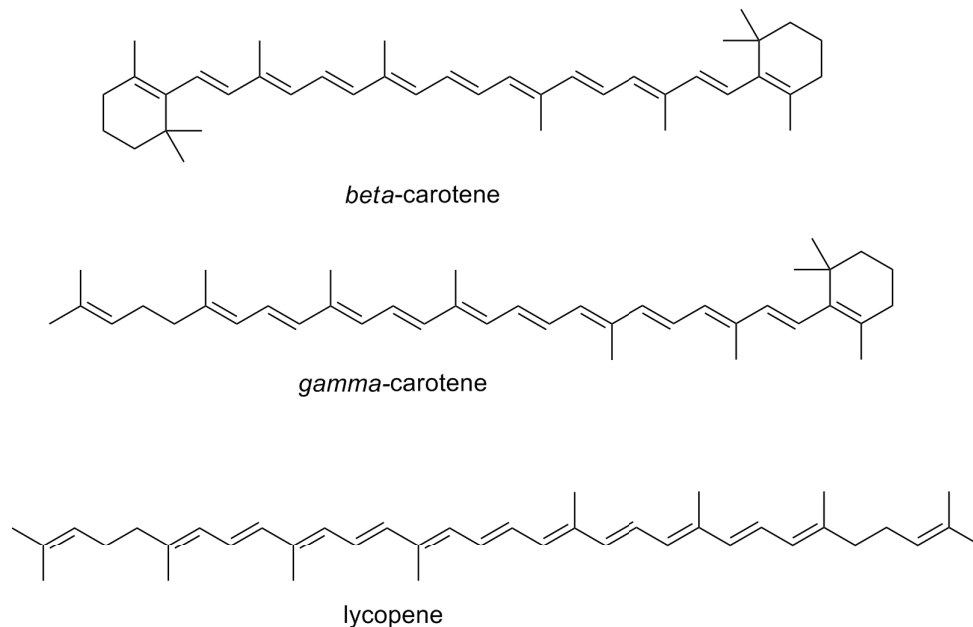


**Figure 91:** Typical examples of the class of carotenoids.

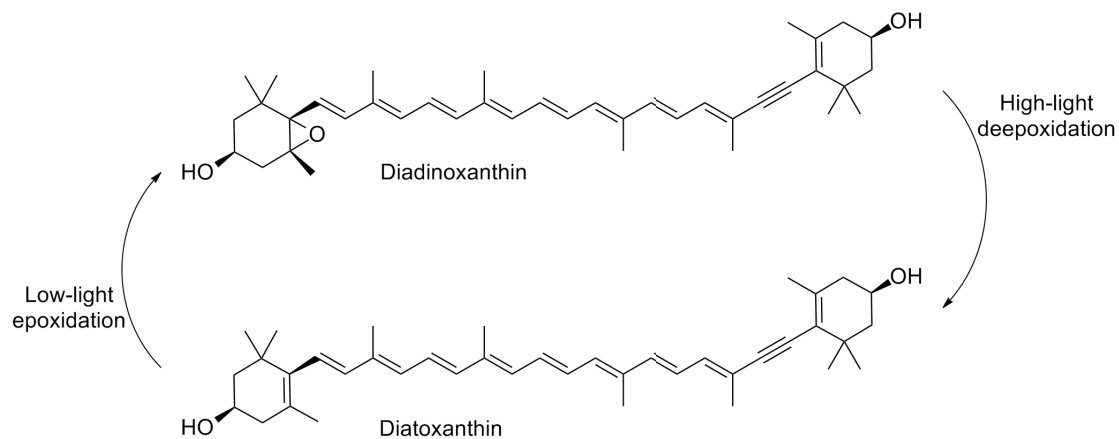


**Figure 92:** Xanthophyll cycle in phytoplankton. [130]

## 7.5 Sulfur content, sulfur balance and mass balance of the separated fractions

### 7.5.1 Determination of the total sulfur content via TXRF

Total reflection X-ray spectrometry (TXRF) is a powerful tool to analyze even small amounts of a certain element. The sample is irradiated at a flat angle, so that the X-ray is totally reflected and only enters to a depth of a few nanometers. That way, no

interactions with the supporting material occur and the signal-to-noise ratio is improved. An internal standard is needed for quantification with TXRF. Here, iron was used in form of ferrocene. Ferrocene is very stable, it is cheap and has a good solubility in organic solvents. Furthermore, iron should only be present in traces in petroleum cuts, so that no major contamination by the sample is expected.

An exact amount of ferrocene is added to the sample and the mixture put on a fused silica sample holder for analysis. The results of the TXRF analysis are presented in table 5.

fraction	determined sulfur content	standard deviation $\sigma$	value determined by BP	value determined by commercial lab.
369-505	6045 ppm	917 ppm	13500 ppm	13045 ppm
	7342 ppm			
505-550	9287 ppm	1991 ppm	15900 ppm	-
	7217 ppm			
	11199 ppm			

**Table 5:** Total sulfur content in Karachaganak fractions 369-505 °C and 505-550 °C according to TXRF, samples determined in duplicate, sulfur content determined by BP and a commercial laboratory.

The high standard deviation, especially for the high boiling sample, shows that the performed quantification is inaccurate. This was probably caused by the inhomogeneous surface of the sample, when applying the crude oils to the sample holder. For TXRF a total reflection is needed to get accurate results. When applying the waxy crude oil samples to the sample holders, uneven surfaces are produced due to the high viscosity of the samples. Heating of the samples on the sample holder might improve the evenness of the sample. The high variations also suggest that no sufficient mixing between the standard and the sample took place. While adding the internal standard, the sample was heated to facilitate a regular distribution of the ferrocene in the sample, but perhaps this mixing was not sufficient enough. Dilution of the sample with highly volatile solvents could improve the mixing and also facilitate the application of the sample onto the sample holder.

The experimental setup of the instrument is challenging for petroleum cut samples, as the sample holder is positioned in a vertical position. Even samples with a high viscosity, such as the Karachaganak 505-550 °C sample, showed some flow behavior on the fused silica surface. Lower boiling samples like the Karachaganak 96-369 °C hence could not



be analyzed at all, as the sample could not be immobilized onto the surface.

The results show that the applied method is not suitable for the analysis at all, as the experimentally determined values are only about half of the expected values. Therefore, the analysis via TXRF was not used for further experiments, but sulfur analysis was performed by a commercial laboratory.

### 7.5.2 Repeatability, mass and sulfur balance of the separations on LEC phases

To verify the results for the vacuum gas oils, repeatability studies were performed. For this purpose, Albacora Leste 369-509 °C and 509-550 °C were used and separated on PdSO<sub>4</sub>-Alox and *h*Ag-MPSG five times each. For repeatability and mass balance, in addition to the general procedure, the solvents were first removed on the rotary evaporator and subsequently the samples were kept at 10<sup>-2</sup> mBar for 15 minutes before the output weight of each fraction was determined.

For the PdSO<sub>4</sub> stationary phase, the results of the repeatability test are displayed in table 6. It is obvious that the results vary strongly. The overdetermination occurring in all samples indicates a methodical error. To exclude the possibility that contaminations from the solvent could increase the output weight of the samples, a blank separation was done. As displayed in figure 6 the mass of the residues of the blank sample are minor and can be neglected.

The results for the *h*Ag-MPSG stationary phase are displayed in table 7. Here, the variation between different sets of sample are even larger.

The most probable cause for the overdetermination error is that the solvents could not be removed completely by the applied method. To verify this assumption, NMR experiments were done. Of course, issues concerning the accuracy of scales should also be kept in mind. Due to the high elution volumes of the fractions, the round bottom flasks used to collect the fractions had also to be upscaled. Therefore, the weight of one flask is approximately about 170 g, whereas the amounts of sample are in the mg range.

**Table 6:** Results of the repeatability studies for separations on PdSO<sub>4</sub>-Alox.~ 200 mg sample, separated on 32 g PdSO<sub>4</sub>-Alox

Albacora Leste 369-509 °C

	amount of sample [in mg]	1st fraction [in g]	2nd fraction [in g]	3rd fraction [in g]	recovery
I	206.05	0.1565 76%	0.0348 17%	0.0567 28%	120%
II	216.81	0.1635 75%	0.0376 17%	0.0188 9%	101%
III	219.3	0.2216 101%	0.0867 40%	0.0922 42%	183%
IV	218.04	0.217 100%	0.1128 52%	0.0868 40%	191%
V	209.74	0.1983 95%	0.1186 57%	0.045 21%	173%

Albacora Leste 509-550 °C

	amount of sample [in mg]	1st fraction [in g]	2nd fraction [in g]	3rd fraction [in g]	recovery
I	191.91	0.1277 67%	0.0527 27%	0.0377 20%	114%
II	192.13	0.1805 94%	0.0362 19%	0.027 14%	127%
III	212.43	0.1837 86%	0.0562 26%	0.0359 17%	130%
IV	186.36	0.1877 101%	0.0377 20%	0.0284 15%	136%
V	220.71	0.1872 85%	0.0391 18%	0.0295 13%	116%

	amount of sample [in mg]	1st fraction [in g]	2nd fraction [in g]	3rd fraction [in g]	recovery
blank		0.001	0.0002	0.0002	-

**Table 7:** Results of the repeatability studies for separations on *hAg*-MPSG.~ 200 mg sample, separated on 32 g *hAg*-MPSG

Albacora Leste 369-509 °C

	amount of sample [in mg]	1st fraction [in g]	2nd fraction [in g]	3rd fraction [in g]	recovery
I	214.28	0.0738 34%	0.0452 21%	0.045 21%	77%
II	213.31	0.1838 86%	0.0425 20%	0.019 9%	115%
III	203.58	0.1569 77%	0.0456 22%	0.0168 8%	108%
IV	192.55	0.1322 69%	0.1629 85%	0.0155 8%	161%
V	197.02	0.2677 136%	0.1136 58%	0.1108 56%	250%

Albacora Leste 509-550 °C

	amount of sample [in mg]	1st fraction [in g]	2nd fraction [in g]	3rd fraction [in g]	recovery
I	235.84	0.3276 139%	0.1574 67%	0.1324 56%	262%
II	201.31	0.1529 76%	0.0475 24%	0.0283 14%	114%
III	211.12	0.1487 70%	0.1297 61%	0.0298 14%	146%
IV	201.36	0.1678 83%	0.0457 23%	0.0309 15%	121%
V	190.19	0.207 109%	0.0222 12%	0.0325 17%	138%

### NMR control of repeatability fractions

To identify possible solvent signals in the samples, NMR experiments were conducted. The literature values for the chemical shifts were gathered from the Spectral Database for Organic Compounds (SDBS) provided by the National Institute of Advanced Industrial Science and Technology, Japan (AIST) and displayed in table 8.

**Table 8:** NMR-shifts of solvents according to AIST-database. [135]

solvent	shift (in ppm)
chloroform in <i>deutero</i> -chloroform	7.24
cyclohexane	1.43
dichloromethane	5.30
isopropanol	4.01, 2.16, 1.20

As displayed in figures 93 to 95, remaining solvents in significant amounts can be found in every fraction. In figure 93 the NMR spectra of the first fraction, which was eluted with cyclohexane, can be found. The peak with the second largest intensity can be assigned to cyclohexane itself. As the remaining peaks are not baseline separated from the solvent peak, a quantification of the remaining solvent is not possible. Another piece of information, which can be gathered from this NMR data is that nearly no aromatics are present in this fraction. The aromatic area, starting at about 6 ppm, is nearly clean. The spectra of the second fraction, which was eluted with a mixture of cyclohexane and dichloromethane, is displayed in figure 94. Here again, one of the larger peaks can be assigned to cyclohexane. Dichloromethane is only present to a very small extent, expected due to the much higher volatility and higher vapor pressure of dichloromethane compared with cyclohexane. Again, the cyclohexane signal is situated in between the signals of the analytes, making a quantification impossible as no baseline separation can be obtained. Comparing this fraction with the first one, it becomes obvious that the amount of aromatic compounds is drastically enlarged. Strong signals for aliphatic protons can be found, indicating the presence of alkyl chains attached to the aromatic compounds. Coupling of the signals is usually used to identify such structures, but due to the high complexity of the sample no such elucidation can be done from these simple NMR experiments. For more insight and structural information about this sample more complex experiments, such as two-dimensional NMR would be needed.

The spectrum of the third fraction, eluted with a mixture of cyclohexane, dichloromethane and isopropanol, is displayed in figure 95. Whereas no signals of the isopropanol could be found, the largest peak of the spectrum corresponds to cyclohexane protons.

Dichloromethane is, as already seen in figure 94, only present in traces. Again, the cyclohexane signal is situated in between signals of the analytes, so that a quantification is not possible, but judging from the size of the signal a significant amount of solvent is still present in this fraction. Concerning the separation efficiency it is nice to see that again no aromatic protons can be found in this fraction. The separation between aromatic sulfur compounds and non-thiophenic sulfur seems to be successful and the compounds present in the third fraction do not possess aromatic protons.

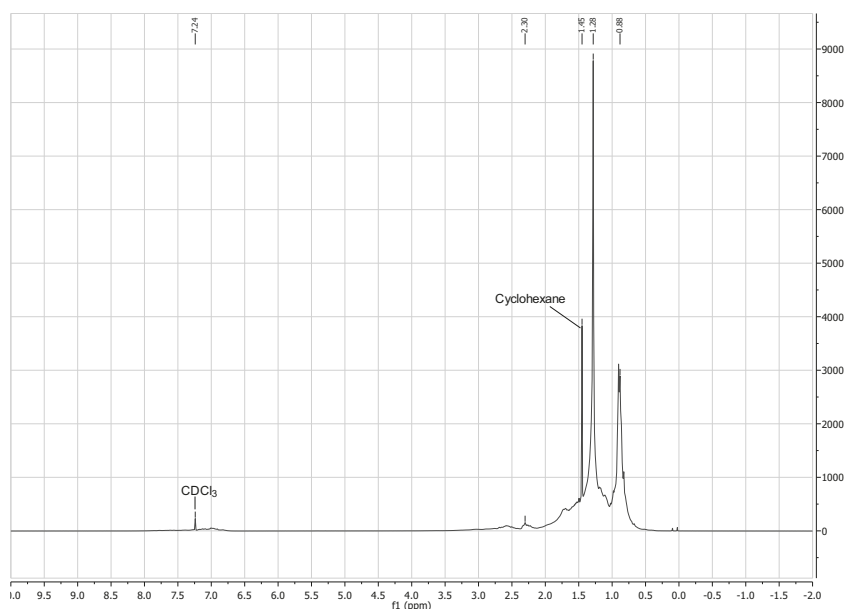


**Figure 93:** NMR spectra of the first fraction of Albacora Leste 369-509°C separated on PdSO<sub>4</sub>-Alox.

NMR studies could show that the method used to remove the solvents from the residues is not sufficient. The use of the rotary evaporator combined with 15 minutes of evaporation at 10<sup>-2</sup> mBar is not able to remove especially cyclohexane completely out of the samples. Therefore, the obtained mass balances should be considered erroneous.

### Use of higher temperatures for recovery and external sulfur quantification

To solve the problem of remaining solvents, higher temperatures were used during evaporation of the samples. Instead of the previously used 40°C during evaporation, the temperature was increased to 60°C.

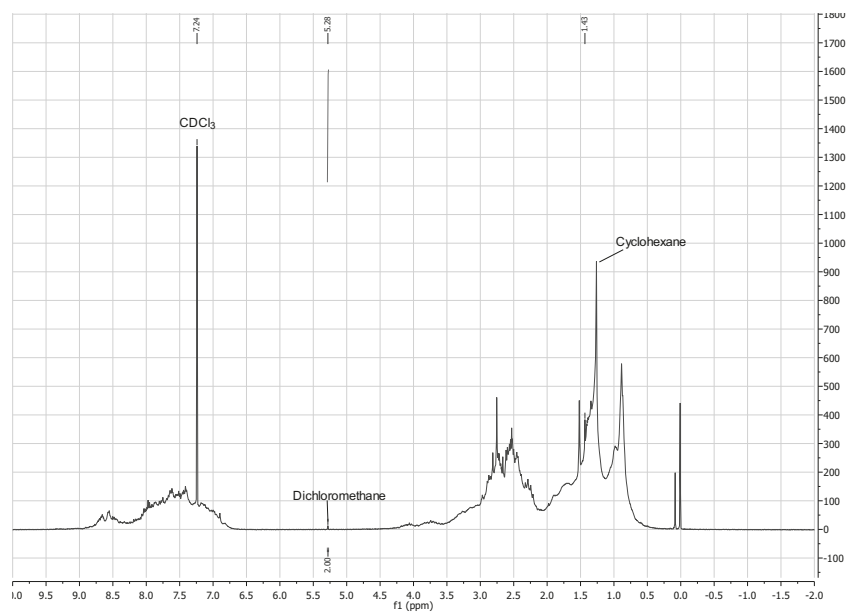


**Figure 94:** NMR spectra of the second fraction of Albacora Leste 369-509°C separated on PdSO<sub>4</sub>-Alox.

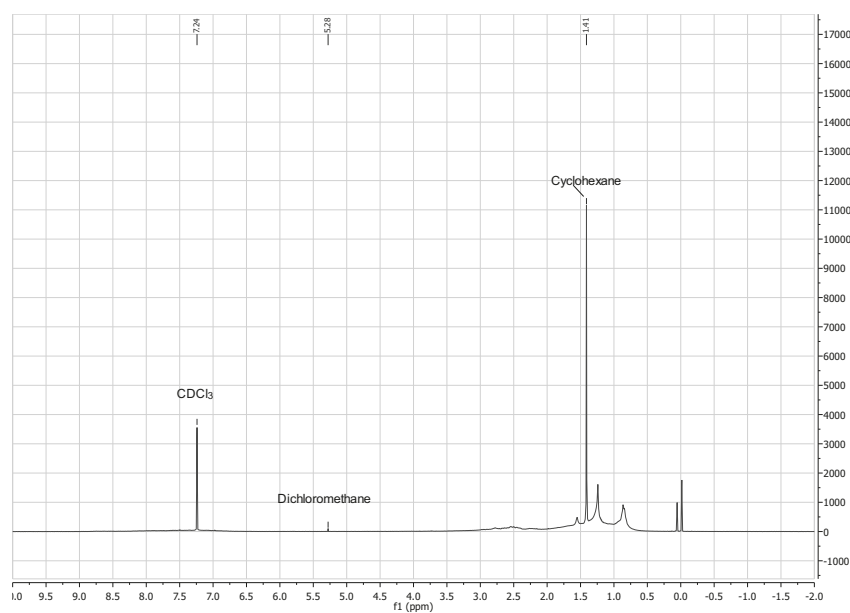


**Figure 95:** NMR spectra of the third fraction of Albacora Leste 369-509°C separated on PdSO<sub>4</sub>-Alox.

In tables 9 and 10 the results of the repeatability test with increased temperature during evaporation are displayed. The sulfur content was now determined externally via sulfur chemiluminescence according to DIN EN ISO 20884 by a commercial laboratory. Table 9 illustrates the successful enrichment of sulfur in the second and third fraction of the separation for both *h*Ag-MPSG and PdSO<sub>4</sub>-Alox. In the first fractions, supposedly containing aliphatics and PAHs, only small amounts of sulfur can be found and the percentage of sulfur is very low. The second fraction, expected to contain PASHs, is high in sulfur content, as well as the third fraction, where non-thiophenic sulfur is eluted. Karachaganak with its high sulfur content in the sample itself also shows much higher percentage of sulfur in the different fractions, indicating the presence of more small sulfur containing molecules than present in Albacora Leste. As the sulfidic-thiophenic ratio in the Karachaganak sample is 4:10 (see also table 13), it is also to be expected that the sulfur content of the second fraction is significantly higher than in the third fraction. For Albacora Leste, a sulfidic-thiophenic ratio of 6:10 was determined by BP, therefore the experimentally found ratio between the sulfur content in the second and third fraction is not expected. Larger amounts of the aromatic sulfur in the sample seem to be lost during the separation, compared to the non-thiophenic sulfur.

Table 10 shows the complete set of data for those separations, including mass balance, sulfur balance and recovery. The mass recovery has improved compared to the data obtained from the previous separations, where evaporation was performed at 40 °C. Concerning the sulfur recovery, there is a huge dependence of the stationary phase used. The separations on the silver phase only lead to a recovery of about 67%, whereas with the separations on palladium about 85% of sulfur can be recovered.

As the palladium phase separations succeeded much better, only those were included for the determination of the sulfur balance for the higher boiling samples. Therefore, the fractions collected for the previous repeatability studies were used. These samples still have high mass recovery variations as they were still evaporated at 40 °C, but remaining solvents should not have an effect on the sulfur balance. Table 11 shows the sulfur content in each of the separated fractions. In contrast to the previous results of the lower boiling cuts, the concentration effect is slightly less drastic. This could be due to the fact that molecules present in this fraction are even larger than the ones in the 369-509 °C fraction and therefore probably contain higher amounts of carbon per molecule.

**Table 9:** Sulfur content of Karachaganak 369-509 °C and Albacora Leste 369-509 °C separated on *h*Ag-MPSG and PdSO<sub>4</sub>-Alox.

E1 to E3 indicate the fractions 1 to 3 collected in the separations.

Sample name	weight of fraction [g]	sulfur content in fraction [mg/kg]	sulfur mass in fraction [ug]	% Sulfur in Fraction
Solvent (CH)	0	<0,5		
K369 Pd E1	0.193	4123	795.74	4%
K369 Pd E2	0.0305	40500	1235.25	41%
K369 Pd E3	0.0172	19600	337.12	20%
K369 Ag E1	0.1646	1052	173.16	1%
K369 Ag E2	0.0338	31000	1116.00	33%
K369 Ag E3	0.0115	51400	591.10	51%
A369 Pd E1	0.2096	2366	495.91	2%
A369 Pd E2	0.0375	11100	416.25	11%
A369 Pd E3	0.0235	14600	343.10	15%
A369 Ag E1	0.15	570	85.50	1%
A369 Ag E2	0.036	12100	408.98	11%
A369 Ag E3	0.0176	17700	311.52	18%

**Table 10:** Sulfur and mass balance of Karachaganak 369-509 °C and Albacora Leste 369-509 °C separated on *h*Ag-MPSG and PdSO<sub>4</sub>-Alox, evaporated at 60 °C.

Sample name	Stationary phase	Initial weight [mg]	sulfur content in sample [mg/kg]	Initial amount of sulfur in sample [ug]	Fraction 1 [g]	Fraction 2 [g]	Fraction 3 [g]	Total output weight [g]	Total sulfur mass in sample [ug]	recovery of sulfur
K369 1	PdSO <sub>4</sub> -Alox	202.29	13500	2730.9	0.193 80%	0.0305 13%	0.0172 7%	0.2407 119%	2368.11	87%
K369 2	<i>h</i> Ag-MPSG	203.51	13500	2747.4	0.1646 78%	0.0338 16%	0.0115 5%	0.2099 103%	1880.26	68%
A369 1	PdSO <sub>4</sub> -Alox	260.87	5790	1510.4	0.2096 77%	0.0375 14%	0.0235 9%	0.2706 104%	1255.26	83%
A369 2	<i>h</i> Ag-MPSG	208.14	5790	1205.1	0.15 74%	0.036 18%	0.0176 9%	0.2036 98%	806.00	67%

Table 12 sums up the mass and the sulfur balance. Mass recovery is still varying because of the lower evaporation temperature, but the sulfur recovery is also decreased compared to the lower boiling sample. With the 509-550 °C sample about 55% of the sulfur can be recovered.

All in all high temperatures during evaporation are essential for the determination of mass balance, as well as recovery. Even at evaporation temperatures of 60 °C recovery is slightly above 100% in nearly all samples with a boiling point of 369-509 °C, suggesting even higher temperatures are needed to completely remove remaining solvents. This makes the treatment of the lower boiling fractions with a boiling point of 96-369 °C almost impossible, as compounds of higher volatility present in the fractions might be lost during the evaporation process.



**Table 11:** Sulfur content of Albacora Leste 509-550 °C separated on PdSO<sub>4</sub>-Alox.

Sample I and III represent two samples from the repeatability tests, where the same crude oil fraction was separated analogously in 5 different batches. E1 to E3 indicate the fractions 1 to 3 collected in the separations.

Sample name	weight of fraction [g]	sulfur content in fraction [mg/kg]	sulfur mass in fraction [ug]	% Sulfur in Fraction
Solvent (CH)	0	<0,5		
A509 Pd I E1	0.1277	1431	182.74	1%
A509 Pd I E2	0.0527	5696	300.18	6%
A509 Pd I E3	0.0377	6197	233.63	6%
A509 Pd III E1	0.1837	990	181.86	1%
A509 Pd III E2	0.0562	5736	322.36	6%
A509 Pd III E3	0.0359	11160	400.64	11%

**Table 12:** Sulfur and mass balance of Albacora Leste 509-550 °C separated on PdSO<sub>4</sub>-Alox, evaporated at 40 °C.

Sample name	Stationary phase	Initial weight [mg]	sulfur content in sample [mg/kg]	Initial amount of sulfur in sample [ug]	Fraction 1 [g]	Fraction 2 [g]	Fraction 3 [g]	Total output weight [g]	Total sulfur mass in sample [ug]	recovery of sulfur
A509 I	PdSO <sub>4</sub> -Alox	191.91	7040	1351.0	0.1277 67%	0.0527 27%	0.0377 20%	0.2181 114%	716.54	53%
A509 III	PdSO <sub>4</sub> -Alox	212.43	7040	1495.5	0.1837 86%	0.0562 26%	0.0359 17%	0.2758 130%	904.87	61%

For the sulfur balance remaining solvents are not problematic, as the total sulfur content in the separated fractions is calculated. Here, for the samples with a boiling point of 369-509 °C the PdSO<sub>4</sub>-Alox phase performed significantly better than the *h*Ag-MPSG phase. Still about 15% of the sulfur is lost during the separation for the 369-509 °C samples and even about 45% for the 509-550 °C samples. The higher loss of sulfur while treating the higher boiling samples might be based on the fact that in polar compounds like asphaltenes and resins the sulfur content is much higher than in lower molecular weight compounds. [14] While performing the separations, very polar compounds are always retained on the column, or in pre-separations according to section 7.2, these compounds are kept on the pre-separating column.

## 7.6 Conclusions

Three different phases PdSO<sub>4</sub>-Alox, *h*Ag-MPSG and Ag<sup>+</sup>-cartridges were applied to VGO samples of different boiling range. For the silver based phases, for some samples strong interactions of large PASHs could be observed resulting in a carry-over of PASHs into the non-thiophenic fraction. For MS detection either ESI after methylation or an

atmospheric pressure ionization technique was applied. The methylation of the non-thiophenic compound classes was previously tested with standards and no methylation could be achieved for disulfides using either iodomethane or trimethyloxonium tetrafluoroborate as methylating agents. In APCI an oxidation of sulfidic standards to sulfoxides within the ion source was observable. Disulfides could not be sufficiently ionized to be even assignable in standard mixtures. Therefore, the used mass spectrometry techniques can still not be applied for the detection of disulfides and the quality of the separations can only be judged by the separation between thiophenic and non-thiophenic S1 compounds and additional parameters like sulfur content of the fractions, mass and sulfur balance.

The Kendrick plots of the separations on the different phases are similar, indicating similar separation abilities of the three phases. As the *h*Ag-MPSG preparation is complicated and inconsistent, the other phases are to be preferred. Also mass and sulfur balance showed a better performance for PdSO<sub>4</sub>-Alox than for *h*Ag-MPSG, as the sulfur recovery was higher and the mass balance more realistic. Ag<sup>+</sup>-cartridges are easy to use, but limited due to the fixed small amount of stationary phase in the prepacked columns, which is only able to separate very small amounts of VGO sample.

To separate the samples as desired no single phase alone will give sufficient results. Instead, using a combination of the LEC phases a separation scheme for non-thiophenic and thiophenic sulfur compounds can be created as displayed in figure 96.

By combining the properties of silver and palladium based phases, a separation into six groups is theoretically possible. After a preseparation on alumina the sample is separated first on the silver ion cartridges, as they are the only phase able to elute disulfides. The combined aliphatic and aromatic fraction are then further separated on the well established Pd-MPSG, as it is able to separate a sample into aliphatics, PAHs and PASHs. If desired, the PASHs can be subsequently separated according to the size of their aromatic ring system using a silver based phase, Ag-MSPG. The non-thiophenic fraction from the separation on Ag<sup>+</sup>-cartridges is divided and one part is analyzed using PdSO<sub>4</sub>-Alox to isolate two individual sulfide classes. The other part can be used for the determination of disulfides. As no stationary phase could be found yet to elute disulfides in an isolated fraction, derivatization of the disulfides and subsequent detection might be the solution here.

Alternatively, the also presented TBAPI oxidation of sulfides can be used as a starting point for the separation of non-thiophenic and thiophenic sulfur (see figure 97).

The advantage of this scheme is that no HPLC separation is needed, but only the Ag<sup>+</sup>-

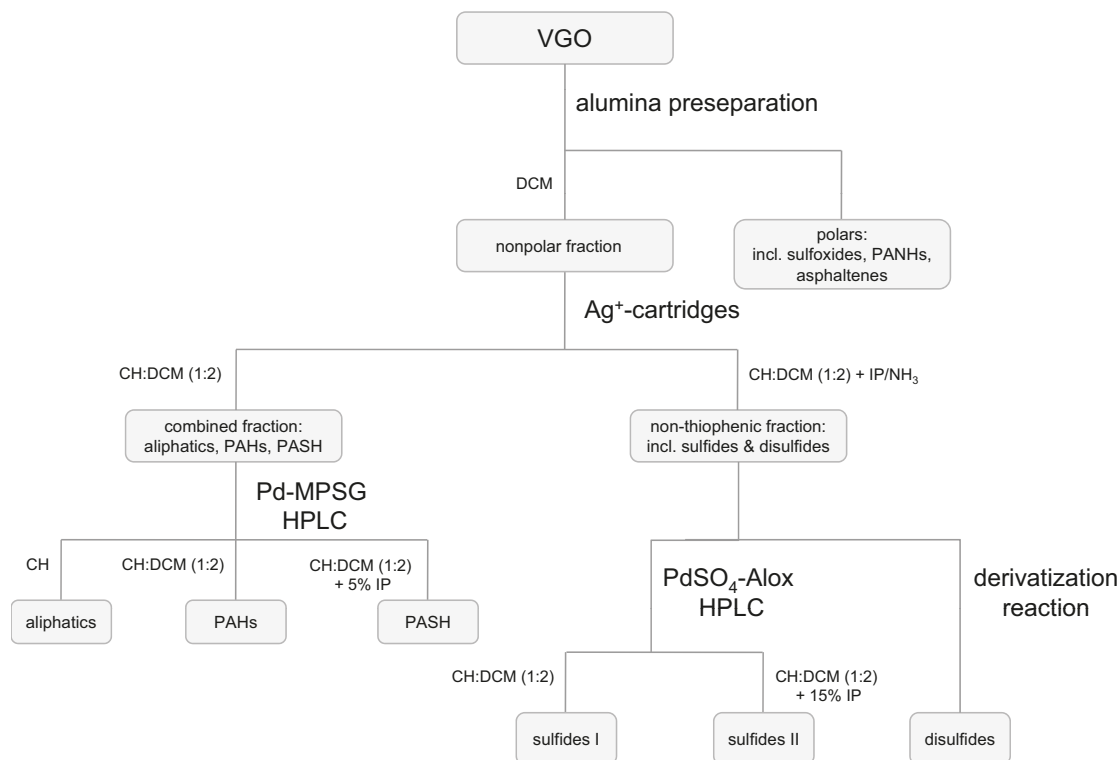


**Figure 96:** Model scheme for the complete separation of thiophenic and non-thiophenic sulfur compounds.

cartridges and conventional silica gel and alumina columns. After a preseparation on alumina the separated VGO is oxidized by TBAPI. On a silica gel column the less polar non-oxidized fraction is separated from the oxidized sulfides, which can be reduced to their original form using lithium aluminum hydride. The non-oxidized fraction can be further separated on Ag<sup>+</sup>-cartridges to obtain the disulfides. The separation of PAHs and PASHs is not as efficient as on Pd-MPSG, but disulfides can be recovered.

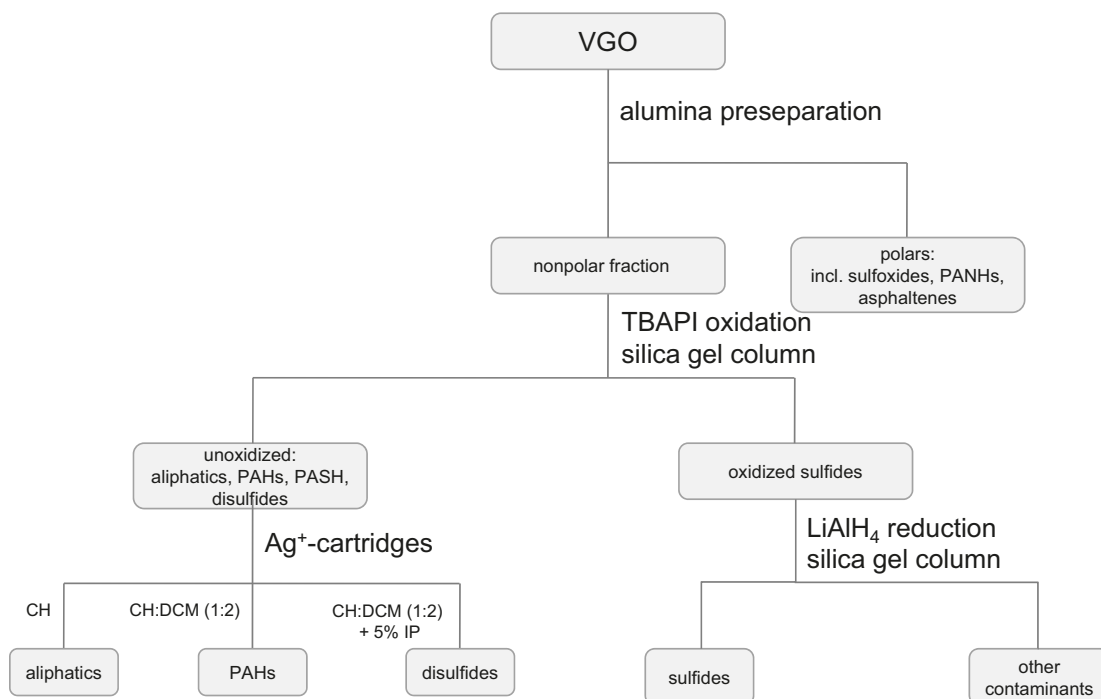


**Figure 97:** Alternative model scheme for the complete separation of thiophenic and non-thiophenic sulfur compounds.

## 8 Alternative approaches towards the analysis of disulfides in VGOs

### 8.1 State of the art: Analysis of disulfides

Organic disulfides occur, for example, in biological material like peptides and proteins. Therefore, many of the known methods for the determination of disulfides were developed for aqueous solutions. To analyze disulfides, usually the disulfide bridge bond is cleaved via reduction. In biochemistry traditionally reagents like dithiothreitol (DTT) and tris(2-carboxyethyl)phosphine (TCEP) are used (displayed in figure 98).

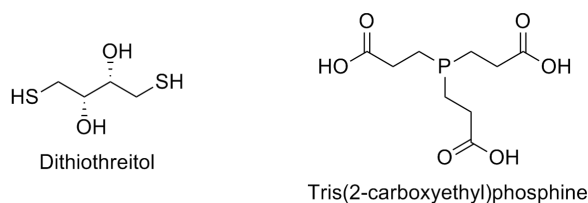


**Figure 98:** Traditionally used biochemical reagents for the cleavage of disulfide bonds.

DTT can be used as a reducing agent, because once oxidized it readily forms a stable six-membered ring with an internal disulfide bond. Even though the reaction with disulfides is a thiol-disulfide-exchange reaction, the equilibrium is shifted towards the cleavage of the disulfide, as the DTT can form a stable ring system. But its reducing abilities are limited to pH values below 7, because only the deprotonated thiolate-group will undergo ring closure, whereas the protonated thiol will not react. [136]

TCEP reduces disulfides stoichiometrically and irreversibly in the aqueous solution. [137] It is more stable than DTT and can be used in a wider pH range (1.5-8.5). [138] The reactivity of both reagents is also influenced by the presence of metal ions, that are able to function as oxidizing agents, e.g.  $\text{Fe}^{3+}$  and  $\text{Ni}^{2+}$ . [137]

In organic synthesis typically hydride reagents are used for the cleavage of disulfide bonds, e.g. sodium borohydride. [139] Various catalysts like zirconium chloride [140] or silver nanoparticle surfaces [141] are also used to enhance the reactivity of the borohydride. One great advantage of sodium borohydride is its solubility in a variety of solvents like alcohols, amines, or other polar solvents such as pyridine, acetonitrile, dimethyl formamide or tetrahydrofuran. In protic solvents like water or methanol it will decompose. [142] In contrast to other disulfide reducing agent like DTT, sodium borohydride is less selective and will also react with ketones, aldehydes, ester and nitro-alkenes. [143]

Historically also techniques like acid-reflux, acid-stirring, polarographic and alkali method were used to reduce disulfides. [144][145] For the acidic methods, disulfides were added to acetic acid and zinc powder and either heated under reflux or stirred with or without heating. In the polarographic method disulfides were reduced at the dropping mercury electrode and in the alkali method disulfides react with Claisen alkali and zinc powder in methanol. Subsequently the resulting thiols were determined by titration with silver nitrate solution. [146]

Nowadays many methods for the photometric detection of thiols have been established. Through derivatization agents photoactive substances are generated and can be detected by spectrometry. For fluorescence detection benzofurazan sulfides can be used [147], manganese(IV) reagents can be used for chemiluminescence [148] and various reagents, i.e. 2,2'-dipyridyl disulfide, can be used for UV/Vis-detection. Recently MONTROYA and PLUTH published a study showing that nitrobenzofurazan-based fluorescence can be quenched in the presence of sulfides. [149]

In the presence of thiols often the disulfide content is determined by difference measures, but thiols present can also be removed as the corresponding silver salts, extracted with alkali or converted to thioethers by unsaturated nitriles. [86]

In biochemistry thiols are often converted to thioesters by reacting with iodoacetamides, benzylic halides or bromomethylketones (see figure 99). Whereas iodoacetamides are mainly used to block reactive thiols on peptides,[150] maleimide derivatives can directly be used for detection and quantification via UV/Vis-spectroscopy. Maleimide derivatives can also be used for mass spectrometric determination of thiols and disulfides, e.g. ferrocene-based maleimides in LC/MS/MS. [151]

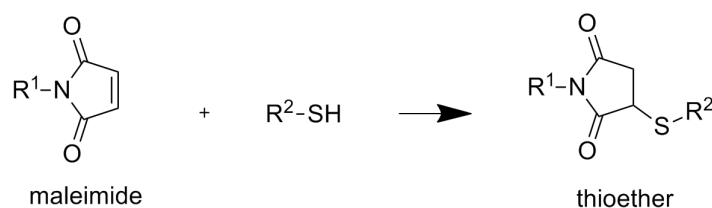


**Figure 99:** Reaction of maleimide and a thiol.

## 8.2 Reduction of disulfides with tris(2-carboxyethyl)phosphine (TCEP)

In addition to the reducing agents that were already tested in previous studies, i.e. sodium borohydride, dithiothreitol and ascorbic acid [85], with TCEP another widely

used reducing agent for the cleavage of disulfides in biochemistry was examined for the derivatization of disulfides in non-aqueous solution. The GC-FID chromatograms

prior to reaction

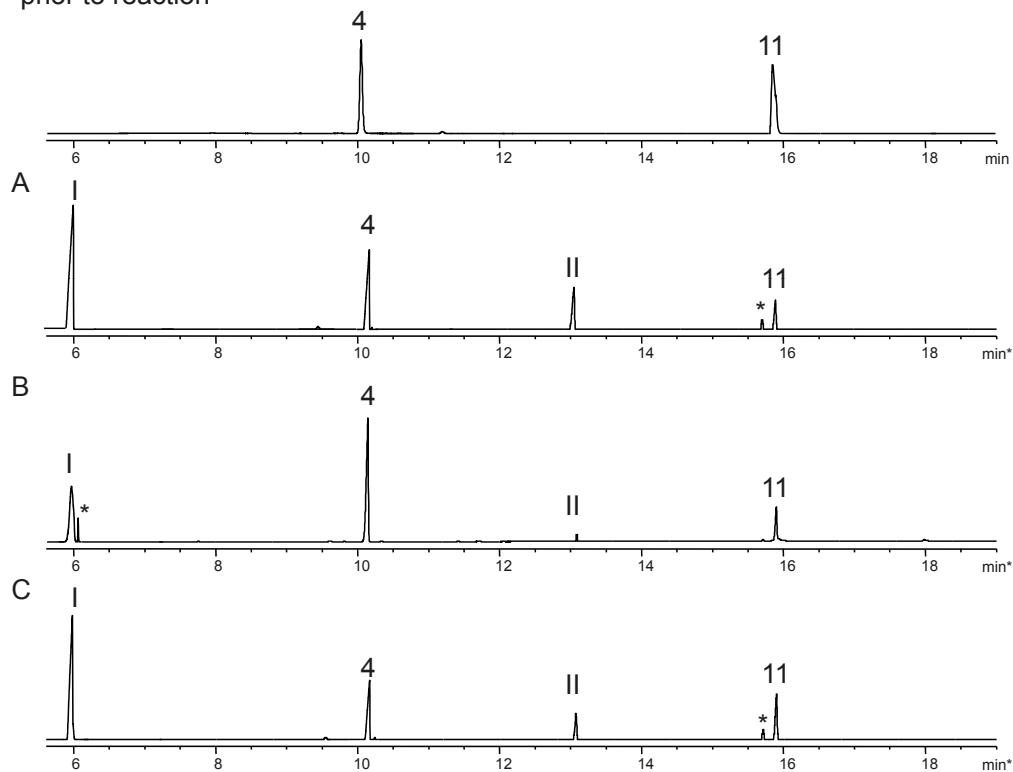


**Figure 100:** GC-FID chromatograms of the reduction of disulfide standards with TCEP in various solvents.

A: ACN/H<sub>2</sub>O, B: DMF/H<sub>2</sub>O, C: IP/H<sub>2</sub>O;

4: *n*-butyl disulfide, 11: phenyl disulfide, I-II: reaction products, \*: contamination.

of the reaction in all three solvent mixtures are displayed in figure 100. In all three cases TCEP was not able to reduce the disulfides completely. The reduction of phenyl disulfide was more efficient than the reduction of the aliphatic *n*-butyl disulfide, but still leftover phenyl disulfide can be found in all three reaction solutions. Under the given conditions TCEP is not able to sufficiently reduce disulfides in the given standard solutions. Therefore, for further experiments the reduction with sodium borohydride will be used. Sodium borohydride might be less selective for disulfide groups than TCEP, which is described to react with disulfide bonds only, but in non-aqueous samples it seems to be the better choice as the reducing abilities of TCEP were shown to be limited in organic solvent mixtures.

### 8.3 Reduction of disulfides and derivatization with ethyl iodoacetate

As sodium borohydride is a well known reagent for the reduction of disulfides in organic synthesis, a standard solution was reacted according to the procedure described in section 10.1.23. As derivatizing agent ethyl iodoacetate was chosen to introduce a polar ester group into the molecule and therefore enable the chromatographic separation of the derivatized product from the unreacted compounds (see figure 101).

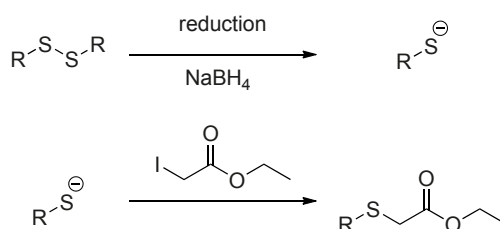


**Figure 101:** Reaction scheme of reduction and consecutive derivatization with ethyl iodoacetate.

The reduction with subsequent derivatization is successful for the simplified standard mixture (see figure 102). *N*-butyl and phenyl disulfide have completely reacted, whereas *t*-butyl disulfide did not react completely due to its steric hindrance. As extremely branched disulfides are presumably not overpresent in the vacuum gas oils, non-reacting tertiary disulfides are not of major concern. The sulfides present in the sample do not react, making the method suitable for the distinction between sulfidic and disulfidic sulfur.

When performing the reaction with a full standard mixture, again only disulfides do react. PASHs and non-sulfur containing compounds do not react under the given conditions. In crude oils, in addition to disulfides, also ketones might react, as sodium borohydride is well known for the reduction of ketones to alcohols, so that an excess of reducing agent should be used.

For the identification of products and byproducts, GC-AED and GC-MS were applied (see also figures 102 and 103). GC-AED was used to determine if compounds contained sulfur and GC-MS was used to determine *m/z*-ratios of the corresponding peaks to assign empirical formulas to the individual peaks. As there is no difference between the masses of isomers, the peaks for *n*-butyl disulfide and *t*-butyl disulfide, as well as the corresponding products can not be differentiated by MS, but only by their retention times in GC using standard substances, which were not available.



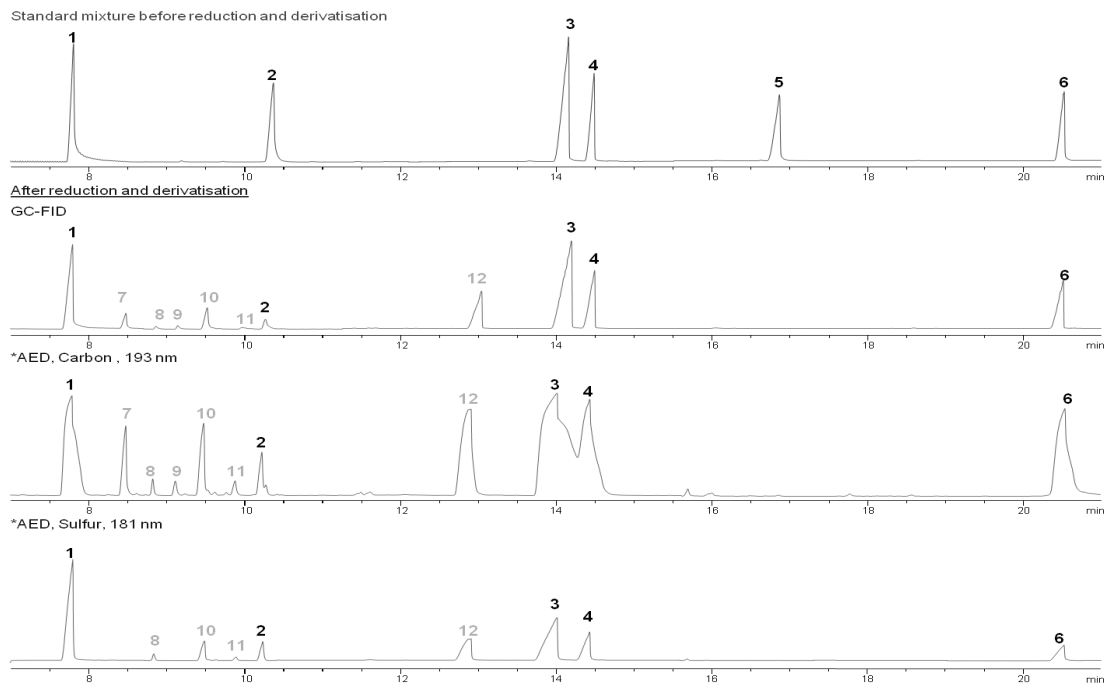


**Figure 102:** Reduction of a standard mixture with sodium borohydride and subsequent derivatization with ethyl iodoacetate. After the reaction GC-FID, GC-AED of the carbon trace (193 nm) and of the sulfur trace (181 nm) are shown, respectively.

Standards in the mixture: 1: *t*-butyl disulfide, 2: *n*-butyl disulfide, 3: dodecyl methyl sulfide, 4: phenyl sulfide, 5: phenyl disulfide, 6: octadecyl methyl sulfide

Products and byproducts of the reaction: 7: unidentified compound, non-sulfur-containing, 8: unidentified compound, sulfur-containing, 9: unidentified compound, non-sulfur-containing, 10: *S*-butyl ethyl acetate, 11: unidentified compound, sulfur-containing, 12: *S*-phenyl ethyl acetate.

Figures 102 and 103 show that the reduction and derivatization with ethyl iodoacetate yielded the desired products. Identification of the products could be performed via GC-MS and furthermore confirmed with GC-AED. For the peaks labeled 7-9 and 11 in figure 102, concentrations were too low to identify them with GC-MS. Judging from the sulfur trace in GC-AED, only compounds 8 and 11 contain sulfur, whereas 7 and 9 only produce emission of carbon atoms.

The reduction with subsequent derivatization appears to be a useful method for modifying disulfides. Aromatic and linear disulfides do react nearly completely under the given conditions, but branched, sterically hindered disulfides do not react. Other sulfur containing compound classes such as sulfides and PASHs also do not react, but of course

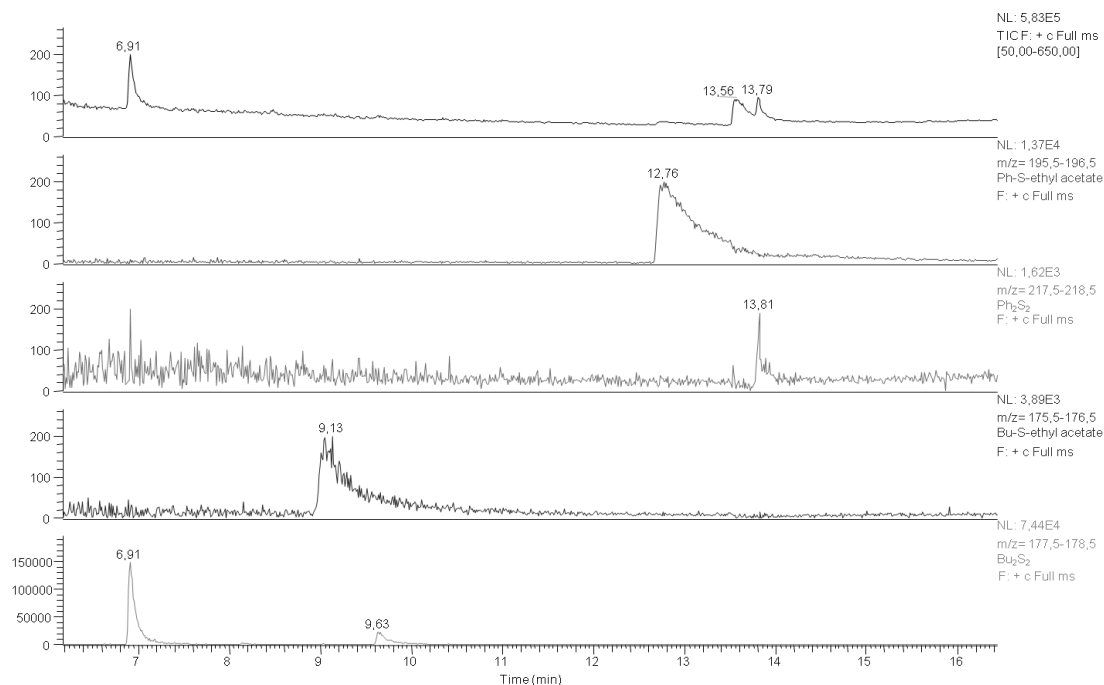


**Figure 103:** Mass spectrum of the standard mixture after reduction and derivatization with ethyl iodoacetate.

Total ion count (top), mass trace of *S*-phenyl ethyl acetate ( $m/z=196$ ), mass trace of phenyl disulfide ( $m/z=218$ ), mass trace of *S*-butyl ethyl acetate ( $m/z=176$ ) and mass trace of butyl disulfide ( $m/z=176$ )(bottom).

possible thiols in the sample would also react with ethyl iodoacetate and would have to be removed before the reaction or differentially determined.

As the exact concentration of disulfides in the sample is unknown, high excess of reagents was to be used in order to ensure sufficient availability. But still the separation of the leftover ethyl iodoacetate is challenging. An easy silica gel column, as well as C18 SPE cartridges is not sufficient for that purpose. Furthermore, mass spectrometric determination of the derivatized disulfides is not trivial. The ester group is not readily ionized in ESI and APCI and as many of the compounds lack larger aromatic systems APPI and APLI are not suited either. Therefore, alternatives to the derivatization with ethyl iodoacetate were tested.

#### 8.4 Reduction and derivatization with iodoacetic acid

As the separation of remaining derivatizing agent was tricky when derivatizing disulfides with ethyl iodoacetate, another set of samples was derivatized with the corresponding

acid, i.e. iodoacetic acid, to introduce a polar functional group, which can be directly introduced and analyzed by ESI-MS. The reaction scheme is analogue to the one presented in figure 101.

The MS detection of the derivatized products should be easily possible, as they are already present as acids. All the more it is surprising to see that even with the addition of bases to deprotonate the acids no peaks for the derivatized products could be found in the ESI mass spectra (see figure 104). As the success of the derivatization in principle was

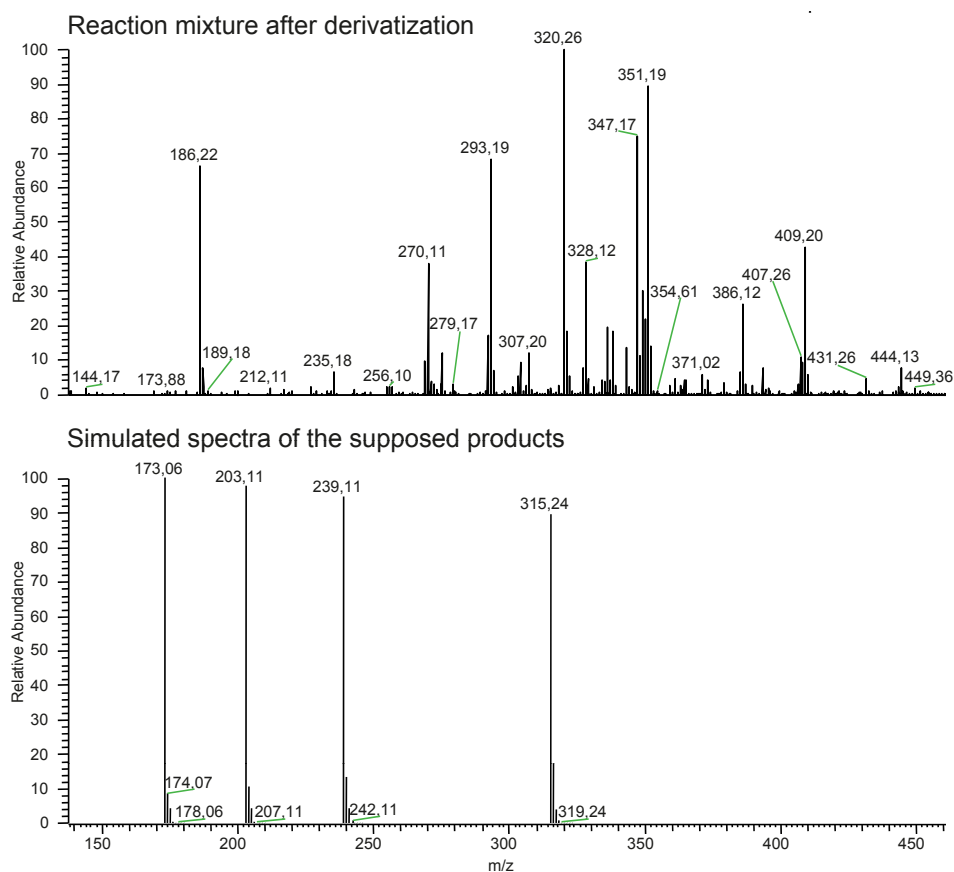


**Figure 104:** ESI-mass spectrum of the reaction of disulfide standards with iodoacetic acid.

Top: Reaction mixture after derivatization, bottom: simulated mass spectra of the desired products.

already shown in GC-FID for the ethyl ester, the structurally similar acid should behave similarly and produce analogous products. However, none of the derivatized disulfide standards could be identified using mass spectrometry. Therefore, the derivatization with iodoacetic acid is not suitable for the easy derivatization of disulfides in non-aqueous solutions.

### 8.5 Reduction and direct determination via ESI-MS as thiolates

After the reduction of disulfides, they are present as thiolates in aprotic environments and thiols in protic neutral to acidic solvents. If it is possible to quantitatively convert the thiols into thiolates, the now already charged molecules would be easily detectable in ESI-MS (see figure 105). With a pre-separation on alumina to remove thiols originating in the sample, the reduction and subsequent detection with ESI would be an easy way to determine disulfides in the VGO samples, as no other compound classes would react and the thiolates should be the only compound class detectable in the ESI negative mode after the pre-separation.

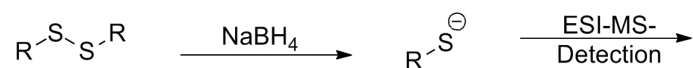


**Figure 105:** Reaction scheme for the direct MS detection as thiolates after the reduction of disulfides

In the literature also the detection of disulfides after an electrochemical reduction is described for biological samples. [152, 153] The disulfide bonds of proteins are cleaved in an electrochemical cell (EC) and through coupling the cell to a mass spectrometer the resulting products can be directly analyzed. This approach could in principal be transferred to the determination of disulfides in petroleum samples, if sufficient conductivity is ensured in the rather lipophilic solvents needed to be able to dissolve especially higher boiling petroleum cuts.

To test this approach, octadecanethiol was dissolved in methanol/potassium hydroxide to deprotonate the thiol to the corresponding thiolate. ESI spectra were recorded in the negative and positive mode, as well as an ESI spectra of the octadecanethiol in pure methanol in negative mode was recorded additionally. The mass spectra including the simulated spectra for the thiolate are displayed in figure 106. Additionally a blank spectra was recorded, but showed no significant signals in the  $m/z$  range of interest.

It is obvious on the first glance that the desired product octadecanethiolate was not detectable in the MS. The addition of potassium hydroxide seems not to be sufficient to effectively deprotonate the thiol. In addition, all mass spectra show the presence of multiple disturbing signals of contaminations. For standards an identification besides multiple interferences might be still doable, but for the supercomplex matrices and analyte compositions found in crude oils, the distinction between analytes and contam-

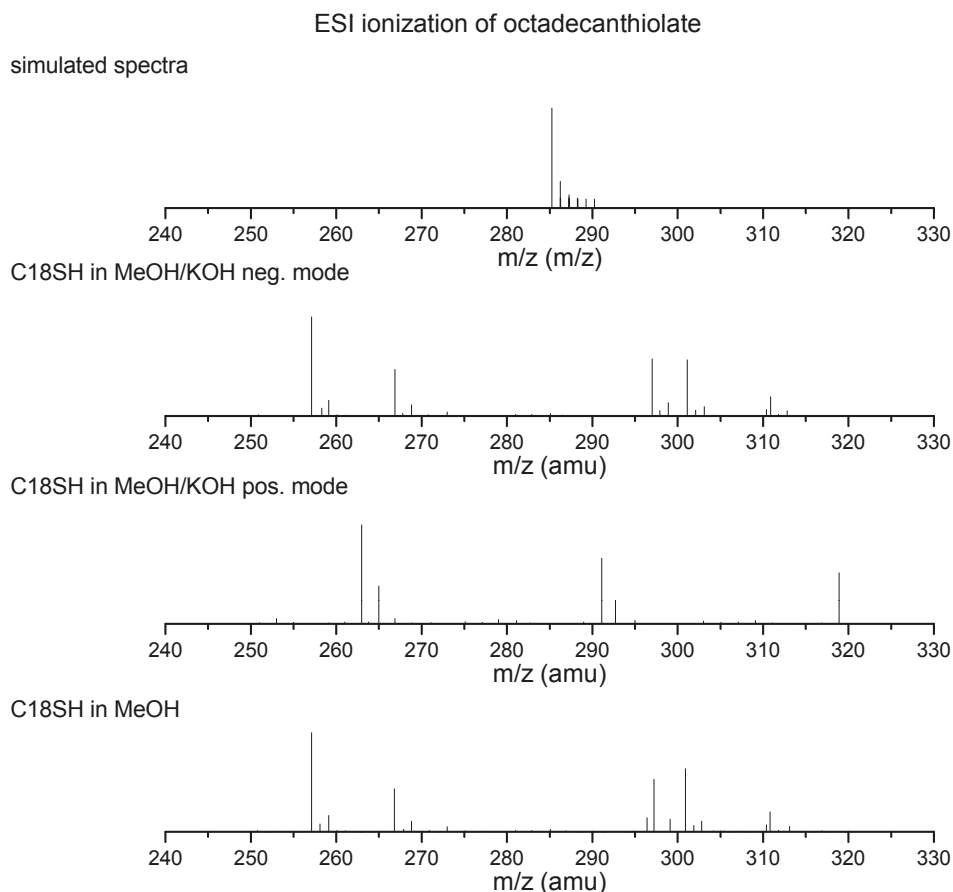


**Figure 106:** ESI-mass spectra of octadecanethiolate ( $C_{18}H_{37}S^-$ ,  $m/z$ : 285,26).

simulated spectrum of the thiolate (top); octadecanethiol in methanol/potassium hydroxide, ESI-spectra in negative mode; octadecanethiol in methanol/potassium hydroxide, ESI-spectra in positive mode; octadecanethiol in pure methanol, ESI-spectra in negative mode (bottom).

inations will be drastically complicated. The methanol/potassium hydroxide mixture was not suitable for the deprotonation of the thiolate. Due to the lipophilic character of the samples, but the need for conductivity in EC and the limited compatibility of many salts in MS, the range of solvents and salts applicable for this kind of detection is very restricted.

The direct MS detection of disulfides after the reduction to thiolates is not as trivial as it seems. It must be guaranteed that the deprotonation of possible thiols is quantitative and no large amount of disturbing signals must be present in the mass spectra. It is a difficult and time-consuming process to find a suitable combination of lipophilic solvent,

that is still able to dissolve sufficient concentrations of salts and to choose the fitting salt, that create a basic solution when dissolved, but can still be injected into a mass spectrometer without causing damage to the instrument or form too many clusters. At this stage of development, the established method cannot be applied to the separation of actual disulfides in VGO samples.

### 8.6 Reduction and derivatization with maleic anhydride

Another approach to derivatize disulfides is the addition to alkenes. The so called disulfidation of carbon-carbon bonds has been widely applied in organic synthesis using various catalysts. Reactions of thiols and disulfides with unsaturated compounds, e.g. alkenes, have been described in literature. [151, 154] The advantage of using maleic anhydride as a derivatizing agent is that hydrolysis leads to a strongly enhanced polarity of the derivatized compound by the two acid functions that may allow analysis via LC-MS (see figure 107).

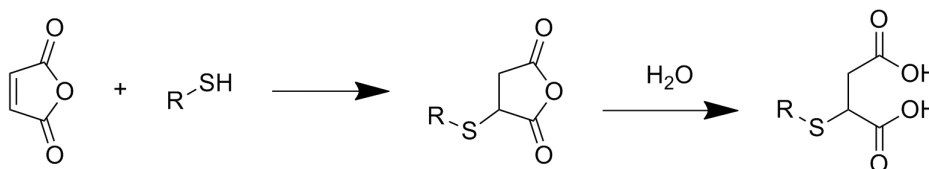


**Figure 107:** Reaction scheme of derivatization with maleic anhydride and subsequent hydrolysis.

The reactions of proteins with unsaturated compounds described in the literature cannot be transferred to the analytes possibly present in the VGO samples without further modifications, as the aqueous work-up step results in hydrolysis of the anhydride (see also [155]). The resulting diacids polarity is increased, so that a distribution of the derivatized standards between the aqueous and organic phase occurred. Processing is more complicated as both phases contain analytes and furthermore additional clean-up steps would be necessary. As the method to be developed should be suitable for routine analysis, further work-up steps would make it non-transferable for routine work and therefore the derivatization with maleic anhydride is not suitable for routine analysis of disulfides in fossil material. As the basic mechanism of this derivatization was successful, further experiments with other unsaturated carbon-carbon bond containing derivatizing agents were performed.

### 8.7 Iodine-catalyzed addition of disulfides to alkenes

As the derivatization with maleic anhydride resulted in issues with the partition equilibrium of the derivatized products, other unsaturated compounds were used to derivatize disulfides accordingly. Based on the method described by WANG and CHEN, disulfide standards were reacted with 4-fluorostyrene and hex-5-enoic acid. [156] The reaction scheme is exemplarily displayed for 4-fluorostyrene in figure 108. The fluorostyrene was chosen for two reasons: firstly to introduce an aromatic ring structure making the derivatized molecule more susceptible to photoionization sources like APPI and APLI and secondly to introduce a fluorine atom. Fluorine does not naturally occur in petroleum samples and is monoisotopic. Therefore, using sufficient mass resolution an unambiguous assignment of the derivatized products would be possible. Hex-5-enoic acid was chosen to introduce an acid function into the disulfides to strongly increase the polarity and therefore drastically change retention. The so derivatized disulfides could be separated from the remaining rather nonpolar sulfur containing compounds like sulfides and PASHs more easily.

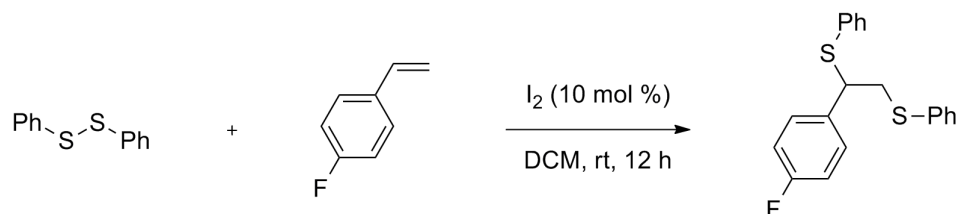


**Figure 108:** Reaction scheme of iodine-catalyzed addition of disulfides to 4-fluorostyrene. [156]

For the derivatization *n*-butyl disulfide and phenyl disulfide were chosen as standards to study the behavior of both aromatic and aliphatic disulfides in the reaction. The GC-FID chromatograms prior to the reaction and after the derivatization with 4-fluorostyrene are displayed in figure 109.

The reaction of the disulfides with 4-fluorostyrene was successful, as nearly all of the starting materials reacted. The peaks for the disulfides nearly vanished during the reaction. Four products could be detected. As displayed in figure 110, besides the symmetric bissulfides also the mixed products, where both *n*-butyl and phenyl thiolates are added to the unsaturated carbon-carbon bond of the fluorostyrene, are formed.

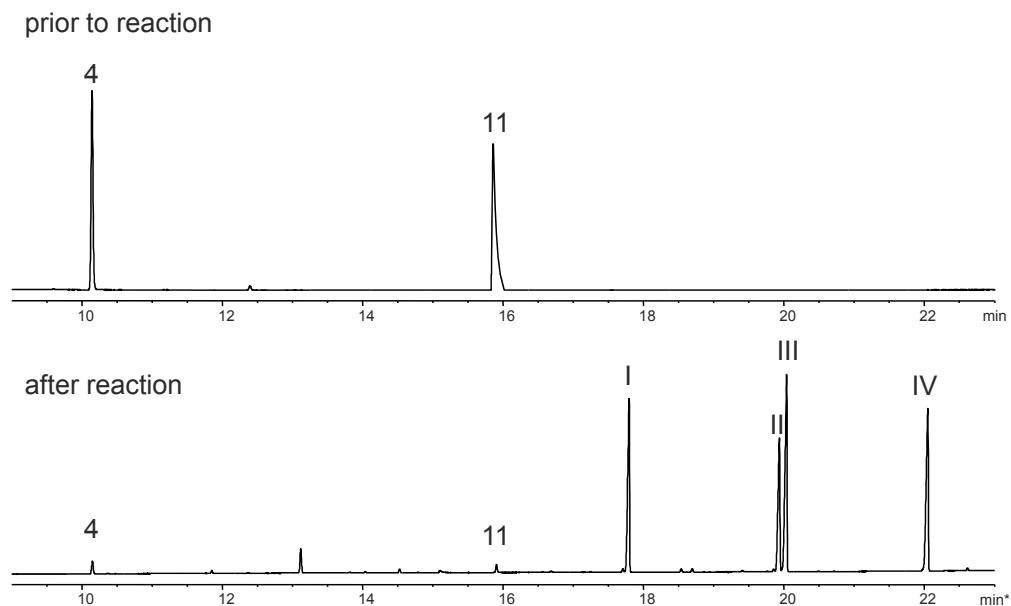


**Figure 109:** GC-FID chromatograms of the derivatization of disulfide standards with 4-fluorostyrene.

4: *n*-butyl disulfide, 11: phenyl disulfide, I-IV: reaction products, for structures see fig. 110.

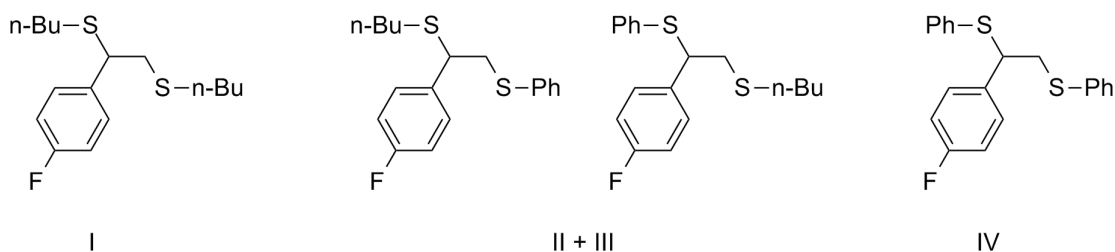


**Figure 110:** Structures of the products of the addition of disulfides standards to 4-fluorostyrene. Besides the symmetric products also the mixed products were found.

The corresponding GC-FID chromatograms for the reaction with hex-5-enoic acid are displayed in figure 111. In contrast to the reaction with fluorostyrene, the reaction with the acid is not as complete. Large amounts of educts remain unreacted. As the conversion is highly incomplete, the reaction products were not further identified.

The reaction of the disulfides with hex-5-enoic acid was not successful, as only small amounts of the educts reacted at all. As for the determination and eventual quantification of non-thiophenic sulfur in a sample, a complete conversion is needed, this derivatization reaction is not suitable for the analytical problem and hence not further investigated.



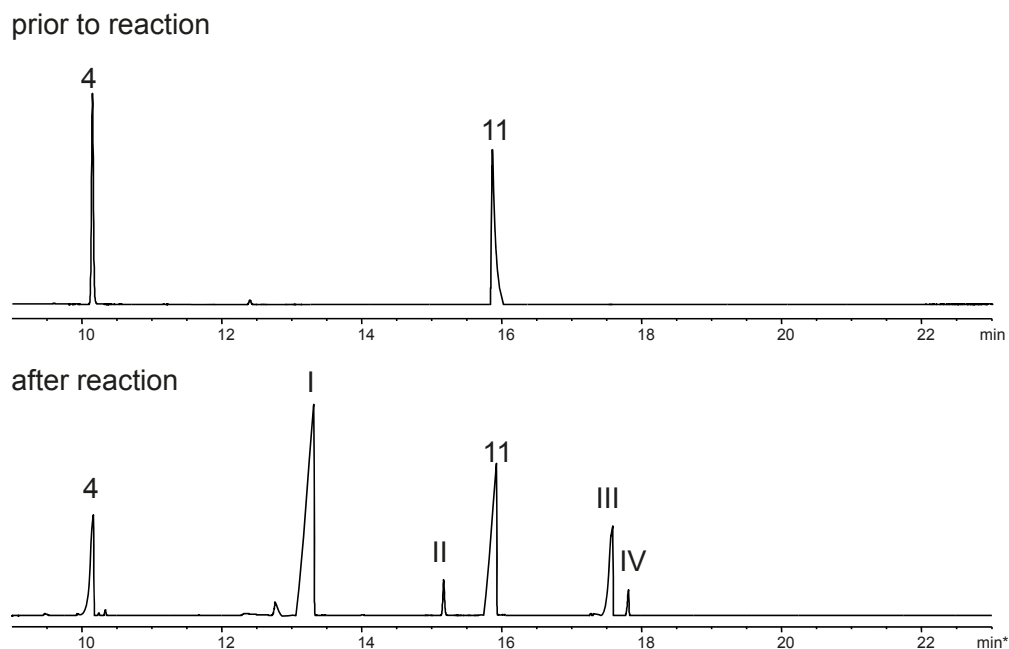


**Figure 111:** GC-FID chromatograms of the derivatization of disulfide standards with hex-5-enoic acid.

4: *n*-butyl disulfide, 11: phenyl disulfide, I-IV: reaction products.

All in all, the derivatization by addition to alkenes is not suitable for the application to real world samples. Using 4-fluorostyrene, mixed products are formed in addition to the desired products. In real world samples the supercomplexity of the matrix would be problematic as reacted disulfides could not be identified correctly and by the creation of mixed products the number of compounds would be enlarged even more. Furthermore, as the reaction does not seem to be intermolecular, other compounds, e.g. thiols or alcohols, might also react with the intermediates and disturb the reaction. Using hex-5-enoic acid, standards do not react even close to quantitatively. For a subsequent determination many analytes would be lost as they would not be derivatized. Therefore, both alkenes 4-fluorostyrene and hex-5-enoic acid are not useful for the derivatization of disulfides in petroleum samples.

## 8.8 Reduction and detection via photometry

### 8.8.1 Derivatization with monobromobimane (mBBr)

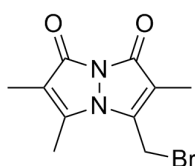


**Figure 112:** Structure of monobromobimane (mBBr).

In biochemistry, bromobimanes are widely used to probe protein structure due to their specificity towards thiol groups, their small size and high reactivity with any natural or mutated SH-function in the protein. [157] Of the available bromobimanes, monobromobimane (mBBr, see figure 112) is the smallest and least water soluble and was therefore chosen to be tested in standard experiments for the derivatization of thiol groups.

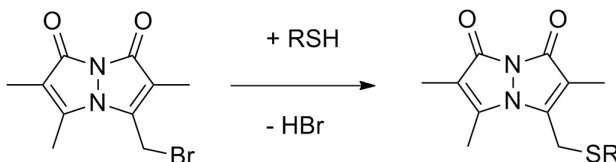


**Figure 113:** Reaction of monobromobimane (mBBr) with R-SH.

The results of the derivatization of different standard compounds with mBBr are displayed in figure 114. In addition to these results, observable differences were noticeable in the samples. When preparing the reagent solution, the color of the mBBr solution was yellowish, after mixing with the standard solutions all colors intensified, but after one night the yellow color vanished and some weak fluorescent purple shimmer was left. Either the reaction takes over night to be completed or the products formed are not very stable and need to be processed right away.

When taking a look at the GC chromatograms, it is noticeable, that only the sulfide seems to react under the given conditions. The retention of neither the disulfides or alcohol nor the thiol is changed. As the reaction scheme requires the elimination of hydrogen bromide (see figure 113), perhaps the use of a two phase system or a proton acceptor is necessary to shift the reaction equilibrium. Under the given conditions the derivatization with monobrombimane is not suitable for the derivatization of disulfides in non-aqueous solutions.

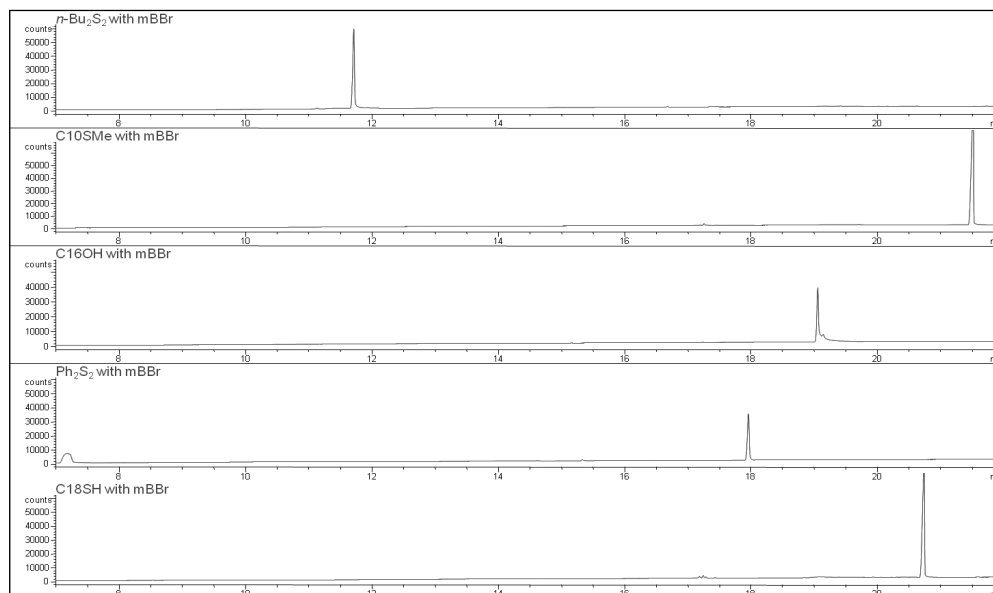


**Figure 114:** GC-FID chromatograms of the reaction mixtures of the different standards with mBBr.

1: *n*-butyl disulfide, retention time of standard: 11.3 min 2: decyl methyl sulfide, retention time of standard: 13.1 min 3: heptadecanol, retention time of standard: n.a. 4: phenyl disulfide, retention time of standard: 18.2 min 5: octadecanethiol, retention time of standard: 21.3 min

### 8.8.2 Derivatization with benzofurazan sulfides

The method for the derivatization of thiols with benzofurazan sulfides described by LI et al. has been modified to test the reaction of nitrobenzofurazan sulfides with several standard substances in non-aqueous solution. In the literature [147] benzofurazan sulfides are used to generate fluorescence from amino acids and derivatives containing thiol groups, whereas amino acids without thiol function do not react (see figure 115). These reactions take place in a buffered solution at pH 7 in a very short time.

As benzofurazan sulfides are readily soluble in acetonitrile, it was chosen as the solvent for the derivatization. Standards containing different functional group such as thiols, alcohols, amines, sulfides and disulfides were given to the benzofurazan sulfide solution and stirred. After 15 min and after 24 h samples were taken. For the amine, a change in color of the reaction mixture was observable immediately: the dark gamboge solution changes immediately to red and after 24 h to a dark green. The alcohol did not change, as well as the sulfur functionalities after 15 min. Both solutions remained gamboge and no

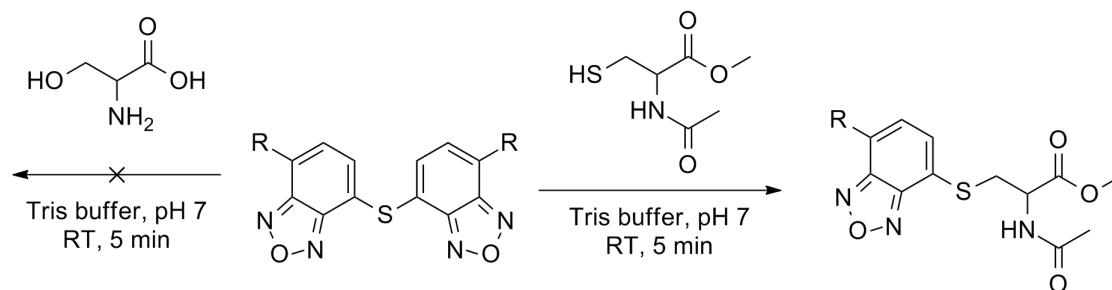


**Figure 115:** Reaction of benzofurazan sulfides with biological thiols in aqueous buffer. [147]  
 R =  $-\text{NO}_2$ ;  $-\text{S}(\text{O})_2\text{N}(\text{CH}_3)_2$ ;  $-\text{S}(\text{O})_2\text{N}(\text{Ph})$ ;  $-\text{S}(\text{O})_2\text{Ph}$

fluorescence was observable, but after 24 h all sulfur containing solutions were completely decolorized and still no fluorescence was observable. Therefore the benzofurazan sulfide itself obviously decomposed in those solutions, but without the creation of the desired fluorescent products described by LI et al.

In experiments with standard solution the derivatization with benzofurazan sulfides was not successful. Immediate changes in color were only observable with the supposedly nonreactive amine, the sulfur functional groups all led to a colorless solution after 24 h and no immediate reaction was observable. Therefore, the fluorescence detection of disulfides in petroleum using benzofurazan sulfides was not successful and hence not suitable for the analytical problem.

Recently, this observation is also supported by the literature. MONTROYA and PLUTH report that hydrogen sulfide is able to deactivate nitrobenzofurazan and results in a quenching of the fluorescence (see figure 116).

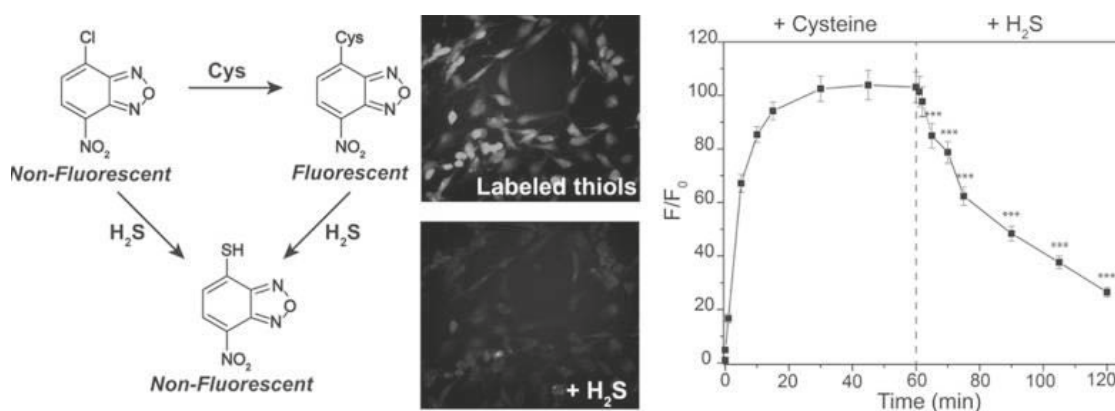


**Figure 116:** Reaction of nitrobenzofurazan with amino acids and its quenching by hydrogen sulfide: Fluorescence images and data. [149]

### 8.9 Isolation of sulfides by oxidation with tetrabutylammonium periodate

In addition to the LEC phases, a different approach towards the detection and identification of non-thiophenic sulfur, as described by PAYZANT et al., was tested (see figure 117). [158]

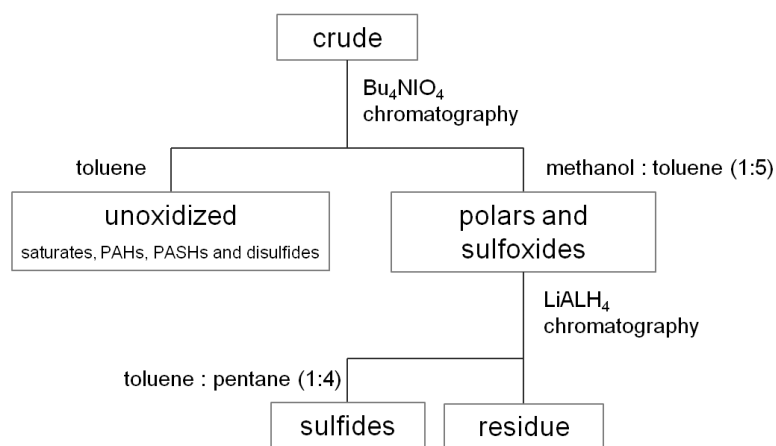


**Figure 117:** Scheme for the alternative separation of sulfides. [158]

Through oxidation of the sulfides to sulfones the polarity of these compounds is increased, so they can be separated from the remaining non-oxidized sulfur containing compounds. Therefore, thiophenic sulfur, as well as disulfides, which are not effected by the oxidation will be collected in one fraction, whereas the sulfides can be isolated. Thiols are already retained irreversibly on the stationary phase in the first step of the separation and cannot be recovered.

To test the method described in the literature, a standard mixture was processed as described and the resulting fractions were analyzed via GC-FID. The chromatograms of the unoxidized fraction, containing saturates, PAHs, PASHs and disulfides, as well as the sulfidic fraction after oxidation and subsequent reduction are displayed in figure 118. Due to multiple evaporation of solvents a lot of the lower boiling and volatile compounds, like naphthalene and the small disulfides, were lost during the evaporation progresses. This might be problematic for the low boiling fraction (96-369 °C), but for the other two fractions (369-509 °C and 509-550 °C) it will be of no concern as the boiling point of the samples is much higher than the boiling point of the used solvents and the compounds present in these two fractions should be less volatile. Apart from this, the separation of sulfides of the standard mixture was successful.

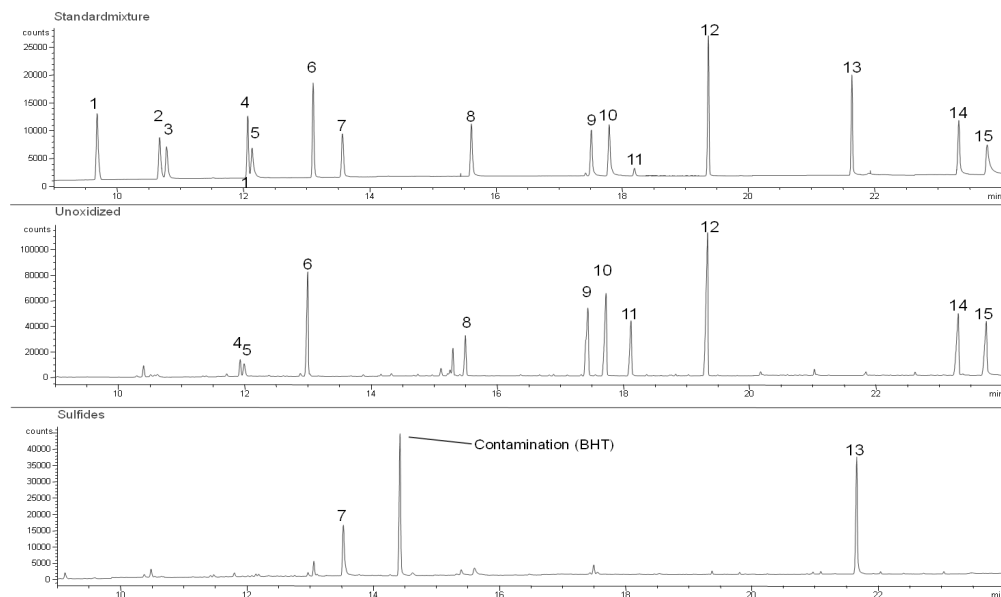


**Figure 118:** Separation via oxidation and reduction of a standard mixture. Top: standards; middle: unoxidized fraction (compare to fig. 117); bottom: sulfide fraction.

1: *t*-butyl disulfide, 2: naphthalene, 3: BT, 4: *n*-butyl disulfide, 5: 2-methylbenzothiophene, 6: tetradecane, 7: decyl methyl sulfide, 8: phenyl sulfide, 9: DBT, 10: phenanthrene, 11: phenyl disulfide, 12: eicosane, 13: octadecyl methyl sulfide, 14: BN[1,2-*d*]T, 15: chrysene.

After testing the method successfully with standard compounds, real world samples were processed. Therefore, Karachaganak 369-509 °C was chosen for its high sulfur content and high amount of non-thiophenic sulfur as provided by BP (see table 13).

To simplify the matrix, a pre-separation on neutral alumina was performed, as described in section 7.2. Kendrick plots of the S1 and S2 compounds present in this fraction before any further separation are displayed in figures 119 and 120.

Here again is proven that non-aromatic sulfur compounds (DBE <3) are eluted in this fraction, as can be clearly seen for the S1 compounds (see figure 119). The smallest S2 compounds detectable via APCI-FT-ICR have a DBE of three. At DBE 4 and higher, they might be aromatic compounds with two sulfur atoms in the aromatic ring. Definitely aliphatic S2 compounds could not be found with APCI. Disulfides cannot be methylated with iodomethane and are only weakly ionizable via APCI, therefore it is hard to detect aliphatic disulfides in these samples if they are present. Both Kendrick plots have a nicely distributed pattern, the maximum for the S1 compounds is at about 5 DBE, for the S2 compounds it can be found at DBE 11, supporting the assumption that the S2 compounds are of an aromatic character.

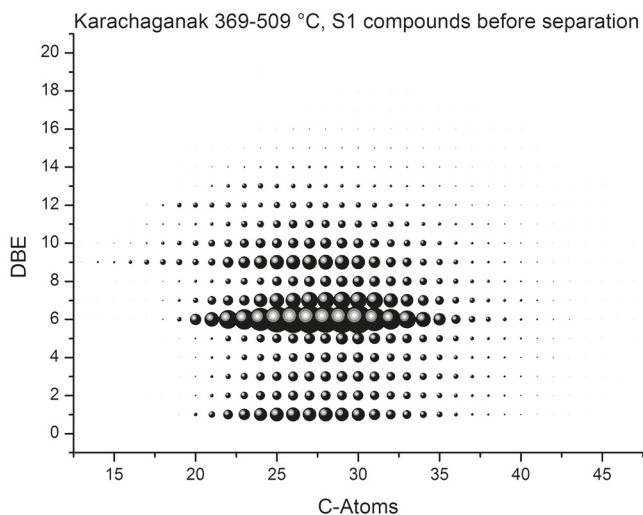


**Figure 119:** Kendrick plot of the S1 compounds from the APCI-FT-ICR spectrum of Karachaganak 369-509 °C before sulfide separation.

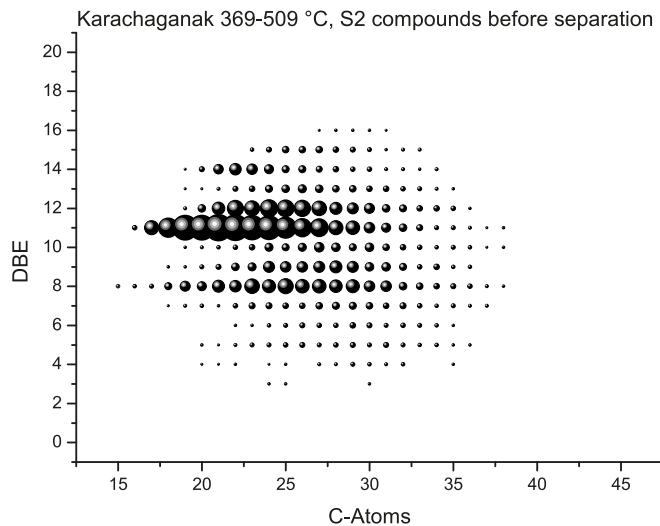


**Figure 120:** Kendrick plot of the S2 compounds from the APCI-FT-ICR spectrum of Karachaganak 369-509 °C before sulfide separation.

The aromatic fraction was processed according to figure 117 and the unoxidized and sulfide fraction were analyzed via MS. As the sulfides are readily methylated, this fraction was directly analyzed via ESI-Orbitrap-MS (see figure 121). The unoxidized fraction,

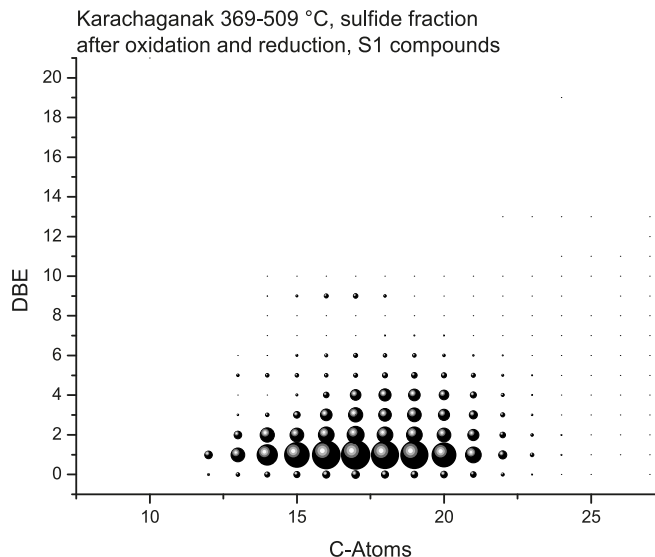


**Figure 121:** Kendrick plot of the S1 compounds of the ESI-Orbitrap-MS spectrum of Karachaganak 369-509 °C, sulfide fraction.

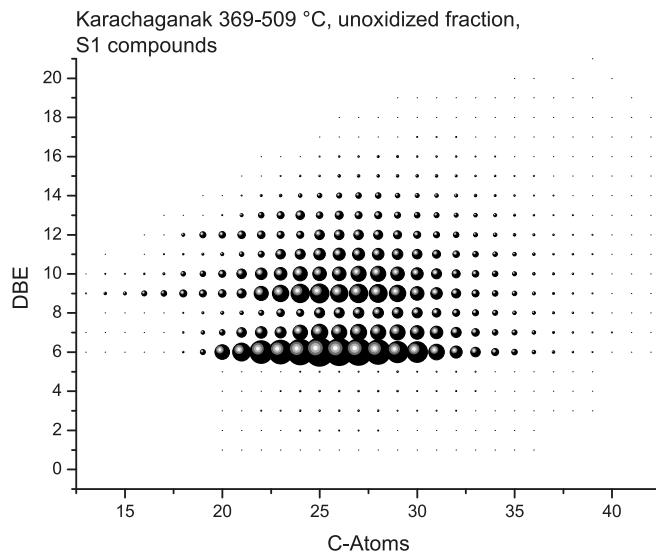
that according to standard experiments might include disulfides and PASHs, was analyzed via APCI-FT-ICR-MS (see figures 122 and 123).

When looking at the Kendrick plot of the S1 compounds of the sulfide fraction in figure 121, it is easy to see that the separation of sulfidic sulfur was successful. The compounds visible in the plot start at a DBE of zero, proving the existence of a very small amount of linear aliphatic sulfides in this sample. The maximum is at DBE 1. This DBE corresponds to cyclic sulfides, which indeed are expected to be the major form of this class of compounds. As the pattern goes up to DBE of 9 either naphthene rings are attached or aromatic rings are incorporated to the sulfidic compounds present in this sample.

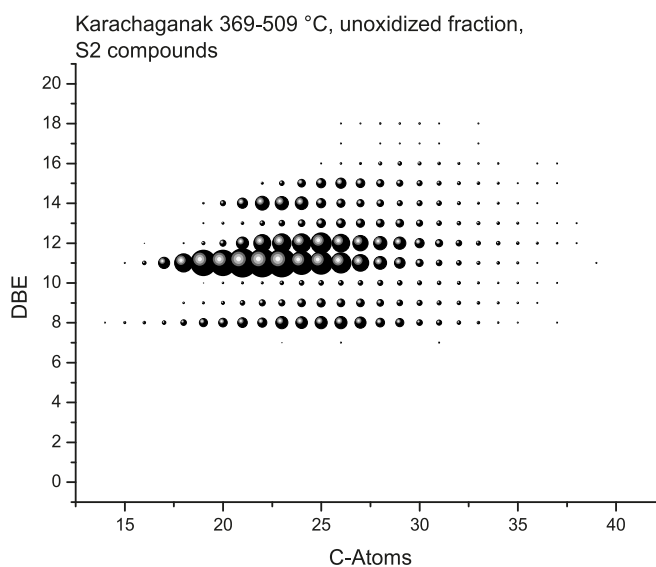
Figures 122 and 123 show the Kendrick plots of the S1 and S2 compounds of the unoxidized fraction, respectively. Taking a closer look at the S1 compounds in figure 122, it becomes obvious that this fraction mainly consists of aromatic sulfur compounds. The maximum can be found at DBE 6, which corresponds to benzothiophenes, and the pattern reaches up to a DBE of 21. The rather broad distribution of C-atoms shows that there is a huge variety of degree of alkylation in this sample, as would be expected of a vacuum gas oil of this boiling range.

Figure 123, displaying the S2 compounds of this sample, shows a different distribution. Starting at DBE 8, the maximum intensity can be found at DBE 11. These high DBEs reaching up to 19 indicate the presence of aromatic S2 compounds like thienothiophenes





**Figure 122:** Kendrick plot of the S1 compounds of the APCI-FT-ICR spectrum of Karachaganak 369-509 °C, unoxidized fraction.



**Figure 123:** Kendrick plot of the S2 compounds of the APCI-FT-ICR spectrum of Karachaganak 369-509 °C, unoxidized fraction.

and derivatives rather than disulfidic compounds. Of course, also disulfides with high DBE are possible in principle, but thienothiophenes are the more probable option and have already been described in the literature. [15] In this fraction also a wide distribution of C-atoms can be found, so the alkylation degree of the S2 compounds in this sample varies a lot as well.

The separation of sulfides via oxidation and reduction was successfully applied to a real world sample. A sulfidic and an unoxidized sulfur containing fraction could be obtained and analyzed via high resolution mass spectrometry. The sulfidic fraction contains various sulfides, starting with aliphatic sulfides and reaching up to DBE 10, indicating either aromatic structures or various ring closures. The unoxidized fraction contains aromatic S1 compounds, starting mainly with benzothiophenes and reaching up to DBE 21. The number of C-atoms of the S1 compounds varies from 12 to 42, so the alkylation pattern is complex. The same applies to the S2 compounds of this fraction (C-atoms from 14 to 39). Here, the distribution pattern starts at DBE 8 and reaches up to DBE 19. Thienothiophenes and similar structures are more probable to be present than highly aromatized disulfides. Especially as disulfides are only weakly ionizable with APCI and even in standard solutions are suppressed by other sulfur containing compounds like PASHs or sulfides.

## 8.10 Conclusions

The detection of disulfides in VGO samples is still the most complex problem to solve. On the tested LEC phases they either are not retained at all or are bound too strongly onto the phase, so that they cannot be released. Only on Ag<sup>+</sup>-cartridges could some disulfides be recovered. That is why alternative methods for the detection and determination of disulfides were tested. As many methods are based on the analysis of thiols different approaches for the cleavage of the disulfide bond were tested. The best results could be obtained using sodium borohydride at elevated temperatures of 60 °C. For the actual derivatization mainly four approaches were tested: iodine containing compounds to introduce more polar groups, direct MS analysis of the thiolates, the addition of disulfides to unsaturated carbon-carbon-bonds and photometrical detection.

For the photometrical approach using nitrobenzofurazan sulfides and monobromobimane no effect could be observable for disulfides. In the case of the mBBr the amine standard reacted as the only tested substance. The addition of disulfides to unsaturated carbon-carbon-bonds was successful in the case of 4-fluorostyrene, but not only the symmetrical products were formed, but also mixed products containing the thioethers originating from different disulfides. Therefore, this method might be used to determine, if disulfides are actually present in a sample, but not to identify them, as the results are distorted by the generation of the mixed thioether species. The direct analysis of the thiolates could not be applied successfully even to standards. The combination of limitations in the choice of solvent and deprotonating salt makes method development demanding

and time-consuming. The derivatization reaction with iodine containing compounds, i.e. iodoacetic acid and ethyl iodoacetate, was successful. The separation of products and educts, as well as the mass spectrometric detection of the generated products, is still to be optimized.

For the detection and determination of disulfides in petroleum samples therefore still no easy method could be developed that is suitable for routine analysis, robust and simple to handle for users without previous technical knowledge. The discussed techniques and approaches can be used as possible entry points for the further optimization and development.

## 9 Summary

In this work, the analysis of non-thiophenic and thiophenic sulfur compounds in vacuum gas oil samples was presented. Ligand exchange chromatography was taken as a starting point, about thirty metal based stationary phases were tested with respect for their separation abilities for sulfur containing compounds. Chromium sulfate, cadmium acetate and cobalt nitrate silica gel showed a separation of either sulfides or disulfides from the remaining standards, but only on  $\text{Ag}^+$ -cartridges was it possible to obtain a fraction containing both non-thiophenic sulfur classes.

Therefore, the cartridges were used for the separation of VGO samples, as well as the previously developed  $\text{PdSO}_4$ -Alox and *hAg*-MPSG. The later two were also transferred to HPLC, where only  $\text{PdSO}_4$  produced separations of a good quality. In general, the silver based phases showed for some samples an increased retention of compounds with large aromatic ring structures based on  $\pi$ - $\pi$ -interactions of the conjugated electrons with the silver ions of the stationary phase. This effect was more pronounced on the *hAg*-MPSG phase. In addition, for this phase irregularities in the separation abilities were observable due to difficulties during the preparation. As a phase for HPLC,  $\text{PdSO}_4$  was able to reveal two individual chromatographic fractions both containing sulfides. As no bleeding or carry-over, but a baseline separation of the fractions was observable and the differences between the polarity and elution strength between the two fraction was significantly different, the two groups of sulfides must have structural differences, which cause significant differences in chromatographic behavior. DBE range and numbers of carbon atoms are similar for the compounds found in both fractions. Hence, only differences in constitution leading to an altered electron density at the sulfur atom.

For the mass spectrometric analysis of the separated fractions, also different ionization techniques were used. ESI after methylation, which is well established for the analysis of PASHs, could be shown to be suitable for the determination of sulfides, but not for disulfides as they are not methylated using neither iodomethane nor trimethyloxonium tetrafluoroborate as methylating agents. Likewise APCI could be applied to the ionization of PASHs and sulfides. The ionization yield of disulfides in APCI is so low that even in directly injected standard solutions an assignment is not possible. APPI and APLI, which were also applied to the separated fractions, did not produce homogenous spectra. In Kendrick plots the lines of homologous series of compounds were often broken when using APPI and APLI, whereas the complete line of compounds could be assigned using APCI and ESI after methylation. The great advantage of APCI compared to ESI is the applicability to online HPLC separations. Whereas for ESI the derivatization reaction,

due to the work-up steps a time-consuming procedure, had to be applied offline, APCI can be directly used for the solvent flow exiting the HPLC.

For the separations of the VGOs on PdSO<sub>4</sub>-Alox and *h*Ag-MPSG also recovery data as well as mass and sulfur balance were evaluated. Again, the separation on PdSO<sub>4</sub>-Alox performed slightly better, as the recovery was more reasonable and the total amount of sulfur recovered was about 85% in contrast to only about 55% of sulfur that could be recovered on *h*Ag-MPSG. The loss might be caused by the removal of polar compounds during the separation. Either using the pre-separation on alumina or on the stationary phases themselves, highly aromatic polar compounds like asphaltenes are irreversibly retained on the phases. As the sulfur content generally increases in the higher molecular weight fractions, the loss of sulfur during the separation is based on this removal. For the high boiling fraction with a boiling point of 509-550 °C the loss of sulfur during the separation is even higher, supporting this assumption.

As no stationary phase tested is able to provide the desired separation on its own, two separation schemes for the combination of different stationary phases and separation steps were presented. For a thorough determination of both non-thiophenic and thiophenic sulfur a combination of Ag<sup>+</sup> cartridges, PdSO<sub>4</sub>-Alox HPLC and Pd-MPSG might be used, whereas disulfides need to be determined by an external derivatization reaction. If only the non-thiophenic sulfur is of interest a combination of an oxidation of the sulfides with TBAPI, open column chromatography and the Ag<sup>+</sup> cartridges can be applied to theoretically obtain sulfides and disulfides in individual fractions. In this scheme the separation between PAHs and PASHs is neglected, as the separation on the silver ion cartridges between those two compound classes is not as good as on Pd-MPSG and small PASHs are already eluted in the PAHs fraction.

For the determination of disulfides four different approaches were presented based on the reduction of the disulfides to thiols. For this reaction sodium borohydride proved to be suited best at slightly elevated temperature. The derivatization itself was either performed using iodoacetic acid and its ethyl ester, compounds with alkene-bonds or photometric reagents. In addition, the direct mass spectrometric detection of the thiols was tested. The best results were obtained using ethyl iodoacetate as a derivatizing agent. The resulting products could be successfully identified using GC-MS, but are not accessible by softer ionization techniques than electron impact ionization (EI). Also the removal of educts is still to be optimized. For the general clarification if disulfides are present in the sample, also the derivatization with 4-fluorostyrene can be applied. But an identification of the disulfides is hardly possible as the derivatization reaction is not only intramolecular, but also intermolecular, so that mixed products are formed.

As a conclusion, the separation of non-thiophenic and thiophenic sulfur is possible to a limited degree, using the methods presented in this work. The successful separation of PASHs and sulfidic sulfur could be shown using high resolution mass spectrometry and comprehensive two-dimensional gas chromatography. The quality of the separations was tested by evaluating recovery, mass and sulfur balance. For disulfides, in addition to the separation on  $\text{Ag}^+$ -cartridges, where disulfide standards could be recovered, alternative methods for the determination were tested.

Yet at the present level of development, no easy, robust and routine technique for the determination of disulfides could be established. Derivatization with ethyl iodoacetate or the MS detection after electrochemical reduction, may be used as starting-points for further development and optimization. The reduction of disulfides with sodium borohydride may also be used as a pretreatment for historical thiol quantification techniques, like the potentiometric titrations, e.g. with silver nitrate, as automation is nowadays available for those techniques.

The presented schemes for a complete separation by combining different stationary phases, may be used to verify if the S<sub>2</sub> compounds present in the sample are in fact disulfides or other compounds containing two sulfur atoms. These methods will not be useful for routine analysis of large batches, but for the initial characterization of a newly established crude oil sources.

For the determination of sulfides in a VGO sample, the newly established palladium phase,  $\text{PdSO}_4$ -Alox may be used to replace the more expensive Pd-MPSG phase. Thus, further experiments concerning repeatability and recovery are needed. For that purpose, multiple crude oil samples of as different composition, degree of saturation and sulfur content as possible should be separated on the phase to characterize it thoroughly.

## 10 Appendix

### 10.1 Experimental

For the preparation of stationary phases 60  $\mu\text{m}$  particles were used, e.g. silica gel, titania and alumina, if not stated otherwise. All chemicals were purchased from Sigma Aldrich, if not stated otherwise.

#### 10.1.1 General preparation of metal coated silica gel

6 g silica gel (SG) was suspended in 60 mL distilled water. 5 wt% of the metal salt was added and the mixture stirred for 3 h at room temperature. After removing the distilled water by filtration, the treated SG was washed with distilled water and dried overnight at 50 °C.

#### 10.1.2 General preparation of metal coated alumina

6 g alumina was suspended in 60 mL distilled water. 5 wt% of the metal salt was added and the mixture stirred for 3 h at room temperature. After removing the distilled water by filtration, the treated alumina was washed with distilled water and dried overnight at 50 °C.

#### 10.1.3 Preparation of silver nitrate titania

12 g titania was suspended in 60 mL distilled water. 5 wt%  $\text{AgNO}_3$  was added and the mixture stirred for 3 h at room temperature. After removing the distilled water by filtration, the  $\text{AgNO}_3$  titania was washed with distilled water and dried overnight at 50 °C.

#### 10.1.4 Preparation of silver nitrate alumina ( $\text{AgNO}_3$ -Alox)

10 g alumina (basic and neutral) was suspended in 60 mL distilled water and 0.5 g  $\text{AgNO}_3$  was added. After stirring for 3 h with exclusion of light, the solvent was removed by filtration and the remaining alumina washed with water and dried at 50 °C. The neutral alumina gave a grayish fine grained powder, whereas the basic alumina gave a white coagulated powder.

### 10.1.5 Preparation of heat-treated Ag-MPSG

20 g silica gel was suspended in 180 mL toluene and 45 mL mercaptopropanotrimethoxysilane was added. After refluxing for 5 h at 120 °C, the solvent was removed by filtration and the product was washed extensively with toluene and methanol. The generated MPSG was dried over night at 50 °C. 5 wt% AgNO<sub>3</sub> was added to the dried MPSG and suspended in 100 mL distilled water. After stirring for 3 h the water was removed, washed with distilled water and the product dried overnight at 50 °C. Subsequently the Ag-MPSG was stored for 3 h at 120 °C to obtain the reddish heat-treated Ag-MPSG (*h*MPSG).

For HPLC material the same procedure was applied to 10 μm silica gel and ca. 8 g *h*Ag-MPSG were packed into a 4.6 mm x 250 mm HPLC column at 400 bar in cyclohexane.

### 10.1.6 Preparation of Ag<sup>0</sup> silica gel

6 g silica gel (SG) was suspended in 80 mL distilled water. 1 g AgNO<sub>3</sub> was added and the mixture stirred for 3 h at room temperature. After removing the water by filtration, the AgNO<sub>3</sub>-SG was washed with water and dried over night at 50 °C.

The dry AgNO<sub>3</sub>-SG was resuspended in 80 mL distilled water. 500 mg of ascorbic acid was added and a color change from white to black was instantly visible. After removing the water, the Ag<sup>0</sup>-SG was washed with water and dried over night at 50 °C.

### 10.1.7 Preparation of silver nanoparticle silica gel (Ag-Nano-SG)[159]

12 g silica gel was suspended in 160 mL toluene and 40 mL mercaptopropanotrimethylsilane was added. The reaction mixture was refluxed for at least 5 h at 120 °C. After removing the solvent by filtration, the remaining mercaptopropano silica gel (MPSG) was washed intensively with toluene and methanol, before drying at 50 °C.

Two different sizes of nanoparticles were produced: 6 g MPSG was suspended in ethylene glycol using sonication and agitation. 0.25 g polyvinylpyrrolidone was added under mild stirring. After 24 h 1000 ppm AgNO<sub>3</sub> was added and the solution was slowly stirred for 30 minutes in order to completely dissolve the AgNO<sub>3</sub>. To produce smaller, homogeneously dispersed nanoparticles the mixture was stirred at room temperature for 18 h, until the solvent was removed, the remaining Ag-Nano-SG washed with acetone and ethanol and dried at 50 °C. For larger nanoparticles with an irregularly increased surface and decreased number of nanoparticles, the mixture was stirred at room temperature for 18 h, at 40 °C for 4 h, at 60 °C for 1 h, at 90 °C for one hour and eventually at



120 °C for 1 h, until the solvent was removed, the remaining Ag-Nano-SG washed with acetone and ethanol and dried at 50 °C.

As the chromatographic behavior of stationary silver phases can be altered by treatment at high temperatures, aliquots of both of the Ag-Nano-SG were heated to 180 °C for 48 h.

#### **10.1.8 Preparation of phenyl silica gel**

10 g silica gel was dried at 240 °C for 20 h. After cooling to room temperature 100 mL dried toluene were added. Under argon 5 mL pyridine and 6.3 mL methyl-diphenylchlorosilane were added and the suspension was refluxed for 19 h. After cooling to room temperature the solvent was removed. The functionalized silica gel was washed with 50 mL toluene, water:methanol (1:1) and acetone, respectively and dried over night at 50 °C.

#### **10.1.9 Preparation of silver coated cationic ion exchanger**

5 g commercially available cationic ion exchange material, based on silica gel, was filled into a 3 x 15 cm open column. 1.5 g silver nitrate dissolved in 100 mL distilled water were passed over the column. After washing with 20 mL dichloromethane the material was dried by passing nitrogen through the column.

#### **10.1.10 Preparation of copper silica gel[160]**

4 g silica gel was filled into a 3 x 15 cm open column. 0.75 g copper sulfate ( $\text{CuSO}_4 \cdot 5 \text{H}_2\text{O}$ ) were dissolved in 300 mL 1 M ammonia solution and passed over the column until the column was saturated and the not longer adsorbable blue copper complex is eluted from the column. The column is washed with dichloromethane and subsequently dried by passing nitrogen through it.

#### **10.1.11 Preparation of palladium 8-hydroxyquinoline silica gel (Pd-8HQSG)[68]**

12 g 8-hydroxyquinoline functionalized silica gel were suspended in 150 mL distilled water and 0.64 g palladium chloride were added. The mixture was stirred for 5 h at room temperature. The solvent was removed by filtration and the Pd-8HQSG was washed with water and dried at 50 °C over night.

### 10.1.12 Preparation of palladium sulfate alumina (PdSO<sub>4</sub>-Alox)

250 mg palladium sulfate were dissolved in 60 mL methanol and 7 g basic alumina were added. The mixture was stirred at room temperature for at least 5 h, while the initially red dispersion turn dark gray and sometimes metallic deposit was observable. After removing the solvent by filtration, the PdSO<sub>4</sub>-Alox was washed with methanol and water before it was dried at 50 °C over night.

For HPLC material the same procedure was applied to 10 μm alumina and ca. 8 g PdSO<sub>4</sub>-Alox were packed into a 4.6 mm x 250 mm HPLC column at 400 bar in cyclohexane.

### 10.1.13 Vacuum gas oils (VGOs)

The samples used in this work were provided by BP USA and consist of different distillation cuts of five crude oils. Geological origin, site of exploration and production and chemical composition vary between the samples to ensure the methods developed are applicable to different kinds of crude oils (see table 13).

**Table 13:** Sulfur content and sulfidic-thiophenic ratio (*s/t*) of the vacuum gas oils.

	96-369 °C ppm wt/wt	<i>s/t</i> ratio	369-509 °C ppm wt/wt	<i>s/t</i> ratio	509-550 °C ppm wt/wt	<i>s/t</i> ratio	origin
Karachaganak	7660	1.1	13500	0.4	15900	0.6	Kazakhstan
Albacora Leste			5790	0.6	7040	0.4 (calculated)	Brazil
Azeri			1740	0.3	2650	0.7	Azerbaijan
West Texas Intermediate			4940	0.5	6380	0.7	Texas, USA
Winter ANS					15200	0.7	Alaska, USA

### 10.1.14 Separation of standards on stationary phases

To ensure comparability of the different separations, each stationary phase was treated in the same way. Thus for each model separation using the standard mixture, identical amounts of stationary phase and standard mixture as well as eluting solvents were used. A solid phase extraction cartridge was filled with 1 g of the stationary phase. After conditioning the phase with cyclohexane, 0.5 mL of the standard mixture was added and three fractions were collected with the solvents indicated:

1. fraction: 10 mL cyclohexane (CH)
2. fraction: 10 mL cyclohexane:dichloromethane (2:1) (CH:DCM)
3. fraction: 10 mL CH:DCM (2:1) + 1.5% isopropanol saturated ammonia (IP/NH<sub>3</sub>)

The solvents were removed and the fractions stored for further analysis.

#### 10.1.15 SARA fractionation of VGOs

Silica gel was activated by storing it at 160 °C over night. On the next day 15 g silica gel were filled into a 25 x 150 mm chromatographic column using cyclohexane. 100  $\mu$ L vacuum gas oil was added and fractions were collected with the solvents indicated:

- aliphatics: 40 mL hexane (CH)
- aromatics: 80 mL toluene
- resins: 50 mL toluene : methanol (80:20)

The solvents were removed and the fractions stored for further analysis.

#### 10.1.16 Preseparation on alumina

A slurry of silica gel in cyclohexane was filled into a chromatographic column with a diameter of 3 cm to a height of 6 cm and subsequently a slurry of neutral alumina in cyclohexane was added on top to a height of 12 cm. 2 mL of vacuum gas oil were loaded onto the column and a combined fraction of aliphatics and aromatics was eluted using 1 L of dichloromethane as eluting solvent. The solvent was removed and the residue dissolved in 10 mL cyclohexane and stored for further analysis.

#### 10.1.17 Separation of VGOs on stationary phases

As early results showed that even an amount of 8 g stationary phase will be easily overloaded with 200  $\mu$ L crude oil, the total amount of stationary phase was increased to 32 g for each separation. The phase was suspended in cyclohexane and filled into a column (2 x 15 cm) and washed with cyclohexane. 200  $\mu$ L sample were loaded and different fractions were collected by elution with the following solvents:

- First fraction: 100 mL cyclohexane
- Second fraction: 100 mL cyclohexane: dichloromethane (2:1)

- Third fraction: 100 mL cyclohexane: dichloromethane (2:1) with addition of ammonia saturated isopropanol

The solvents were removed and the sample stored for further analysis.

#### 10.1.18 Separation of VGOs on Ag<sup>+</sup>-cartridges

As only prepacked cartridges with 750 mg supporting material are commercially available, the separation of VGOs had to be modified to fit the drastically reduced capacities of the cartridges. The phase was conditioned with cyclohexane and 20  $\mu$ L sample were loaded and different fractions were collected by elution with the following solvents:

- First fraction: 50 mL cyclohexane
- Second fraction: 50 mL cyclohexane: dichloromethane (2:1)
- Third fraction: 50 mL cyclohexane: dichloromethane (2:1) with addition of ammonia saturated isopropanol

The solvents were removed and the sample stored for further analysis.

#### 10.1.19 Derivatization by methylation with methyl iodide

For the methylation reaction a modification of the method described by ACHESON and HARRISON was used [109].

For the methylation of standard compounds, 2.0 mL of the standard solution were mixed with 3 mL 1,2-dichloroethane and 100  $\mu$ L of methyl iodide was added. 50 mg silver tetrafluoroborate was added and the mixture stirred for 10 min. The solvents were removed in a stream of dry nitrogen. The residue was suspended in 2 mL 1,2-dichloroethane and the precipitate was removed by filtration using a PTFE filter with a pore size of 0.2  $\mu$ m. After removal of the solvent in a stream of dry nitrogen, the thiophenium salts were dissolved in 1 mL acetonitrile and stored in the refrigerator at 4 °C.

For derivatization of the separated fractions from LEC, 100  $\mu$ L methyl iodide and 50 mg silver tetrafluoroborate were added to each sample. The mixtures were stirred for 10 min and the solvents removed in a stream of dry nitrogen. After the residue was suspended in 2 mL 1,2-dichloroethane, the precipitate was removed by filtration using a PTFE filter with a pore size of 0.2  $\mu$ m. Finally, after the solvent was removed in a stream of dry nitrogen, the residue was dissolved in 1 mL acetonitrile and stored the refrigerator at 4 °C.

### 10.1.20 Derivatization by methylation with oxonium salts

For the methylation reaction a modification of the methods described by DUBS et al. and HELMKAMP et al. was used [112, 113].

For the methylation of standard compounds, 2.0 mL of the standard solution were mixed with 2 mL nitromethane or 1,2-dichloroethane, respectively. 100 mg of trimethyl- or triethyloxonium tetrafluoroborate was added, respectively. After the mixture was stirred for 1 h, the reaction was quenched by the addition of 1 mL distilled water. The organic phase was dried with sodium sulfate and the solvents were removed in a stream of dry nitrogen. The residue was suspended in 1 mL acetonitrile and stored in the refrigerator at 4 °C.

### 10.1.21 Reaction monitoring by NMR

To follow the the reaction progress of the derivatization, samples were taken at different stages of the reaction (immediately, after 30 min, after 60 min and after 24 h) and analyzed via NMR.

For the reaction with methyl iodide a given amount of sample was taken from the reaction vessel, the solvents were removed *in vacuo* and the residue was dissolved in deuterated chloroform. The remaining silver iodide precipitate was removed by filtration and the sample analyzed using NMR.

For the reaction with trimethyloxonium tetrafluoroborate a given amount of sample was taken from the reaction vessel and the methylation agent was removed by extraction with water (hydrolysis). After removing the organic solvent *in vacuo*, the residue was dissolved in deuterated chloroform and the sample analyzed using NMR.

### 10.1.22 Reduction of disulfides with TCEP

450 mg tris(2-carboxyethyl)phosphine is dissolved in 9 mL distilled water. To be able to apply the method to petroleum samples, solubility and feasibility of the reaction in lipophilic solvents had to be tested. Therefore 3 mL of the solution were added to 3 mL acetonitrile, dimethylformamide and isopropanol, respectively. To each mixture disulfide standards, i.e. 55 mg phenyl disulfide and 45 mg *n*-butyl disulfide, were added and the resulting mixture stirred for 12 h at room temperature. The phases were separated by the addition of cyclohexane and the organic phase dried over magnesium sulfate and stored for further analysis.

### 10.1.23 Reduction of disulfides and derivatization with ethyl iodoacetate

1 mL of a sulfide/disulfide standard mixture, containing *t*-butyl disulfide, *n*-butyl disulfide, dodecyl methyl sulfide, octadecyl methyl sulfide, phenyl sulfide and phenyl disulfide, was mixed with 5 mL dimethylformamide and 0.1 g sodium borohydride was added. After stirring for 6 h at 60 °C, 0.2 mL ethyl iodoacetate was added and the solution was stirred over night at RT. The generated white precipitate was dissolved by adding 5 mL distilled water. The aqueous phase was extracted with cyclohexane (3 x 10 mL) and the combined organic phases were dried over MgSO<sub>4</sub>.

### 10.1.24 Reduction of disulfides and derivatization with iodoacetic acid

1 mL of a disulfide standard mixture, containing *n*-octyl disulfide, *n*-heptyl disulfide, cyclohexyl disulfide, undecyl disulfide and hexadecyl disulfide, was mixed with 5 mL dimethylformamide and 0.1 g sodium borohydride was added. After stirring for 6 h at 60 °C, 0.25 g iodoacetic acid was added and the solution was stirred over night at RT. The generated white precipitate was dissolved by adding 5 mL distilled water. After adding cyclohexane for phase separation, the products were extracted using ethyl acetate (3 x 10 mL). After the solvents were evaporated, the residue was dissolved in ethyl acetate and directly analyzed via ESI-MS.

### 10.1.25 Reaction of disulfides and thiols with maleic anhydride

0.2 g octadecanethiol and 0.2 g maleic anhydride were dissolved in tetrahydrofuran and 1 mL diethylamine was added. The reaction mixture was stirred for 12 h. At this point the diethylamine was evaporated and the remaining solution was transferred into a vial to be analyzed by GC-FID.

To test if the reaction is also possible with disulfides, which have to be reduced first, the following reaction was tested: 0.2 g phenyl disulfide was dissolved in cyclohexane and 0.18 g maleic anhydride as well as 0.23 g iodine in diethylether were added. The reaction mixture was stirred at 40 °C for 12 h. The product was hydrolyzed with water and the organic phase removed. Remains of iodide were precipitated with silver nitrate solution and the emerging silver iodide precipitate was removed by filtration. The solvent was removed and the product stored for further analysis.

### 10.1.26 Isolation of sulfides by oxidation with tetrabutylammonium periodate[158]

1 mL Karachaganak 369-509 °C was separated on a neutral aluminum oxide column into an aliphatic and an aromatic fraction, using 200 mL cyclohexane and 200 mL toluene. The solvents were removed and the residue of the aromatic fraction was dissolved in 30 mL methanol:toluene (1:5) and tetrabutylammonium periodate (0.15 g) was added. The mixture was stirred and refluxed for 30 minutes. After cooling the resulting mixture to room temperature and the addition of *n*-pentane (25 mL) the organic phase was washed with water. After removal of the solvent in vacuo the residue was applied to a silica gel column (2 x 15 cm) prewashed with *n*-pentane.

The first fraction, containing the unoxidized nonpolar compounds, was eluted with *n*-pentane (50 mL), followed by toluene (200 mL). The second fraction, containing the oxidized sulfides and other polars, was eluted with methanol:toluene (1:4, 200 mL). The solvents were removed.

The second fraction was further treated by reduction of the sulfoxides to sulfides. Therefore the residue was dissolved in dioxane (15 mL) and lithium aluminum hydride (0.2 g) was added. The reaction mixture was stirred and refluxed for 1 hour. While cooled with ice water excess lithium aluminum hydride was destroyed by careful addition of water (10 mL), toluene (20 mL), *n*-pentane, and 10 % sulfuric acid (30 mL) and afterwards stirred for 15 min at room temperature.

After washing the organic phase with 5% sulfuric acid (1 x 30 mL) and water (2 x 30 mL), the solvent was removed and the residue applied to a silica gel column (2 x 15 cm) prewashed with *n*-pentane. The reduced sulfides were eluted with toluene:*n*-pentane (1:4, 200 mL) and the solvent was removed.

### 10.1.27 Derivatization of standards with monobromobimane (mBBr)

Several standards with different functional groups were given to a solution of mBBr in a mixture of methanol, cyclohexane and dichloromethane and stirred at room temperature for 15 minutes. The resulting fluorescent solutions were analyzed via GC-FID to check if stable reaction products had formed.

Standard solutions of the following compounds solved in cyclohexane were used:

- octadecanethiol
- heptadecanol
- phenyl disulfide

- *n*-butyl disulfide
- octadecyl methyl sulfide

#### 10.1.28 Iodine-catalyzed addition of disulfides to 4-fluorostyrene[156]

100 mg phenyl disulfide and 90 mg *n*-butyl disulfide were dissolved in 5 mL dichloromethane. 150 mg 4-fluorostyrene and 25 mg iodine were added. After stirring for 12 h at room temperature, the reaction was stopped by quenching it by the addition of 5 mL sodium sulfite solution. The product was extracted with ethyl acetate (3 x 5 mL) and the combined organic phases were dried over magnesium sulfate. The solvents were removed and the residue dissolved in 1 mL cyclohexane and stored for further analysis.

#### 10.1.29 Synthesis of benzofurazan sulfides[147]

0.8 g 4-chloro-7-nitrobenzofurazan was dissolved in 10 mL acetonitrile and under argon atmosphere a solution of 0.28 g sodium thiolate in 2 mL distilled water was added dropwise. The reaction mixture was stirred for 30 min at 70°C. After cooling to room temperature the solvent was removed and the residue dissolved in a little amount of acetonitrile. The solution was purified using a 3 x 30 cm silica gel column. After washing with 250 mL ethyl acetate : cyclohexane (1:1), the benzofurazan sulfide was eluted with 250 mL ethyl acetate. The solvent was removed and the nitrobenzofurazan sulfide bis(7-nitrobenzo[1,2,5]oxadiazol-4-yl)sulfane was obtained as a reddish yellow powder.

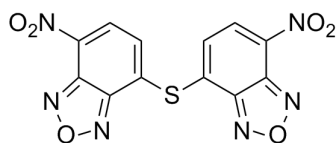


**Figure 124:** Bis(7-nitrobenzo[1,2,5]oxadiazol-4-yl)sulfane

#### 10.1.30 Derivatization of standards with nitrobenzofurazan sulfides

130 mg of bis(7-nitrobenzo[1,2,5]oxadiazol-4-yl)sulfane were dissolved in 50 mL acetonitrile and added to standard solutions. Standard solutions of the following compounds solved in cyclohexane were used:



- 
- octadecanethiol
  - heptadecanol
  - dodecyl amine
  - sulfide and disulfide mixture containing: phenyl disulfide, *n*-butyl disulfide, phenyl sulfide and octadecyl methyl sulfide

## 10.2 Instrumental

GC x GC SCD experiments were performed at BP Refining & Logistics Technology Naperville, IL, USA. Sulfur content determinations were done at ASG Analytik-Service Gesellschaft mbH, Augsburg according to DIN EN ISO 20884.

### 10.2.1 GC-FID parameters

Gas chromatograph:	Agilent 5890 Series II
Autosampler:	Agilent 7673
Injector:	split/splitless (splitless)
Injector temperature:	280 °C
Detector temperature:	350 °C
Capillary column:	Supelco SLB5ms, 30 m x 0,25 mm x 0,25 $\mu$ m
Temperature program:	60 °C - 1 min, 5 °C/min to 300 °C, 5 min
for 509-550 °C samples:	60 °C - 1 min, 5 °C/min to 330 °C, 15 min
Injection volume:	1 $\mu$ L
Carrier gas:	Hydrogen 4.8

### 10.2.2 GC-AED analysis

Gas chromatograph:	Agilent 6890N GC and a G2350A AED
Autosampler:	Gerstel MPS2
Capillary column:	Agilent HP-5MS, 30 m x 0.25 mm x 0.25 $\mu$ m
Injector:	Gerstel CIS injector
Injector temperature:	300 °C
Transfer line temperature:	300 °C
Cavity temperature:	300 °C
Detection wavelength:	carbon: 193 nm, sulfur: 181 nm
Temperature program:	60 °C - 1 min, 20 °C/min to 300 °C, 5 min
for 509-550 °C samples:	60 °C - 1 min, 5 °C/min to 330 °C, 15 min
Injection volume:	1 $\mu$ L
Carrier gas:	Helium 5.0
Carrier gas velocity:	40 $\mu$ L/min
Helium makeup flow:	300 mL/min
Hydrogen plasma gas pressure:	15 psi
Oxygen plasma gas pressure:	20 psi

### 10.2.3 GC-MS parameters

GC-MS:	Gaschromatograph Finnegan MAT GCQ
Mass spectrometer:	Finnegan MAT GCQ Polaris MS
Injector:	split / splitless (60 s)
Injector temperature:	300 °C
Column:	Supelco SLB5ms, 30 m x 0,25 mm x 0,25 $\mu$ m
Carrier gas:	Helium 6.0 (BIP), 40 cm/s (constant flow)
Transfer line:	300 °C
Ionization conditions:	EI positive mode, 70 eV, Ion source 200 °C
Mass range:	Full Scan (50-600 amu)
Temperature program:	60 °C - 1 min, 5 °C/min to 300 °C, 5 min
Solvent delay:	6 min
Injection volume:	1 $\mu$ L

### 10.2.4 RP-HPLC parameters

HPLC system:	Merck Hitachi D-6000 interface
Pump:	L-6200A intelligent pump
Autosampler:	AS-2000A autosampler
Detector:	L-4500 diode array detector
Column:	4.6 mm x 250 mm PdSO <sub>4</sub> -Alox column
Gradient:	100% cyclohexane for 4 min; 67% cyclohexane, 33% dichloromethane for 4 min, 52% cyclohexane, 33% dichloromethane, 15% isopropanol for 4 min
Flow rate:	1.5 mL/min
Injection volume:	10-50 $\mu$ L
Detection wavelength:	254 nm

**10.2.5 ESI-Orbitrap MS**

Syringe pump:	Fusion 100 classic syringe pump
Flow rate:	10 $\mu\text{L}/\text{min}$
Ionization mode:	ESI (+)
AGC target:	balanced
Sheath gas:	Nitrogen
Sheath gas flow:	10 a.u.
Spray voltage:	3.6 kV
Capillary temperature:	275 $^{\circ}\text{C}$
Capillary current:	30.0 V
Tube lens current:	135 V
Skimmer current:	20.0 V
Max. injection time:	100 s
Mass range:	200-600 m/z

**10.2.6 APCI- and APPI Orbitrap MS**

Syringe pump:	Fusion 100 classic syringe pump
Flow rate:	300 $\mu\text{L}/\text{min}$
Ionization mode:	APCI (+) or APPI (+)
Source Current:	6 $\mu\text{A}$
Vaporizer Temperature:	350 $^{\circ}\text{C}$
Sheath gas:	Nitrogen
Sheath Gas Flow Rate:	40 a.u.
Aux Gas Flow Rate:	5 a.u.
Sweep Gas Flow Rate:	5 a.u.
Capillary Temperature:	270 $^{\circ}\text{C}$
Max. injection time:	100 s
Mass range:	200-1000 m/z

### 10.2.7 APCI-FT-ICR MS

FT-ICR:	Bruker solariX
Flux density:	12 T (actively shielded)
Syringe pump:	Fusion 100 classic syringe pump
Flow rate:	25 $\mu\text{L}/\text{min}$
Ionization mode:	APCI (+)
Source Current:	6 $\mu\text{A}$
Vaporizer Temperature:	400 $^{\circ}\text{C}$
Sheath gas:	Nitrogen
Drying gas temperature:	250 $^{\circ}\text{C}$
Drying gas flow:	4 L/min
Nebulizer pressure:	2.5 bar
Capillary voltage:	-2000 V
Corona needle current:	3000 nA
Transient time:	4.18 s
Mass range:	184-3000 m/z
Resolution (at $m/z=400$ ):	1,000,000

### 10.2.8 APLI-Orbitrap MS

Syringe pump:	Fusion 100 classic syringe pump
Flow rate:	300 $\mu\text{L}/\text{min}$
Ionization mode:	APLI (+) (modified APCI-source)
Laser:	ATL Lasertechnik GmbH KrF*excimer laser
Radiation wavelength:	248 nm
Laser pulse:	50 Hz, 8 mJ
Nebulizer temperature:	240 $^{\circ}\text{C}$
Sheath gas flow:	16 a.u.
Auxiliary gas flow:	5 a.u.
Max. injection time:	100 s
Mass range:	200-1000 m/z

**10.2.9 NMR**

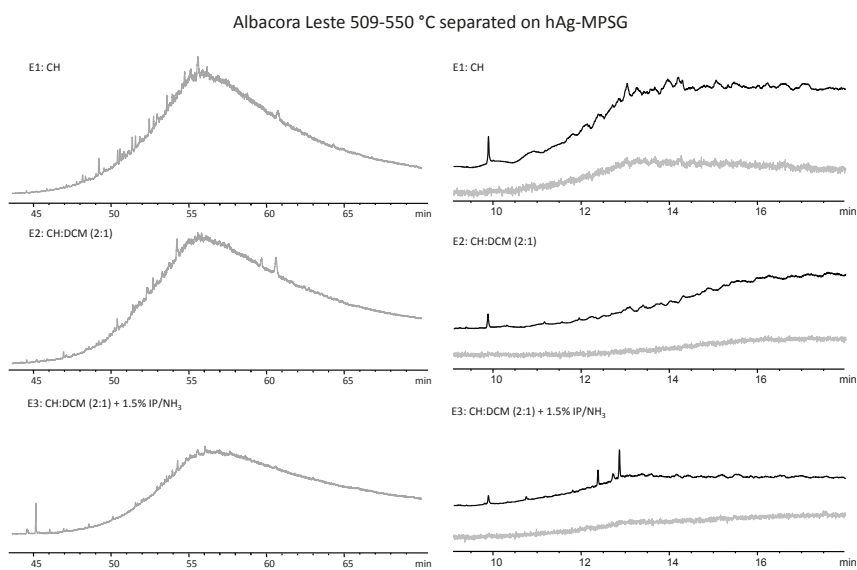
Instrument type: Bruker AVANCE III  
Sample head: BBFO,  $z$ -gradient  
Frequency: 400,03 MHz  
Temperature: 300 K

**10.2.10 TXRF**

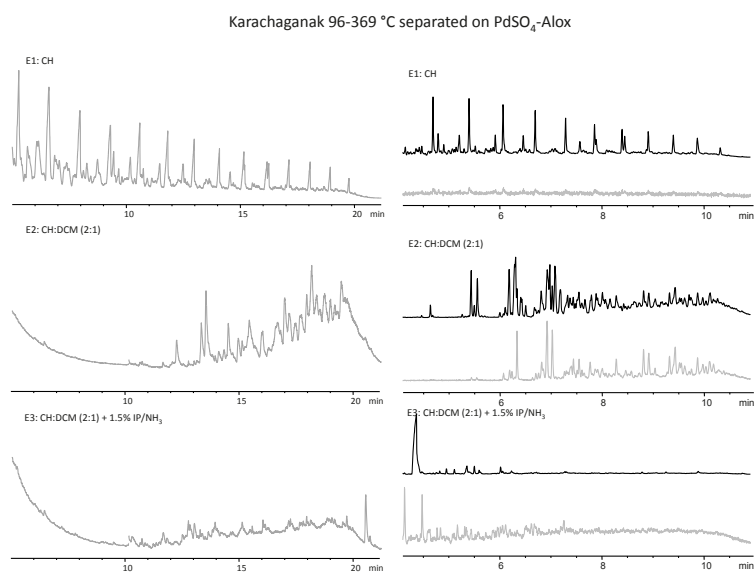
Instrument type: Bruker S2 Picofox  
X-ray tube: 30 W metal-ceramic, max. 50 kV, 1 mA, Mo target  
X-ray optics: multilayer monochromator  
Detector: Peltier-cooled silicon drift detector  
Energy resolution: <150 eV at 100 keps

### 10.3 Additional figures

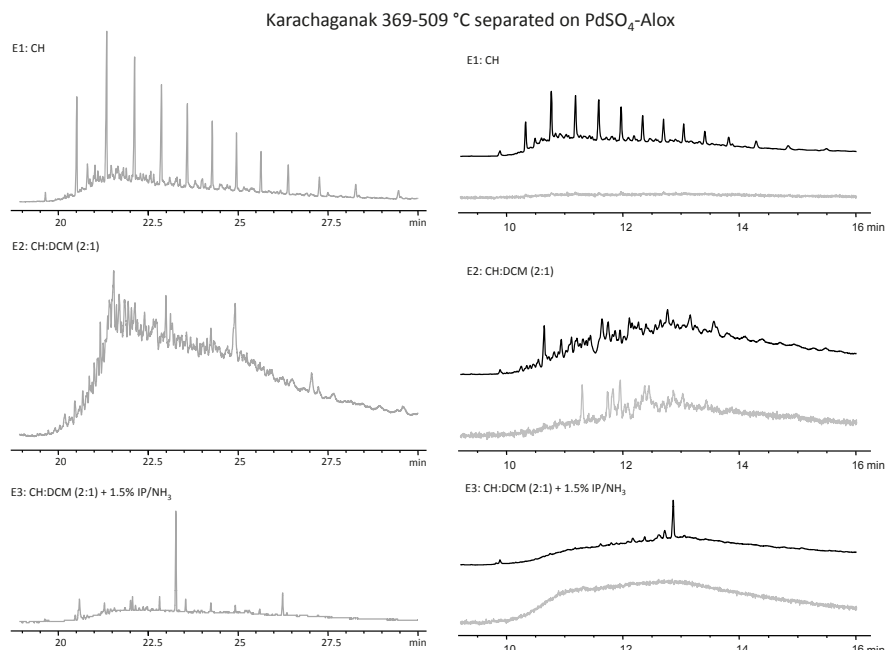
#### GC-FID and GC-AED chromatograms of separated VGOs



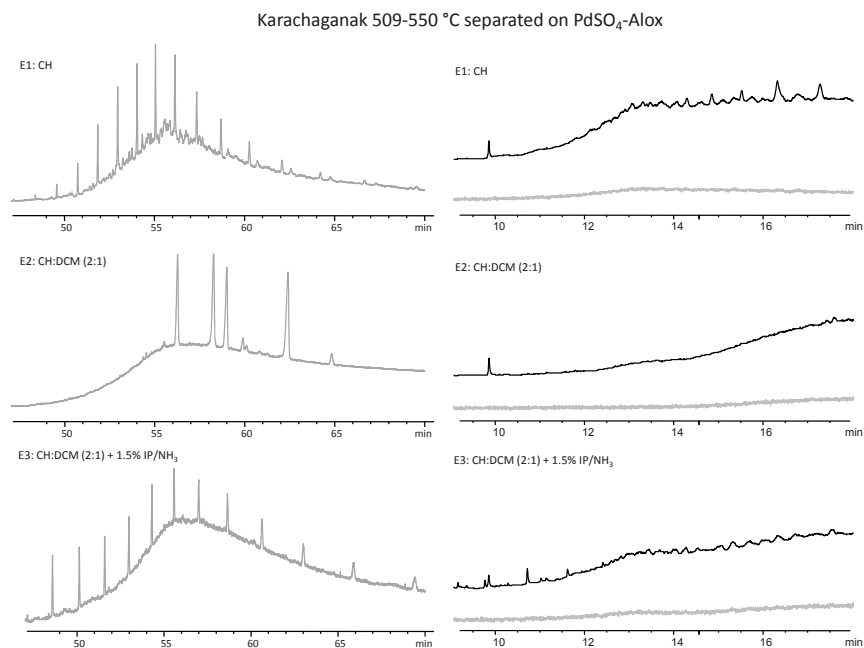
**Figure 125:** GC chromatograms of the separation of Albacora Leste 509-550 °C. Left: GC-FID, right: GC-AED with carbon (upper) and sulfur trace (lower).



**Figure 126:** GC chromatograms of the separation of Karachaganak 96-369 °C on PdSO<sub>4</sub>-Alox. Left: GC-FID, right: GC-AED with carbon (upper) and sulfur trace (lower).

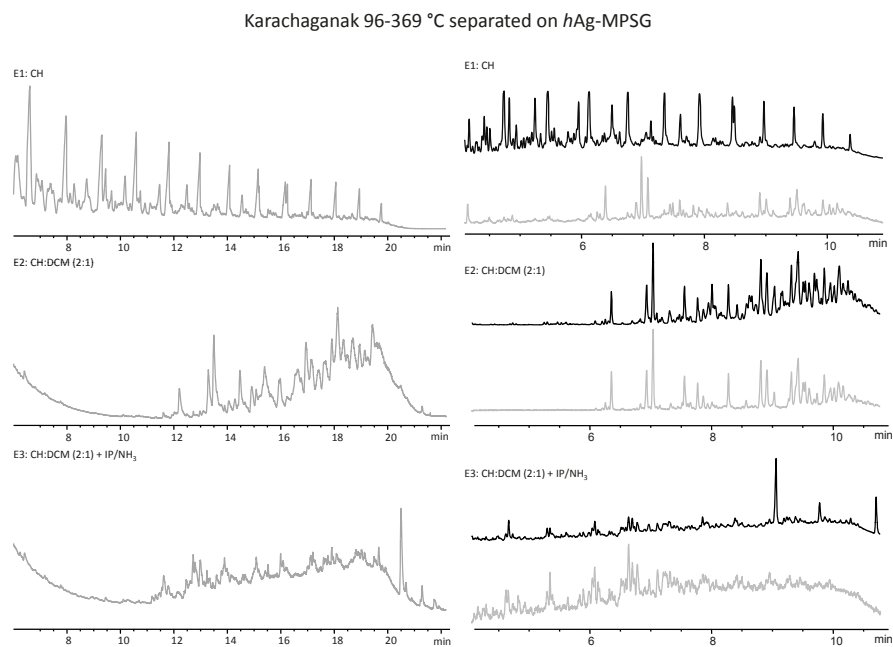


**Figure 127:** GC chromatograms of the separation of Karachaganak 369-509 °C on PdSO<sub>4</sub>-Alox. Left: GC-FID, right: GC-AED with carbon (upper) and sulfur trace (lower).

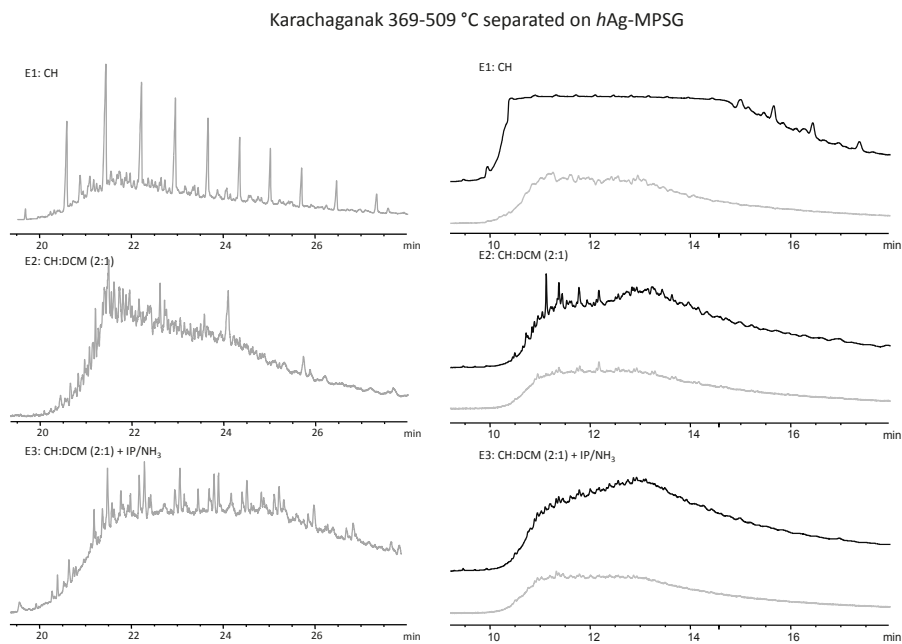


**Figure 128:** GC chromatograms of the separation of Karachaganak 509-550 °C on PdSO<sub>4</sub>-Alox. Left: GC-FID, right: GC-AED with carbon (upper) and sulfur trace (lower).

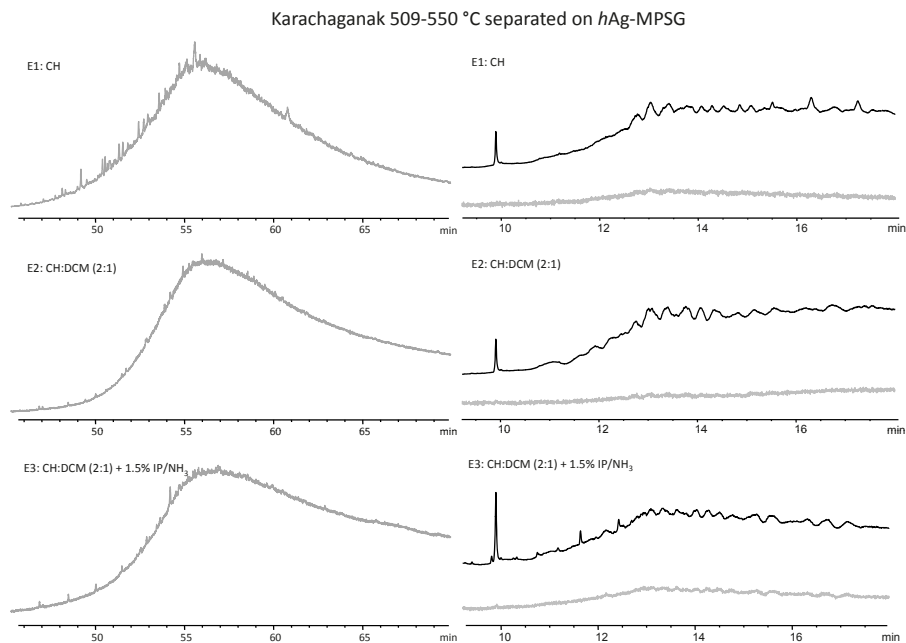




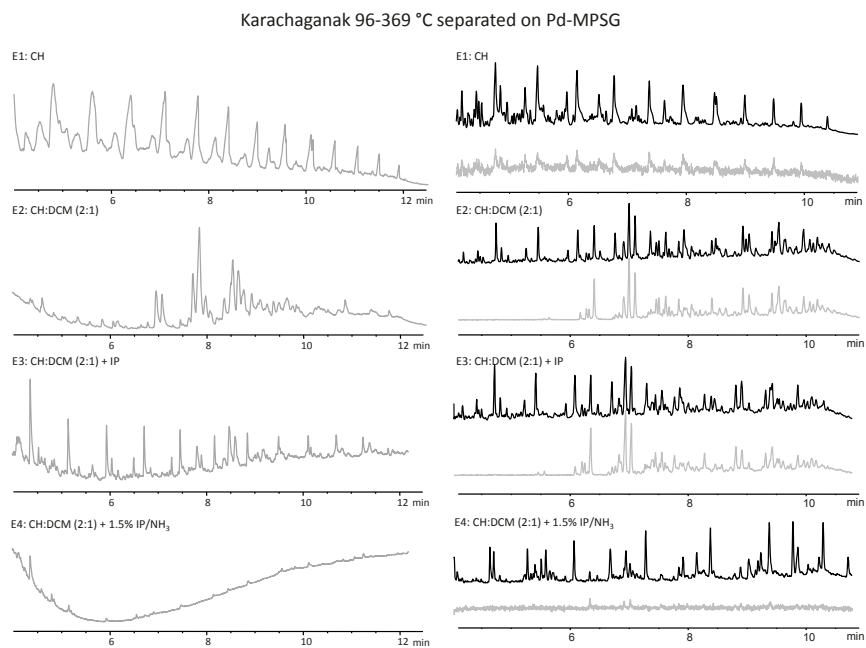
**Figure 129:** GC chromatograms of the separation of Karachaganak 96-369 °C on *h*Ag-MPSG. Left: GC-FID, right: GC-AED with carbon (upper) and sulfur trace (lower).



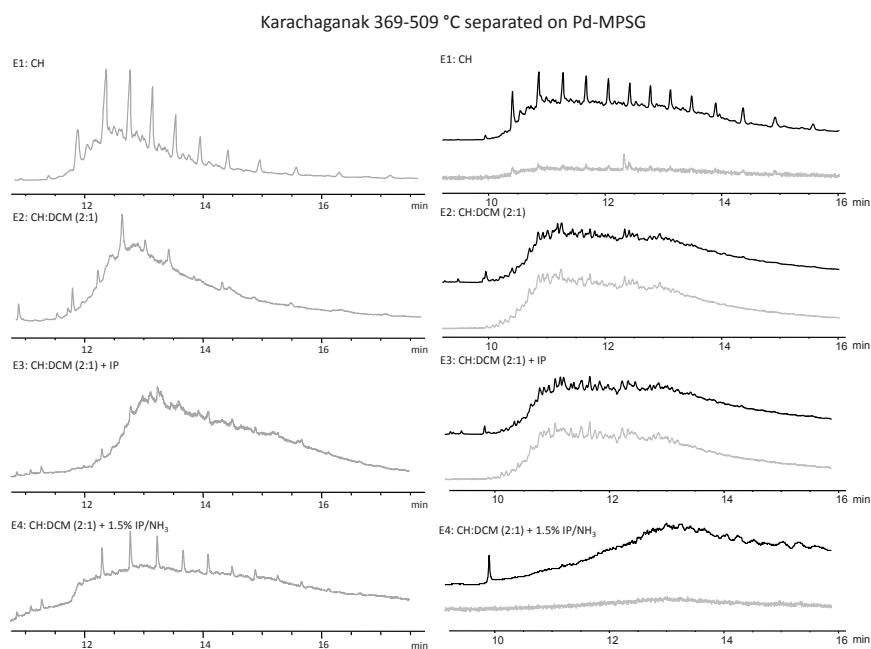
**Figure 130:** GC chromatograms of the separation of Karachaganak 369-509 °C on *h*Ag-MPSG. Left: GC-FID, right: GC-AED with carbon (upper) and sulfur trace (lower).



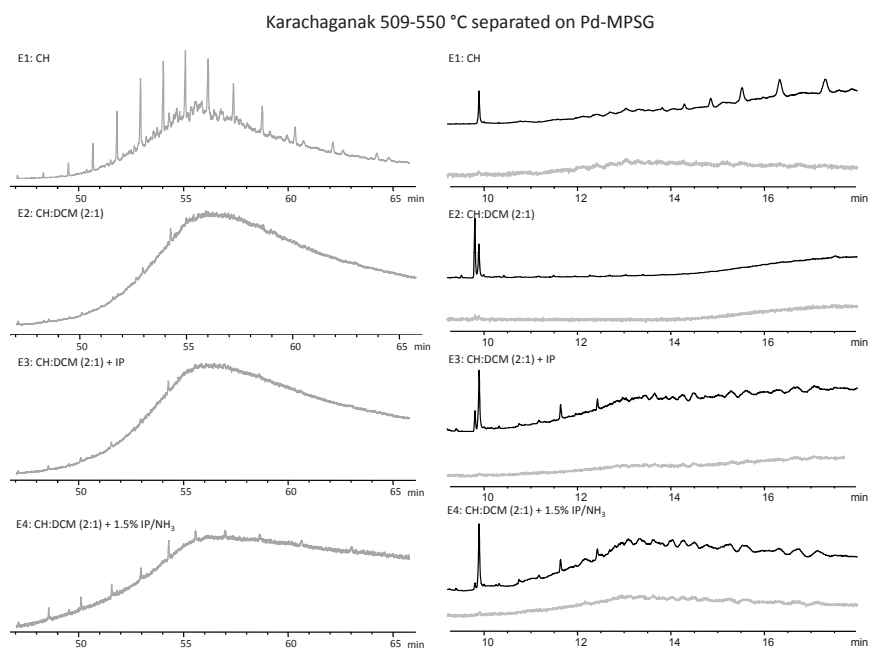
**Figure 131:** GC chromatograms of the separation on Karachaganak 509-550 °C on *h*Ag-MPSG. Left: GC-FID, right: GC-AED with carbon (upper) and sulfur trace (lower).



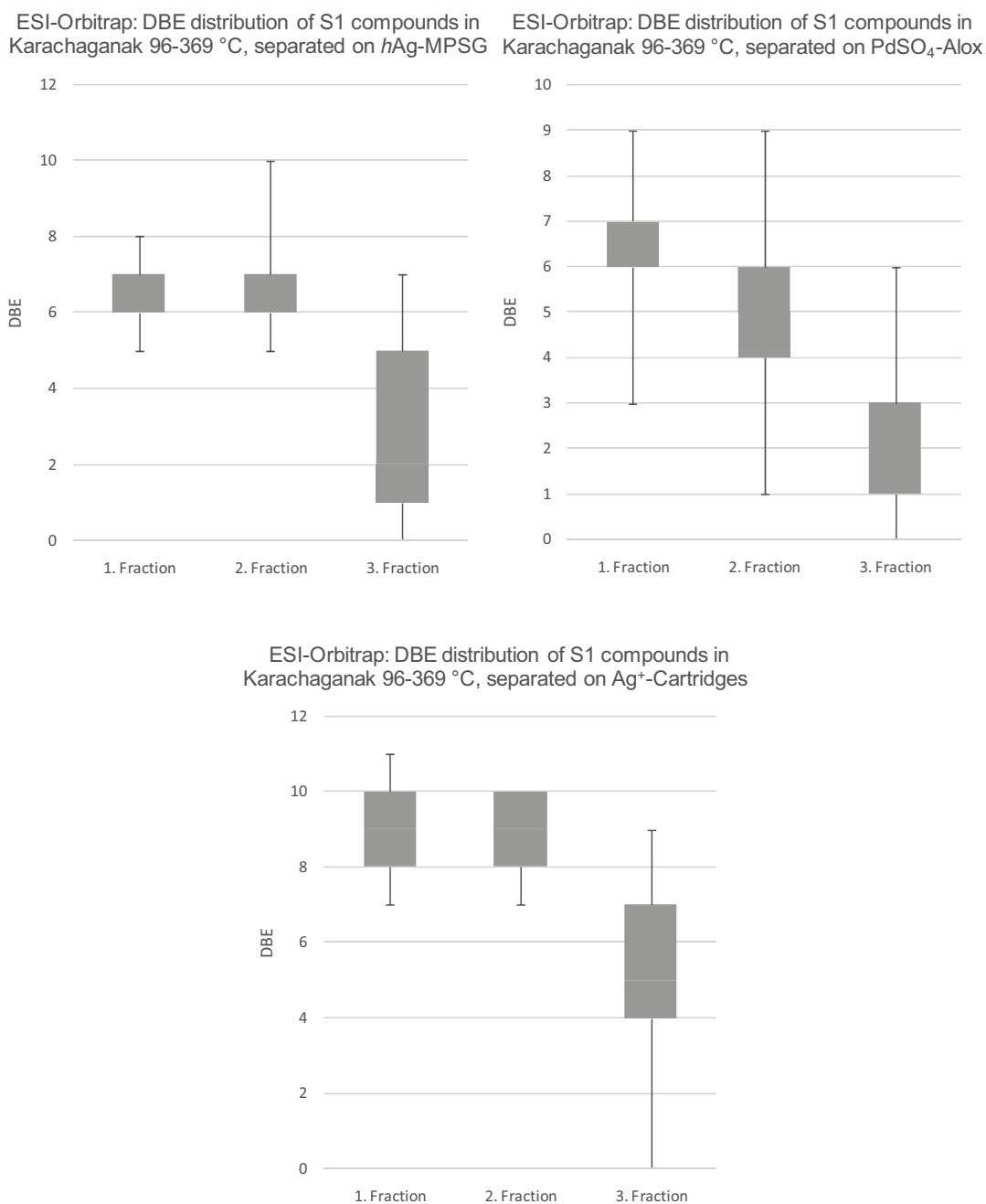
**Figure 132:** GC chromatograms of the separation of Karachaganak 96-369 °C on Pd-MPSG. Left: GC-FID, right: GC-AED with carbon (upper) and sulfur trace (lower).



**Figure 133:** GC chromatograms of the separation of Karachaganak 369-509 °C on Pd-MPSG. Left: GC-FID, right: GC-AED with carbon (upper) and sulfur trace (lower).

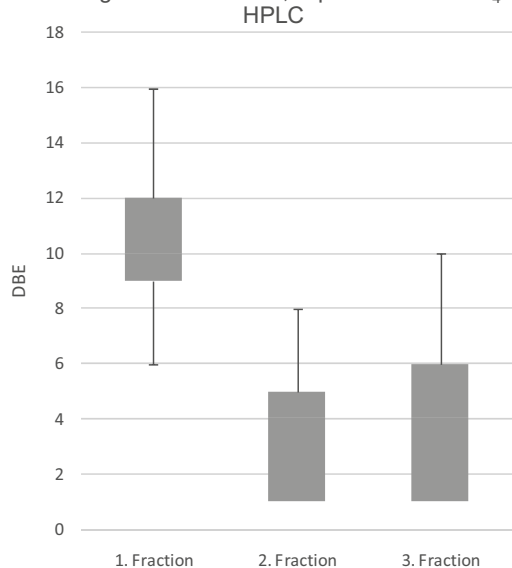


**Figure 134:** GC chromatograms of the separation on Karachaganak 509-550 °C on Pd-MPSG. Left: GC-FID, right: GC-AED with carbon (upper) and sulfur trace (lower).

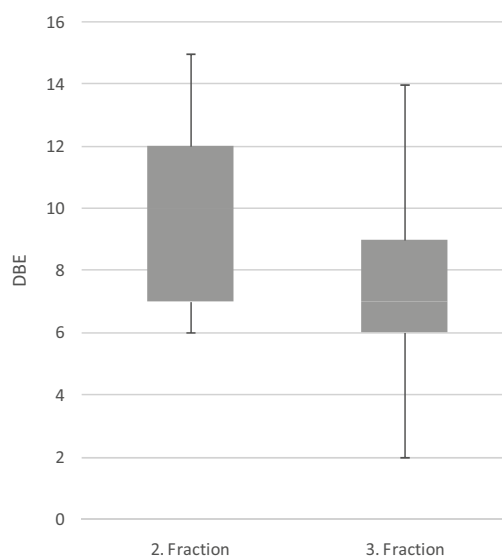
**Box plots**

**Figure 135:** Box plots of the S1 compounds of the ESI mass spectra of the separations of Karachaganak 96-369 °C on different phases. Upper left: PdSO<sub>4</sub>-Alox, upper right: *h*Ag-MPSG, bottom: Ag<sup>+</sup>-cartridges.

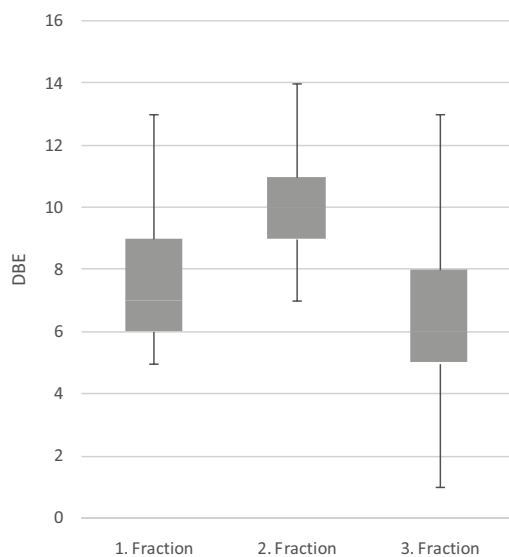
Online-APCI-Orbitrap: DBE distribution of S1 compounds in Karachaganak 369-509 °C, separated on PdSO<sub>4</sub>-Alox HPLC



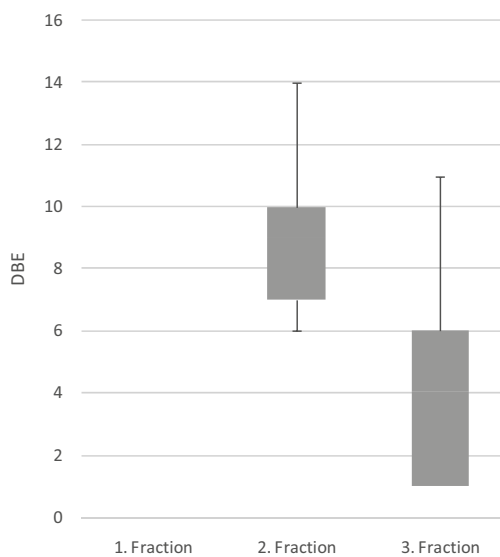
APCI-FT-ICR: DBE distribution of S1 compounds in Karachaganak 369-509 °C, separated on hAg-MPSG



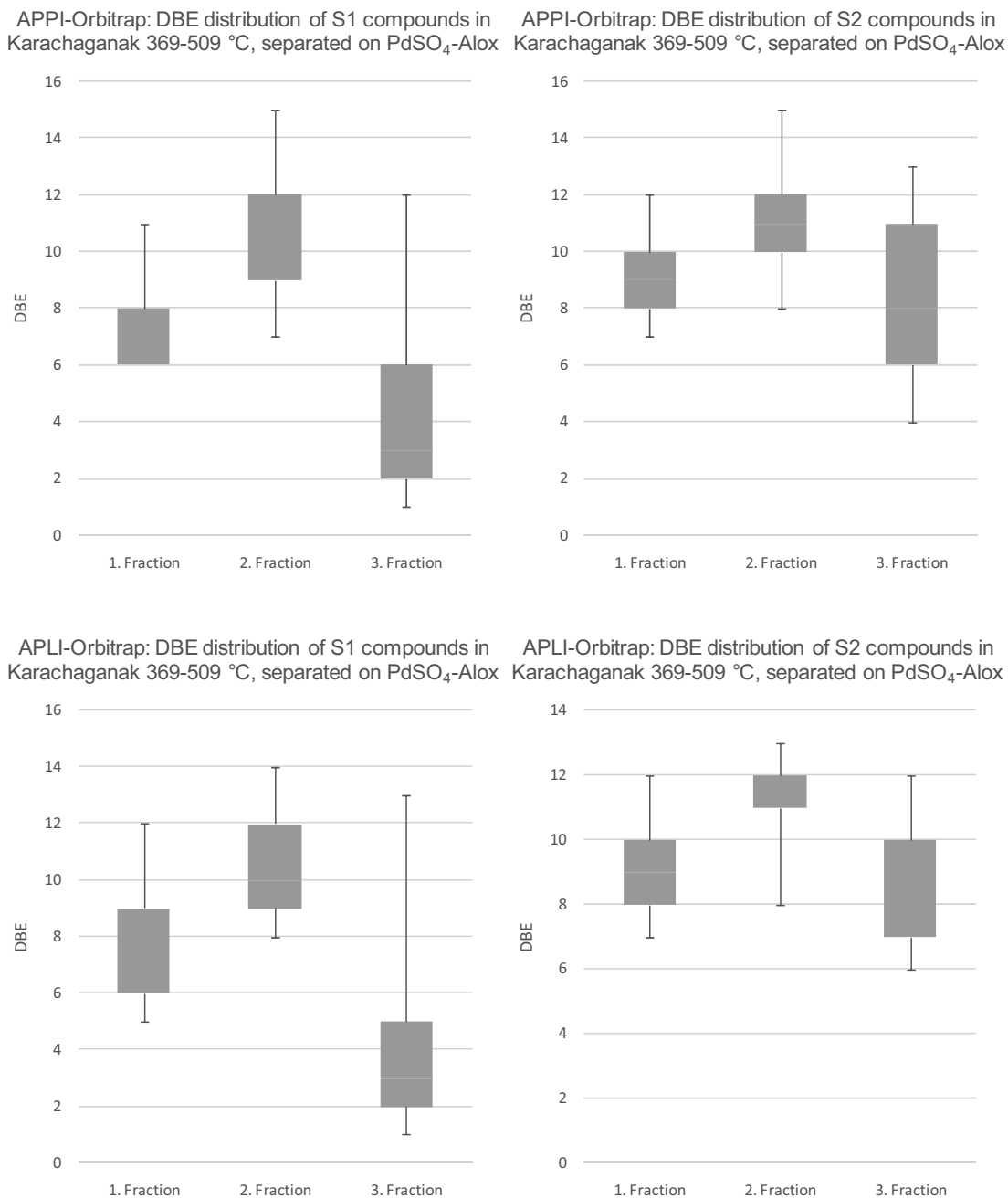
ESI-Orbitrap: DBE distribution of S1 compounds in Karachaganak 369-509 °C, separated on Ag<sup>+</sup>-Cartridges



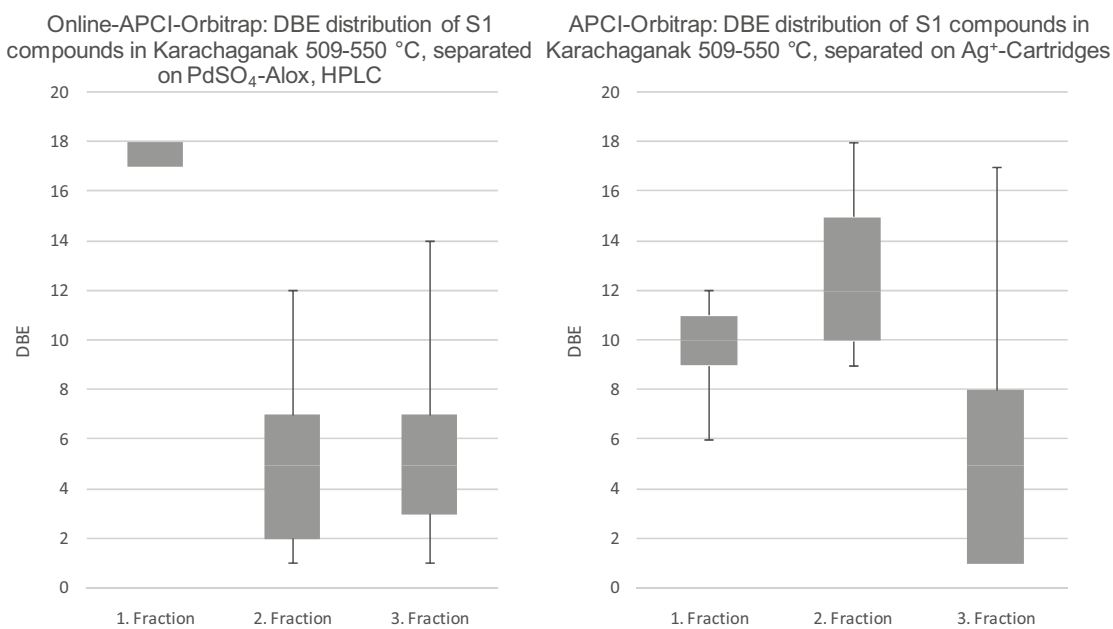
APCI-Orbitrap: DBE distribution of S1 compounds in Karachaganak 369-509 °C, separated on Ag<sup>+</sup>-Cartridges



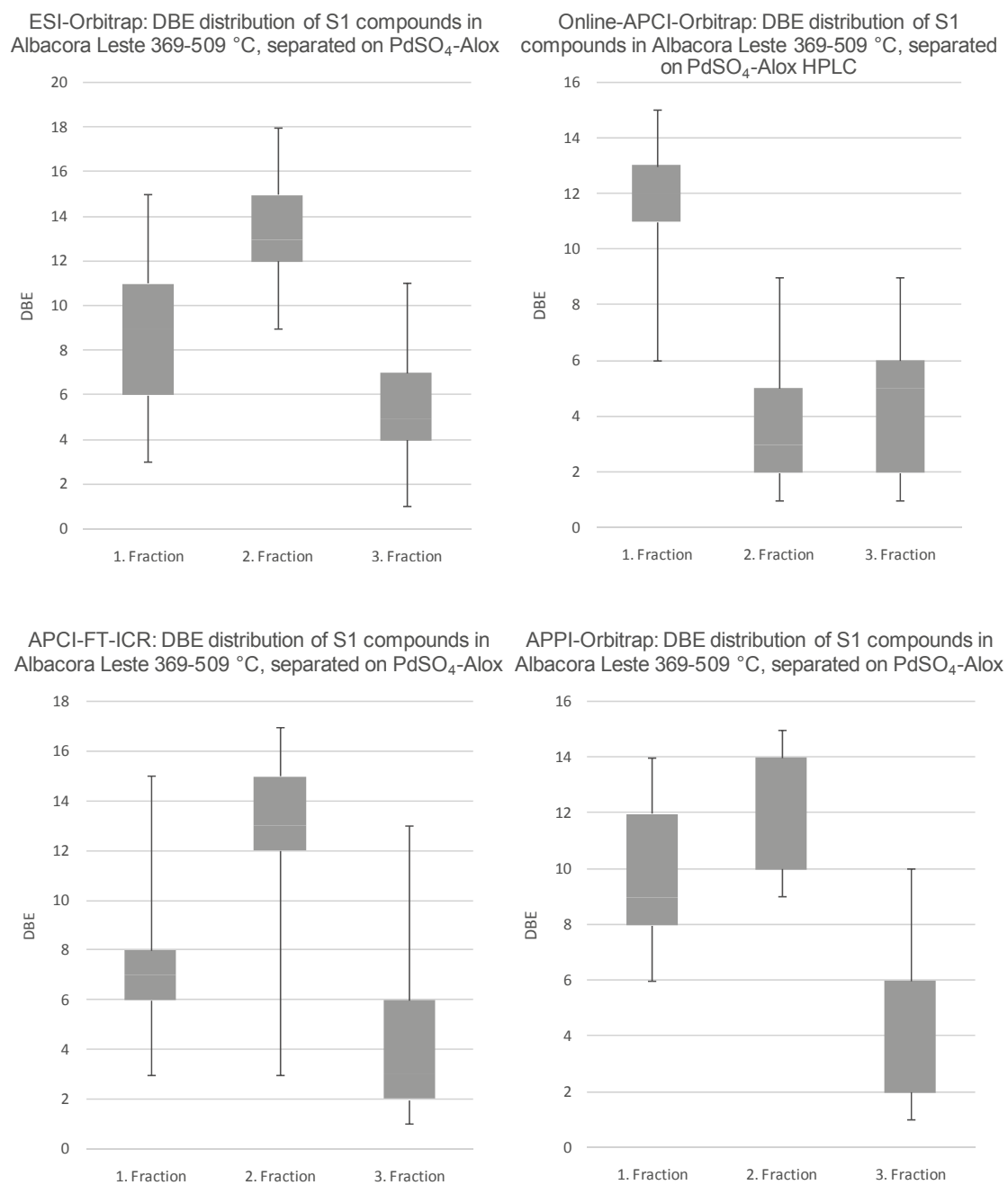
**Figure 136:** Box plots of the S1 compounds of ESI and APCI mass spectra of the separations of Karachaganak 369-509 °C on different phases. Upper left: APCI-Orbitrap MS, online PdSO<sub>4</sub>-Alox HPLC separation; upper right: APCI-FT-ICR MS, hAg-MPSG; bottom left: ESI-Orbitrap MS, Ag<sup>+</sup>-cartridges; bottom right: APCI-Orbitrap MS, Ag<sup>+</sup>-cartridges.



**Figure 137:** Box plots of the S1 and S2 compounds of APPI and APLI mass spectra of the separations of Karachaganak 369-509 °C on PdSO<sub>4</sub>-Alox. Upper row: APPI-Orbitrap MS; bottom row: APLI-Orbitrap MS.

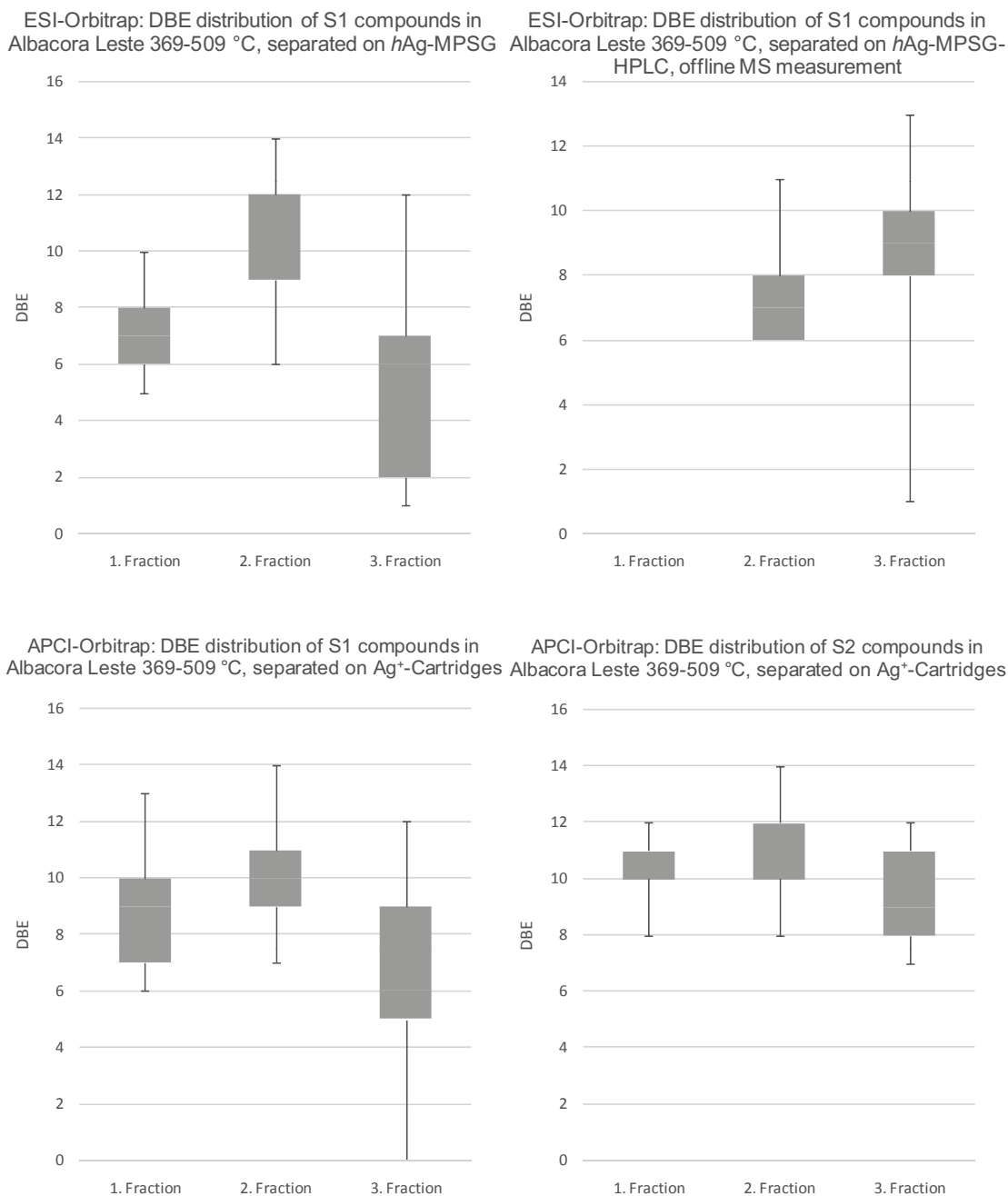


**Figure 138:** Box plots of the S1 compounds of APCI mass spectra of the separations of Karachaganak 509-550 °C on different phases. Left: online PdSO<sub>4</sub>-Alox HPLC separation; left: Ag<sup>+</sup>-cartridges.

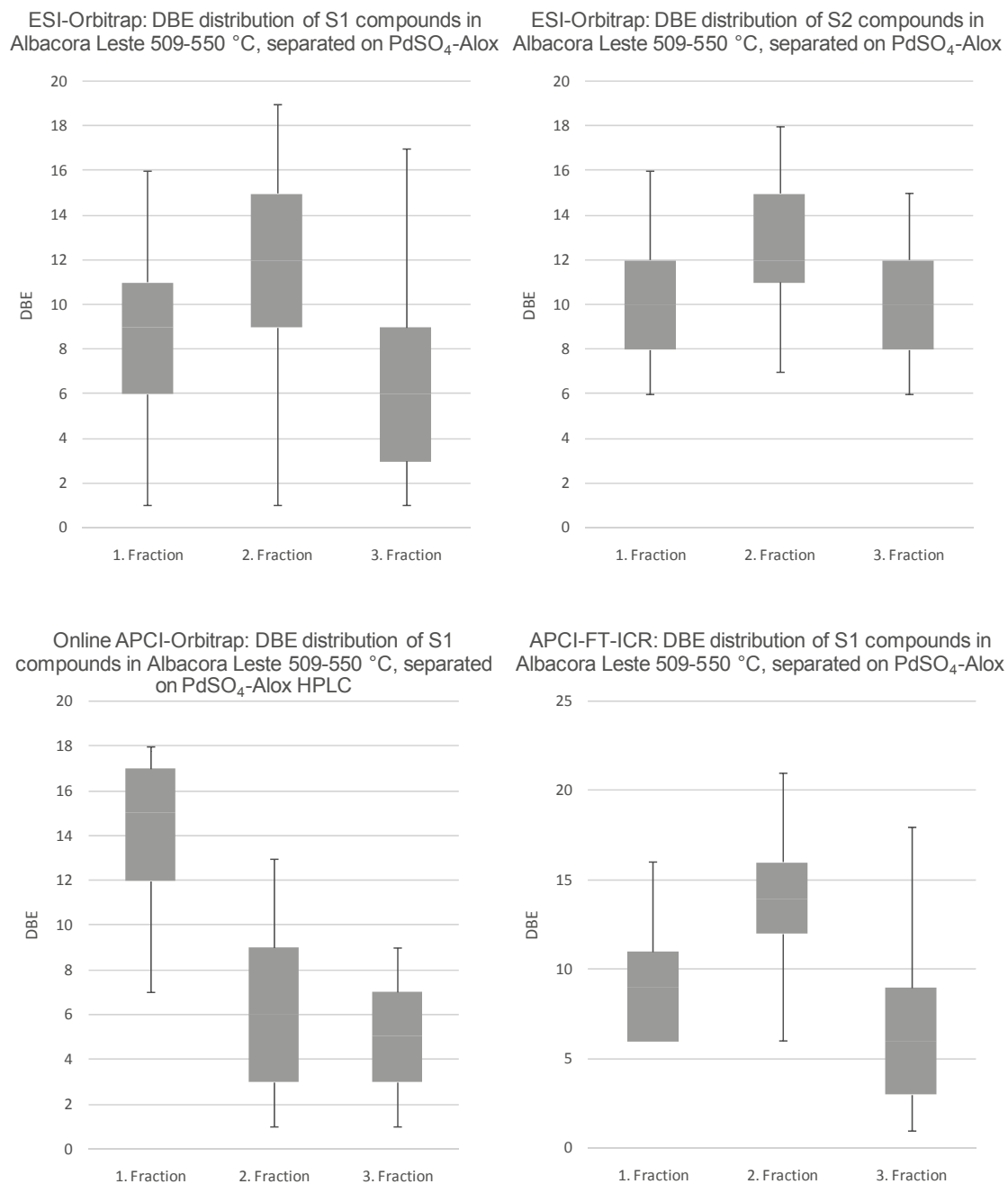


**Figure 139:** Box plots of the S1 compounds of APCI, ESI and APPI mass spectra of the separations of Albacora Leste 369-509 °C on PdSO<sub>4</sub>-Alox. Upper left: ESI-Orbitrap; upper right: online APCI-Orbitrap; bottom left: APCI-FT-ICR; bottom right: APPI-Orbitrap.

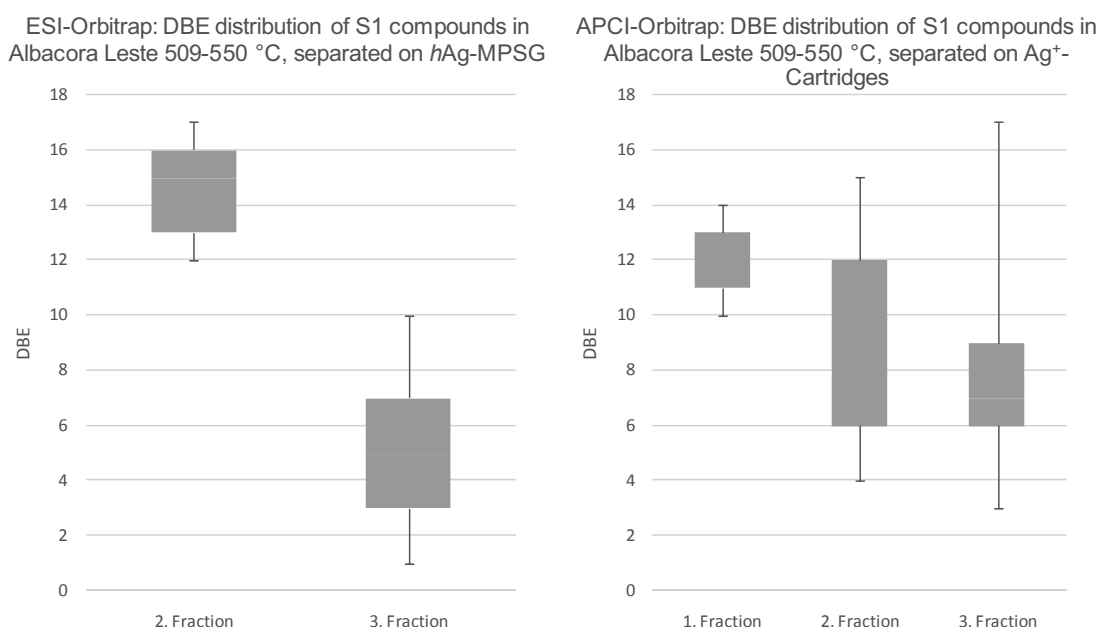




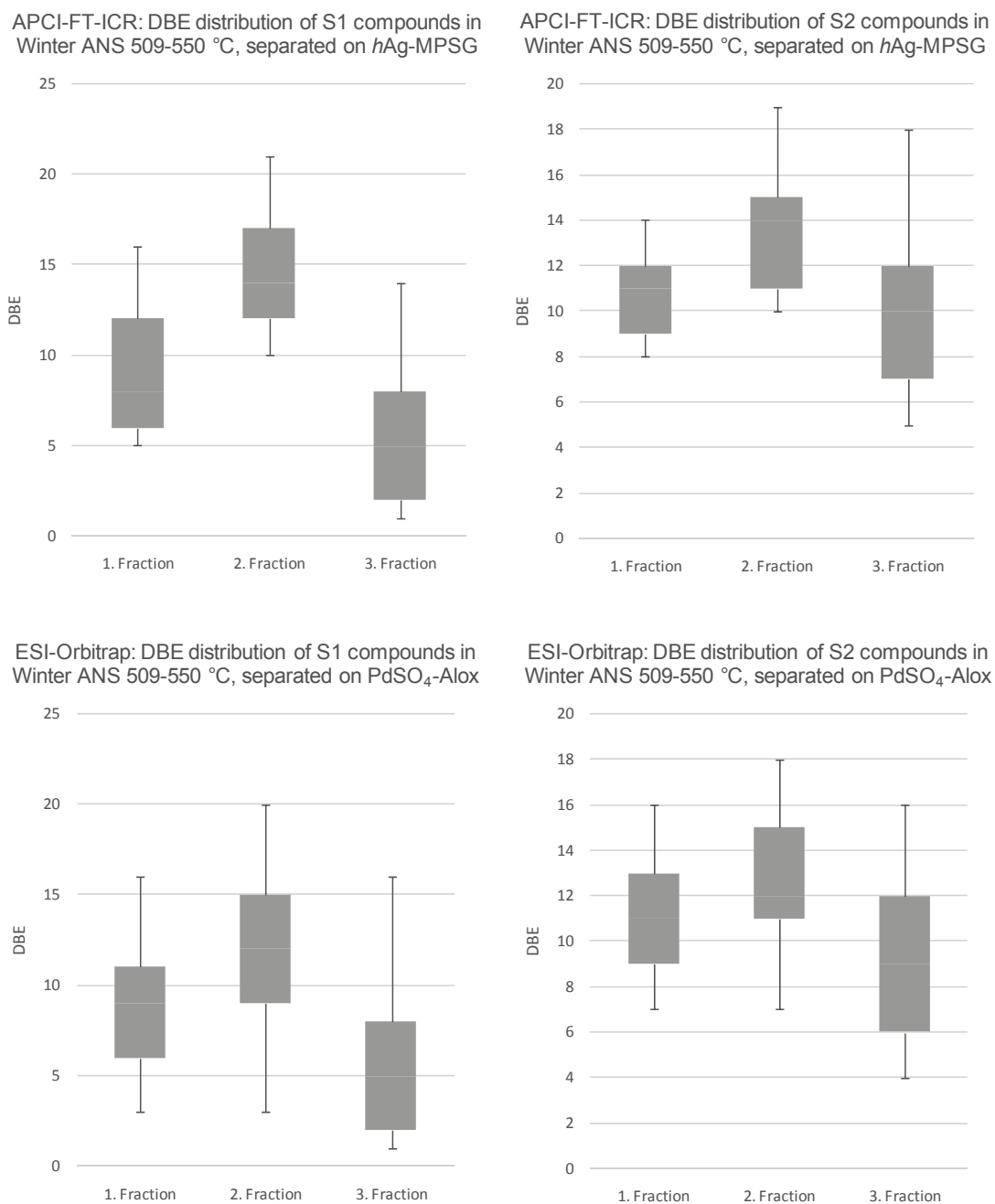
**Figure 140:** Box plots of the S1 and S2 compounds of ESI and APCI mass spectra of the separations of Albacora Leste 369-509 °C on different phases. Upper left: ESI-Orbitrap, *h*Ag-MPSG; upper right: offline ESI-Orbitrap, *h*Ag-MPSG-HPLC; bottom row: APCI-Orbitrap, Ag<sup>+</sup>-cartridges.



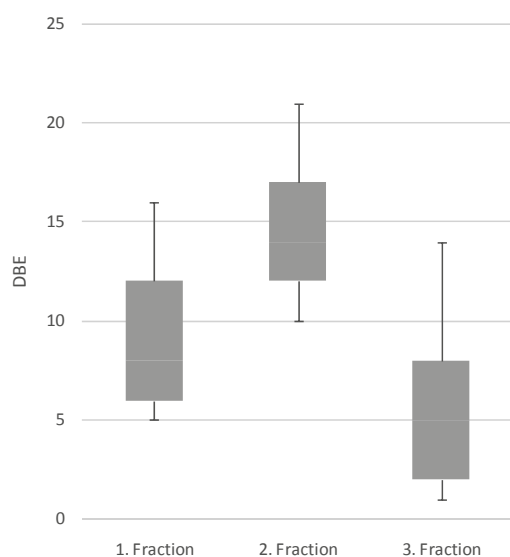
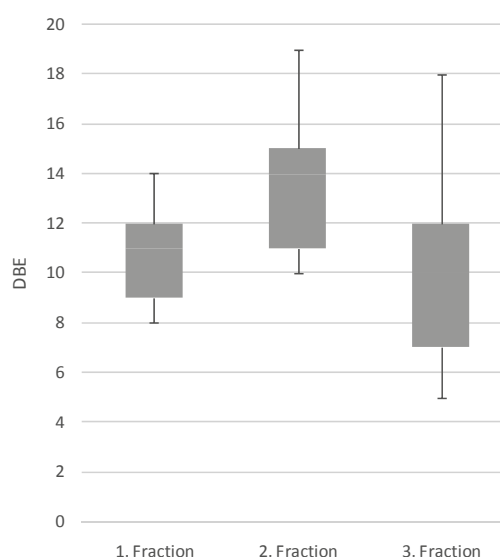
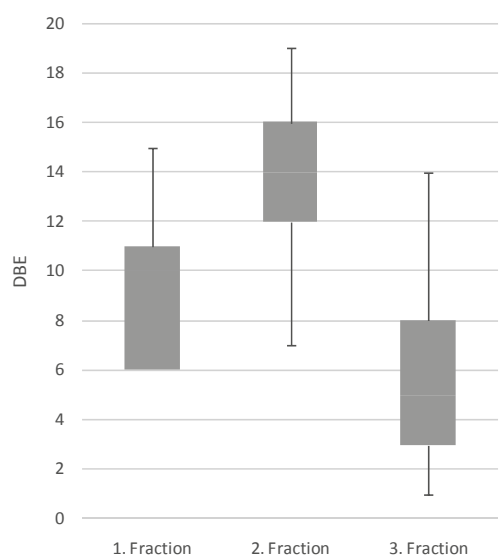
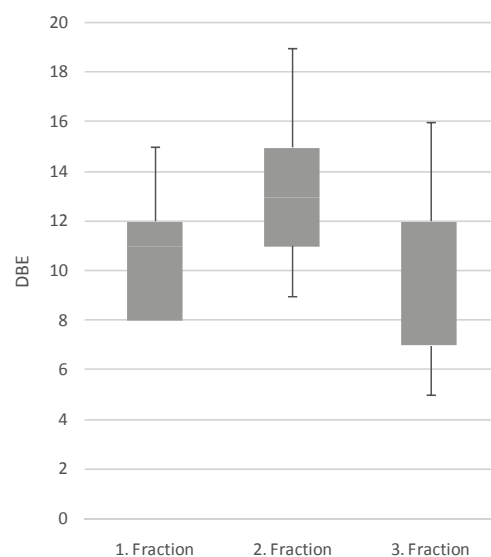
**Figure 141:** Box plots of the S1 and S2 compounds of ESI and APCI mass spectra of the separations of Albacora Leste 509-550 °C on PdSO<sub>4</sub>-Alox. Upper row: ESI-Orbitrap; bottom left: online APCI-Orbitrap; bottom right: APCI-FT-ICR.



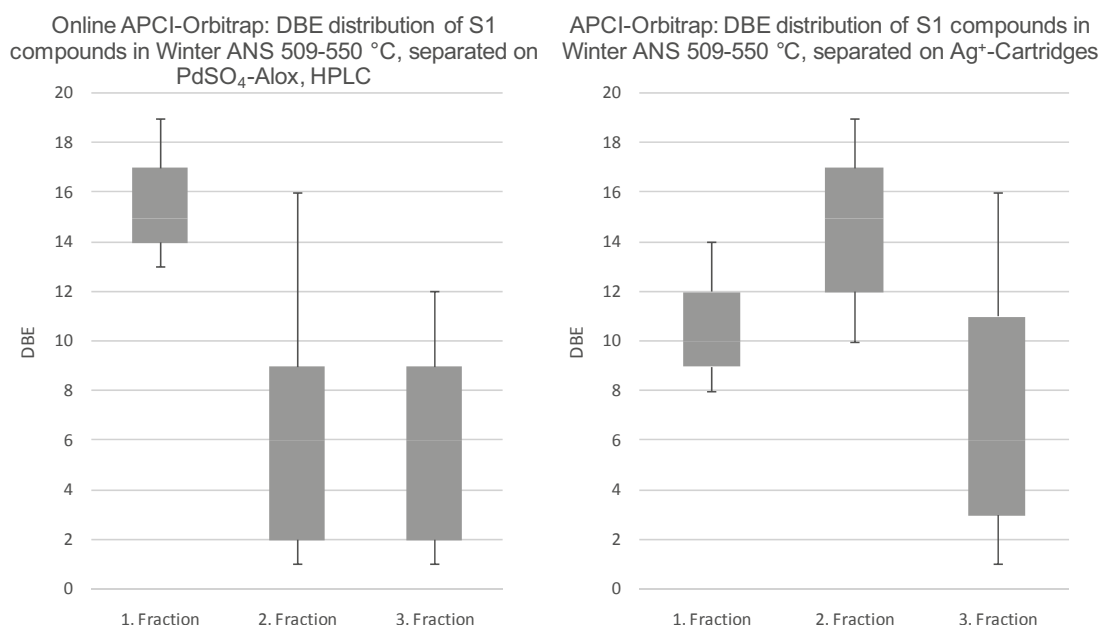
**Figure 142:** Box plots of the S1 compounds of ESI and APCI mass spectra of the separations of Albacora Leste 509-550 °C on different phases. Left: ESI-Orbitrap, *h*Ag-MPSG; right: APCI-Orbitrap, Ag<sup>+</sup>-cartridges.



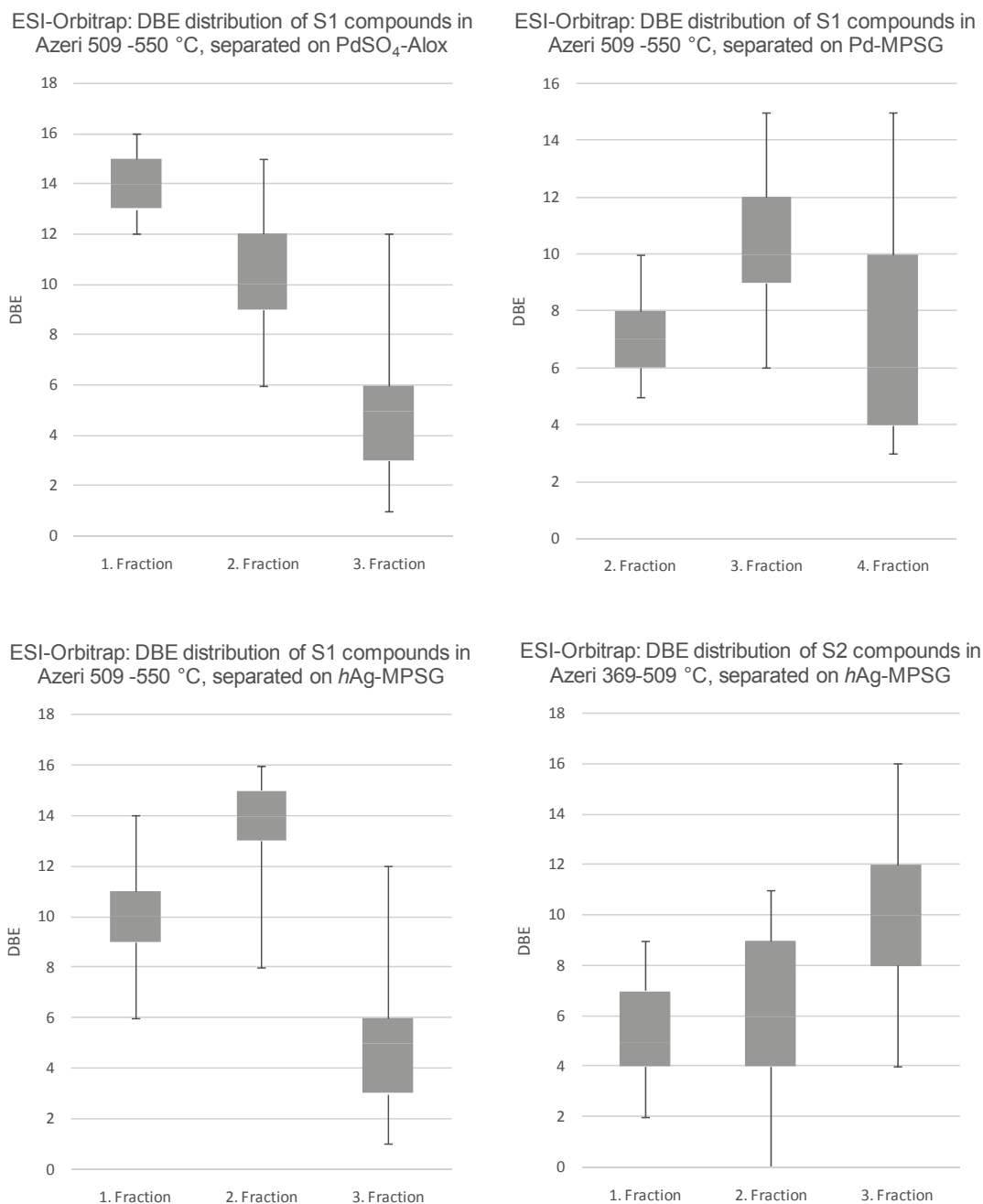
**Figure 143:** Box plots of the S1 and S2 compounds of ESI and APCI mass spectra of the separations of Winter ANS 509-550 °C on PdSO<sub>4</sub>-Alox. Upper row: APCI-FT-ICR; bottom row: ESI-Orbitrap.

APCI-FT-ICR: DBE distribution of S1 compounds in Winter ANS 509-550 °C, separated on *hAg*-MPSGAPCI-FT-ICR: DBE distribution of S2 compounds in Winter ANS 509-550 °C, separated on *hAg*-MPSGESI-Orbitrap: DBE distribution of S1 compounds in Winter ANS 509-550 °C, separated on *hAg*-MPSGESI-Orbitrap: DBE distribution of S2 compounds in Winter ANS 509-550 °C, separated on *hAg*-MPSG

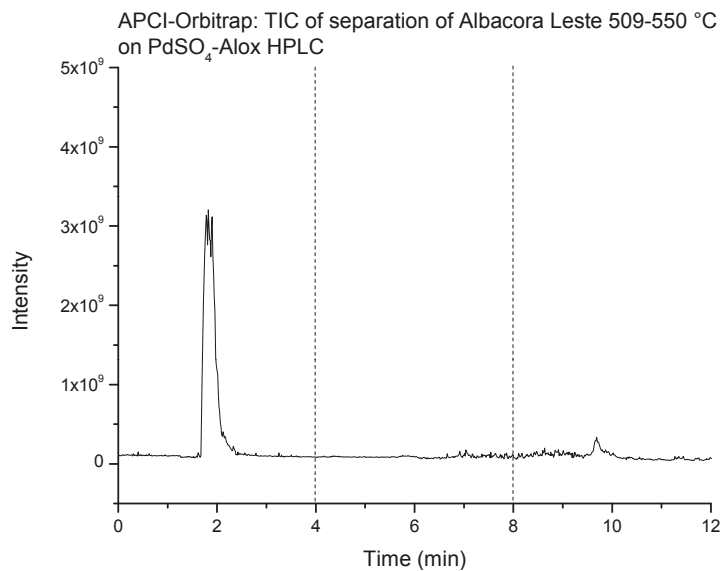
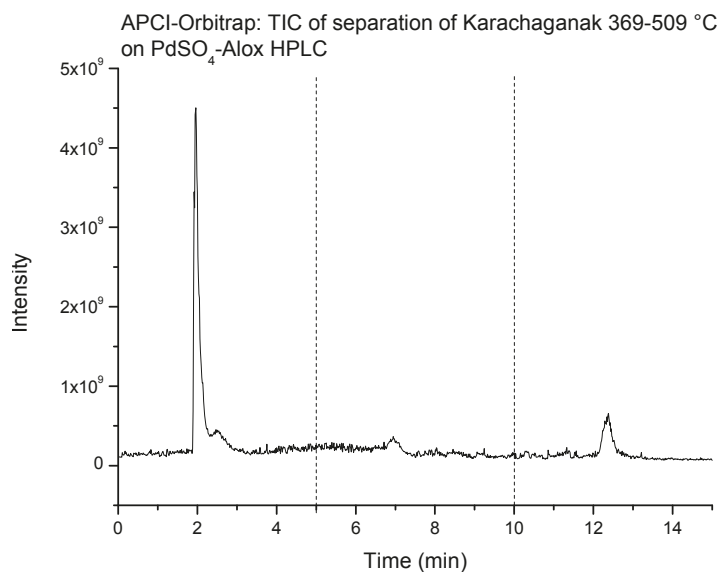
**Figure 144:** Box plots of the S1 and S2 compounds of ESI and APCI mass spectra of the separations of Winter ANS 509-550 °C on *hAg*-MPSG. Upper row: APCI-FT-ICR; bottom row: ESI-Orbitrap.



**Figure 145:** Box plots of the S1 compounds of APCI mass spectra of the separations of Winter ANS 509-550 °C on different phases. Left: online APCI-Orbitrap, PdSO<sub>4</sub>-Alox HPLC separation; right: APCI-Orbitrap, Ag<sup>+</sup>-cartridges.



**Figure 146:** Box plots of the S1 and S2 compounds of APCI mass spectra of the separations of Azeri 369-509 °C on different phases. Upper left: ESI-Orbitrap, PdSO<sub>4</sub>-Alox; upper right: ESI-Orbitrap, Pd-MPSG; bottom row: ESI-Orbitrap, hAg-MPSG.

**TIC of the HPLC separations of VGO****Figure 147:** TIC of the HPLC-separation of Albacora Leste 509-550 °C on PdSO<sub>4</sub>-Alox.**Figure 148:** TIC of the HPLC-separation of Karachaganak 369-509 °C on PdSO<sub>4</sub>-Alox.



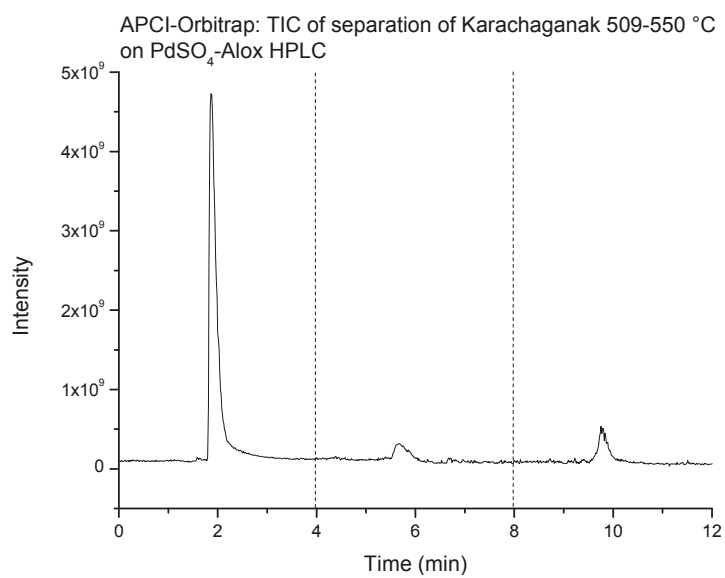


**Figure 149:** TIC of the HPLC-separation of Karachaganak 509-550 °C on PdSO<sub>4</sub>-Alox.

	<u>AgNO<sub>3</sub>-TiO<sub>2</sub></u>			<u>MnSO<sub>4</sub>-SG</u>			<u>ZnCl<sub>2</sub>-SG</u>			<u>CrSO<sub>4</sub>-SG</u>			<u>Ag-Alox (b)</u>			<u>Ag-Alox (n)</u>			<u>Ag-Alox (n)</u>			<u>Ag-Alox (a)</u>		
	A	B	C	A	B	C	A	B	C	A	B	C	A	B	C	A	B	C	A	D	C	A	B	C
<u>Alkanes:</u>																								
<i>n</i> -C <sub>16</sub> or <i>n</i> -C <sub>14</sub>	X			X			X			X			X			X			X			X		
<i>n</i> -C <sub>20</sub>	X			X			X			X			X			X			X			X		
<i>n</i> -C <sub>24</sub>	X			X			X			X			X			X			X			X		
<u>PASHs:</u>																								
benzothiophene	X	X		X			X			X			X			X			X				X	
3-methylbenzothiophene		X		X			X			X			X			X			X				X	
dibenzothiophene		X		X			X			X				X		X			X				X	
benzonaphtho[1,2- <i>d</i> ]thiophene		X		X			X			X				X			X		X				X	
<u>PAHs:</u>																								
naphthalene	X	X		X			X			X			X			X			X				X	
phenanthrene		X		X			X			X				X		X			X				X	
chrysene		X		X				X		X	X			X			X			X			X	X
<u>non-thiophenic sulfur:</u>																								
<i>t</i> -Bu <sub>2</sub> S <sub>2</sub>			X	X			X			X			-	-	-	X			X			-	-	-
<i>n</i> -Bu <sub>2</sub> S <sub>2</sub>			X	X			X			X				X		-	-	-	-	-	-	-	-	-
Ph <sub>2</sub> S <sub>2</sub>	-	-	-	X			X			X				X			X			X			-	-
PhS <sub>2</sub>	-	-	-	X			X			X				X			X			X			X	X
C <sub>12</sub> SMe		X		X				X			X				X			X			X		X	
C <sub>18</sub> SMe		X		X				X		X	X				X			X			X		X	X

A: CH

B: CH:DCM 2:1

C: CH:DCM 2:1 + 1.5% IP/NH<sub>3</sub>

X = recovered

- = not recovered

n = neutral, b = basic, a = acidic

Table 14: Overview over the tested stationary phases. Part 1

	<u>Ag-nano-SG I</u>			<u>Ag-nano-SG II</u>			<u>h Ag-MPSG</u>			<u>h Ag-MPSG</u>			<u>MnCl<sub>2</sub>-SG</u>			<u>Cd(OAc)<sub>2</sub>-SG</u>			<u>CdCl<sub>2</sub>-SG</u>			<u>Co(NO<sub>3</sub>)<sub>2</sub>-SG</u>			
	A	B	C	A	B	C	A	B	C	A	B	P	A	B	C	A	B	C	A	B	C	A	B	C	
<b>Alkanes:</b>																									
<i>n</i> -C <sub>16</sub> or <i>n</i> -C <sub>14</sub>	X			X			X			X			X			X			X			X			
<i>n</i> -C <sub>20</sub>	X			X			X			X			X			X			X			X			
<i>n</i> -C <sub>24</sub>	X			X			X			X			X			X			X			X			
<b>PASHs:</b>																									
benzothiophene	X			X			X			X			X			X			X			X			
3-methylbenzothiophene	X			X			X			X			X			X			X			X			
dibenzothiophene	X			X			X			X			X			X			X			X			
benzonaphtho[1,2- <i>d</i> ]thiophene		X		X				X			X		X			X	X		X			X			
<b>PAHs:</b>																									
naphthalene	X			X			X			X			X			X			X			X			
phenanthrene		X		X			X			X			X			X			X			X			
chrysene		X		X				X		X			X			X	X		X	X		X			
<b>non-thiophenic sulfur:</b>																									
<i>t</i> -Bu <sub>2</sub> S <sub>2</sub>	X				X			X		X			X			X			X				-	-	-
<i>n</i> -Bu <sub>2</sub> S <sub>2</sub>	X			-	-	-	-	-	-	-	-	-	X			X			X			X			
Ph <sub>2</sub> S <sub>2</sub>	-	-	-	X			-	-	-	-	-	-	X			X			X				X		
PhS <sub>2</sub>		X		X			X			X			X			X	X		X				X		
C <sub>12</sub> SMe		X			X			X		X			X			X	X		X	X		X			
C <sub>18</sub> SMe		X			X			X		X			X			X	X		X	X		X			

A: CH

B: CH:DCM 2:1

C: CH:DCM 2:1 + 1.5% IP/NH<sub>3</sub>

X = recovered

- = not recovered

Table 15: Overview over the tested stationary phases. Part 2

	<u>Cu(OAc)<sub>2</sub>-SG</u>			<u>Cu(I)Cl-SG</u>			<u>Ni(OAc)<sub>2</sub>-SG</u>			<u>FeCl<sub>3</sub>-SG</u>			<u>Zn(NO<sub>3</sub>)<sub>2</sub>-SG</u>			<u>Pb(NO<sub>3</sub>)<sub>2</sub>-SG</u>			<u>Cr(SO<sub>4</sub>)<sub>3</sub>-Alox</u>			<u>VCl<sub>3</sub>-Alox</u>				
	A	B	C	A	B	C	A	B	C	A	B	C	A	B	C	A	B	C	A	B	C	A	B	C		
<u>Alkanes:</u>																										
<i>n</i> -C <sub>16</sub> or <i>n</i> -C <sub>14</sub>	X			X			X			X			X			X			X			X				
<i>n</i> -C <sub>20</sub>	X			X			X			X			X			X			X			X				
<i>n</i> -C <sub>24</sub>	X			X			X			X			X			X			X			X				
<u>PASHs:</u>																										
benzothiophene	X			X			X			X			X			X			X	X		-	-	-		
3-methylbenzothiophene	X			X			X			X			X			X			X	X		-	-	-		
dibenzothiophene	X			X			X		X	X			X			X			X	X		X				
benzonaphtho[1,2- <i>d</i> ]thiophene	X	X		X	X		X	X		X	X		X	X		-	-	-	X	X		X				
<u>PAHs:</u>																										
naphthalene	X			X			X			X			X			X			X	X		-	-	-		
phenanthrene	X			X	X		X	X		X	X		X	X		X			X	X		-	-	-		
chrysene	X	X		X	X			X		X	X		X	X		-	-	-	X	X		-	-	-		
<u>non-thiophenic sulfur:</u>																										
<i>t</i> -Bu <sub>2</sub> S <sub>2</sub>	-	-	-	-	-	-	-	-	-	-	-	-	-	-	-	X			X			-	-	-		
<i>n</i> -Bu <sub>2</sub> S <sub>2</sub>	-	-	-	X			-	-	-	-	-	-	-	-	-	X			X			-	-	-		
Ph <sub>2</sub> S <sub>2</sub>	-	-	-	-	-	-	-	-	-	-	-	-	-	-	-	X			X	X		X				
PhS <sub>2</sub>	-	-	-	X			X	X		X			X	X		X			X	X		X				
C <sub>12</sub> SMe		X		-	-	-		X		X			X		(X)			(X)		X	X		-	-	-	
C <sub>18</sub> SMe		X		-	-	-		X		X			X	X		(X)			X			-	-	-		

A: CH

B: CH:DCM 2:1

C: CH:DCM 2:1 + 1.5% IP/NH<sub>3</sub>

X = recovered

- = not recovered

Table 16: Overview over the tested stationary phases. Part 3

	<u>Cd(OAc)<sub>2</sub>-Alox</u>			<u>CdCl<sub>2</sub>-Alox</u>			<u>Pb(NO<sub>3</sub>)<sub>2</sub>-Alox</u>			<u>H<sub>3</sub>BO<sub>3</sub>-SG</u>			<u>CuCl<sub>2</sub>-SG*</u>			<u>Phenyl-SG</u>			<u>Gold-Nano-SG</u>			<u>Ag-Cartridges</u>					
	A	B	C	A	B	C	A	B	C	A	B	C	A	B	C	A	B	C	A	B	C	A	B	C			
<u>Alkanes:</u>																											
<i>n</i> -C <sub>16</sub> or <i>n</i> -C <sub>14</sub>	X			X			X			X			X			X			X			X			X		
<i>n</i> -C <sub>20</sub>	X			X			X			X			X			X			X			X			X		
<i>n</i> -C <sub>24</sub>	X			X			X			X			X			X			X			X			X		
<u>PASHs:</u>																											
benzothiophene	X			X			X			X			X			X			X			X			X		
3-methylbenzothiophene	X			X			X			X			X			X			X			X			X		
dibenzothiophene	X			X	X		X	X		X	X		X	X		X	X		X	X		X		X			
benzonaphtho[1,2- <i>d</i> ]thiophene	X				X			X		X			X			X			X					X			
<u>PAHs:</u>																											
naphthalene	X			X			X			X			X			X			X			X					
phenanthrene	X				X			X		X			X			X			X					X			
chrysene	X				X			X		X			X			X			X					X			
<u>non-thiophenic sulfur:</u>																											
<i>t</i> -Bu <sub>2</sub> S <sub>2</sub>	X			X			X			X			X			X			X								X
<i>n</i> -Bu <sub>2</sub> S <sub>2</sub>	X			X			X			X			X			X			X								X
Ph <sub>2</sub> S <sub>2</sub>	X			X			X			X			X				X		X								X
PhS <sub>2</sub>	X			X			X			X			X			X			X								X
C <sub>12</sub> SMe	X			X	X		X			X			X			X	X		X						-	-	-
C <sub>18</sub> SMe	X			X	X		X			X			X			X			X						-	-	-

A: CH

B: CH:DCM 2:1

C: CH:DCM 2:1 + 1.5% IP/NH<sub>3</sub>

X = recovered

- = not recovered

\* = deprotonated with NH<sub>3</sub>

Table 17: Overview over the tested stationary phases. Part 4

## 11 References

- [1] Arbeitsgemeinschaft Energie e.V, Auswertungstabellen zur Energiebilanz für die Bundesrepublik Deutschland 1990 bis 2012 - Berechnungen auf Basis des Wirkungsgradansatzes -, **2013**.
- [2] *Bundesgesetzblatt Teil I* **2011**, (43), 1704–1705.
- [3] World DataBank - World Development Indicators, **12.06.2014**, URL <http://databank.worldbank.org/data/home.aspx>.
- [4] OPEC, The new OPEC Reference Basket (ORB), **2014**, URL [http://www.opec.org/opec\\_web/en/data\\_graphs/40.htm](http://www.opec.org/opec_web/en/data_graphs/40.htm).
- [5] J. V. Headley, K. M. Peru, M. P. Barrow, *Mass Spectrometry Reviews* **2009**, 28 (1), 121–134.
- [6] W. Jörß, L. Emele, M. Scheffler, V. Cook, J. Theloke, B. Thiruchittampalam, F. Dünnebeil, W. Knörr, C. Heidt, M. Jozwicka, J. Kuenen, H. D. van der Gon, A. Visschedijk, R. van Gijlswijk, B. Osterburg, B. Laggner, D. R. Stern, *Luftqualität 2020/2030: Weiterentwicklung von Prognosen für Luftschadstoffe unter Berücksichtigung von Klimastrategien*, Bd. 35, Umweltbundesamt, **2014**.
- [7] *The 0.1 An assessment of available impact studies and alternative means of compliance*, European Maritime Safety Agency, **2010**, technical Report.
- [8] J. G. Speight, *Petroleum Chemistry and Refining*, Taylor & Francis, **1998**.
- [9] B. P. Tissot, D. H. Welte, *Petroleum Formation and Occurrence*, Springer Verlag, 2. Aufl., **1984**.
- [10] P. H. Albers, *Handbook of Ecotoxicology*, Kap. Petroleum and Individual Polycyclic Aromatic Hydrocarbons, 341–360, Lewis Publishers, **1995**.
- [11] J. H. Gary, G. E. Handwerk, *Petroleum Refining Technology and Economics*, Marcel Dekker, 4. Aufl., **2001**.
- [12] J. G. Speight, *The Chemistry and Technology of Petroleum*, Marcel Dekker, 3. Aufl., **1999**.
- [13] G. F. Bolshakov, *Sulfur reports* **1986**, 5 (2), 103–393.

- [14] W. L. Orr, J. S. S. Damste, *Geochemistry of Sulfur in Petroleum Systems*, Bd. 429, Kap. 2, 2–29, American Chemical Society, **1990**.
- [15] C.-D. Czogalla, F. Boberg, *Sulfur Reports* **1983**, 3 (4), 121–167.
- [16] W. Orr, J. S. S. Damsté, *Geochemistry of Sulfur in Fossil Fuels: Sulfur in Petroleum and Related Bitumens*, ACS Symposium Series American Chemical Society: Washington, DC, **1990**.
- [17] T. Cyr, J. Payzant, D. Montgomery, O. Strausz, *Organic Geochemistry* **1986**, 9 (3), 139 – 143.
- [18] S. C. Brassell, C. A. Lewis, J. W. D. Leeuw, F. D. Lange, J. S. S. Damste, *Nature* **1986**, 320, 160–162.
- [19] J. S. S. Damste, J. W. De Leeuw, *International Journal of Environmental Analytical Chemistry* **1987**, 28 (1-2), 1–19.
- [20] M. Kohnen, T. Peakman, J. Damste, J. de Leeuw, *Organic Geochemistry* **1990**, 16 (4-6), 1103 – 1113, proceedings of the 14th International Meeting on Organic Geochemistry.
- [21] J. Poinot, P. Schneckenburger, J. Trendel, *Chem. Commun.* **1997**, 2191–2192.
- [22] J. C. Schmid, J. Connan, P. Albrecht, *Nature* **1987**, 329, 54–56.
- [23] A. Charrie-Duhaut, C. Schaeffer, P. Adam, P. Manuelli, P. Scherrer, P. Albrecht, *Angewandte Chemie International Edition* **2003**, 42 (38), 4646–4649.
- [24] S. R. C. Douglas A. Skoog, F. James Holler, *Instrumentelle Analytik*, Springer Spektrum, 6. Aufl., **2013**.
- [25] L. Molin, P. Traldi, *Advances in LC-instrumentation, Journal of Chromatography Library*, Bd. 72, Kap. Basic Aspects of electrospray ionization, 1–8, Elsevier, **2007**.
- [26] K. Cammann, *Instrumentelle Analytische Chemie. Verfahren, Anwendungen und Qualitätssicherung*, Spektrum Verlag Heidelberg, **2010**.
- [27] A. Raffaelli, *Advances in LC-instrumentation, Journal of Chromatography Library*, Bd. 72, Kap. Atmospheric Pressure chemical ionization (APCI), 11–24, Elsevier, **2007**.

- [28] D. B. Robb, T. R. Covey, A. P. Bruins, *Analytical Chemistry* **2000**, *72* (15), 3653–3659, PMID: 10952556.
- [29] A. Raffaelli, A. Saba, *Mass Spectrometry Reviews* **2003**, *22* (5), 318–331.
- [30] M. P. Balogh, *Advances in LC-instrumentation, Journal of Chromatography Library*, Bd. 72, Kap. A case for congruent multiple ionization modes in atmospheric pressure ionization mass spectrometry, 65–88, Elsevier, **2007**.
- [31] O. J. Schmitz, T. Benter, *Advances in LC-instrumentation, Journal of Chromatography Library*, Bd. 72, Kap. Atmospheric pressure laser ionization (APLI), 89–114, Elsevier, **2007**.
- [32] M. Constapel, M. Schellenträger, O. J. Schmitz, S. Gäb, K. J. Brockmann, R. Giese, T. Benter, *Rapid Communications in Mass Spectrometry* **2005**, *19* (3), 326–336.
- [33] S. Schmidt, M. F. Appel, R. M. Garnica, R. N. Schindler, T. Benter, *Analytical Chemistry* **1999**, *71* (17), 3721–3729.
- [34] S. K. Panda, K.-J. Brockmann, T. Benter, W. Schrader, *Rapid Communications in Mass Spectrometry* **2011**, *25* (16), 2317–2326.
- [35] D. R. Demartini, *Tandem Mass Spectrometry - Molecular Characterization*, Kap. A Short Overview of the Components in Mass Spectrometry Instrumentation for Proteomics Analyses, InTech, **2013**.
- [36] R. H. Perry, R. G. Cooks, R. J. Noll, *Mass Spectrometry Reviews* **2008**, *27* (6), 661–699.
- [37] R. A. Zubarev, A. Makarov, *Analytical Chemistry* **2013**, *85* (11), 5288–5296.
- [38] A. Makarov, E. Denisov, O. Lange, *Journal of the American Society for Mass Spectrometry* **2009**, *20* (8), 1391 – 1396.
- [39] A. Makarov, E. Denisov, O. Lange, S. Horning, *Journal of the American Society for Mass Spectrometry* **2006**, *17* (7), 977 – 982.
- [40] A. G. Marshall, C. L. Hendrickson, *International Journal of Mass Spectrometry* **2002**, *215*, 59–75.



- [41] M. B. Comisarow, A. G. Marshall, *Chemical Physics Letters* **1974**, *25* (2), 282–283.
- [42] E. N. Nikolaev, Y. I. Kostyukevich, G. N. Vladimirov, *Mass Spectrometry Reviews* **2014**, n/a–n/a.
- [43] *Pressemitteilung Bruker vom 16.06.2014*, **2014**, URL <http://www.bruker.com/products/mass-spectrometry-and-separations/news/single-view/article/worlds-highest-field-21-tesla-magnet-for-ft-icr-mass-spectrometry-installed-at-national-high-magn.html>.
- [44] A. G. Marshall, R. P. Rodgers, *Accounts of Chemical Research* **2004**, *37* (1), 53–59.
- [45] M. Witt, J. Friedrich, *ASMS annual conference* **2013**.
- [46] R. Rodgers, F. White, C. Hendrickson, A. Marshall, K. Andersen, *Analytical Chemistry* **1998**, *70* (22), 4743–4750, cited By (since 1996)69.
- [47] Y. Cho, A. Ahmed, A. Islam, S. Kim, *Mass Spectrometry Reviews* **2014**.
- [48] E. Kendrick, *Analytical Chemistry* **1963**, *35* (13), 2146–2154.
- [49] M. Nocun, *Chromatographische und massenspektrometrische Methoden für die Untersuchung von polycyclischen aromatischen Schwefelheterocyclen in Rohölen*, Dissertation, Westfälische Wilhelms-Universität Münster, **2012**.
- [50] S. Panda, *Liquid Chromatography and High Resolution Mass Spectrometry for the Speciation of High Molecular Weight Sulfur Aromatics in Fossil Fuels*, Dissertation, Westfälische Wilhelms-Universität Münster, **2006**.
- [51] A. Japes, *Untersuchungen schwer entschwefelbarer Verbindungen aus Erdöl und seinen Fraktionen*, Dissertation, Westfälische Wilhelms-Universität Münster, **2008**.
- [52] F. Helfferich, *Nature* **1961**, *189*, 1001–1002.
- [53] V. A. Davankov, A. V. Semechkin, *Journal of Chromatography* **1977**, *141*, 313–353.
- [54] R. G. Pearson, *Journal of the American Chemical Society* **1963**, *85* (22), 3533–3539.

- [55] J. W. Vogh, J. E. Dooley, *Journal of Analytical Chemistry* **1975**, *47* (6), 816–821.
- [56] H. Takayanagi, O. Hgtano, K. Fujimura, T. Ando, *Journal of Analytical Chemistry* **1985**, *57*, 1840–1846.
- [57] M. Nishioka, R. S. Tomich, *Fuel* **1993**, *72* (7), 1007 – 1010.
- [58] G. Blanco-Brieva, J. M. Campos-Martin, S. M. Al-Zahrani, J. L. G. Fierro, *Fuel* **2011**, *90*, 190–197.
- [59] D. Peralta, G. Chaplais, A. Simon-Masseron, K. Barthelet, G. D. Pirngruber, *Energy & Fuels* **2012**, *26*, 4923–4960.
- [60] M. Guadalupe, V. C. Branco, J. Schmid, *Organic Geochemistry* **1991**, *17* (3), 355–361.
- [61] N. H. Jiang, G. Y. Zhu, S. C. Zhang, Z. J. Wang, *Chinese Science Bulletin* **2008**, *53* (3), 396–401.
- [62] R. Vivilecchia, M. Thiebaud, R. W. Frei, *Journal of Chromatographic Science* **1972**, *10*, 411–416.
- [63] A. Samokhvalov, E. C. Duin, S. Nair, B. J. Tatarchuk, *Applied Surface Science* **2011**, *257*, 3226–3232.
- [64] M. Nishioka, *Energy & Fuels* **1988**, *2*, 214–219.
- [65] U. Pyell, S. Schober, G. Stork, *Fresenius Journal of Analytical Chemistry* **1997**, *359*, 538–541.
- [66] K. Sripada, J. T. Andersson, *Analytical and Bioanalytical Chemistry* **2005**, *382*, 735–741.
- [67] A. Japes, M. Penassa, J. T. Andersson, *Energy & Fuels* **2009**, *23* (4), 2143–2148.
- [68] B. Yang, W. Hou, K. Zhang, X. Wang, *Journal of Separation Science* **2013**, *36* (16), 2646–2655.
- [69] V. P. Sergun, R. S. Min, *Petroleum Chemistry* **2012**, *52* (2), 68–73.
- [70] C.-C. Hu, Y. Liu, *Analytical Chimica Acta* **1996**, *332*, 23–30.
- [71] K. Beiner, P. Popp, R. Wennrich, *Journal of Chromatography A* **2002**, *968*, 171–176.

- [72] T. Kaimai, A. Matsunaga, *Analytical Chemistry* **1978**, *50* (2), 268–270.
- [73] V. Horak, M. D. V. Guzman, G. Weeks, *Analytical Chemistry* **1979**, *51*, 2248–2253.
- [74] C.-Y. Liu, C.-C. Hu, K.-Y. Yeh, M.-J. Chen, *Fresenius Journal of Analytical Chemistry* **1991**, *339* (12), 877–881.
- [75] N. Ghaloum, G. Michael, Z. Khan, *Journal of Liquid Chromatography and Related Technology* **2002**, *25*(9), 1409–1420.
- [76] G. Michael, H. Al-Rabiah, R. Kadmi, M. Al-Mojbel, *Journal of Liquid Chromatography and Related Technologies* **2007**, *30*, 1577–1601.
- [77] H. Wei, X. Wang, Q. Liu, Y. Mei, Y. Lu, Z. Guo, *Inorganic Chemistry* **2005**, *44*, 6077–6081.
- [78] I. M. Klotz, B. J. Campbell, *Archives of Biochemistry and Biophysics* **1962**, *96*, 92–99.
- [79] S. Chowdhury, S. Roy, *Tetrahedron Letters* **1997**, *38* (12), 2149–2152.
- [80] G. Danno, K. Kanazawa, M. Nataka, *Agricultural and Biological Chemistry* **1975**, *39* (7), 1379–1384.
- [81] A. Müller, E. Diemann, R. Jostes, H. Bögge, *Angewandte Chemie, International Edition* **1981**, *20*, 934–955.
- [82] S. E. Livingstone, *Quarterly Reviews, Chemical Society* **1965**, *19*, 386–425.
- [83] H. Sigel, K. H. Scheller, V. M. Rheinberger, B. E. Fischer, *Dalton Transactions* **1980**, *7*, 1022–1028.
- [84] D. Dyrssen, *Marine Chemistry* **1988**, *24*, 143–153.
- [85] I. Möller, *Chromatographische Trennung von Sulfiden und Disulfiden auf metallbeschichteten Kieselgelen*, Diplomarbeit, Westfälische Wilhelms-Universität Münster, **2011**.
- [86] T. E. Earle, *Analytical Chemistry* **1953**, *25* (5), 769–771.
- [87] Y. Miki, M. Toba, Y. Yoshimura, *Journal of the Japan Petroleum Institute* **2008**, *51* (4), 225–233.

- [88] S. Nair, B. J. Tatarchuk, *Fuel* **2010**, *89*, 3218–3225.
- [89] C. Yin, D. Xia, *Fuel* **2001**, *80*, 607–610.
- [90] M. Penassa, *The Class of Hexahydrobenzothiophenes in Petroleum Distillates - Chromatographic Methods for Sample Preparation and Analysis on Modern Desulfurized Middle Distillates*, Dissertation, Westfälische Wilhelms-Universität Münster, **2008**.
- [91] M. Nocun, J. T. Andersson, *Journal of Chromatography A* **2012**, *1219* (0), 47 – 53.
- [92] S. K. Panda, W. Schrader, A. al Hajji, J. T. Andersson, *Energy & Fuels* **2007**, *21* (2), 1071–1077.
- [93] H. Willsch, H. Clegg, B. Horsfield, M. Radke, H. Wilkes, *Analytical Chemistry* **1997**, *69* (20), 4203–4209.
- [94] G. Felix, C. Bertrand, F. Van Gastel, *Chromatographia* **1985**, *20* (3), 155–160.
- [95] G. M. Janini, K. Johnston, W. L. Zielinski, *Analytical Chemistry* **1975**, *47* (4), 670–674, pMID: 1137143.
- [96] P. L. Grizzle, D. M. Sablotny, *Analytical Chemistry* **1986**, *58* (12), 2389–2396.
- [97] D. M. Jewell, J. H. Weber, J. W. Bungler, H. Plancher, D. R. Latham, *Analytical Chemistry* **1972**, *44* (8), 1391–1395.
- [98] G. S. Frysinger, R. B. Gaines, *Journal of Separation Science* **2001**, *24* (2), 87–96.
- [99] G. S. Frysinger, R. B. Gaines, *Journal of High Resolution Chromatography* **1999**, *22* (5), 251–255.
- [100] G. S. Kapur, S. Berger, *Energy & Fuels* **2005**, *19* (2), 508–511.
- [101] E. Ragazzi, G. Veronese, *Journal of Chromatography A* **1973**, *77* (2), 369 – 375.
- [102] J. Rolfes, J. T. Andersson, *Anal. Commun.* **1996**, *33*, 429–432.
- [103] T. E. Cogswell, J. F. McKay, D. R. Latham, *Analytical Chemistry* **1971**, *43* (6), 645–648.

- [104] A. Gole, *Entwicklung neuer Materialien zur chromatographischen Klassentrennung aromatischer Stickstoffverbindungen in fossilen Brennstoffen*, Dissertation, Westfälische Wilhelms-Universität Münster, **2013**.
- [105] J. T. Andersson, *Analytical and Bioanalytical Chemistry* **2002**, *373* (6), 344–355.
- [106] R. Hua, Y. Li, W. Liu, J. Zheng, H. Wei, J. Wang, X. Lu, H. Kong, G. Xu, *Journal of Chromatography A* **2003**, *1019* (1-2), 101 – 109, first International Symposium on Comprehensive Multidimensional Gas Chromatography.
- [107] R. Ruiz-Guerrero, C. Vendevre, D. Thiébaud, F. Bertoncini, D. Espinat, *Journal of Chromatographic Science* **2006**, *44* (9), 566–573.
- [108] G. S. Waldo, R. M. Carlson, J. Moldowan, K. E. Peters, J. E. Penner-hahn, *Geochimica et Cosmochimica Acta* **1991**, *55* (3), 801 – 814.
- [109] R. M. Acheson, D. R. Harrison, *Journal of the Chemical Society C: Organic* **1970**, (13), 1764–1784.
- [110] T. Nolte, J. T. Andersson, *Analytical and bioanalytical chemistry* **2009**, *395*, 1843–1852.
- [111] T. K. Green, P. Whitley, K. Wu, W. G. Lloyd, L. Z. Gan, *Energy & Fuels* **1994**, *8* (1), 244–248.
- [112] G. K. Helmkamp, H. N. Cassey, B. A. Olsen, D. J. Pettitt, *The Journal of Organic Chemistry* **1965**, *30* (3), 933–935.
- [113] P. Dubs, R. Stüssi, *Helvetica Chimica Acta* **1976**, *59* (4), 1307–1311.
- [114] A. Gaspar, E. Zellermann, S. Lababidi, J. Reece, W. Schrader, *Analytical Chemistry* **2012**, *84*, 5227–5267.
- [115] A. Gaspar, E. Zellermann, S. Lababidi, J. Reece, W. Schrader, *Energy & Fuels* **2012**, *26* (6), 3481–3487.
- [116] Y. Cho, J.-G. Na, N.-S. Nho, S. H. Kim, S. Kim, *Energy & Fuels* **2012**, *26* (5), 2558–2565.
- [117] J. M. Purcell, C. L. Hendrickson, R. P. Rodgers, A. G. Marshall, *Analytical Chemistry* **2006**, *78* (16), 5906–5912.

- [118] J. M. Purcell, P. Juyal, D.-G. Kim, R. P. Rodgers, C. L. Hendrickson, A. G. Marshall, *Energy & Fuels* **2007**, *21*, 2869–2874.
- [119] H. Müller, J. T. Andersson, W. Schrader, *Analytical Chemistry* **2005**, *77*, 2536–2543.
- [120] J. M. Purcell, P. Juyal, D.-G. Kim, R. P. Rodgers, C. L. Hendrickson, A. G. Marshall, *Energy & Fuels* **2007**, *21* (5), 2869–2874.
- [121] V. V. Lobodin, P. Juyal, A. M. McKenna, R. P. Rodgers, A. G. Marshall, *Energy & Fuels* **2014**, *28* (1), 447–452.
- [122] E. P. Maziarz III, G. A. Baker, T. D. Wood, *Canadian Journal of Chemistry* **2005**, *83* (11), 1871–1877.
- [123] K. K. Laali, S. Hupertz, A. G. Temu, S. E. Galembeck, *Organic & Biomolecular Chemistry* **2005**, *3*, 2319–2326.
- [124] W. E. Rudzinski, K. Zhou, X. Luo, *Energy & Fuels* **2004**, *18* (1), 16–21.
- [125] W. L. Orr, *Analytical Chemistry* **1966**, *38* (11), 1558–1562.
- [126] W. L. Orr, *Analytical Chemistry* **1967**, *39* (10), 1163–1164.
- [127] S. Lababidi, S. K. Panda, J. T. Andersson, W. Schrader, *Analytical Chemistry* **2013**, *85* (20), 9478–9485.
- [128] I. Marchi, S. Rudaz, J.-L. Veuthey, *Talanta* **2009**, *78* (1), 1 – 18.
- [129] S. K. Panda, J. T. Andersson, W. Schrader, *Angewandte Chemie* **2009**, *121* (10), 1820–1823.
- [130] C. Dimier, F. Corato, F. Tramontano, C. Brunet, *Journal of Phycology* **2007**, *43* (5), 937–947.
- [131] J. S. S. Damste, M. P. Koopmans, *Pure and Applied Chemistry* **1997**, *69* (10), 2067–2074.
- [132] E. C. Hopmans, S. Schouten, W. I. C. Rijpstra, J. S. S. Damste, *Organic Geochemistry* **2005**, *36* (3), 485 – 495.
- [133] J. D. Payzant, D. S. Montgomery, O. P. Strausz, *Organic Geochemistry* **1986**, *9* (6), 357–369.

- [134] M. E. L. Kohnen, J. S. S. Damsté, A. C. K.-V. Dalen, J. W. D. Leeuw, *Geochimica et Cosmochimica Acta* **1991**, *55*, 1375–1394.
- [135] AIST, *Spectral Database for Organic Compounds (SDBS); NMR spectrum*, (accessed May 14, 2013).
- [136] W. W. Cleland, *Biochemistry* **1964**, *3* (4), 480–482.
- [137] E. B. Getz, M. Xiao, T. Chakrabarty, R. Cooke, P. R. Selvin, *Analytical Biochemistry* **1999**, *273* (1), 73 – 80.
- [138] J. Han, G. Han, *Analytical Biochemistry* **1994**, *220* (1), 5 – 10.
- [139] A. Ookawa, S. Yokoyama, K. Soai, *Synthetic Communications* **1986**, *16* (7), 819–825.
- [140] K. P. Chary, S. Rajaram, D. S. Iyengar', *Synthetic Communications* **2000**, *30* (21), 3905–3911.
- [141] A. R. Kiasat, R. Mirzajani, F. Ataeian, M. Fallah-Mehrjardi, *Chinese Chemical Letters* **2010**, *21*, 1015–1019.
- [142] L. Banfi, E. Narisano, R. Riva, *e-EROS Encyclopedia of Reagents for Organic Synthesis* **2001**.
- [143] J. Clayden, N. Greeves, S. Warren, P. Wothers, *Organic Chemistry*, Oxford University Press, **2009**.
- [144] R. L. Hubbard, W. E. Haines, J. S. Ball, *Analytical Chemistry* **1958**, *30* (1), 91–93.
- [145] J. H. Karchmer, M. T. Walker, *Analytical Chemistry* **1958**, *30* (1), 85–90.
- [146] ASTM Standard D3227, 2013, Standard Test Method for (Thiol Mercaptan) Sulfur in Gasoline, Kerosine, Aviation Turbine, and Distillate Fuels (Potentiometric Method), **2013**.
- [147] Y. Li, Y. Yang, X. Guan, *Analytical Chemistry* **2012**, *84*, 6877–6883.
- [148] G. P. McDermott, J. M. Terry, X. A. Conlan, N. W. Barnett, P. S. Francis, *Analytical Chemistry* **2011**, *83* (15), 6034–6039.
- [149] L. A. Montoya, M. D. Pluth, *Analytical Chemistry* **2014**.

- [150] C. V. Smythe, *Journal of Biological Chemistry* **1936**, *114* (3), 601–612.
- [151] B. Seiwert, U. Karst, *Analytical Chemistry* **2007**, *79*, 7131–7138.
- [152] Y. Zhang, H. D. Dewald, H. Chen, *Journal of Proteome Research* **2011**, *10* (3), 1293–1304.
- [153] A. Kraj, H.-J. Brouwer, N. Reinhoud, J.-P. Chervet, *Analytical and Bioanalytical Chemistry* **2013**, *405* (29), 9311–9320.
- [154] B. S. Fröhlich, *Wachse der Honigbiene Apis mellifera carnica Pollm.*, Dissertation, Julius-von-Sachs-Institut für Biowissenschaften, University Würzburg, **2002**.
- [155] J. Rosenfeld, C. Murphy, *Talanta* **1967**, *14* (1), 91 – 96.
- [156] X.-R. Wang, F. Chen, *Tetrahedron* **2011**, *67*, 4547–4551.
- [157] C. Joe-Wong, E. Shoenfelt, E. J. Hauser, N. Crompton, S. C. B. Myneni, *Environmental Science & Technology* **2012**, *46* (18), 9854–9861.
- [158] J. D. Payzant, T. W. Mojelsky, O. P. Strausz, *Energy and Fuels* **1989**, *3*, 449–454.
- [159] J.-M. Lee, D.-W. Kim, Y.-D. Jun, S.-G. Oh, *Materials Research Bulletin* **2006**, *41*, 1407–1416.
- [160] A. Foucault, M. Caude, *Journal of Chromatography* **1979**, *185*, 345–360.











